# DISENTANGLING THE COMPLEXITY OF CHEMICAL AND PHYSICAL STRESSORS IMPACTING RIVER SYSTEMS

**Laia Sabater Liesa**

DOCTORAL THESIS

November 2020

Laia Sabater Liesa

# Disentangling the complexity of chemical and physical stressors impacting river systems

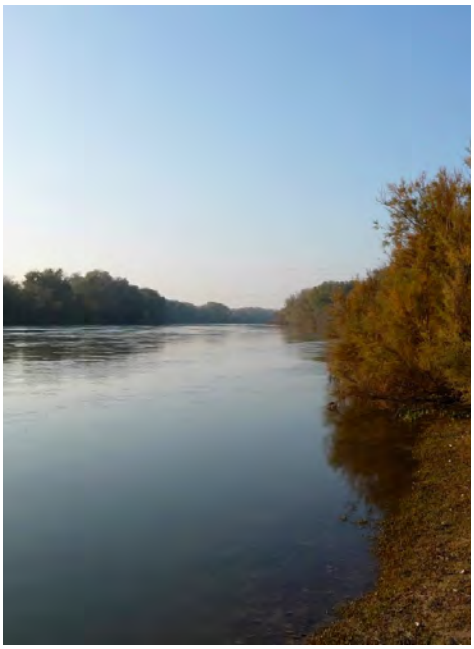

**Universitat de Girona**
Doctoral program in Water Science and Technology

Universitat de Girona

idaea

CSIC
CONSEJO SUPERIOR DE INVESTIGACIONES CIENTIFICAS

Universitat de Girona

idaea

CSIC
Consejo Superior de Investigaciones Científicas

Doctoral Thesis

Doctoral program in Water Science and Technology

# Disentangling the complexity of chemical and physical stressors impacting river systems


Laia Sabater Liesa

Supervised by

Dr. Damià Barceló i Cullerés

Institute of Environmental Assessment
Water Research
Catalan Institute for Water Research

Dr. Antoni Ginebreda Martí

Institute of Environmental Assessment
Water Research

Tutored by

Dr. Anna Maria Romaní i Cornet

University of Girona


Thesis submitted in fullfilment of the requirements for the doctoral degree at the University of Girona

A la Maria, a la Sara i al Pol

## Agraïments

M'agradaria expressar el meu sincer agraïment a totes aquelles persones i institucions que han fet possible la realització d'aquesta tesi doctoral.

En primer lloc als meus directors de tesi, en **Damià Barceló** i l'**Antoni Ginebreda**, per donar-me l'oportunitat d'unir-me al grup de recerca de química de l'aigua, medi ambient i aliments de l'IDAEA-CSIC. Gràcies per confiar en mi, i guiar-me en aquesta gran aventura científica. La realització d'aquesta tesi no hagués estat possible sense el suport econòmic dels projectes SCARCE [Consolider-Ingenio CSD2009-00065] i GLOBAQUA [Grant Agreement No. 603629].

A la meva tutora a la UdG, **Anna Romaní**, per la dedicació en el seguiment de la tesi doctoral. Així com a tots els membres de la comissió de seguiment del programa de doctorat de ciència i tecnologia de l'aigua de la UdG. I també als revisors d'aquesta tesi pels seus consells i aportacions.

A la **Sandra** per la química que ens ha unit, i la que m'has ensenyat juntament amb mil consells i necessàries correccions. Sandra, la meva més sincera gratitud pel teu interès i suport al llarg de tot aquest temps. I també al **Peter** pels seus valuosos comentaris i revisions.

A tots els del grup de recerca de química de l'aigua, medi ambient i aliments de l'IDAEA-CSIC, per l'ajuda rebuda al llarg d'aquest període de tesi. Gràcies **Maja**, **Alícia**, **Cris**, **Marianne**, **Mar**, **Jaume**, **Juan**, **Bozo**, **Massimo**, **Miren**, **Ethel**, **Marinella**, **Núria**, **Roser** i **Dori** entre d'altres. A l'**Àngels** pels bons moments compartits que hem passat xerrant i rient mentre construíem una amistat inoblidable. Al **Nicola** que des de que ens vam conèixer fent un curs a Itàlia, ha estat una persona imprescindible en aquest camí.

A totes les persones de l'ICRA (**Carmen**, **Maria**, **Vicenç**, **Anna**, **Bet**, **Julio**...) que van donar-me suport durant els mesos que va durar l'experiment als canals artificials. A la **Míriam** pels seus consells en els últims mesos de la tesi. Al **Ferran** i a l'**Olatz** per compartir un magnífic experiment, envoltats d'efluent de la depuradora. Al **Juan David** per estar sempre disposat a ajudar-me amb el millor dels somriures.

A la meva família, **Sergi**, **Celi**, **Núria** i **Pau**, pel seu suport incondicional i el seu amor. Entre moltes altres coses, gràcies **pares** per estimar i tenir cura de les nétes al llarg de tots aquests anys. I molt especialment al meu pare doncs amb tu va començar tot...

Al **Nabil** per estar al meu costat en els moments més difícils d'aquest camí. El teu optimisme i valentia són els que m'han ajudat a seguir endavant. A les meves filles i fill, **Maria**, **Sara i Pol**, per fer-me creure que tot és possible. Us estimo molt!

A tots aquells que d'una manera o altra m'han ajudat, encara que el seu nom no figuri de forma explicita en aquestes línies; sense ells tampoc hauria estat possible!

Novembre 2020

# Publications List

## Scientific publications included in this thesis

Sabater-Liesa, L., Ginebreda, A. & Barceló, D. (2018) Shifts of environmental and phytoplankton variables in a regulated river: A spatial-driven analysis. *Science of the Total Environment*; 642: 968-978. https://doi.org/10.1016/j.scitotenv.2018.06.096

Sabater-Liesa, L., Montemurro, N., Font, C., Ginebreda, A., González-Trujillo, J.D., Mingorance, N., Pérez, S. & Barceló, D. (2019) The response patterns of stream biofilms to urban sewage change with exposure time and dilution. *Science of the Total Environment*; 674: 401-411. https://doi.org/10.1016/j.scitotenv.2019.04.178

Sabater-Liesa, L., Montemurro, N., Barceló, D., Eichhorn, P., Ginebreda, A. & Pérez, S. (2020) Retrospective mass spectrometric analysis of wastewater-fed mesocosms to assess the degradation of drugs and their human metabolites. *Journal of Hazardous Materials*. Under Review

## Scientific publications derived from this thesis

Ginebreda, A., Sabater-Liesa, L., Rico, A., Focks, A., Barceló, D. (2018) Reconciling monitoring and modeling: An appraisal of river monitoring networks based on a spatial autocorrelation approach - emerging pollutants in the Danube River as a case study. *Science of the Total Environment*; 618: 323-335 https://doi.org/10.1016/j.scitotenv.2017.11.020

Sabater, S., Bregoli, F., Acuña, V., Barceló, D., Elosegi, A., Ginebreda, A., Marcé, R., Muñoz, I., Sabater-Liesa, L., Ferreira, V. (2018) Effects of human-driven water stress on river ecosystems: a meta-analysis. *Scientific Report*s 8, 11462. https://doi.org/10.1038/s41598-018-29807-7

Ginebreda, A., Sabater-Liesa, L., Barceló, D. (2019) Quantification of ecological complexity and resilience from multivariate biological metrics datasets using singular value decomposition entropy. *MethodsX* 6. https://doi.org/10.1016/j.mex.2019.07.020

# List of acronyms

| | |
|---|---|
| 4-OH-OMZ | 4-Hydroxy omeprazole sulfide |
| AFDM | Ash-free dry mass |
| APA | Alkaline phosphatase activity |
| ATL | Atenolol |
| ATV | Atorvastatin |
| AZY | Azythromycin |
| BLG | Benzoylecgonine |
| CBZ | Carbamazepine |
| Chl-*a* | Chlorophyll-*a* content |
| CLT | Citalopram |
| CTP | Clarithromycin |
| DCF | Diclofenac |
| DCF | Diclofenac |
| DIC | Dissolved Inorganic Carbon |
| DIN | Dissolved inorganic nitrogen |
| DOC | Dissolved organic carbon |
| DON | Dissolved Organic Nitrogen |
| DTZ | Diltiazem |
| DZP | Diazepam |
| EAEE | Erythromycin A enol ether |
| EPS | Eprosartan |
| EU | European Union |
| F0 | Basal fluorescence |
| FLZ | Fluconazole |
| H′ | Shannon diversity index |
| HB | Erythro/threo-Hydrobupropion |

| | |
|---|---|
| HRMS | High-resolution mass spectrometry |
| KTF | Ketoprofen |
| LAP | Leucine-aminopeptidase activity |
| LC-MS | Liquid chromatography mass spectrometry |
| Leu-AMC | l-leucine-4-methyl-7-coumarinylamide |
| LMG | Lamotrine |
| LMZ | Lormetazepam |
| LRMS | Low-resolution mass spectrometry |
| *m/z* | Mass/charge |
| MLE | Maximum likelihood estimation |
| MS/MS | Tandem mass spectrometry |
| MTB | Metabolite |
| MTF | Metformin |
| MUF | 4-methylumbelliferyl |
| N | Nitrogen |
| NCC | Norcocaine |
| NDZP | Nordiazepam |
| $NH_4^+$ | Ammonium |
| $NO_2^-$ | Nitrite |
| $NO_3^-$ | Nitrate |
| NSAIDs | Non-steroidal anti-inflammatory drugs |
| OLS | Ordinary least squares |
| P | Phosphorus as phosphate |
| PAR | Photosynthetic active radiation |
| PCA | Principal Components Analysis |
| PE | population equivalent |
| PPCPs | Pharmaceuticals and personal care products |

| | |
|---|---|
| $PO_4^{3-}$ | Phosphate |
| QTOF-MS | Quadrupole time-of-flight mass spectrometry |
| $R^2$ | Regression of coefficient |
| RDA | Redundancy Analysis |
| RSE | Residual standard error |
| SAR | Spatial autoregression model |
| SRP | Soluble reactive phosphorus |
| STG | Sitagliptin |
| SVD | Singular value decomposition |
| TLS | Telmisartan |
| TMP | Trimethoprim |
| TMZ | Temazepam |
| TOC | Total organic carbon |
| ToF | Time-of-flight |
| TPs | Transformation products |
| TU | Toxic Units |
| UPLC | Ultra-high performance liquid chromatography |
| VFX | Venlafaxine |
| VLS | Valsartan |
| WFD | Water framework directive |
| WWTP | Wastewater treatment plant |
| $Y_{eff}$ | Photosynthetic efficiency |
| ZPD-CA | Zolpidem phenyl-4-carboxylic acid |

# List of Tables

## Introduction



## **Paper I** Supplementary information



## Paper II



## **Paper II** Supplementary information



## Paper III



## **Paper III** Supplementary information

# List of Figures

## Introduction



## Paper I



## Paper I Supplementary information



## Paper II



## Paper II Supplementary information

## Paper III



## Paper III Supplementary information



## General discussion

# Contents

# Summary
# Resumen
# Resum

# Summary

Humanity has always been closely linked to rivers, benefiting from their resources (i.e. water, fishing, energy), while producing impacts associated with their activity, such as the alteration of the river flow after dam construction, pollution, or changes in the land uses. Thus, river systems have been exposed to multiple stressors, which have affected the quality of water and their biological communities. These impacts, which are both physical (e.g. regulation) and chemical (e.g. wastewater discharge), not only have local effects but can spread their effects in space and time to the fluvial network. The effects of these impacts can change the structure and functioning of the biological communities inhabiting there, such as those attached to substrata (biofilms) or those that are suspended in water (phytoplankton). On the other hand, biological communities also respond and contribute to the transformation and/or degradation of certain anthropogenic organic compounds. Among them, pharmaceutically active compounds are of special concern since they are biologically active compounds and make up the most continuous input into the environment as their consumption is increasing due to the expanding population, and their elimination by conventional wastewater treatment plants (WWTP) remains incomplete. Moreover, the long-term effects of these physical and chemical impacts on biological communities are still poorly understood. Any thorough analysis should then consider the physical impairments occurring in the river, as well as the chemical compounds, not only the parent compounds but also the metabolites (compounds resulting from the metabolism of drugs in humans) and the transformation products (compounds resulting from abiotic and biotic degradation in the river system). In this way, a more accurate 'photograph' of the physical impacts and the presence of active and resistant drugs needs to be achieved to perform a more precise risk assessment.

This thesis aims to investigate the chemical state of the river systems and their impacts on the biological communities, using different approaches and scales. This goal has been developed through several papers, which approach this issue from different perspectives. The first paper analyzes the chemical and biological longitudinal structure of a river system impacted by dams. By analyzing the spatial connectivity of variables through mathematical models, and by using a preexistent database of the Ebro river, the responses of biological and chemical variables were determined. We aimed to define how much the chemical and biological responses were related to each other, and how much they were affected by the physical structure of the river system. In the second paper of this thesis,

the effects of chemical variables (nutrients and micropollutants) on a biological community (biofilms) have been described, by using a manipulative experiment in artificial rivers (mesocosms). These were subjected to a gradient of WWTP effluent dilution which simulated the real situation of a river system, especially in the Mediterranean area where the seasonal alteration of flows is noticeable, due to both natural and anthropogenic causes. The third paper explored, through a retrospective analysis, the unnoticed pharmaceuticals compounds occurring in the WWTP effluent used in the mesocosm experiment. This retrospective analysis determined that some human drugs and metabolites suffered from hydrolysis (such as atenolol, benzoylecgonine and norcocaine), or underwent oxidative biodegradation (such as valsartan), and finally a large majority of compounds were persistent and hard to degrade (such as carbamazepine, diclofenac ...). These different chapters of the thesis show that the chemicals present in river systems play an essential role in a multiplicity of processes, but that this may differ according to the considered scale. In the case of the Ebro river mainstream, being regulated by dams, the chemical state of a certain section of the river becomes influenced by the contiguous sections, highlighting that it is necessary to consider the physical frame of the system to establish the complex interactions between chemical and biological processes. When the interaction of thousands of chemicals (including nutrients, organic matter, and/or micropollutants) is analyzed against the biological communities (biofilm) in more detail it arises that they may act as enhancers or stressors of biological activity depending on concentration. Further, the intrinsic dynamics of the community itself plays an important role in the response to the potential effects caused by chemical stress. Our results also highlight that the continued chemical and/or physical impact irreversibly affects biological communities, which does not fully recover even after restoring the initial conditions. Both in the Ebro river and the artificial streams, the new environmental conditions favor opportunistic organisms and the substitution of species, the community shifting to a different stage. A closer look at the multiplicity of chemicals and their degradation products suggests that their identification is crucial in assessing the overall impact of pollutants on river systems. It may be seen as a final implication of our findings that chemical and biological complexity has various temporal and spatial scales, which must be considered for the improvement of the diagnosis of the impact of chemical contamination in the aquatic environment and on its biological communities.

# Resum

La humanitat ha estat sempre íntimament lligada als rius, beneficiant-se dels seus recursos (aigua, pesca, energia, etc.) però també produint impactes associats a la seva activitat tal com l'alteració del cabal del riu per la a construcció de preses, la contaminació o els canvis en els usos del sòl. Així doncs, els sistemes fluvials han estat exposats a múltiples estressos, que han afectat la qualitat de l'aigua així com a l'ecosistema de les seves comunitats biològiques. Aquests impactes, tan físics (com una presa) com químics (com l'abocament de l'aigua residual), no només tenen efectes locals sinó que poden estendre els seus efectes en espai i temps en els sistemes fluvials. Els efectes d'aquests impactes es poden manifestar en canvis en l'estructura i funcionament de les comunitats biològiques que hi viuen, com les adherides al biofilm o bé les que estan en suspensió a l'aigua, com el fitoplàncton. A més, les comunitats biològiques també responen i contribueixen a la transformació i/o degradació d'alguns compostos orgànics d'origen antropogènic. Entre ells son d'especial importància els fàrmacs, ja que a més de ser compostos biològicament actius, la seva aportació al medi és continua a partir del seu consum creixent per part de la població, i la seva incompleta eliminació en els sistemes de depuració convencionals. Per altra banda, els seus efectes a llarg termini sobre molts dels organismes vius presents als ecosistemes son pràcticament desconeguts. Per això, és important fer un anàlisi complet on no només s'identifiquin els compostos originals sinó també els metabòlits (compostos resultants de la metabolització dels fàrmacs en els humans) i els productes de transformació (compostos resultants de la degradació biòtica o abiòtica al sistema fluvial). D'aquesta manera es pot aconseguir una 'fotografia' més precisa de la presència de fàrmacs actius i resistents durant llarg temps en els sistemes fluvials, i per tant es pot fer una avaluació de riscos més acurada.

Aquesta tesi té per objectiu investigar l'estat químic dels sistemes fluvials, i els seus impactes, utilitzant diferents aproximacions i escales. Aquest objectiu s'ha desenvolupat donant lloc a diferents articles. En el primer, s'analitza l'estructura longitudinal química i biològica d'un sistema fluvial impactat per preses. Analitzant la connectivitat espacial de variables mitjançant models matemàtics, i usant una base de dades preexistent del riu Ebre, es va determinar de quina manera les respostes de variables biològiques i químiques s'acoblen o es relacionen entre elles, i quin paper hi juga cada una d'elles en el sistema fluvial. En el segon article d'aquesta tesi, s'han descrit els efectes de les variables

químiques (nutrients i microcontaminants) sobre una comunitat biològica (biofilms), usant per a això un experiment manipulatiu en rius artificials (mesocosmos), sotmesa a un gradient de dilució d'aigua residual que simula la situació real del medi fluvial, especialment a l'àrea Mediterrània on l'alteració estacional dels cabals es notable, tant per causes naturals com antròpiques. I per últim, al tercer article es va fer un anàlisi retrospectiu dels fàrmacs presents en les mostres d'aigües residuals recollides de l'experiment de mesocosmos. Així s'ha determinat l'existència de productes de transformació i metabòlits humans, i s'ha relacionat amb els processos físics i biològics que podrien haver donat lloc a aquests. Aquest anàlisi restrospectiu va determinar que alguns fàrmacs i metabòlits humans van experimentar hidròlisi (com atenolol, benzoylecgonina i norcocaïna), altres com el valsartan va experimentar una biodegradació oxidativa, i finalment que una gran majoria eren persistents (com carbamazepina, diclofenac...) i de difícil degradació. La tesi mostra que els productes químics presents en els sistemes fluvials juguen un paper essencial en multiplicitat de processos, però de forma diferent segons l'escala considerada. En el cas del riu Ebre en el seu eix, molt regulat per preses, l'estat químic d'un tram determinat de riu estava molt influenciat pels trams contigus, el que indicava que cal tenir en compte el marc físic del sistema per establir les complexes interaccions entre processos químics i biològics. Quan es mira a escala física amb més detall, la interacció de milers de productes químics (nutrients i/o microcontaminants) amb les comunitats biològiques, s'observa que els uns i altres actuen com a potenciadors o estressors de l'activitat biològica depenent de la concentració, però que la dinàmica intrínseca de la pròpia comunitat com a resposta als efectes potencials causats per l'estrès químic hi juga un paper important. Aquest impacte químic i/o físic continuat afecta irreversiblement les comunitats biològiques, i no es recupera completament fins i tot després de restablir les condicions inicials. Tant al riu Ebre com als canals artificials, les noves condicions ambientals afavoreixen els organismes oportunistes i la substitució d'espècies. L'estudi, encara a escala amb més detall, de la multiplicitat dels productes químics i dels seus productes de degradació suggereix que la seva identificació és crucial per avaluar l'impacte global dels microcontaminants en els sistemes fluvials.

La complexitat química i biològica travessa diverses escales temporals i espacials, els quals s'ha de tenir en compte per a la millora de la diagnosi de l'impacte de la contaminació química en el medi aquàtic i al seu sistema biològic.

# Resumen

La humanidad ha estado desde siempre íntimamente ligada a los ríos, beneficiándose de sus recursos (agua, pesca, energía, etc.) pero también produciendo impactos asociados a su actividad tales como la alteración del caudal del río por la construcción de presas, la contaminación o los cambios en los usos del suelo. Así pues, los sistemas fluviales han sido expuestos a múltiples factores de estrés, que han afectado a la calidad del agua, así como al ecosistema de sus comunidades biológicas. Estos impactos, tanto físicos (como una presa) como químicos (como el vertido de agua residual), no sólo tienen efectos locales, sino que pueden extenderse en espacio y tiempo en los sistemas fluviales. Los efectos de estos impactos pueden manifestarse en cambios en la estructura y funcionamiento de las comunidades biológicas, como las adheridas a un sustrato (biofilms) o bien las que están en suspensión en el agua (fitoplancton). Además, las comunidades biológicas también responden y contribuyen a la transformación y/o degradación de algunos compuestos orgánicos de origen antropogénico. Entre ellos son de especial importancia los fármacos, ya que además de ser compuestos biológicamente activos, hay una continua aportación al medio debido al creciente consumo de la población, y su incompleta eliminación en las depuradoras. Además, sus efectos a largo plazo en los organismos vivos presentes en los ecosistemas son prácticamente desconocidos. Por ello, es importante hacer un análisis completo de caracterización en el que no sólo se identifiquen los compuestos originales sino también los metabolitos (compuestos resultantes de la metabolización de los fármacos en los humanos) y los productos de transformación (compuestos resultantes de la degradación biótica o abiótica en el medio acuático). De esta manera podemos tener una 'fotografía' más realista de la presencia de fármacos activos en los sistemas fluviales, y por lo tanto una evaluación de riesgos más precisa.

Esta tesis tiene por objetivo investigar el estado químico de los sistemas fluviales, y sus impactos, utilizando diferentes aproximaciones y escalas. Este objetivo se ha desarrollado dando lugar a diferentes artículos. En el primero, se analiza la estructura longitudinal química y biológica de un sistema fluvial impactado por presas. Analizando la conectividad espacial de variables mediante modelos matemáticos, y usando una base de datos preexistente del río Ebro, se determinó de qué manera las respuestas de variables biológicas y químicas estaban o no acopladas, y qué papel jugaba cada una de ellas en el sistema fluvial. En el segundo artículo de esta tesis, se han descrito los efectos de las

variables químicas (nutrientes y microcontaminantes) sobre una comunidad biológica (biofilms), usando para ello un experimento manipulativo en ríos artificiales, sometida a un gradiente de dilución de agua residual que simula la situación real de un sistema fluvial, especialmente en el área Mediterránea donde la alteración estacional, por causas tanto naturales como antrópicas, de los caudales es notable. Y, por último, en el tercer artículo se hizo un análisis retrospectivo de los fármacos presentes en las muestras de aguas residuales recogidas del experimento de mesocosmos. Así se determinó la existencia de productos de transformación y metabolitos humanos, y se relacionó con los procesos físicos y biológicos que podrían haber dado lugar a éstos. Este análisis retrospectivo permitió establecer que algunos fármacos y metabolitos humanos experimentaron hidrólisis (como atenolol, benzoylecgonina y norcocaína), otros como el valsartán experimentó una biodegradación oxidativa, y finalmente una gran mayoría de compuestos químicos resultaron ser persistentes y de difícil degradación (como carbamazepina, diclofenaco ...). La tesis muestra que los productos químicos presentes en los sistemas fluviales juegan un papel fundamental en una multiplicidad de procesos, pero de forma diferente según la escala considerada. En el caso del río Ebro en su eje principal, muy regulado por presas, el estado químico de un tramo determinado de río estaba muy influenciado por los tramos contiguos, lo que indicaba que hay que tener en cuenta el marco físico del sistema para establecer las complejas interacciones entre procesos químicos y biológicos. Cuando se mira a una escala con más detalle, la interacción de múltiples productos químicos (nutrientes y/o microcontaminantes) con las comunidades biológicas, se observa que actúan como potenciadores o estresores de la actividad biológica dependiendo de la concentración, pero que la dinámica intrínseca de la propia comunidad como respuesta a los efectos potenciales causados por el estrés químico juega un papel importante. Este impacto químico y/o físico continuado afecta irreversiblemente las comunidades biológicas, y no se recupera completamente incluso después de restablecer las condiciones iniciales. Tanto en el río Ebro como en los canales artificiales, las nuevas condiciones ambientales favorecen los organismos oportunistas y la sustitución de especies. El estudio, a escala más detallada, de la multiplicidad de los productos químicos y de sus productos de degradación sugiere que su identificación es crucial para evaluar el impacto global de los microcontaminantes en los sistemas fluviales. La complejidad química y biológica atraviesa varias escalas temporales y espaciales, los cuales se deben tener en cuenta para mejorar el diagnóstico del impacto de la contaminación química en el medio acuático y su sistema biológico.

# Introduction

# Introduction

## River systems

Most of the planet is covered by water, although the majority of resources remain unavailable to freshwater and terrestrial ecosystems, stored in the ice caps, soils, and being part of the oceans. Freshwater lakes and rivers hold 100.000 $km^3$ globally, less than 0.01% of all water on earth (Jackson et al., 2001). Therefore, water is a limited resource while remaining absolutely essential for humans life as well as for nature (Naiman and Dudgeon, 2011). Rivers connect the atmosphere and oceans with the biotic compartments and soil processes (Meybeck, 2003). Changes induced in this complex global water cycle may imply important consequences in terrestrial, lacustrine and marine ecosystems' health, affecting the ecosystem services and so, the benefits they provide (Sabater et al., 2013; Strayer and Dudgeon, 2010). As a matter of fact, the availability of good water quality in sufficient quantity is an essential condition for human societies to succeed (Haidvogl, 2018).

Human demands on water resources have increased over the past century, creating an evident anthropogenic footprint on them (Ercin and Hoekstra, 2014). Tightly connected to water quantity, water quality is affected by the multiple and continued human water uses, affecting ecosystems all over the world. Inland waters, and particularly rivers, may be especially vulnerable to Anthropocene impacts because of their strategic position within the global water cycle. Only a few rivers on our Planet remain in pristine condition and have not been altered by humans (Sabater et al., 2019), this, being expressed on dam building, river channelization or land-use change. These actions affect the morphology, hydrology, and aquatic biota of streams and rivers (Sabater et al., 2008), and all of these also affect water quality, i.e. the presence and concentration of nutrients, dissolved organic matter, and contaminants (Petrovic et al., 2016).

Effects on water quantity and quality are particularly pronounced in Mediterranean regions, where dry periods (i.e. winter and summer), account for low precipitation. Mostly during summer, when temperatures are high and plants are in their most active phase, high evapotranspiration causes a further decrease in the water level of superficial and groundwater, which sometimes forces the systems to become intermittent. Water scarcity is not exclusive of Mediterranean water courses (Mekonnen and Hoekstra, 2016),

but the density of population and the diverse water demands, contribute in making this as an area of marked water resource deficits (Navarro-Ortega et al., 2015). Pressures on water resources are going together with low dilution, and indeed Mediterranean watercourses present extensive issues on water quality and quantity (Petrovic et al., 2011).

Pressure on river systems is currently enhanced by the occurring climate change and human demands, and models predict an increase in anthropogenic and climatic impacts (Döll and Schmied, 2012). Together with air temperatures increase, precipitation patterns are fluctuating and becoming more extreme (IPCC, 2014), particularly in the Mediterranean (Mas-Pla et al., 2016; Sergi Sabater et al., 2016a). As a result, rivers are submitted to longer than normal periods of basal low flows, but also are affected by more intense floods. Climate change predictions together with rising pressures associated to land-use changes (i.e. those resulting from the transformation in agricultural areas, or those associated to urbanization, or industrialization) (Steffen et al., 2008) make river systems more vulnerable to the arrival of contaminants, again, particularly in the Mediterranean. Therefore, it is necessary to protect and preserve river systems, and understanding the relevance of chemical pollution as stressor is a necessary step to achieve a suitable conservation. This urgency is matching to the requirements of the European Union's Water Framework Directive 2000/60/EC, a legislative framework aiming to protect and enhance the status of aquatic ecosystems while promoting the sustainable use of available water resources (Pistocchi, 2019). The Water Framework Directive (WFD) represented a landmark in water management in the European Union (EU) countries, which connected ecosystem preservation to the secure use of water resources. The WFD moved priorities from those purely based on the water economy and use to those based on the prevention of impacts onto freshwater ecosystems.

However, after twenty years of implementation of the WFD, several issues require further refinement before the goal of a better status of the European waterbodies might be achieved. One recently signaled is to improve our knowledge of the chemical status and their effects on the ecosystems (Vermeulen et al., 2019). This would include setting river quality standards to all EU member states, updating the list of priority substances, and evaluating the risk to the environment in the form of combined chemical mixtures rather than single substances. A further challenge is the difficulty of making compatible the

rising pressure on water resources with the preservation of biodiversity (Vorosmarty et al., 2010).

**Physical stressors as modulators of chemical risk**

Rivers are characterized by their high spatial connectivity and hierarchical structure, which configure drainage networks (Allan and Castillo, 2007), and define the nature of hydrological and geomorphological patterns. Rivers are highly dynamic systems, on which the unidirectional water flow from headwaters to the river mouth configures particular spatial and temporal dynamics (Johnson et al., 1995). This structure may favour cumulative influences of stressors traveling downstream, and including both biological as well as physical and chemical (Helmut Segner et al., 2014; Strayer et al., 2010). The occurrence and potential impact of anthropogenic stressors multiply (Meybeck, 2004; Piggott et al., 2016; Helmut Segner et al., 2014) throughout river networks.

As a consequence, stressors and impacts affect river systems beyond the local influence, so a local physical stressor may extend other spaces and persist through time (Elosegi et al., 2019). Usually, impacts become stronger towards the medium and lower parts of river networks. Here is where impacts in land use (agriculture, forestry), flow modification and over-extraction of water (Jackson et al., 2001), chemical contaminants (Carey and Migliaccio, 2009; Kuzmanovic et al., 2015), the impact of invasive species (Gallardo et al., 2016), or the destruction or degradation of habitat (Sabater et al., 2013), are the most pronounced. Overall, impacts are less intense in headwaters and progressively stronger towards the most humanized areas.

One of the main physical stressors imposed on river systems is *regulation*, which is achieved through the construction of small dams, irrigation channels, and large reservoirs. Dams respond to the long-lasting influence which humans have inflicted on river networks, and have disrupted the river continuum, since early historical times (Vörösmarty et al., 2004). Their spread construction throughout many world river basins is aimed mostly to take advantage of river water resources. Reservoirs diverge in size, and are used for irrigation, drinking water supply, hydroelectric power, and floods control; these uses account for the enormous number of dams all over the world (Nilsson et al., 2005). Regarding its effect on rivers, damming alters the hydrology, geomorphology, and ecology of the river downstream. Effects include alterations in the

flow pattern and thermal regime, the capture of fine sediments, and the reduction of habitat availability for many inhabiting species (Nilsson and Renofalt, 2008).

In the Mediterranean regions, which already suffer from a large deficit of water resources (Barceló and Sabater, 2010), the effects of large dams and flow regulation are highly relevant. In large and medium-sized Mediterranean rivers, reservoirs are managed with the ultimate goal to store as much water resources as possible to provide water supplies for human activities (Piqué et al., 2016). The alteration of the natural flow regime because of the dams' presence establishes new conditions for the biota, and certainly affects the river water quality. The natural biogeochemical cycles of carbon, nutrients and metals become altered, accounting for the large differences in the chemical water quality between upstream and downstream of a reservoir (Roura-Carol, 2004). Thus, modifications in the flow regime reduce rivers' connectivity and the downstream effects of dams are maintained tens of kilometers downstream and the effects may persist down to the river mouth (Goodwin et al., 2006). Overall, reservoirs produce extensive consequences for the biota and the water quality in river networks.

**Figure I1.** Ebro river

**Chemical stressors reaching river systems**

Water draining a basin does carry many dissolved substances into river systems, which then become net receivers of chemical pollution, including organic matter and inorganic nutrients (phosphorus, nitrogen) in excess, and many micropollutants such as pharmaceuticals, pesticides or industrial products. Nutrients are essential elements for primary producers such as algae and other plants, but when concentrations are too high, they result in impairment of the system condition, providing a clear example of the complex relationship between human influence and river health. In fact, chemical pollution is recognized as one of the major causes of rivers impairment (Vorosmarty et al., 2010) as it is involved in the majority of stress situations in surface waters (Noges et al., 2016). As said, the intensity of this threat is magnified in those rivers with reduced dilution capacity (Dudgeon, 2010; Petrovic et al., 2011), such as those in the Mediterranean basin.

Organic micropollutants find their way into the aquatic environment either from point (localized) or diffuse (multiple pathways) sources (Gros et al., 2007; Schwarzenbach et al., 2006). Micropollutants such as pesticides can reach river systems through diffuse pollution as a result of the runoff in agriculture, or as industrial contaminants following atmospheric deposition (Mandaric et al., 2016). Fish farms, landfill sites, power stations, and oil spillage from pipelines can be included as point sources of contaminants (Mandaric et al., 2016), but the main source of contaminants occurring in superficial waters are wastewaters collecting industrial or urban uses (Posthuma et al., 2008). These arrive at river systems, either before being treated or after treatment. Regarding wastewater treatment, the current legislation for urban wastewaters (Directive 91/271/EEC) is aimed at the reduction of suspended solids, organic load, and in areas declared vulnerable, nutrients (nitrogen and phosphorus) as well. Therefore, urban WWTPs generally consist of secondary treatment, and eventually, tertiary treatment for nutrient reduction, but they are not designed for the elimination of micropollutants. For that reason, they do not entirely remove the contaminants they receive (Navarro-Ortega et al., 2015). Therefore, WWTP effluents are currently the main route of entry of many contaminants into the aquatic environment.

Once released into the environment, contaminants are subjected to physical processes (dilution, dispersion, volatilization). These processes do not affect the chemical structure of the molecules, but indeed may decrease their concentration with respect to the waters

received from the WWTP. Sorption (including adsorption and absorption) is another physical process which may also affect the chemicals concentrations. Further effects on chemicals can also follow because of a variety of biotic and chemical processes (e.g., photolysis, hydrolysis, or biodegradation). Biodegradation is perhaps one of the most important processes in river systems, particularly regarding polar micropollutants such as pharmaceuticals, to which microorganisms inhabiting the streambed and the water column may degrade, partially or completely making part of the ecosystem process of attenuation (Acuña et al., 2015b). Some contaminants may bioaccumulate by aquatic organisms, either through direct partitioning from the abiotic environment or directly from dietary sources (Ruhí et al., 2016). All these processes contribute to the transformation of the original molecules (Barret et al., 2010; Petrovic et al., 2007), leading to the so-called transformation products (TP) (Längin et al., 2008).

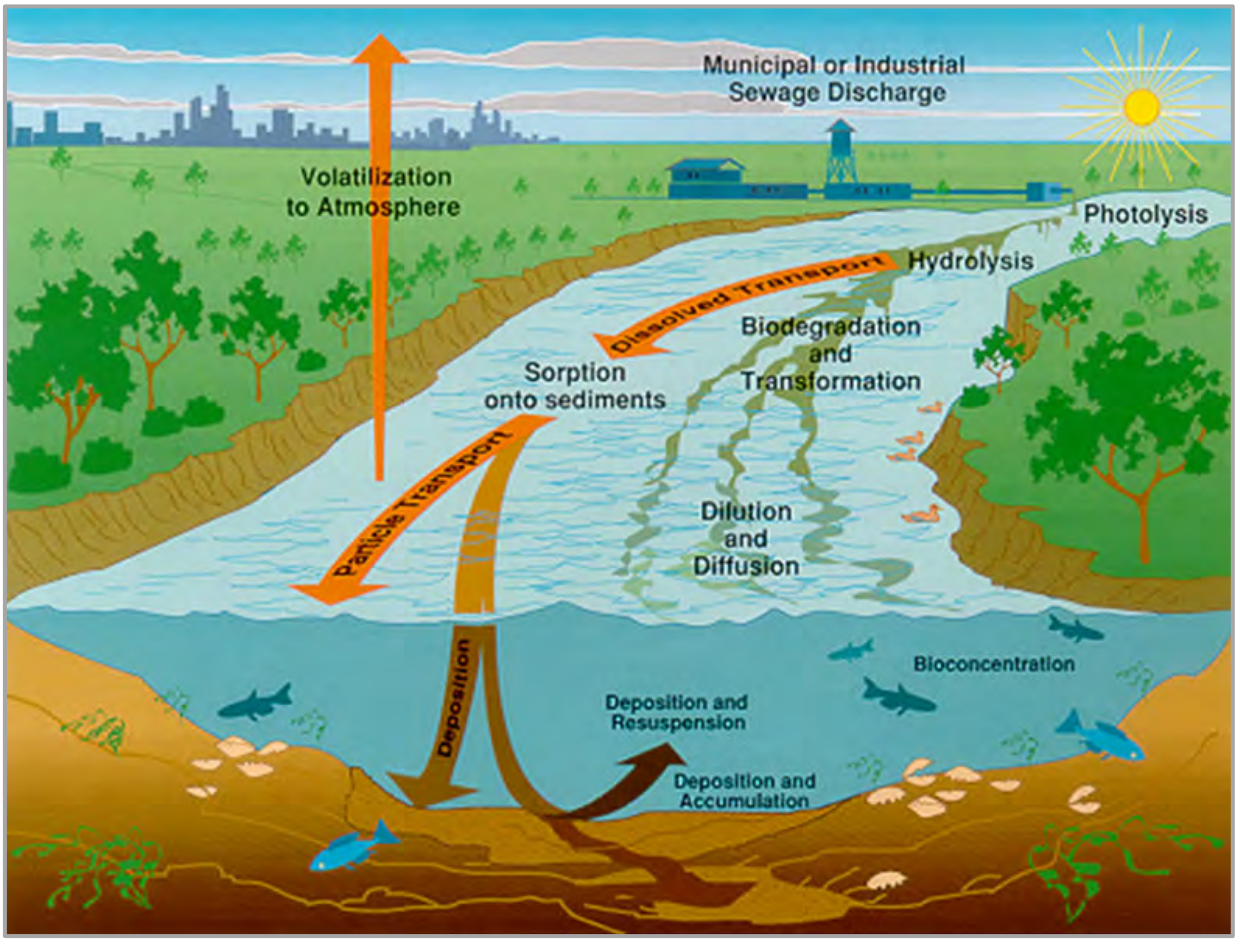


**Figure I2.** Processes controlling the fate of organic contaminants in the aquatic environment. Figure from USGS Circular 1133, p. 114-135

The WFD (Directive 2000/60/EC, 2000) regulates 45 priority substances and established a watch list with 10 additional substances of possible concern (Directive 2013/39). However, these regulated or suspected chemicals of concern are just a small fraction of numerous chemicals present in different environmental compartments (rivers, lakes, groundwaters, sediments, wastewaters, drinking waters) (Daughton and Ternes, 1999; Delgadillo-Mirquez et al., 2011). Their continuous release into the environment makes these contaminants potentially hazardous (Barceló and Petrovic, 2007), at least for the aquatic systems, and the long-term environmental effects are still unknown, especially because they occur in the form of complex chemical mixtures rather than alone, and usually as long-term (chronic) low dose exposures. As commented previously, incorporating more chemicals into these surveillance lists needs to be addressed through legislative intervention.

**Pharmaceutical products as contaminants in river systems**

Among the vast array of contaminants of anthropogenic origin reaching watercourses, pharmaceuticals are of environmental concern, for both their continuous release through human wastes and their inherent biological activity. The pharmaceuticals most frequently detected in surface waters in Europe are usually high consumption drugs. The most relevant therapeutic groups include analgesics, anti-inflammatory drugs, β-blocker agents, antibiotics, and antihypertensives (aus der Beek et al., 2016), though many other classes such as psychiatric drugs and cytotoxic drugs should not be disregarded due to their environmental concerns. The constant entrance of antibiotics into the aquatic environment through the WWTPs, and the increasing use of antibiotics in livestock and aquaculture has led to the selection of resistant bacteria, which is a matter of great concern (Chu et al., 2018; Rodriguez-Mozaz et al., 2015a).

Pharmaceuticals previously administered to humans or animals are excreted via urine or feces as a mixture of parent compounds (unmetabolized forms) and biotransformation products (metabolites). These metabolites originating from the enzyme-mediated changes of the structure of pharmaceuticals within the treated organism, and they may be more potent than the parent compound or display off-target selectivity (Halling-Sørensen et al., 1998; Längin et al., 2008). Once excreted, these substances reach WWTP through the sewer system. While they are not completely removed in conventional WWTPs (Jelić et al., 2012) enhanced elimination rates can be achieved with advanced treatment

technologies (Rodriguez-Mozaz et al., 2015b). Ultimately, a significant fraction of wastewater-relevant pharmaceutical substances is discharged into receiving water bodies (rivers, lakes, and seas) yielding concentrations in the ng $L^{-1}$ to µg $L^{-1}$ range (Luo et al., 2014). Also, many pharmaceutical products remain in the aquatic environment for long periods of time such as atenolol, carbamazepine, diclofenac, iopromide, metoprolol, sulfamethoxazole, and trimethoprim, which can be biologically active and are particularly resistant to elimination (Montemurro et al., 2018; Patel et al., 2019; Pérez et al., 2006; Pérez and Barceló, 2008). This indeed poses a risk to the environment, which can be potentially extended to humans when waters are used as sources for drinking purposes (Daughton and Ternes, 1999). Therefore, the presence of pharmaceuticals in the environment as well as in drinking waters are of concern for human health and biodiversity (Gros et al., 2012).

The identification and quantification of organic micropollutants at low concentrations in aquatic environmental matrices requires analytical methods of high sensitivity and selectivity, which mostly rely on liquid chromatography coupled to mass spectrometry (LC-MS). Currently, the most frequently types of mass spectrometry used for the detection of organic compounds in environmental samples are low-resolution MS (LRMS) and high-resolution (HRMS). In the 1990s, LRMS instruments were considered the best strategy for routine quantitative analysis of small molecules in environmental samples and HRMS was almost exclusively used for structure elucidation of metabolites and degradation products (Aceña et al., 2015a). However, in the last decade HRMS has become much more affordable to research laboratories, mostly because of the development of user-friendly Orbitrap-MS-based instruments and quadrupole time-of-flight MS (QToF-MS) systems suitable for the sensitive determination of polar organic compounds (Aceña et al., 2015b). Both platforms are compatible with ultra-high performance LC (UPLC), offer high sensitivity, and record full-scan chromatograms with high mass accuracy and resolution (Eichhorn et al., 2012; Kern et al., 2009).

LC–HRMS provides robust analysis with high selectivity into three different analytical applications: target analysis of known analytes; suspect screening of known structures but without standards; and non-target screening of unknown compounds (Krauss et al., 2010). Also, the LC-HRMS allows retrospective analysis of the samples, therefore providing a powerful tool for monitoring.

In the suspect screening mode, preliminary information is available including the compound names, molecular and fragment ions as well as retention time if they are available. Then the list is screening to the samples files obtained in the HR-MS instrument in order to extract the masses of those suspected compounds. Then a match is required between the isotopic profile and the fragments from the analytes detected in the samples and the ones from the suspected list. Also, they can be confirmed with theoretical MS/MS spectra (from base data or modelling sources). After that, one can get a list of suspect compounds in the sample.

The application of advanced HRMS in environmental analysis to monitor a broader range of compounds has enabled a more comprehensive assessment of the level of pollution (Aceña et al., 2016). Still, the regulated chemicals that are monitored frequently are just a small fraction of the numerous chemicals present in the environment, and most analytical methods focus only on targeted parent compounds and rarely include metabolites and transformation products, which sometimes can be more persistent than the original compounds.

**Assessing the effects of stressors in river systems**

The co-occurring chemical and physical stressors in river systems produce pressure on the inhabiting biota. Organisms living in river systems, including bacteria, algae, invertebrates, or fish, respond individually, or as assemblages, to the occurring stressors. Specific responses of each group of organisms are related to their life cycle and habitat that they occupy and translate in specific roles in the energy and matter flux in the ecosystem.

Shorter life-cycle organisms (bacteria, algae) may rapidly respond to changes occurring in the river environment, being these both physical (e.g. temperature, pH) and chemical (e.g. nutrient, organic matter, contaminants). Amongst these, biofilms are consortia of algae, bacteria, and fungi, assembled on solid surfaces in a very efficient manner (Lock, 1993). Biofilms may colonize all solid river substrata (sediments, rocks, stones), where bacteria are the dominant component especially in light-limited systems, and algae become dominant when light is available. Biofilms are the first receptors of environmental and chemical stress because of their position in the interface between water and sediments (Sabater et al., 2007). Stream biofilms drive a large part of the ecosystem metabolism and biogeochemical cycling, this being shared by the primary producers

(algae) and the heterotrophs (bacteria, fungi). Biofilms are sensitive to a wide array of chemical substances as nutrients or organic and inorganic contaminants (Corcoll et al., 2012a). These elements may reflect on their structure (i.e., biomass and taxonomic composition), since pollutants may affect the growth rate of particular species as well as the equilibrium between the competing species within the community. Contaminants are also able to affect biofilm functioning, both that of the primary producers (photosynthesis), as well as that of the heterotrophs, such as the transformation capacity of dissolved materials (enzymatic activities) (Sabater et al., 2007). Accordingly, biofilm responses may be evaluated through a set of structural (i.e. ash-free dry mass (AFDM), chlorophyll-*a* content (Chl-*a*)) and functional variables (i.e. photosynthetic efficiency ($Y_{eff}$), or transformation of organic phosphorus by alkaline phosphatase activity (APA)).

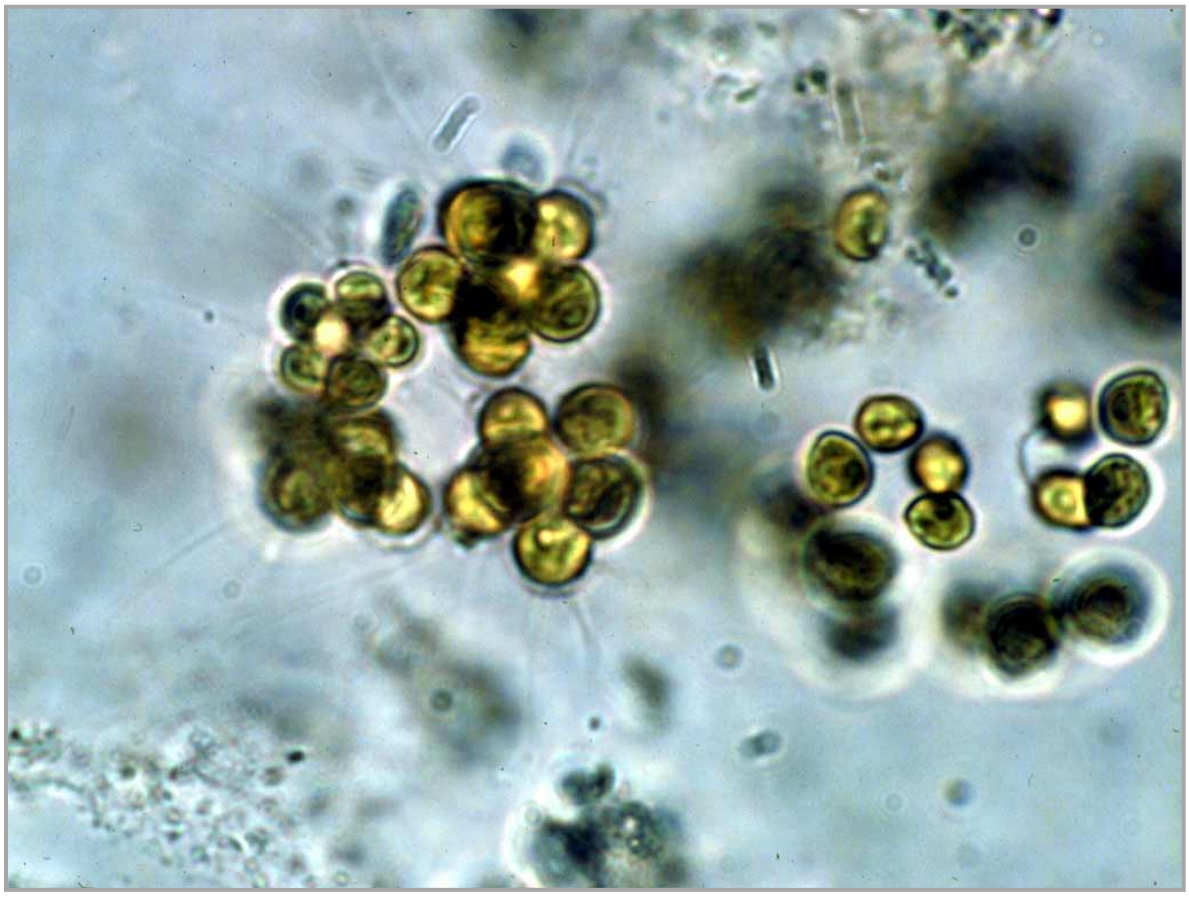

**Figure I3.** Planktonic green alga in riverine plankton

In the water column, phytoplankton mostly occurs under suitable hydrological and hydrodynamic conditions. That is, high discharge (or low water residence time) affects planktonic development and causes low planktonic densities. In river systems, phytoplankton is constrained by the drift of the algal cells downstream and the decrease

of the population growth rates (Reynolds, 2006). Planktonic chlorophyll in river systems is affected by the occurrence of reservoirs, which promote cell settlement, and a complete reset in the biogeochemical water conditions. Reservoirs cause that the expected pattern of a downstream increase in planktonic chlorophyll becomes interrupted. The potential pattern, associated with the time available for plankton to develop, and the corresponding higher nutrient concentrations downstream (Jones, 1984; Köhler, 1994), is completely altered. The absence of longitudinal coincidence between nutrients and chlorophyll reinforces the role that hydraulics may exert on the development of phytoplankton in large rivers (Reynolds and Descy, 1996).

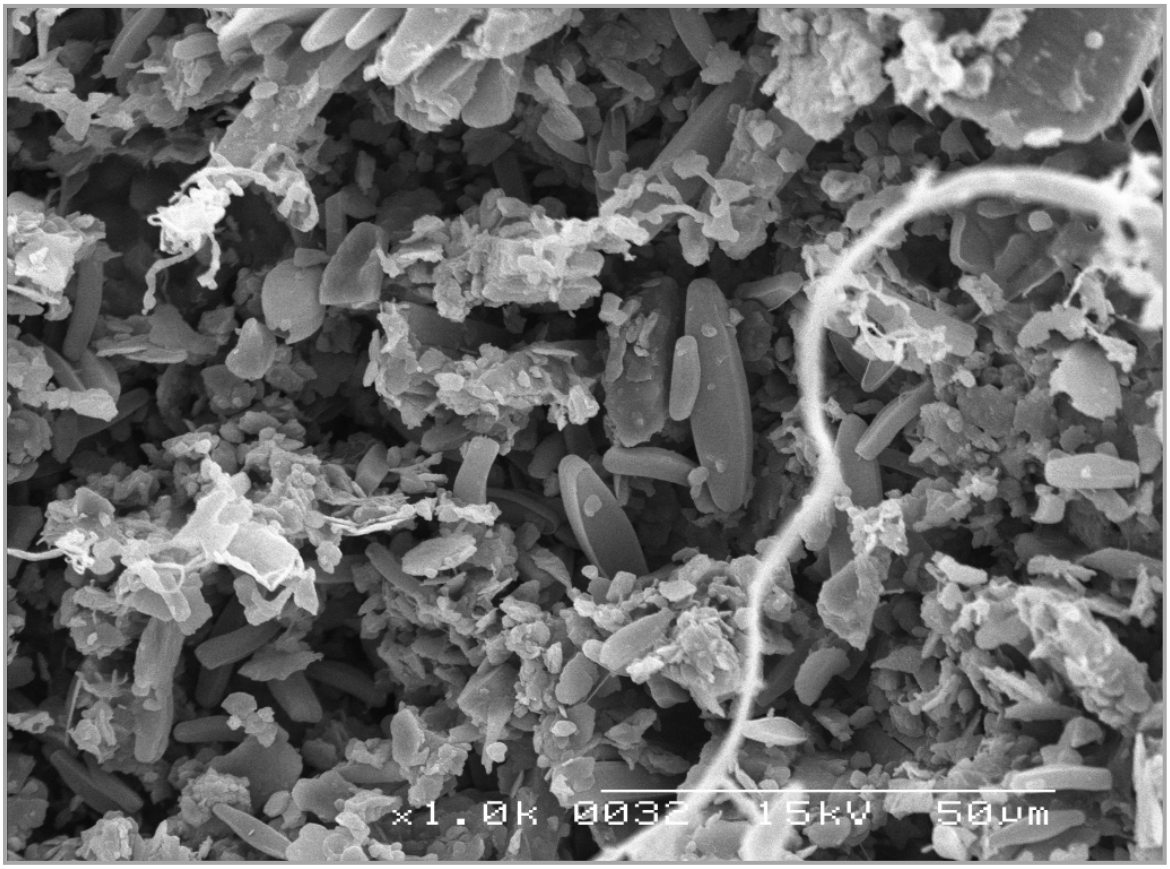


**Figure I4.** Scanning microscope photograph of a biofilm in a small stream

Either in the water column, or associated with every substratum in the river bottom, the complex composition of contaminants reaching river waters, which also include nutrients, organic matter, and emerging contaminants, makes it difficult to predict which might be the environmental effects they produce. The subsidy-stress framework (Odum et al., 1979) indicates that contaminants may act either as a subsidy or as a stressor for biological activity regarding their concentration and mode-of-action. Assimilable contaminants such as dissolved nutrients and organic matter subsidize biological activity, at least up to a

threshold, beyond which they can suppress it. On the other hand, some contaminants are deleterious to organisms and tend to suppress biological activity. Therefore, because of their mixed composition and the resulting concentrations in river ecosystems can be either a subsidy or stress for the receiving ecosystem. Furthermore, the potential response to contaminants differs between the different groups of organisms, and ecological interactions add a level of complexity (Segner et al., 2014). Thus, the response to pollution can differ from the scale of the river biofilm to the scale of the whole ecosystem.

## Thesis objectives and hypotheses

The overall **aim** of this thesis has been to investigate the chemical status of river systems at different scales of analysis and submitted to different influences. More specifically, this thesis aimed to answer the following questions:

1. In which manner the longitudinal structure of river networks affects its chemical status? Were discontinuities, associated with the presence of tributaries or dams, the two equally effective on the chemical and biological river components? In the present work the effect of reservoirs on the longitudinal structure of the system was approached using a regulated river data set, which allowed to determine whether the responses of biological and chemical variables were or not coupled, this being related to the occurrence of dams. This question was investigated by analyzing the spatial connectivity of variables through mathematical approaches and modeling (Paper I).

2. Which was the influence of chemical variables, including contaminants, on the biota submitted to their effects? Were these effects linearly produced, or followed other patterns? These questions were investigated by means of a replicated manipulative experiment in artificial streams, which performed as smaller river systems onto which environmental conditions were controlled. In these systems, biofilms were subjected to a gradient of wastewater effluents, and their responses analyzed (Paper II).

3. Are human metabolites and pharmaceutical transformation products present on mesocosm wastewater-fed? Are they mediated by the physical and biological processes co-occurring in river systems? The chemical dynamics of pollutants were investigated by means of the screening of wastewater samples collected from the mesocosm experiment, using retrospective HRMS analysis. The identification of TPs and metabolites is crucial to assess the overall impact of pollutants on river systems (Paper III).

The above objectives were designed to test the **general hypothesis** that *chemicals present in river systems are the result not only of the incoming inputs, but also derive from a*

*multiplicity of processes occurring on them, these being different according to the scale considered*.

The interactions between the three main papers included in this thesis are depicted in the following figure, all structured around the main issue of the chemical status of river ecosystems, and the associated complexities and biological implications:

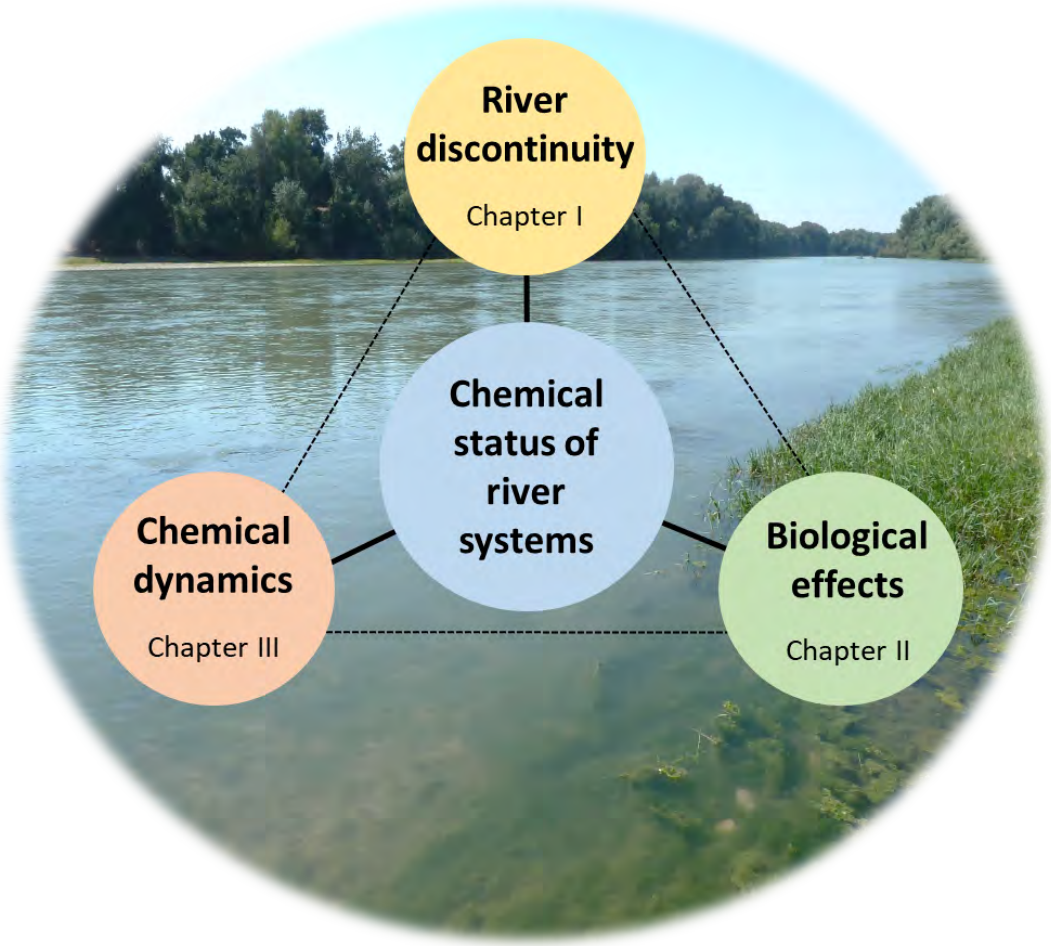


**Figure I5**. Interaction between the three main papers included in the thesis

# Thesis papers

# Paper I

## Shifts of environmental and phytoplankton variables in a regulated river: A spatial-driven analysis

Laia Sabater-Liesa, Antoni Ginebreda, Damià Barceló
Science of the Total Environment; 642: 968-978 (2018)

# Paper I. Shifts of environmental and phytoplankton variables in a regulated river: A spatial-driven analysis

Laia Sabater-Liesa[a], Antoni Ginebreda[a,*], Damià Barceló[a,b]

[a] Department of Environmental Chemistry, IDAEA-CSIC, Jordi Girona 18-26, 08034 Barcelona, Spain

[b] ICRA, Carrer Emili Grahit 101, Girona 17003, Spain

## Abstract

The longitudinal structure of the environmental and phytoplankton variables was investigated in the Ebro River (NE Spain), which is heavily affected by water abstraction and regulation. A first exploration indicated that the phytoplankton community did not resist the impact of reservoirs and barely recovered downstream of them. The spatial analysis showed that the responses of the phytoplankton and environmental variables were not uniform. The two set of variables revealed spatial variability discontinuities and river fragmentation upstream and downstream from the reservoirs. Reservoirs caused the replacement of spatially heterogeneous habitats by homogeneous spatially distributed water bodies, these new environmental conditions downstream benefiting the opportunist and cosmopolitan algal taxa. The application of a spatial auto-regression model to algal biomass (chlorophyll-a) permitted to capture the relevance and contribution of extra-local influences in the river ecosystem.

**Keywords**: Phytoplankton; Environmental variables; Ebro River; Spatial autocorrelation; Longitudinal connectivity; Resistance and resilience

## 1. Introduction

River networks have an asymmetrical configuration which determines unidirectional physical and chemical processes (Frissell et al., 1986). The imposed downstream direction in environmental conditions greatly determines the biological structure of river (Vannote et al., 1980; Wehr and Descy, 1998), though geomorphological complexity configures non-linear connections (Delong and Thorp, 2006). So forth, neighbouring sites are not independent one from the other, and this can be reflected both in the hydrological and environmental conditions as well as in the composition and relative abundance of biological assemblages (Amoros and Bornette, 2002; Tockner et al., 1999; Ward and Stanford, 1995). This complex pattern is further complicated when hydraulic infrastructures (dams, weirs, channels) occur in the river (Lobera et al., 2017). Largely regulated rivers show alterations of the water regime and its chemical quality, which affect biological assemblages (Dynesius and Nilsson, 1994; Nilsson et al., 2005). The regulation capacity of reservoirs is one of the strongest causes for river discontinuity (Ward and Stanford, 1983), but their impact on environmental and biological variables is not necessarily analogous (Bunn and Arthington, 2002). It is unknown yet if the ability to resist regulation effects, and the ability to recover after them, is parallel between ones and the others.

One of the most sensitive elements in large river ecosystems is phytoplankton. The phytoplankton community plays a central role as primary producers in the functioning of large rivers (Dale and Beyeler, 2001; Wehr and Descy, 1998). River phytoplankton occurs as a balance result of the advocative forces occurring in flowing waters and the in situ population growth rates (Reynolds, 2006). In this delicate balance, river phytoplankton is affected both by local environmental factors (light and nutrient availability, water temperature, grazing pressure) as well as by the upstream influence of continuous seeding and hydrological and chemical conditions. Here we use the phytoplankton community composition and its associated biomass (planktonic chlorophyll-a) as the biological receptors to be tested in the river because of regulation, and compare their changes in structure with those occurring in the environmental variables.

In that context, the Ebro River offers a suitable case study to explore the spatial structure of an ecosystem impacted by man-made perturbation. The Ebro River is one of the largest rivers in the Iberian Peninsula, strongly regulated by dams since the 1940s'. Around 190

dams are spread across the whole basin, impounding 57% of the mean annual runoff (Romaní et al., 2010). The location of the three large reservoirs (Mequinenza, Ribarroja and Flix) in the middle-lower section of the river cause a large disruption to the sites downstream. These reservoirs cause water thermal alteration downstream (Prats et al., 2010), contribute to retain sediments (Batalla and Vericat, 2011), and disrupt the biogeochemical nutrients cycles and the phytoplankton community structure (Sabater et al., 2008; Tornes et al., 2014). Since the basin is subjected to multiple human activities which produce impacts like inorganic and organic pollution and water abstraction (Batalla et al., 2004; Lacorte et al., 2006; Navarro-Ortega and Barceló, 2010), effects might be complex on both water quality and phytoplankton assemblages. The size and position of these reservoirs offer a good setting for the analysis of the phytoplankton and environmental variables responses to the impact, showing in which way their respective spatial patterns differ or resemble.

In order to do so, we apply an analogous approach to that used on trophic webs and metapopulations analysis, able to deal with complex systems in which different constituents ("nodes") interact ("links") to each other (Nordström and Bonsdorff, 2017; Wallach et al., 2017). We use this as starting point to capture the river topology and connections among neighboring nodes, where variables were measured (monitoring sites) and the anthropogenic effects on this arrangement were evaluated by using appropriate tools commonly used in the spatial analysis (Fischer and Wang, 2011; Ginebreda et al., 2018). Whereas either time or spatial data series could be in principle equally used in autocorrelation modeling of phytoplankton indicators, their performance depends on (a) the connectivity and heterogeneity of the area under study, (b) the spatial and temporal scales of the variable considered and (c) the easiness of monitoring. Spatial autocorrelation works better on heterogeneous environments, and its analysis takes into account the connectivity (Dakos et al., 2010). On the other hand, the timescales that govern phytoplankton succession (weeks) require of an extensive monitoring effort far beyond the one required for a spatial study. Based on that, the spatial analysis approach is a convenient alternative to time series when available data are not sufficiently complete. In this paper we implement a method to analyze and compare the spatial patterns of environmental and biological variables in rivers systems submitted to regulation. The identification of 'stability' properties (resistance and resilience), and thus, the interpretation in terms of connectivity and longitudinal patterns are aimed to test the

hypothesis that regulation produces uncoupled responses on the environmental and phytoplankton variables, further compromising the ability of phytoplankton community to resist and recover. While the longitudinal dynamics of environmental variables supposedly has a strong neighbor influence, the response of phytoplankton is likely more complex as a result of conjoint local and extra-local influences. The spatial dimension may then provide understanding on how the different elements of river ecosystem respond to regulation.

## 2. Material and methods

### *2.1 Study area*

The Ebro basin is located in the Northeastern part of the Iberian Peninsula occupying a total surface of 85362 km2. The main river is 910 km length and flows from the Cantabrian mountains to the Mediterranean Sea (Romaní et al., 2010). In the Ebro mainstream there is a system of three consecutive large reservoirs, Mequinenza (1500 x 106 m3), Riba-roja (210 x 106 m3) and Flix (11 x 106 m3) that regulate the hydrology of the lower part (Prats et al., 2010). These reservoirs cause major changes in the hydromorphological dynamics by altering floods peaks (López-Moreno et al., 2002) as well as by retaining sediments (Buendia et al., 2016).

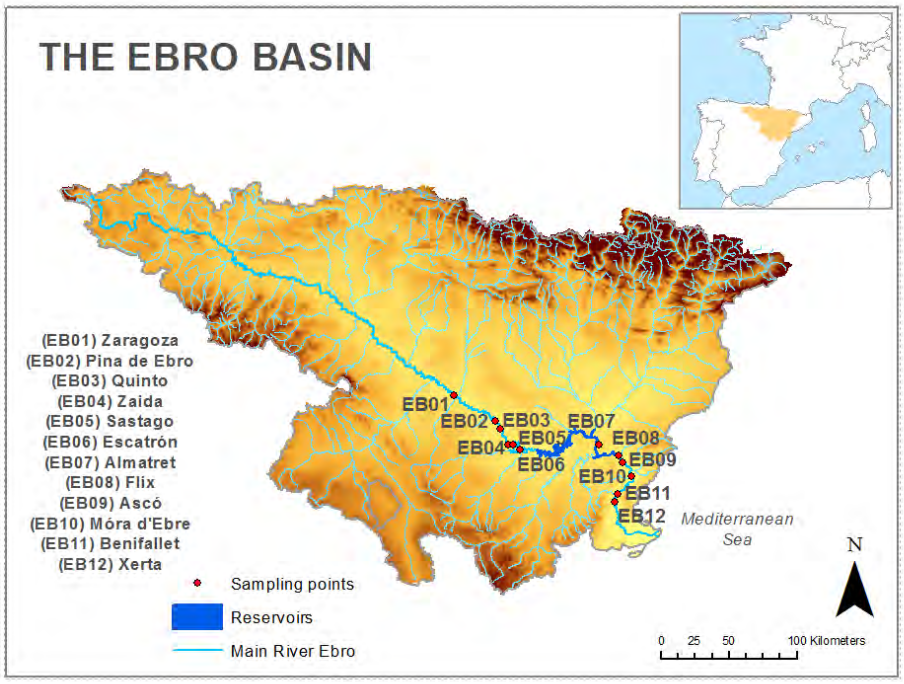


**Figure PI *1*.** The Ebro river basin. The reservoirs are highlighted and the sampling points are numbered

*2.2 Data collection*

For this study we used data from several published studies (Artigas et al., 2012; Sabater et al., 2008; Tornes et al., 2014), as well as public data from the Confederación Hidrográfica del Ebro webpage (http://www.chebro.es). Using these sources, we selected data from twelve sites located in the mid-lower course from Zaragoza to the proximity of the river mouth (Figure 1). Six of the sites (Zaragoza, EB01; Pina Ebro, EB02; Quinto, EB03; Zaida, EB04; Sástago, EB05; Escatrón, EB06) were located upstream of the Mequinenza, Riba-roja and Flix reservoirs. One site (Almatret, EB07) was placed between the first two dams, and the remaining five (Flix, EB08; Ascó, EB09; Móra d'Ebre, EB10; Benifallet, EB11; Xerta, EB12) were located downstream to the reservoirs.

We collected some data on abiotic and biotic variables to characterize the ecosystem response to regulation. Regarding biological variables, we used metrics on the phytoplankton biomass (biovolume and chlorophyll-*a* concentration) and community structure (Shannon-Wiener diversity, cell density). Both biovolume and chlorophyll-a concentration have been used as surrogate of biomass (Hillebrand et al., 1999); while the Shannon diversity index (H') characterizes the taxonomic diversity in a community. The selected physical and chemical variables included water temperature, conductivity, water flow and nutrients. NH4+ and NO3- were considered together as dissolved inorganic nitrogen (DIN), comparable to, soluble reactive phosphorus (SRP), Dissolved Inorganic Carbon (DIC), Dissolved Organic Carbon (DOC) and Dissolved Organic Nitrogen (DON).

Phytoplankton and environmental data covered eighteen sampling campaigns between 2008 to 2013. The dataset included samples from different hydrological conditions, low waters and high water periods, occurring in the river (Artigas et al., 2012). Therefore, the data we used accounted for 350 km of the main river axis over 5 years (Table S1a and S1b).

*2.3. Data analysis*

The sequence of analysis is summarized in Figure 2. Briefly, the stress effect of reservoirs into phytoplankton was analyzed by means of two stability properties, i.e., resilience and resistance (Grimm and Wissel, 1997). These are dynamic properties largely dependent on the connections of the ecosystem (Pimm, 1984); resilience is the capacity of the system

to return to a reference state after a disturbance, while resistance refers to staying essentially unchanged despite the perturbation (Holling, 1973). To that end, appropriate indexes quantifying these properties are proposed.

In a second phase of the analysis, we examined the spatial distribution of the biological and environmental variables, separating the variability in the river sections upstream and downstream the reservoirs. We further explored the spatial connectivity of these variables using spatial autocorrelation indicators (i.e., global and local Moran autocorrelation index and correlation lengths) based on the observed data. The degree of connection between consecutive neighboring sites for each measured variable was also analyzed in order to obtain a quantitative estimation of the nearest neighbors influence to each site in terms of its contribution to the total variability. This allowed attributing the remaining variability to local factors.

In a final step of the analysis, a spatial autoregression model has been used to explore the potential influence of imposed environmental conditions on algal biomass (chlorophyll-a), considering the joint contribution of neighbors and local effects (Fischer and Wang, 2011). While neighbors' influence was captured by an autocorrelation term, local effects were embodied in the model by introducing environmental measurements as explanatory independent variables.

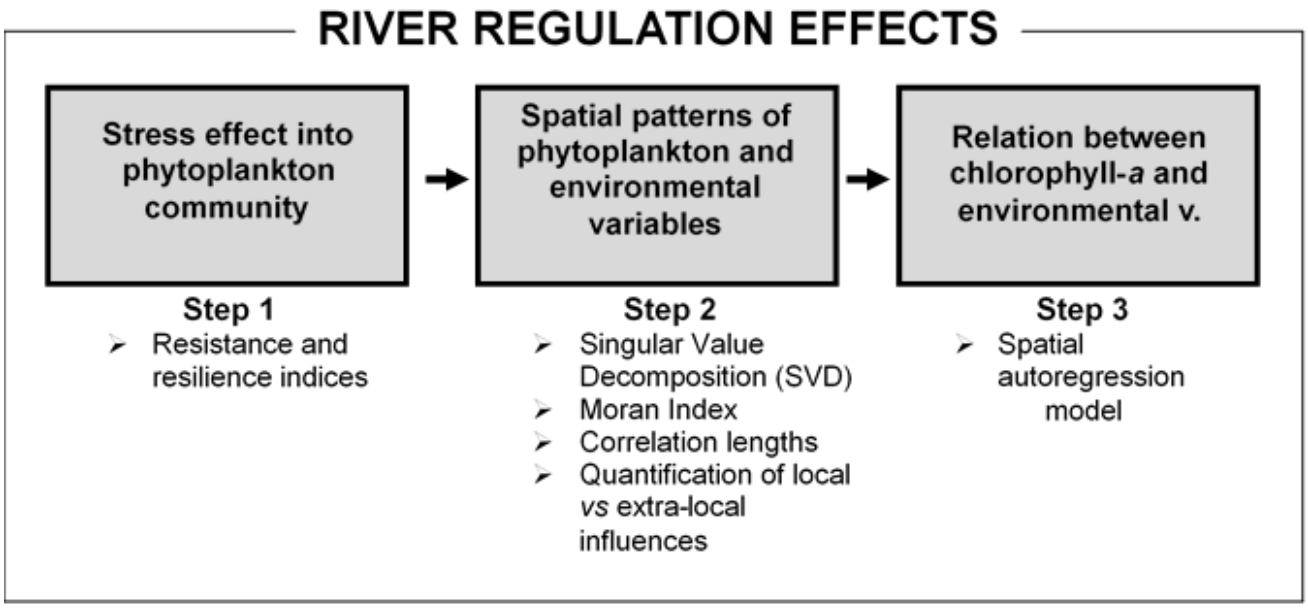


**Figure PI 2**. The methodological workflow

*2.3.1. Quantification of resistance and resilience*

We quantified the stress effects of reservoirs into phytoplankton community by defining its resistance and resilience. The calculation of phytoplankton community resistance and resilience were performed comparing values taken upstream (not regulated) and downstream the reservoirs (regulated). In order to better capture the phytoplankton pattern of upstream sites, we used the mean of sites EB04, EB05 and EB06 named as XUP, because of their proximity to the reservoirs. We therefore considered the mean of the upstream sites as the control on which to compare the sites impacted by regulation (Griffiths and Philippot, 2013).

Resistance is an indicator of the capacity of minimal change and was calculated as the difference between the variable measured immediately downstream reservoirs (site EB08) and the corresponding variable measured in upstream sites (XUP).

$$\text{Resistance (\%)} = (X_{EB08} / X_{UP}) \cdot 100 \quad (1)$$

Where X stands for the phytoplankton variables measured (biovolume, cell density, chl-*a* and diversity) at the site indicated by the superscript.

Resilience indicates the ability of phytoplankton to return to initial levels (recovery) after disturbance. Resilience was estimated on the downstream reservoir sites using the following ratio:

$$\text{Resilience (\%)} = (X_{DOWN} / X_{UP}) \cdot 100 \quad (2)$$

DOWN indicates the different sites in downstream section (from EB08 to EB12 sites).

*2.3.2. Spatial Structure analysis using Singular Value Decomposition (SVD)*

The spatial structure of the phytoplankton community and environmental variables was analyzed by means of singular value decomposition (SVD). This is a technique of data dimensionality reduction and may be seen as a generalization of eigenvalue decomposition for rectangular matrices. It consists of a decomposition of rectangular matrix into a product of three matrices which help to interpret the data structure.

Briefly, we constructed a dataset for every measured variable constituted by tables of space × time. These are handled as rectangular matrices *M* of *m* columns (*m*: number of spatial sites) and *n* rows (*n*: number of campaigns). *M* matrix can be conveniently

factorized in its time and space components using the SVD. Briefly, matrix $M$ is factorized as $M = U \cdot \Sigma \cdot VT$, where $U$ is an $m \times m$ unitary matrix, $\Sigma$ is a $m \times n$ rectangular diagonal matrix with non-negative real numbers on the diagonal, and $V$ is an $n \times n$ real or complex unitary matrix. The diagonal entries $\sigma_i$ of Σ are known as the singular values of M. The columns of U and the columns of V are called the left-singular vectors and right-singular vectors of $M$, which in our case captured the time and space contributions respectively. Furthermore, U vectors are the eigenvectors of $MM^T$ and $V$ vectors are the eigenvectors of $M^TM$. The non-zero singular values of $M$ (the diagonal entries of $\Sigma$) are the square roots of the non-zero eigenvalues of both $M^TM$ and $MM^T$.

Contribution $c_i$ of each site $i$ to the spatial variability can be calculated using the right singular vectors V, according to the following expression:

$$c_i = \frac{\sum_{j=1}^{n} \sigma_j V_{ij}^2}{\sum_{j=1}^{n} \sigma_j} \quad (3)$$

where $v_{ij}$ is the component $i$ of the of the $j$ right-singular vector. The sum in the denominator normalizes the weight of the singular values $\sigma j$ so that their sum equals unity, and taking into account that V vectors are normalized (i.e., $\sum_{j=1}^{n} V_{ij}^2 = 1$); altogether $\sum_{i=1}^{n} c_i = 1$.

### *2.3.3. River Network analysis*

Network analysis was used to explore the structural properties of the set of items (nodes, sites) and the connections between them (links). We characterized each sampling site as the node $i$ linked with a neighbor node $j$. Its network structure can be captured by means of the adjacency matrix A, known as spatial-neighborhood matrix, defined as $A_{ij} = 1$ if nodes $i$ and $j$ are connected, $A_{ij} = 1$ otherwise. Also, we considered that a given node was not affected by itself, so $A_{ii} = 0$. This implies restricting the neighbors' influence to those nodes directly linked to the one considered. In our case, we assumed that the adjacency matrix A associated to the river was not symmetrical since measured variables under concern could only run downstream on the direction of river flow. Thus, the adjacency matrix is assumed to be low-triangular (i.e., a node can be only affected by those located upstream). Therefore, for two connected nodes $i,j$ $A_{ij} = 1$ if i>j and $A_{ji} = 0$ otherwise. Hence, this implies that the end nodes are considered closed and their measured values taken as boundary conditions (Ginebreda et al., 2018).

### *2.3.4. Spatial correlation: The Moran Index*

We explored the continuity and the degree of connection between neighbouring sites and identified the influence of neighbours and local factors into the variability of the phytoplankton variables by means of spatial autocorrelation indexes (global and local Moran indexes). We used the Moran index to obtain a first picture of the continuity patterns of the environmental and biological variables of the Ebro. The Moran index (López-Moreno et al., 2011) is widely used as a measure of spatial autocorrelation in exploratory analyses (Li et al., 2007), and is defined as the two-point correlation for all pairs of consecutively connected sites or lag-1 correlation:

$$Moran\_I = \frac{n\sum_{i=1}^{n}\sum_{j=1}^{n}A_{ij}(x_i-\mu)(x_j-\mu)}{\left(\sum_{i=1}^{n}\sum_{j=1}^{n}A_{ij}\right)\left(\sum_{i=1}^{n}(x_i-\mu)^2\right)} \quad (4)$$

Where xi is the observation of variable *x* at site *i,* $\mu$ its mean and *n* the number of monitoring sites (Chen, 2013; López-Moreno et al., 2011). Since Moran_I calculation requires the use of a symmetric adjacency matrix, here we used $1/2(A^T+A)$ as a symmetrized version of matrix A. Furthermore, it is row-standardized (i.e., rows sum up to 1) (Li et al., 2007). Moran_I was conveniently calculated following (Chen, 2013). This author showed that equation (4) is equivalent to:

$$Moran\_I = \sum_i \sum_j \bar{A}_{ij} z_i z_j = z^T \bar{A} z \quad (5)$$

Where $z = (x-\mu)/\sigma$ (*x* standardized) and Ā is a normalized version of A, so that $\bar{A}_{ij} = A_{ij} / \sum_{ij} A_{ij}$ and $\sum_{ij} \bar{A}_{ij} = 1$.

The Moran_I indicates the correlation between neighboring spatial observations of a given variable, and so forth it is a measure of spatial association. Spatial autocorrelation among similar neighbour sites results on positive values of Moran_I and conversely, lack of similarity is reflected on negative Moran_I. For the absence of correlation, the expected Moran_I value is given by the expression $-1/(n-1)$ (*n* = number of sites), which is close to zero for high *n* values.

Moran_I can be disaggregated into local node contributions giving way to the so called "Local Indicator of Spatial Association" (LISA) or in short, Local Moran_I (Anselin, 1995):

$$I_i = z_i \sum_j \bar{A}_{ij} z_j \quad (6)$$

with $$Moran\_I = \sum_i I_i \quad (7)$$

Moran's local measures assess the spatial autocorrelation associated with one particular area unit (Fischer and Wang, 2011) which is well suited to do an exploratory analysis of the spatial structure of the river.

### *2.3.5. Correlation lengths*

The correlation length $\ell$ can be interpreted as the distance threshold, from which a site no longer has influence on the next one (Ginebreda et al., 2018). In order to study how much the spatial correlation between nodes (sites) varies with the separation distance, we calculated Moran_I at higher lags up to 4 (note that at distance 0 Moran_I equals 1). This requires the use of appropriate lower-triangular adjacency matrices $A_{(d)}$ (d =2, 3, 4) describing the topology at the respective distances. These matrices can be readily obtained multiplying $A$ (actually $A_{(1)}$) by itself the required number of times, i.e., $A_{(2)} = A \cdot A$; $A_{(3)} = A \cdot A \cdot A = A_{(2)} \cdot A$, and so on. The so-called 'correlation length' $\ell$ is the distance at which Moran_I=0, and it was estimated from the linear fit of Moran_I as a function of the topological distance (Dakos et al., 2010) taking it as the intercept with the x-axis. Topological distances can be approximately converted to real distances (in km) multiplying by the mean separation distance (km) between consecutive sites (Ginebreda et al., 2018). This was calculated for phytoplankton and environmental variables.

### *2.3.6. Quantifying local and neighbor contributions*

For a given variable the effect of neighbor sites on each site can be generally described using a simple spatial autoregression model (SAR). This can be simply expressed by means of the spatial autocorrelation equation (8) (Fischer and Wang, 2011):

$$x_i = \rho \cdot \sum_{j=1}^{n} A_{ij} \cdot x_j + \varepsilon_i \quad (8)$$

Where $x_i$ can be a measured variable at node $i$ and $\rho$ an autocorrelation parameter to be determined. Written in compact matrix form:

$$x = \rho \cdot Ax + \varepsilon \quad (9)$$

Where A is the above-mentioned adjacency matrix, x is an n-dimension vector ($n$ = number of nodes) of measurements of the variable considered, ε is an $n$-dimension vector reflecting the local effects and $\rho$ is a correlation coefficient to be determined. The two

terms in equations (8) and (9), capture respectively the neighbors' and local influences. The correlation parameter $\rho$ was calculated by both ordinary least squares (OLS) and maximum likelihood estimation (MLE), being the latter considered the most reliable method (Fischer and Wang, 2011).

The relative contributions of both neighbors and local sources on the variables can be quantified at the river network scale. To do so, equation (9) was left multiplied by $x^T$ and both terms were divided by $x^T x$:

$$1 = \rho \cdot \frac{x^T A\, x}{x^T x} + \frac{x^T \varepsilon}{x^T x} \qquad (10)$$

The first and second terms respectively provide quantitative estimations of the overall neighbor influence and of the local contributions normalized to unity for the variable under study at the river stretch level (Ginebreda et al., 2018). In the present study equation (10) was applied to the phytoplankton and environmental variables.

### *2.3.7. The Spatial Autoregression model (SAR model)*

We performed a spatial autoregression model (SAR) to take into account neighbor effects and local contributions of environmental variables to algal biomass (chlorophyll-*a*). The SAR model can be generalized by combination with a conventional linear regression multivariate model (Fischer and Wang, 2011), as per equation:

$$x_i = \rho \cdot \sum_{j=1}^{n} A_{ij}\, x_j + \sum_{q=1}^{m} \beta_q y_{iq} + \varepsilon_i \qquad (11)$$

Where $y_{iq}$ *(q=1…m)* is a vector of independent variables associated to site $i$, $\beta_q$ are the corresponding coefficients, and $\varepsilon_i$ an error term. Written in compact matrix form, equation 11 reads:

$$x = \rho \cdot Ax + y\beta + \varepsilon \qquad (12)$$

We analyzed the relationship between chlorophyll-*a* (dependent variable) and nutrients, temperature, conductivity and water flow as independent variables using the above SAR model (equations 11, 12). Parameters $\rho$ and $\beta_q$ were determined by regression.

We first developed models for the whole river section and later we explored separate models for upstream and downstream stretches to check for differences between the two. Therefore, separate models were calculated for (a) sites upstream the dams (sites EB01

to EB06); (b) sites downstream the dams (sites EB07 to EB012) and (c) all sites. Best independent variables were selected by step-wise regression.

All calculations were carried out in a spread sheet using Excel (Microsoft®) and graphs were performed using SigmaPlot 13.

## 3. Results

### *3.1 Spatial indicators of phytoplankton's response to stress: resistance and resilience*

The resistance of chlorophyll-*a* to the reservoirs impact was low (17.3%) while phytoplankton diversity showed a substantially larger resistance (>100%). Biovolume resistance accounted for 32.3% and cell density for 24.8% (Table 1a).

The resilience, that is, the rate of recovery for the phytoplankton variables, was incomplete for biovolume, cell density and chlorophyll-a. The maximum recovery with respect the mean of the previous upstream sites (EB04, EB05 and EB06) ranged 19.4-39.1% (Table 1b). The distance needed by biovolume and chlorophyll-*a* to reach the new maximum after the reservoirs impact was at the Ascó site (EB09), while the maximum achieved by cell density was shorter (Flix site, EB08). Contrastingly, diversity completely recovered and even increased slightly after the reservoirs.

**Table PI 1**. **(a)** Resistance and **(b)** resilience of studied phytoplankton variables

a)

| Resistance | % |
|---|---|
| Biovolume | 32.3 |
| Cell density | 24.8 |
| Chlorophyll-*a* | 17.3 |
| Diversity | 113.5 |

b)

| Resilience % | Distance 1 (EB08) | Distance 2 (EB09) | Distance 3 (EB10) | Distance 4 (EB11) | Distance 5 (EB12) |
|---|---|---|---|---|---|
| Biovolume | 32.3 | 39.1 | 34.7 | 21.4 | 20.1 |
| Cell density | 24.8 | 21.9 | 23.3 | 8.6 | 10.1 |
| Chlorophyll-*a* | 17.3 | 19.4 | 15.6 | 14.8 | 13.5 |
| Diversity | 113.5 | 104.9 | 108.9 | 100.1 | 105.2 |

*3.2. River Spatial Structure of environmental variables*

The spatial pattern of environmental variables (conductivity, temperature, water flow and nutrients) was captured by singular value decomposition (SVD) analysis of the corresponding data matrices using V vectors (right singular vectors). The first two vectors (Figures 3a-f) accounted for ca. 80% of the data variability (conductivity 93.1%; temperature 89.1%; water flow 85.8%; SRP 73.4%; DIN 80.9% and DON 70.7%). The analysis indicated that for all these variables the upstream sites were well separated from the downstream sites. The Almatret site (EB07), located in between the dams, was mostly grouped with downstream sites. In all cases, the discrimination was only related to the second singular vector (V2).

The respective site contributions to the variability of environmental variables (Figure S1) indicates a rather regular variability among all sites. Conductivity, DIN, and DON had a major contribution in the first six upstream sites (61.6 – 62.3%). Temperature, water flow and SRP in the six upstream sites contribution amounted to 44%. In general, for a given river section (upstream or downstream) sites have a similar contribution to the variability of the environmental variables.

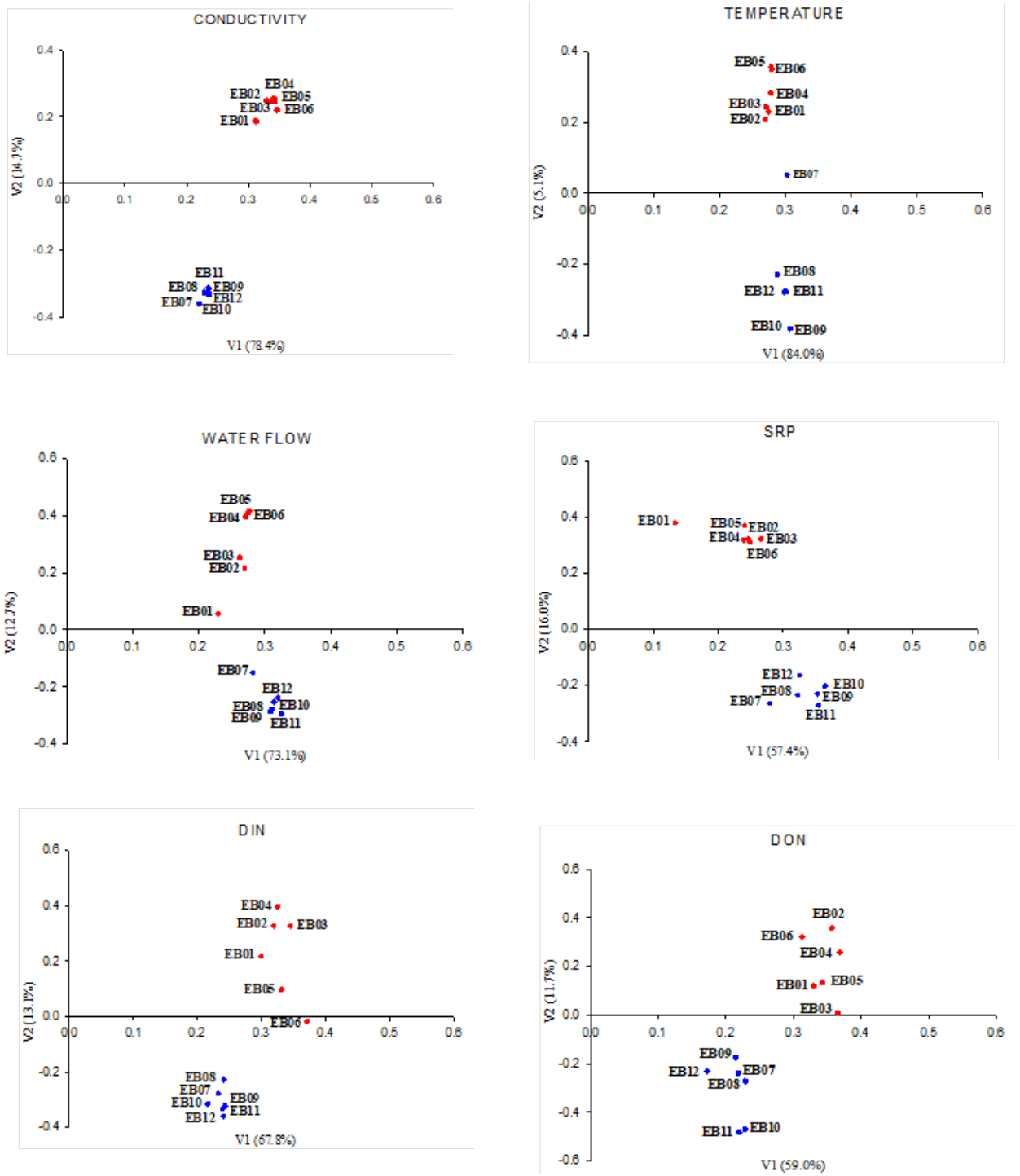


**Figure PI3.** Representation of the first two Right Singular Vectors (explained variance given in parentheses) for the environmental variables. **Upstream sites** (EB01 to EB06) are circled in red; **Downstream sites** (EB07 to EB12) are circled in blue. EB01, Zaragoza; EB02, Pina de Ebro; EB03, Quinto; EB04, Zaida; EB05, Sástago; EB06, Escatrón; EB07, Almatret; EB08, Flix; EB09, Ascó; EB10, Móra d'Ebre; EB11, Benifallet; EB12, Xerta

### *3.3. River Spatial Structure of phytoplankton variables*

The spatial pattern of phytoplankton (biovolume, cell density, chlorophyll-a, and diversity) captured by the SVD analysis showed that the first two vectors accounted for ca. 70% of the data variability (biovolume 70.6%; cell density 80.1%; chlorophyll-*a* 72.5% and diversity 68.8%, Figures 4a-d). The upstream sites were separated from the downstream sites for all the considered variables. The Almatret site (EB07), located in between the dams, was grouped with the downstream sites for chlorophyll-*a* and diversity, but close to sites upstream for cell density and biovolume. The first right singular vector (V1) separates upstream and downstream sites for biovolume, cell density, and chlorophyll-a, while discrimination in the case of diversity was related to the second singular vector (V2). The first six upstream sites were the main contributors to variability (65.2 – 80.2%) in biovolume, cell density, and chlorophyll-*a* (Figure S2). However, diversity variability was evenly divided among all sites (mean per site: 8.3%; upstream and downstream sites had a similar contribution of ca. 50%).

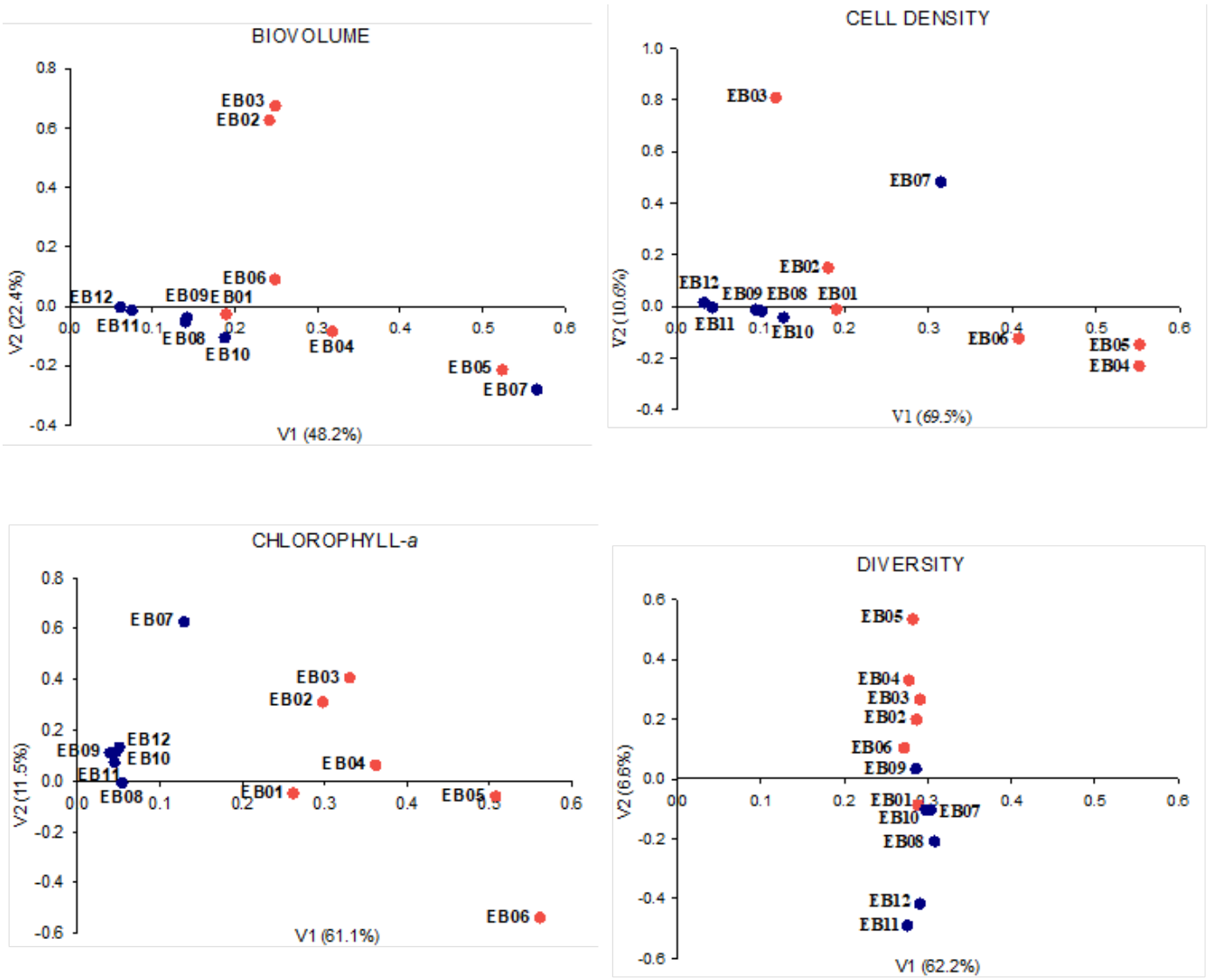


**Figure PI4**. Representation of the first two Right Singular Vectors (explained variance given in parentheses) for the phytoplankton variables studied. **Upstream sites** (EB01 to EB06) are circled in red; **Downstream sites** (EB07 to EB12) are circled in blue. EB01, Zaragoza; EB02, Pina de Ebro; EB03, Quinto; EB04, Zaida; EB05, Sástago; EB06, Escatrón; EB07, Almatret; EB08, Flix; EB09, Ascó; EB10, Móra d'Ebre; EB11, Benifallet; EB12, Xerta

### *3.4. Longitudinal variations of phytoplankton taxa*

In terms of abundance, diatoms dominate the upstream sites while green algae prevailed in the downstream section. Phytoplankton composition of the more abundant taxa (Table 2) upstream of the reservoirs (*Skeletonema potamos*, *Limnothrix planctonica*, *Micractinium pusillum* and large centric diatoms) differed from that downstream of the reservoirs (*Aphanocapsa* sp. and *Oscillatoria* sp.).

**Table PI 2**. The average abundance values (cells/ml) of phytoplankton taxa in the upstream (EB01-EB06) and the downstream (EB07-EB12) sections of all sampling campaigns. The table includes the more abundant taxa from both sections.

| Taxa | Upstream | Downstream |
|---|---|---|
| *Skeletonema potamos* | 570 | 4 |
| Large centric diatoms | 180 | 14 |
| *Limnothrix planctonica* | 109 | 57 |
| *Micractinium pusillum* | 107 | 5 |
| *Planktothrix agardhii* | 85 | 36 |
| Small centric diatoms | 76 | 6 |
| *Aulacoseira granulata* var. *angustissima* | 71 | 6 |
| *Actinastrum hantzschii* | 43 | 0 |
| *Oscillatoria sp.* | 37 | 61 |
| *Pseudanabaena sp.* | 31 | 10 |
| *Aphanocapsa sp.* | 6 | 123 |
| *Cocconeis cf. placentula* | 6 | 19 |
| Large volvocales | 2 | 17 |
| *Planktothrix sp.* | 2 | 31 |
| *Coelosphaerium sp.* | 0 | 29 |
| *Pediastrum simplex* | 0 | 19 |

### *3.5. Spatial correlation and connectivity*

Spatial autocorrelation (Moran_I) for phytoplankton (biovolume, cell density, chlorophyll-*a* and diversity) and environmental variables (conductivity, temperature, water flow, SRP, DON, and DIN) was calculated taking the variables' mean value for each site averaged from the respective time series. The global Moran_I (Figures 5a and 6a) indicated a positive spatial autocorrelation for all environmental variables (range: 0.52 − 0.72, the lowest value corresponding to SRP, and the highest to temperature) as well as for chlorophyll-a, biovolume and cell density (range: 0.57 − 0.73), but negligible correlation for diversity (0.09).

The global Moran_I disaggregated into their local site contributions, that is the local Moran_I, showed a sharp decrease of spatial correlation roughly coincident with the dams' occurrence (EB06 and EB07), followed by a progressive recovery downstream (sites EB09 - EB12) for both variables (Figure 5b and 6b). Biovolume shifted from 0.102

to -0.002, cell density from 0.12 to 0.017 and chlorophyll-*a* from 0.085 to -0.017. The Shannon-Wiener diversity showed erratic values along the studied section.

The spatial correlation of conductivity, temperature, water flow, DIN, and DON decreased in Escatrón (EB06) close to 0, indicating lack of similarity between consecutively connected sites (EB05 and EB07). The spatial correlation of conductivity, DIN and DON decreased further in Almatret (EB07) followed by a recovery downstream (Figure 5b). SRP presented a smooth positive spatial correlation (0.02-0.04) along the upstream sites (EB01 to EB06), and reached a minimum at Almatret (EB07), followed by an increase up to 0.14 from Flix (EB08) to Benifallet (EB11). Sites EB01 and EB12 are considered end nodes (i.e., without external connections) implying that their measured values provide boundary conditions. These results on spatial correlations slightly decreased with respect to their immediate internal neighbors. This situation was observed, for instance, in Xerta (EB12) with respect to Benifallet (EB11) for all the aforementioned environmental variables.

The distance threshold (based on the correlation lengths) at which a site has no influence on the next site downstream was calculated in topological units (TU). Even though monitoring sites are not evenly distributed along the river, one might consider the mean distance between sampling sites (30.5 km) to be roughly equivalent to a topologic distance of 1. Hence, the correlation lengths can be readily transformed into real distances (km) after multiplying by this factor. Correlation lengths of phytoplankton and environmental variables were lower (2.0 - 4.3 TU) when the whole river section was considered than when river sections were considered separately (2.8 – 16.5 TU, Upstream; 2.4 – 17.2 TU, Downstream), with the only exception of SRP (Table 3, Figure S3 and S4). The distances of environmental variables were within the range 3.4 – 17.2 TU, slightly higher than those of phytoplankton variables, 2.0 – 13.4 TU.

The correlations lengths of environmental variables (except SRP) were about four topologic units (120 km) in the whole river. The correlation length of the two sections (upstream and downstream) showed high values for all variables, being DIN (13.5 – 17.2 TU) the highest, and SRP (3.1 – 3.6 TU) the lowest. Conductivity, temperature, and DON presented higher values in the upstream section while water flow, SRP and DIN were higher in the downstream segment (Table 3a and Figure S1).

**Table PI 3**. Estimation of correlation length (L) expressed in topological units (TU) for (**a**) environmental variables and (**b**) phytoplankton variables, considering the whole river and the upstream and downstream sections

**(a)**

| | All sites | Upstream | Downstream |
|---|---|---|---|
| Conductivity | 3.7 | 16.5 | 5.6 |
| Temperature | 3.9 | 15.8 | 6.9 |
| Water flow | 4.3 | 6.3 | 9.2 |
| SRP | 3.4 | 3.1 | 3.6 |
| DIN | 3.7 | 13.5 | 17.2 |
| DON | 4.0 | 7.6 | 5.0 |

**(b)**

| | All sites | Upstream | Downstream |
|---|---|---|---|
| Biovolume | 3.3 | 3.6 | 3.7 |
| Cell density | 2.8 | 2.9 | 4.2 |
| Chlorophyll-*a* | 3.3 | 8.4 | 13.4 |
| Diversity | 2.0 | 2.8 | 2.4 |

Regarding the correlation lengths of phytoplankton variables, biovolume, cell density and chlorophyll-*a* were about three topologic units (90 km), while diversity showed a lower value (60 km) when all river sites were considered. Diversity had lower values (2.8 – 2.4 TU) and chlorophyll-*a* the highest (up to 8.3 TU) upstream, and increased up to 13.4 TU, downstream. As a matter of fact, the downstream section showed the maximum values, with the exception of diversity (Table 3b and Figure S2). In all cases, values of $r^2$ ranged from 0.75 to 0.99.

a

| | Global Moran I. |
|---|---|
| Conductivity | 0.69 |
| Temperature | 0.72 |
| Water flow | 0.60 |
| SRP | 0.52 |
| DIN | 0.63 |
| DON | 0.69 |

b

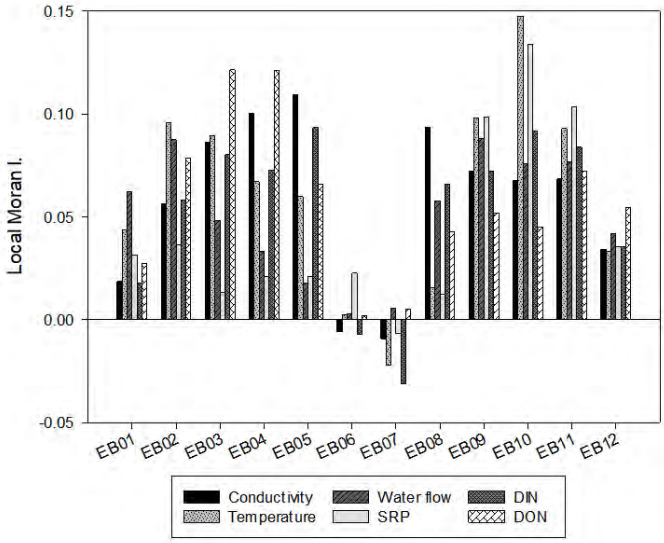


**Figure PI5**. a) Spatial correlation of environmental variables using Local Moran_I b) Global Moran Index

a

| | Global Moran I. |
|---|---|
| Biovolume | 0.57 |
| Cell density | 0.73 |
| Chlorophyll-a | 0.71 |
| Diversity | 0.09 |

b

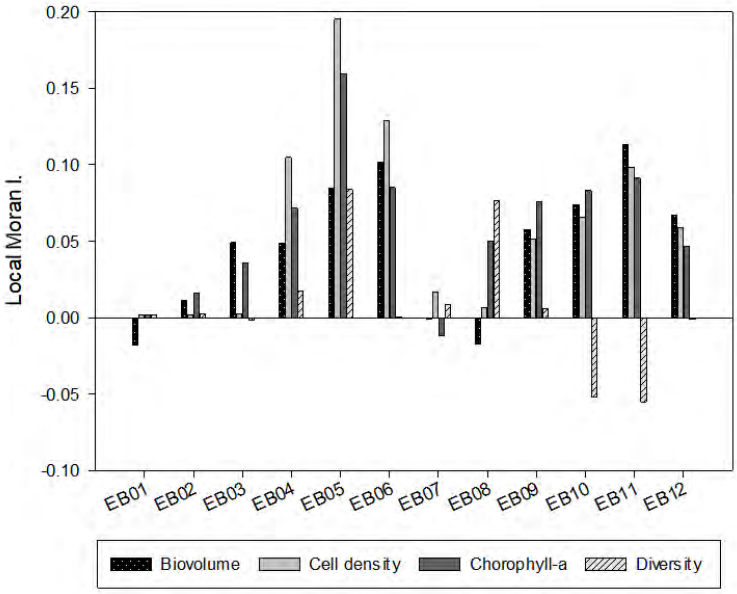


**Figure PI 6**. a) Spatial correlation of phytoplankton variables using Local Moran_I b) Global Moran Index

### *3.6. Local and neighbor contributions*

The respective contributions of neighboring vs. local factors were over 60% in environmental variables. The highest extra-local contribution was for temperature (86%) and water flow (87%), while nutrients (62-79%) and conductivity (70%) had a lower neighbor contribution (Figure 7a). The neighbour's contribution of phytoplankton variables was ca. 30 % for biovolume and diversity, 63.3% for cell density and 55.4% for chlorophyll-*a* (Figure 7b). The results indicated that phytoplankton variables had greater local contribution than environmental variables.

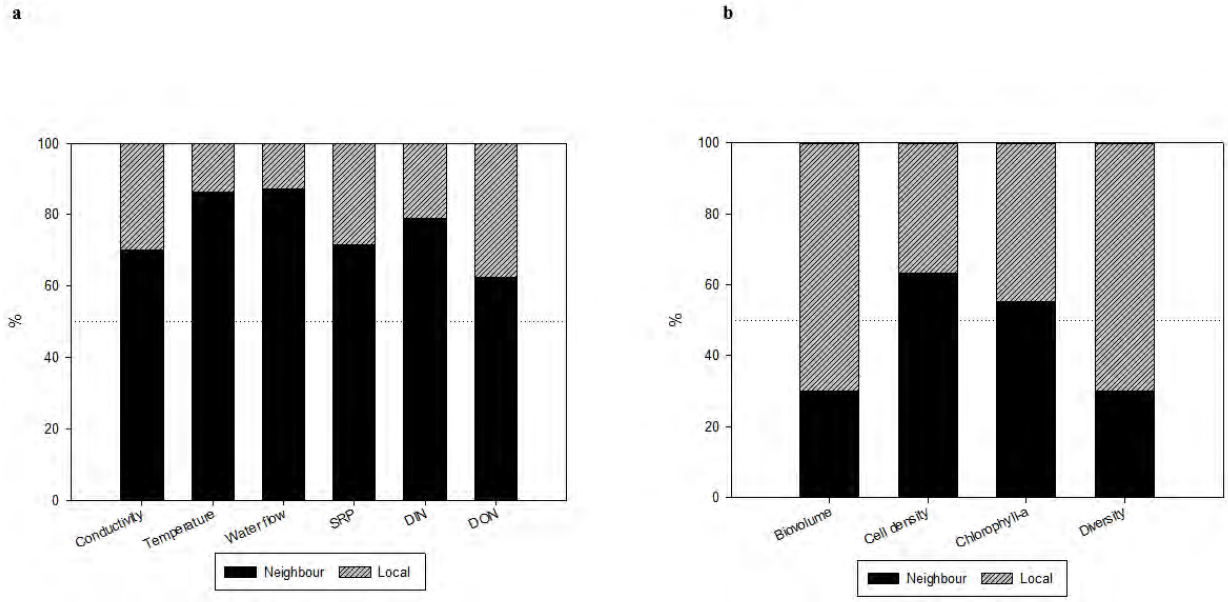


**Figure PI 7**. Local and neighbor contribution using equation 10 (autocorrelation parameter ρ estimated by MLE) (**a**) environmental variables (**b**) phytoplankton variables

### *3.7. Algal biomass Spatial Autoregression model*

The longitudinal distribution of algal biomass (chlorophyll-a) was analyzed using spatial multilinear regressions together with the most closely related environmental variables (nutrients, temperature, conductivity and water flow). The best model for the whole river section and for the upstream and downstream sections are summarized in Table 4. The obtained correlation coefficients ($r^2$) were good for the whole river and the upstream section (0.60 and 0.83 respectively) and poor for the downstream section (0.26), but statistically significant in the three cases. The F-value was high for the upstream section (173.34), which gave extra confidence on the $r^2$ value.

**Table PI 4**. Multilinear spatial autoregression models relating the planktonic chlorophyll-a (Chl-a) to environmental factors. The number of observations/cases (n), correlation coefficient ($r^2$), data variability (F) and significance (p-value) are given. A is the adjacency matrix; the product A·Chl-a captures the neighbor effect (equation 10); SRP, Soluble Reactive Phosphorus; Cond, conductivity; DON, Dissolved Organic Nitrogen; WF, Water Flow

| Relationships | n | *r2* | *F-value* | *p-value* |
|---|---|---|---|---|
| *The whole river* | | | | |
| Chl-a= -2.47 + 0.64 A·Chl-a + 0.01 Cond - 0.09 SRP | 228 | 0.60 | 110.18 | 7.50E-44 |
| *Upstream section* | | | | |
| Chl-a= 10.4 + 0.97 A·Chl-a - 0.01 WF - 0.10 SRP | 114 | 0.83 | 173.34 | 1.57E-41 |
| *Downstream section* | | | | |
| Chl-a= 8.41 + 0.13 A·Chl-a - 0.004 Cond - 0.001 DON | 114 | 0.26 | 13.03 | 2.42E-07 |

Chlorophyll-*a* appeared positively related with conductivity and negatively correlated with soluble reactive phosphorus (SRP) when the whole river section was considered. When only the upstream section was considered, chl-*a* appeared negatively related to SRP and water flow. Chl-*a* in the downstream stretch was negative related to conductivity and DON.

The inclusion of the neighbor effects contributed positively to all models improving the correlation between chl-*a* and environmental variables. So forth, the upstream stretch was more influenced by neighbors (coefficient 0.97) than those in the downstream section (coefficient 0.13).

## 4. Discussion

Chlorophyll-*a* and its associated biomass variables biovolume and cell density were affected by the reservoirs presence, showing a low resistance as well as a poor recovery downstream. However, diversity even increased downstream of the reservoirs; the substantial loss of biomass contrasted to the increase of species diversity, possibly a result of species replacement by means of some opportunistic algae which took advantage of the new environmental conditions imposed by the reservoirs (Petraitis et al., 1989).

Not only the phytoplankton variables were affected by the reservoirs; also the environmental variables were affected on their spatial variability, which showed a clear

separation between the sites located upstream (sites EB01 to EB06) versus those downstream (EB08 to EB12) the reservoirs. The reservoirs, therefore, fragmented the river (Dynesius and Nilsson, 1994) in both the biological and environmental compartments of the river ecosystem. The separate analysis of the different environmental variables reflected the higher contribution to variability patterns in the upstream sites, especially for conductivity and nitrogenous forms (DIN and DON) as well as a more homogenous pattern downstream. The large reservoirs in the Ebro, interrupt the exchange of nutrients between the two river sections (Friedl and Wüest, 2002; von Schiller et al., 2015), which were not so obvious in the water flow and temperature which show more homogeneous patterns in the two river sections. The conductivity and nutrient fluctuations could co-occur with the spatial distribution of the phytoplankton variables, which also showed higher variability pattern in the upstream sites. The hydraulic regulation in the downstream stretch probably was behind the decrease of this conjoint variability. Overall, there was a higher spatial variability in the upstream section, a reflection of the heterogeneous structure of the river, which potentially allowed rapid ecosystem reorganizations and interactions (Petraitis et al., 1989). However, the downstream stretch increased in local homogeneity, as said, mostly reflected in the patterns of biovolume, cell density, and chlorophyll-a, but not in the diversity pattern which was evenly distributed among the sites of the two sections.

The difference between phytoplankton variables associated with biomass (biovolume, cell density, chlorophyll-a) with respect to those describing the community structure (diversity) was also highlighted by the spatial analysis. As previously suggested, diversity remains steady because species replacement rather than the decrease in the number of species is the operating mechanism. This follows the adaptive response or autogenic changes of the phytoplankton taxa (Peterson and Stevenson, 1992) to the different environmental conditions occurring in each river section. The phytoplankton community in the Ebro is strongly affected in its composition by the reservoirs (Sabater et al., 2008; Tornes et al., 2014), in a similar way as it occurs in other systems elsewhere (Billen et al., 1994; Istvánovics et al., 2010; Picard and Lair, 2005). On the other hand, the variations in biomass are guided by local factors (i.e. nutrient availability, light, temperature) which determine the growth and success of phytoplankton assemblages (Reynolds, 2006).

The respective site's contribution (Local Moran I) to the spatial variability highlights the existence of an increasing spatial correlation upstream the dams and a decrease in between

the reservoirs. The loss in spatial correlation in the environmental and phytoplankton variables in this area can be attributed to the effects that reservoirs produce both on the immediate river upstream site (EB06, Escatrón) as well as in the site placed in between (EB07, Almatret). This pattern confirms the extent that the hydrological river fragmentation shaped the longitudinal structure of environmental conditions and phytoplankton variables.

The topological distance threshold at which a site had no influence on the next downstream was longer for environmental than for phytoplankton variables. This difference highlight the fact that most of the sensitivity of river ecosystems is constrained within the framework of the physical-chemical conditions. This accounts for the increase in connectivity which can be seen when considering separately the upstream and downstream sections emphasizing their functioning as two distinct rivers. The reason for this difference lies in the evidence that the longitudinal dynamics of environmental variables have a strong neighbor influence, stronger than the phytoplankton variables. The longitudinal dynamics of these are more complex and results of a mixture of local and neighbor influences. In particular, cell density and chlorophyll-*a* were more influenced by the contiguous river stretches (or neighbors) than diversity which was seemingly more affected by local factors because of the rapid colonization of opportunist species after the reservoirs.

The application of spatial multivariate auto-regression models to chlorophyll-*a* patterns, allowed to separate the contribution of the spatial autocorrelation term as well as the relevance of local environmental variables (nutrients, water flow, temperature, and conductivity) as independent explanatory variables. Both the overall river as well as the separated two river segments showed that neighbors' effect on the chlorophyll-*a* was positive, that is, that values in each river sites were influenced by upstream ones. However, that influence of neighbor sites decreases considerably downstream of the dams, leading to individuality. Planktonic chlorophyll-*a* correlated differently with environmental variables in upstream or downstream sections. The soluble reactive phosphorus (SRP) contributed negatively to the upstream part, meaning that this nutrient was in deficit because of the large growth of phytoplankton and the associated depletion of this nutrient. This is a common situation observed elsewhere (Smith, 1984), which might lead even to the activation of enzymatic extracellular packages to use organic

phosphorus (Artigas et al., 2012). Whereas, conductivity and dissolved inorganic nitrogen (DON) were negatively related to the phytoplankton biomass in the downstream section.

Our analysis shows that effects of dams cause river fragmentation in terms of the structure and functioning of environmental characteristics and phytoplankton community. The presence of dams caused a disruption of the spatial autocorrelation as well as a decrease in the natural connectivity. Our study highlighted a clear separation between the river segments upstream and downstream the dams which is reflected in the spatial characteristics of phytoplankton and environmental variables. Even though phytoplankton and environmental variables are tightly related, the dynamics of the two is complex and does not follow linear patterns.

**Acknowledgments**

This study has been financially supported by the EU FP7 project GLOBAQUA [Grant Agreement No. 603629], the NET-Scarce project [Redes de Excelencia CTM2015-69780-REDC] and by the Generalitat de Catalunya [Consolidated Research Groups: 2014 SGR 418−Water and Soil Quality Unit].

Supplementary information

# Paper I. Shifts of environmental and phytoplankton variables in a regulated river: A spatial-driven analysis

Laia Sabater-Liesa[a], Antoni Ginebreda[a,*], Damià Barceló[a,b]

[a] Department of Environmental Chemistry, IDAEA-CSIC, Jordi Girona 18-26, 08034 Barcelona, Spain

[b] ICRA, Carrer Emili Grahit 101, Girona 17003, Spain

**Figure PI S1.** Site contributions to variability obtained from Singular Value Decomposition right vectors (see text, equation 3)

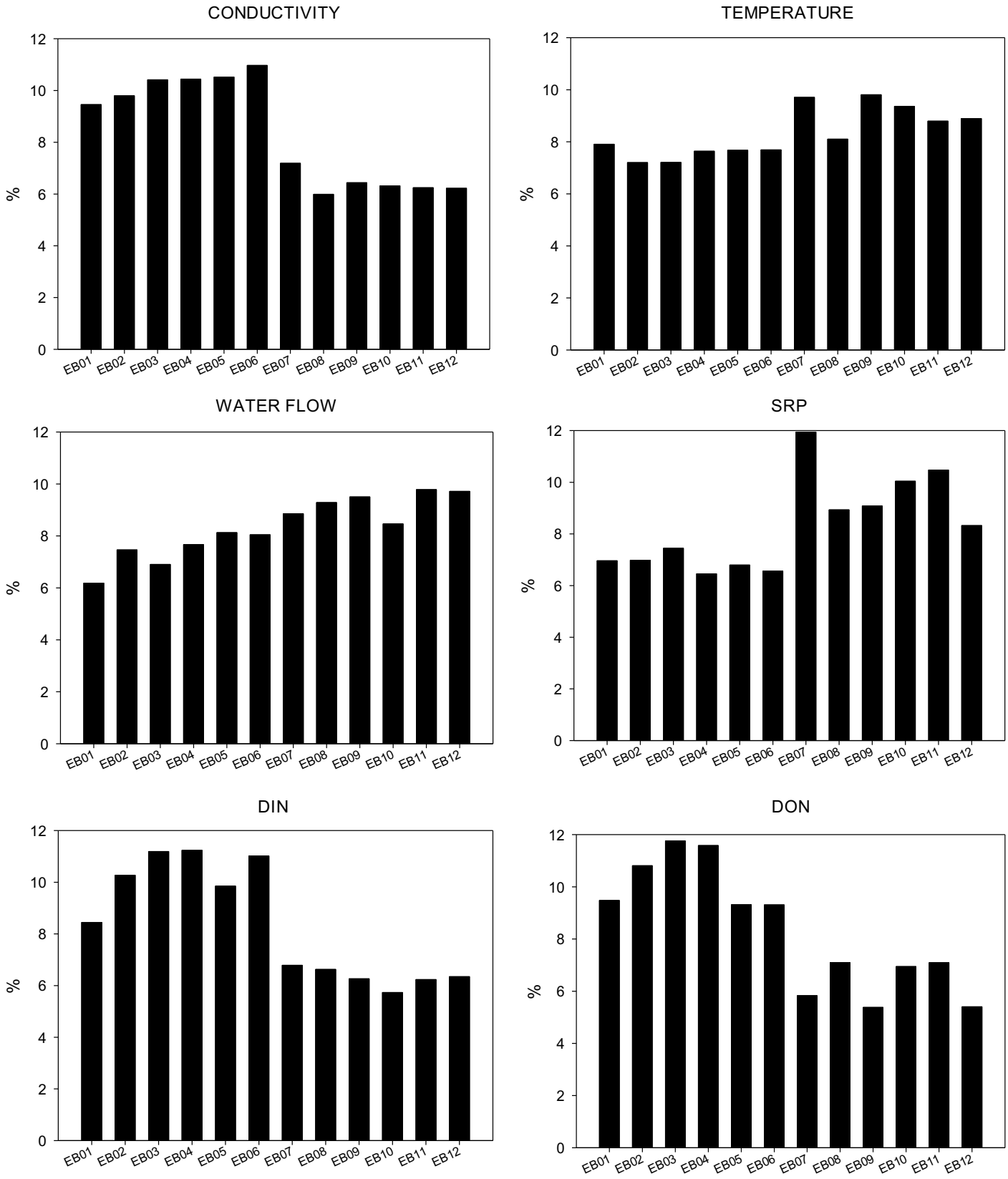

**Figure PI S2.** Site contributions to variability obtained from Singular Value Decomposition right vectors (see text, equation 3)

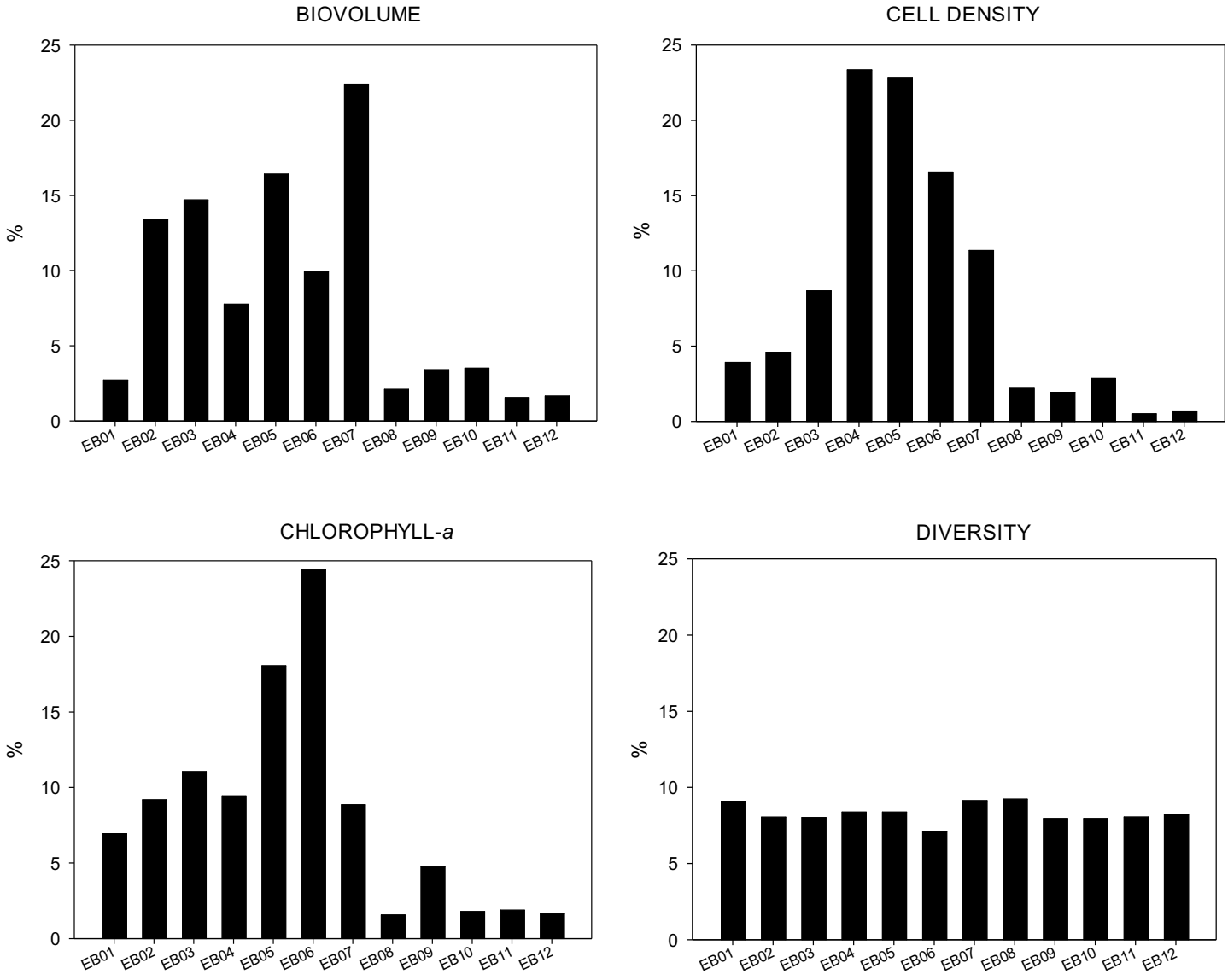

**Figure PI S3.** Estimation of correlation length (L) for environmental variables in all river sites. Distance is expressed in topological units

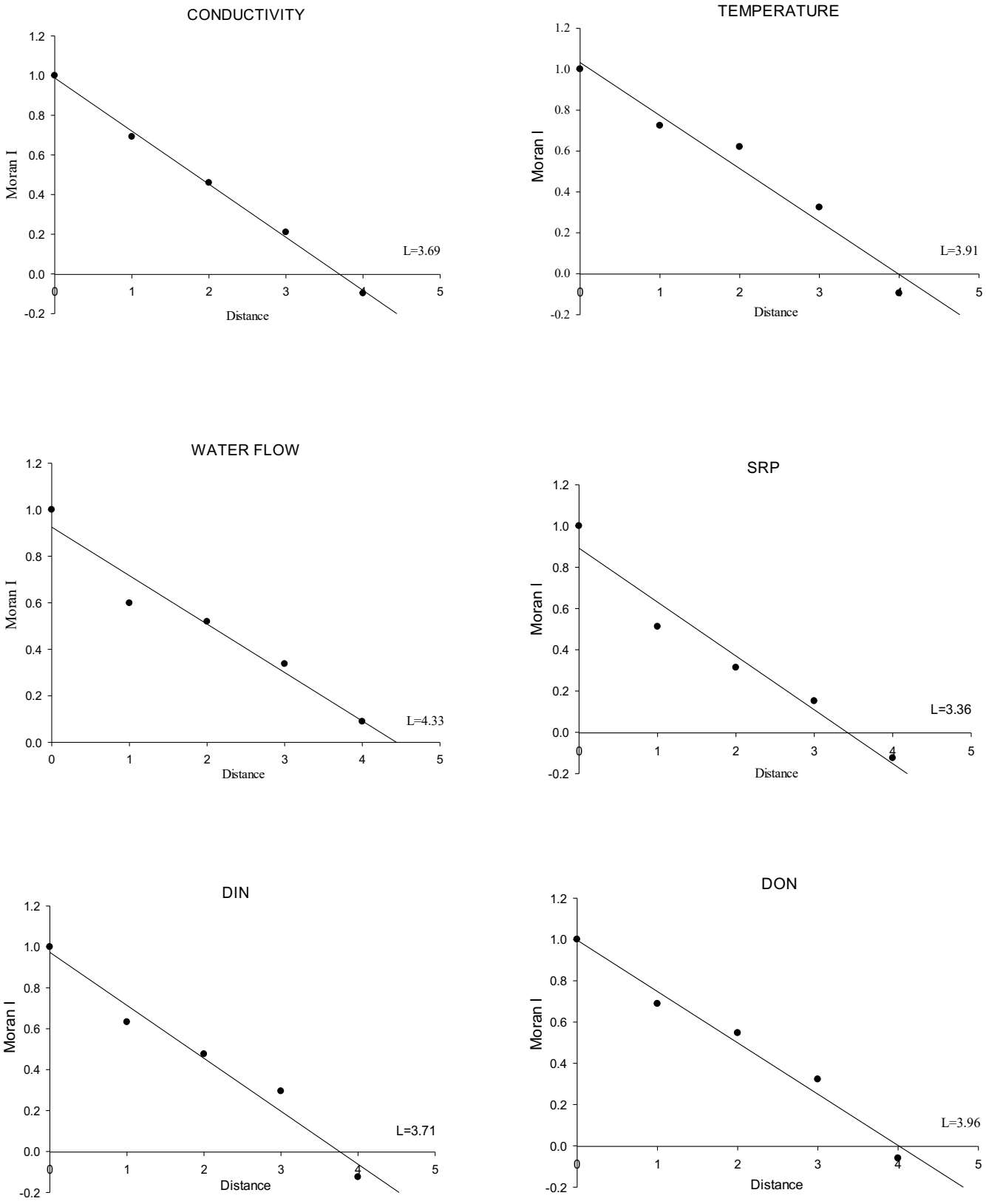

**Figure PI S4.** Estimation of correlation length (L) for phytoplankton variables in all river sites. Distance is expressed in topological units. Each variable has a different colour.

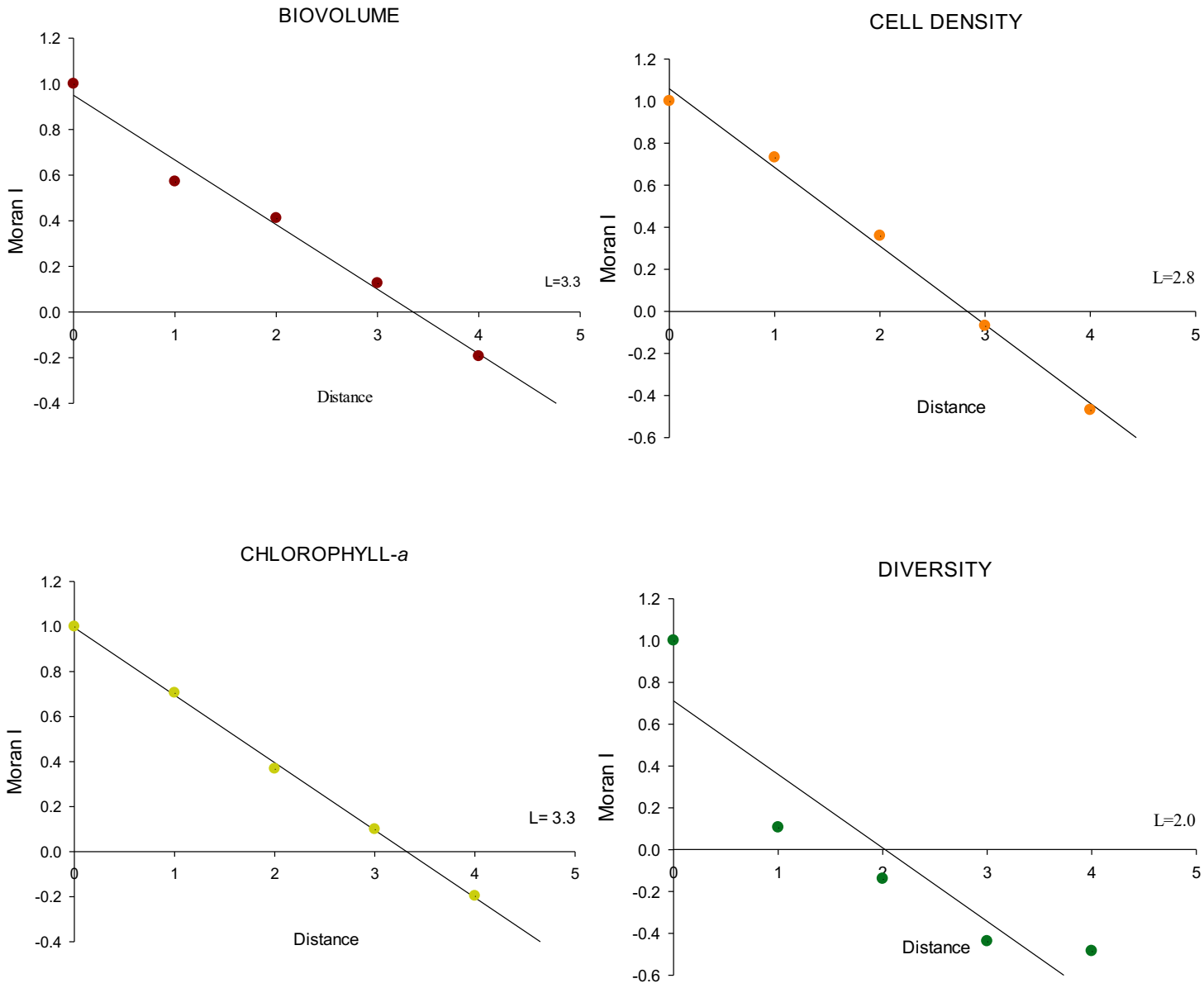

**Table PI S1**. Average (± Standard deviation) of variables measured in each sampling site (**a)** phytoplankton variables and (**b)** environmental variables

**a)**

| **Ebro Sites** | **Biovolume** (μm3/mL) | **Cell density** (cells/mL) | **Chlorophyll-*a*** (mg/m³) | **Diversity** |
|---|---|---|---|---|
| EB01 | 4.6E+05 ± 8.1E+05 | 1244.4 ± 2994.5 | 10.3 ± 12.9 | 2.9 ± 0.8 |
| B02 | 9.4E+05 ± 1.6E+05 | 1498.8 ± 2709.6 | 13.1 ± 13.7 | 2.8 ± 0.7 |
| EB03 | 1.1E+06 ± 1.6E+06 | 1680.0 ± 2337.0 | 13.8 ± 15.9 | 2.8 ± 0.9 |
| EB04 | 8.6E+05 ± 1.3E+06 | 3320.1 ± 8670.6 | 15.1 ± 16.4 | 2.8 ± 0.8 |
| EB05 | 1.2E+06 ± 2.3E+06 | 3412.6 ± 8624.9 | 19.1 ± 24.9 | 2.7 ± 1.1 |
| EB06 | 1.0E+06 ± 1.0E+06 | 3177.7 ± 6193.2 | 21.7 ± 27.7 | 2.6 ± 1.0 |
| EB07 | 1.1E+06 ± 2.7E+06 | 2304.8 ± 4942.8 | 7.5 ± 9.0 | 2.9 ± 1.1 |
| EB08 | 3.4E+05 ± 6.2E+05 | 818.8 ± 1625.3 | 3.2 ± 2.2 | 3.1 ± 0.8 |
| EB09 | 4.1E+05 ± 6.5E+05 | 723.1 ± 1526.3 | 3.6 ± 4.5 | 2.8 ± 0.7 |
| EB10 | 3.6E+05 ± 8.9E+05 | 768.4 ± 2101.3 | 2.9 ± 3.0 | 3.0 ± 0.7 |
| EB11 | 2.2E+05 ± 2.6E+05 | 284.5 ± 543.0 | 2.8 ± 3.0 | 2.7 ± 0.9 |

| | | | | |
|---|---|---|---|---|
| EB12 | 2.1E+05 ± 3.4E+05 | 332.1 ± 691.1 | 2.5 ± 2.6 | 2.9 ± 0.9 |

**b)**

| Ebro Sites | Distance between sites (km) | Conductivity (µS/cm) | Temperature (ºC) | Water flow ($m^3/s$) | SRP (µg $P\text{-}PO_4/L$) | DIN (µg N/L) | DON (µg N/L) |
|---|---|---|---|---|---|---|---|
| EB01 | 0 | 1358.3 ± 498.8 | 16.2 ± 6.5 | 215.5 ± 202.5 | 23.9 ± 18.4 | 2626.2 ± 1572.9 | 2622.5 ± 1861.5 |
| EB02 | 53.5 | 1423.5 ± 563.7 | 16.0 ± 6.2 | 265.6 ± 222.2 | 36.4 ± 23.1 | 2779.7 ± 1764.6 | 2731.1 ± 2178.0 |
| EB03 | 10.4 | 1462.5 ± 578.5 | 16.0 ± 6.3 | 258.1 ± 217.7 | 36.5 ± 28.2 | 2920.6 ± 2009.2 | 2919.6 ± 2037.2 |
| EB04 | 18.2 | 1470.1 ± 598.1 | 16.3 ± 6.8 | 267.9 ± 232.1 | 34.2 ± 24.0 | 2774.7 ± 1946.1 | 2891.9 ± 2150.5 |
| EB05 | 3.2 | 1476.1 ± 594.9 | 16.3 ± 7.1 | 274.1 ± 236.9 | 35.7 ± 23.7 | 2828.0 ± 1822.99 | 2748.3 ± 1836.3 |
| EB06 | 36.4 | 1494.7 ± 586.0 | 16.3 ± 7.0 | 273.0 ± 235.93 | 33.1 ± 22.9 | 3097.3 ± 2115.3 | 2463.6 ± 1858.2 |
| EB07 | 125 | 1015.8 ± 317.9 | 18.0 ± 6.7 | 296.2 ± 208.0 | 32.9 ± 39.2 | 1914.9 ± 1505.9 | 1891.7 ± 1087.9 |
| EB08 | 29.9 | 1054 ± 278.6 | 17.4 ± 5.6 | 319.2 ± 237.7 | 43.4 ± 33.0 | 2015.6 ± 1475.8 | 2040.5 ± 1109.0 |
| EB09 | 11.7 | 1083.5 ± 290.5 | 18.7 ± 5.8 | 325.5 ± 225.9 | 45.6 ± 36.9 | 2016.7 ± 1547.7 | 1743.2 ± 1204.9 |
| EB10 | 15.6 | 1084.6 ± 290.8 | 18.7 ± 5.5 | 315.1 ± 248.6 | 47.4 ± 37.1 | 1829.5 ± 1355.9 | 2015.3 ± 1249.0 |

| | | | | | | | |
|---|---|---|---|---|---|---|---|
| EB11 | 23.6 | 1078.4 ± 283.7 | 18.2 ± 5.7 | 319.9 ± 268.4 | 45.9 ± 38.2 | 1971.1 ± 1561.8 | 1930.7 ± 1282.7 |
| EB12 | 8.2 | 1085.1 ± 287.7 | 18.1 ± 5.7 | 320.6 ± 255.7 | 43.0 ± 32.4 | 1980.5 ± 1577.7 | 1456.5 ± 1057.4 |

# Paper II

## The response patterns of stream biofilms to urban sewage change with exposure time and dilution

Laia Sabater-Liesa, Nicola Montemurro, Carme Font, Antoni Ginebreda, Juan David González-Trujillo, Natalia Mingorance, Sandra Pérez, Damià Barceló, Science of the Total Environment; 674: 401-411

# Paper II. The response patterns of stream biofilms to urban sewage change with exposure time and dilution

Laia Sabater-Liesa[a], Nicola Montemurro[a], Carme Font[b], Antoni Ginebreda[a*], Juan David González-Trujillo[b], Natalia Mingorance[b], Sandra Pérez[a], Damià Barceló[a,b]

[a]Department of Environmental Chemistry, IDAEA-CSIC, Jordi Girona 18-26, Barcelona, Spain

[b]ICRA, Carrer Emili Grahit 101, Girona, Spain *corresponding author

## Abstract

Urban wastewater inputs are a relevant pollution source to rivers, contributing a complex mixture of nutrients, organic matter and organic microcontaminants to these systems. Depending on their composition, WWTP effluents might perform either as enhancers (subsidizers) or inhibitors (stressors) of biological activities. In this study, we evaluated in which manner biofilms were affected by treated urban WWTP effluent, and how much they recovered after exposure was terminated. We used indoor artificial streams in a replicated regression design, which were operated for a total period of 56 days. During the first 33 days, artificial streams were fed with increasing concentration of treated effluents starting with non-contaminated water and ending with undiluted effluent. During the recovery phase, the artificial streams were fed with unpolluted water. Sewage effluents contained high concentrations of personal care products, pharmaceuticals, nutrients, and dissolved organic matter. Changes in community structure, biomass, and biofilm function were most pronounced in those biofilms exposed to 58% to 100% of WWTP effluent, moving from linear to quadratic or cubic response patterns. The return to initial conditions did not allow for complete biofilm recovery, but biofilms from the former medium diluted treatments were the most benefited (enhanced response), while those from the undiluted treatments showed higher stress (inhibited response). Our results indicated that the effects caused by WWTP effluent discharge on biofilm structure and function respond to the chemical pressure only in part, and that the biofilm dynamics (changes in community composition, increase in thickness) imprint particular response pathways over time.

**Keywords**: Biofilm, mesocosm experiment, pharmaceuticals and personal care products (PPCPs), wastewater treatment plant effluent, stream, subsidy-stress

## 1. Introduction

The functioning of wastewater treatment plants (WWTPs) has improved water quality of many river systems (Carey and Migliaccio, 2009), but they are still major sources of nutrients (i.e. phosphorus, nitrogen) and dissolved organic matter to receiving rivers (Walsh et al., 2005). WWTP effluents also carry contaminants of emerging concern, such as pharmaceuticals and personal care products (PPCPs) (Gros et al., 2012). Many contaminants are not completely degraded by conventional treatment. Due to this persistence and continuous release, they reach the aquatic environment in low yet steady concentrations (Kuzmanovic et al., 2015; Luo et al., 2014; Noguera-Oviedo and Aga, 2016). The presence in receiving waters bodies of PPCPs ranges from ng L−1 to μg L−1 (Luo et al., 2014), and they affect river ecosystems particularly those with a low capacity to dilute the effluents (Martí et al., 2010). Limited dilution threatens water quality and has negative implications for biological communities (Marti et al., 2004; Sutton and al., 2011; Vorosmarty et al., 2010). Nutrients and contaminants present in sewage discharges can cause unexpected effects in river ecosystems (Aristi et al., 2016) because of either beneficial or detrimental effects. Nutrients and organic matter are assimilable compounds up to a certain threshold beyond which they may become harmful. Increasing nutrient concentrations tend to enhance or subsidize biological activity (Odum et al., 1979), but higher concentrations may become unfavorable or even toxic (Giorgi, 1995). Overall, nutrient resources may result in a subsidy-stress pattern for the biota (Wagenhoff et al., 2011). In regards to the organic contaminants, it is known that chronic exposure to a mixture of PPCPs adversely affects aquatic organisms (Corcoll et al., 2014; Huerta et al., 2016; Ricart et al., 2010; Wilson et al., 2003). Biological communities respond by shifting towards more tolerant species, and many biological functions become impaired (Lawrence et al., 2005; Meyer et al., 2005; Munn et al., 2002; Sabater et al., 2007). Overall, potential effects produced by WWTP effluent discharges extend through different compartments of river ecosystems, hence predicting the actual consequences and their legacy effects are far from being straightforward. Biofilms are the first biological compartment to show the effects of sewage effluents exposure. Epilithic biofilms are communities of heterotroph (bacteria, protozoa, fungi, meiofauna) and autotroph organisms (algae and cyanobacteria) are embedded in a matrix of hydrated extracellular polymeric substances (Sabater et al., 2016b). Biofilms participate in the river functioning through the uptake of organic and inorganic nutrients, as well as in the

transient or permanent retention of pollutants (Allan, 1995; Battin et al., 2016; Kaplan et al., 1987) as occurs, for instance, on trickle filter systems in WWTPs (Huerta et al., 2016). Biofilm structure and function are sensitive to changes in temperature, nutrient content, oxygen, water flow, and light irradiance (Romaní et al., 2013). As a result, biofilms integrate environmental changes and respond rapidly to chemical pressures, such as organic matter or nutrients in excess, or exposure to contaminants (Sabater et al., 2007). Their effects may be expressed as variations on biomass, community composition, and on functions such as photosynthesis or dissolved organic assimilation; responses may be either stimulatory (Taylor et al., 2004) or inhibitory (Biggs, 2000; Loza et al., 2014; Wagenhoff et al., 2013), depending on the type and concentration of chemicals. Chemicals can affect some structural components such as algal growth or community structure or functions like respiration or production of biofilms (Corcoll et al., 2014; Rosi-Marshall et al., 2013), but others can show higher resistance (Segner et al., 2014). Given the variety of elements within biofilms, and the chemical complexity of sewage effluents, effects on system components are expected to be diverse and even of opposite nature during the exposure but also when effluents are no longer received. Accordingly, in this study, we selected a set of structural and functional variables to monitor a wide range of biofilm responses and covering both shorter- or longer-term responses.

We performed laboratory experiments to assess in which manner biofilms were affected by different dilutions of urban wastewater effluents and to determine their ability to recover. The eight treatments ranged from pure WWTP effluent (undiluted) to unpolluted water in a regression design, using 24 artificial streams. This setup allowed to determine potential thresholds on the response of biofilms to contaminants (Navarro et al., 2000). In this study, we aimed to test three main hypotheses. The first hypothesis was that the biofilm responses to increasing effluent concentrations would not follow linear patterns, but would resemble hump-shape subsidy-stress curve, where WWTP effluent components would subsidize biofilm activities up to a certain threshold to beyond which stress would become dominant. The second one was that the exposure to effluent water would produce a faster response of the functional variables (photosynthesis, organic matter use), but a slow one at the structural variables (community composition, biomass). The third hypothesis was that biofilm intrinsic changes produced during the exposure phase (such as community composition, biomass, and thickness) would modify its recovery when initial conditions were restored.

## 2. Material and methods

### *2.1. Experimental conditions*

Experiments were performed in a series of artificial indoor streams located at the Experimental Streams Facility of the Catalan Institute for Water Research (ICRA, Girona, Spain) between January 19th and March 31st, 2017. The artificial streams consisted of 24 independent methacrylate channels (length, 200 cm; width, 10 cm; and depth, 10 cm). Water was maintained under continuous recirculation for 72 h using a water tank to feed each of the channels at a flow of 50 mL $s^{-1}$. The average water mean velocity was 0.71 cm $s^{-1}$ and the water depth over the plane bed ranged from 3 to 3.5 cm. Each artificial stream was filled with 5 L of fine sediment and 14 cobblestones, all of them extracted from an unpolluted segment of the Llémena River (Sant Esteve de Llémena, NE Spain). The Llémena (41°59'43'' N, 2°44'19'' E) is a tributary of the Ter river (NE Iberian Peninsula). The geological substratum of the stream is calcareous, and has a total length of 31.6 km and a basin area of 185 $km^2$. This Mediterranean system receives rainfall mostly fall and spring (700-900 mm per year), with very little precipitation in the summer. The water flow of the Llémena closely reflects the rainfall pattern, and thus nearly dries up during summer (average water flow in the last 75 years was 0.94 $m^3s^{-1}$). Water conductivity ranges between 430-700 $\mu Scm^{-1}$, and water pH is commonly around 7.5-8.0.

The hydraulic and physical parameters (water velocity, temperature and light cycles) in the artificial streams simulated those of the Llémena River during early spring. Daily cycles of photosynthetic active radiation (PAR) were defined as 10 h daylight (09:00-19:00) and 14 h darkness (19:00-09:00) and were simulated with LED lights (120 W; Lightech, Girona, Spain). PAR was held constant at 173.99 ± 33 $\mu E\ m^{-2}\ s^{-1}$ during the daytime and recorded every 10 min using four quantum sensors (sensor LI-192SA, LiCOR Inc, Lincoln, United States) located across the whole array of streams.

The biofilm-colonized substrata were transported to the artificial streams in less than one hour and uniformly distributed to facilitate biofilm growth from the inoculum present on the cobblestones. At the beginning of the recovery phase, newly collected cobblestones from the aforementioned river were incorporated again at the head of the channels to enable their colonization, and to avoid the lack of inoculum that would hamper the recovery. Previous characterization of the microbial community (Romero et al., 2019)

had demonstrated the high stability of the natural community on the cobblestones when transferred from the natural environment into the experimental system.

The wastewater effluents were obtained from the WWTP of Quart (Girona, Spain) which treats sewage from c. 2750 population equivalents (PE). The plant integrates a primary and a secondary treatment with an activated sludge process to treat urban sewage water before discharging into the receiving Onyar River. The effluent water was transported in 200-L plastic tanks to the laboratory and transferred to the artificial streams in less than two hours. Water from the channels was replaced twice a week with fresh WWTP effluent.

The active charcoal-filtered rainwater used for the effluent dilutions and the acclimation and recovery phases in the artificial streams had a pH similar to that of the Llémena river, because rainwater was stored in a large container where it was naturally neutralized.

We used eight treatment conditions (N=3) with contents of WWTP effluent of 100, 86, 72, 58, 43, 28, 14, and 0%. These dilutions ratios were selected to simulate the river's capacity to dilute WWTP effluent. The 24 streams were distributed in four separate arrays (six channels par section) and were randomly assigned. Biofilms were first acclimated to non-contaminated water (rainwater) for two weeks. During the following 33 days, streams received their respective treatment. Following this exposure phase, all channels were loaded again with unpolluted water for 23 days (recovery phase) (Figure 1). At the end of each week of the exposure and recovery phase, one cobblestone sample was collected and examined for changes in the structure and function of the biofilms from each artificial stream.

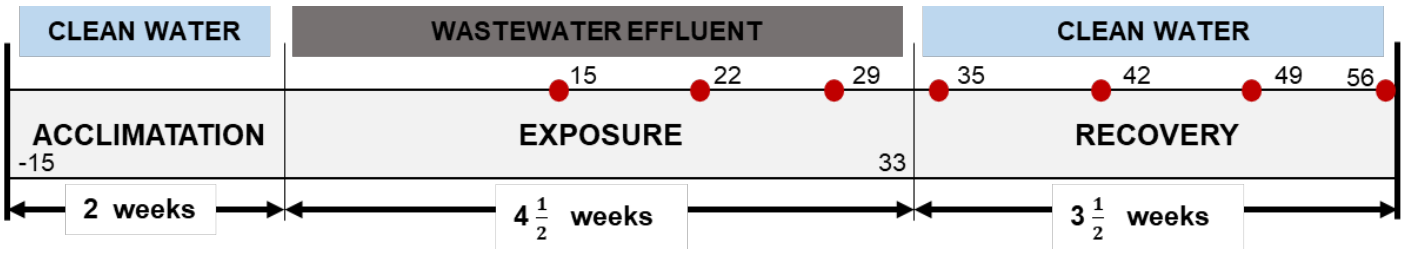


**Figure PII 1**. Experimental design and timeline. Periodic red circles indicate the biofilm sampling days.

*2.2. Water sampling, sample processing, and analysis*

Dissolved oxygen concentration and saturation level, pH, temperature, and conductivity were measured at noon in all artificial streams by twice a week using a hand-held multi-probe (WTW multiline 3310, Weilheim, Germany).

The concentration of nutrients and dissolved organic carbon (DOC) were determined 24 hours after each water renewal. Water was collected from the channel outlet and immediately filtered through 0.2 μm pore size nylon filters (Whatman, Kent, UK) into pre-washed polyethylene containers. The phosphorus ($P\text{-}PO_4^{3-}$) concentration was determined colorimetrically using a fully automated discrete analyzer Alliance Instruments Smartchem 140 (AMS, Frépillon, France). Samples for dissolved organic carbon (DOC) were analyzed using a Shimadzu DOC-V CSH coupled to a TNM module (Shimadzu Corporation, Kyoto, Japan). The nitrate ($N\text{-}NO_3^-$), nitrite ($N\text{-}NO_2^-$) and ammonium ($N\text{-}NH_4^+$) concentrations were determined on a Dionex ICS-5000 ion chromatograph (Dionex Corporation, Sunnyvale, United States).

*2.3. Pharmaceuticals and Personal Care Products (PPCPs) analysis*

The artificial streams receiving undiluted WWTP effluent were analyzed for polar compounds, specifically pharmaceuticals and personal care products, before and after each water renewal in the exposure phase, and once per week in the recovery phase. Water from the unpolluted treatment (0%) was used as a control and was sampled with less frequency. The concentrations of PPCPs for the other treatments were estimated from the measured 100% treatments after using the chloride values, a marker of dilution because of its conservative character (Davis et al., 1998; Katz et al., 2011). We simply assumed that the effluent concentration would dilute in the different treatments according to the presence of the conservative tracers, and by subtracting the presence in the 0% treatment. This was done through the analysis of chloride in all the samples, which allowed adjusting the dilution to the exact proportion for any channel and date.

Samples were kept in 750 mL PET bottles and stored at -20ºC until analysis by high pressure liquid chromatography tandem mass spectrometry (LC-MS) as described in the Supplementary Material.

*2.4. Biofilm sampling and analysis*

The response of the biofilms to the different WWTP effluent dilutions was evaluated by measuring a set of structural and functional variables. Biomass measurements included ash-free dry mass (AFDM) and chlorophyll-*a* content (Chl-*a*). The basal fluorescence (F0), is a surrogate of the chlorophyll present in the biofilm (Serôdio et al., 1997) but results cannot be extrapolated between the two because the method is limited by the biofilm thickness (Guasch et al., 2003; Schmitt-Jansen and Altenburger, 2008). The functional response of the autotrophs in the biofilm was evaluated by the photosynthetic efficiency ($Y_{eff}$), while the responses mediated by heterotrophs were estimated by the transformation of organic phosphorus (alkaline phosphatase activity, APA) and peptides (leucine-aminopeptidase activity, LAP). The identification of algal groups was performed at the end of the exposure phase (day 29), and at the end of the recovery phase (day 49).

Measurements were performed on one cobble randomly collected from each of the artificial streams, on days 15, 22, 29, 35, 42, 49, and 56. The material from the upper part of the cobblestone was scrapped off with a knife and a toothbrush was used to detach the biofilm with a surface area of about 35 $cm^2$. This sample was suspended to a final volume of 40 mL and later divided in different aliquots for the determination of AFDM, chl-*a*, enzyme activities, and algal identification.

The AFDM was determined by drying the biofilm material at 105 °C to constant weight followed by combustion at 450 °C for 4 h. Chl-*a* concentration (μg $cm^{-2}$) was quantified spectrophotometrically using a UV/VIS spectrophotometer (U-2000 Spectrophotometer; Hitachi, Tokyo, Japan) according to Jeffrey and Humphrey (1975). The basal fluorescence was determined in vivo using a Diving pulse amplitude modulated fluorimeter (Heinz Walz, Effeltrich, Germany). The F0 accounts for the chl-*a* fluorescence emission in a non-excited status (Corcoll et al., 2012b; Serôdio et al., 1997). The photosynthetic efficiency ($Y_{eff}$) reflects the algal capacity to convert photoenergy into chemical energy (Bilger and Björkman, 1990). This parameter was used to evaluate the physiological state of algae in the biofilm and its response to environmental stressors (Corcoll et al., 2012b; Schreiber et al., 2002). Photosynthetic efficiency was also determined in vivo using the Diving-PAM (Genty et al., 1989). The enzymatic activities APA and LAP were determined using substrate of 4-methylumbelliferyl (MUF) and l-leucine-4-methyl-7-coumarinylamide (Leu-AMC) (APA, LAP from Sigma Aldrich). Four millimetres of the biofilm suspension were mixed with 0.12 mL of substrate to yield a final concentration of 0.3 mM, thereby to ensure saturating condition (Romani, 2000).

Incubation was carried out in the dark conditions with continuous shaking for 1 h at 20 ºC. Two blanks of filtered artificial stream water (Whatman nylon membrane, 0.2 µm) were incubated alongside MUF and Leu-AMC blanks. After adding 4 mL of 0.05 M glycine buffer (pH 10.4), fluorescence was quantified at 365/455 nm excitation/emission by spectrofluorometry (Hitachi fluorescence spectrophotometer F-7000, Tokyo) (Sabater and Romani, 1996).

Samples for algal composition were preserved in 40% formaldehyde until analysis. The algae were characterized at the genus level by light microscopy (Nikon E200, Tokyo, Japan) with the support of specialized monographs (Wehr et al., 2015). Data were expressed as the relative abundance of algae (Diatoms, Rhodophyta and, Chlorophyta) and cyanobacteria, for each treatment.

### *2.5. Calculations and statistical methods*

#### *2.5.1. Regression models for the effluent effects on biofilm characteristics*

We used a curve-fitting approach to assess which polynomial linear regression (linear, quadratic or cubic models) best described the biofilm's response to the different WWTP effluent exposure scenarios. We explored the response of each biofilm descriptor ($Y_{eff}$, APA, LAP, F0, AFDM, and chl-*a*) at each sampling date, in order to obtain the response curves succession. A linear relationship implied that the biofilm response was proportional to the % of WWTP effluent in the streams, due to either subsidy (increase) or stress (decrease). A quadratic relationship could display either "U"-shape or "hump"-shape profiles, with the latter could imply subsidy-stress effect. In this instance, it consisted of a peak at intermediate effluent concentration but then drops at higher effluent concentration due to inhibition. The cubic pattern, in turn, has two maxima and one minimum (or one maximum and two minima); the curve goes down, back up, then back down again (or vice-versa). A cubic pattern might potentially show a subsidy or stress effect related to effluent concentration. The best model was selected based on the lowest residual standard error (RSE) and the highest coefficient of determination ($R^2$). The residuals of all adjusted models followed a normal distribution. We performed this model fitting procedure in the R software (R version 3.4.2 2017) using the function 'lm' in the stats package.

#### *2.5.2. Ordination of chemical variables*

We used principal component analyses (PCA) to explore water chemistry changes across the WWTP effluent dilution range during the exposure and recovery phases. In the ordination of the exposure phase, we included the concentrations of nitrite, nitrate, ammonium, phosphate, dissolved organic carbon, and sulfate as variables, as well as the total concentrations of pharmaceutical compounds belonging to six families (five antibiotics, two antihypertensives, one β-blocker, seven psychiatric drugs, four non-steroidal anti-inflammatory drugs and, one contrast agent) and three personal care products (complete list in Table S3). The concentrations of the PPCPs in each of the dilutions were interpolated based on the concentrations in the 0% and 100% treatments setting after normalization by the chloride content. The PCA for the recovery phase did not include the PPCPs concentrations, because no-statistically significant differences between the rainwater-fed streams were observed. All variable data were previously normalized by log-transformation. PCA computing and graphical outputs were done with SPSS statistics v.25.

### *2.6. Relationships between biofilm and chemical variables*

The relationship between epilithic biofilm metrics and water chemistry variables (nutrients, organic matter, and PPCPs) was explored by means of a Redundancy Analysis (RDA). Two separate RDAs were performed for the exposure and the recovery phases. We performed a forward selection procedure using the 'ordiR2step' function of the Vegan Package (Oksanen et al., 2019) to retain the best predictors of the variance of biofilm variables. We included the same chemical variables as in the PCA and four descriptors of the biofilm structure and functioning (chl-*a*, APA, LAP, and $Y_{eff}$). F0 and AFDM were not included because of their repetitive information as biomass estimators. Water chemistry variables were standardized by subtracting the mean and dividing by the standard deviation. Analysis and graphs were done with R software (R version 3.4.1.) using the package 'vegan' (Oksanen et al., 2019).

## 3. **Results**

### *3.1. Water characterization during the exposure and recovery phases*

Water chemistry varied according to the treatment (concentration of WWTP effluent in the channel water) and phases (exposure vs recovery). Physical and chemical differences between treatments disappeared after the input of unpolluted water to the channels.

Water temperature did not change between treatments and ranged between 19.2 ± 0.9 ºC and 22.1 ± 0.6 ºC throughout the experiments (Table 1). The pH of the water in the 0% treatment was 8.3 ± 0.3 in the exposure phase, and only slightly higher during the recovery phase (8.5 ± 0.3). Water conductivity increased with the percentage of WWTP effluent; it run from 400.4 ± 53.4 µS $cm^{-1}$ in the 14% treatment to 1368.6 ± 313.1 µS $cm^{-1}$ in the 100% treatment (Table 1). Dissolved oxygen also changed with the WWTP effluent content, decreasing from 9.1 ±0.3 mg $L^{-1}$ at the 14% to 6.9 ± 1.6 mg $L^{-1}$ in the undiluted treatment. After three weeks of exposure, treatments from 72% to undiluted effluent concentration reached anoxia during the night. Minima of dissolved oxygen were detected at 72% (3.3 mg $L^{-1}$), 86% (0.6 mg $L^{-1}$) and 100% (2.2 mg $L^{-1}$) treatments. Dissolved oxygen concentrations during the recovery phase ranged from 9.0 to 9.4 mg $L^{-1}$ in all the treatment channels (Table 1).

Inorganic nutrients ($N\text{-}NO_3^-$, $N\text{-}NO_2^-$, $N\text{-}NH_4^+$, $P\text{-}PO_4^-$) and dissolved organic carbon (DOC) concentrations increased with the proportion of WWTP effluent. Nitrate ($N\text{-}NO_3^-$) concentrations ranged from 1.2 (± 0.2) in the unpolluted treatment to 18.6 ± 5.7 mg N L-1 in the 100% treatment, and phosphate ($P\text{-}PO_4^-$) from 0.1±0.2 in the 0% treatment to 1.2 ± 0.5 mg P L-1 in the 100% treatment. DOC ranged from 1.18 ±0.1 in the unpolluted treatment to 13.42± 2.1 mg C $L^{-1}$ in the 100% treatment. During the recovery phase, all treatments showed similar nutrient concentrations (Table 1).

The chloride concentrations measured during the exposure phase ranged from 17.3 ± 7.8 in the unpolluted treatment to 198.1 ± 42.0 mg $L^{-1}$ in the 100% treatment (Table S2). Its levels increased linearly ($R^2$=0.992) with growing WWTP effluent concentration (Figure S1).

Twenty-three drugs from six therapeutic groups of pharmaceuticals and several PCPs were detected in the sewage effluent. Among the detected groups were ß-blockers, antibiotics, psychiatric drugs, non-steroidal anti-inflammatory drugs, antihypertensive and, contrast agents. The highest concentrations were of contrast agents (9792.4 ng $L^{-1}$) and antihypertensives (3214.2 ng $L^{-1}$). In particular, iopromide (9792.4 ng $L^{-1}$), valsartan (3201.6 ng $L^{-1}$), and the PCP, benzotriazole (2412.5 ng $L^{-1}$) were the most abundant ones (Table S3). No drugs were detectable in the unpolluted (0%) treatment.

**Table PII 1**. Physico-chemical water variables measured in the streams during the exposure and recovery phases. Mean values (± standard deviation) of three sampling campaigns during the exposure phase, n=9, and four samplings campaigns during the recovery phase, n=12. DOC, dissolved organic carbon; $Cl^-$, chloride; T, temperature; DO, dissolved oxygen; PPCPs, personal care products and pharmaceuticals

| Treatment | $N\text{-}NO_3^-$ (mg N $L^{-1}$) | $N\text{-}NO_2^-$ (mg N $L^{-1}$) | $N\text{-}NH_4^+$ (mg N $L^{-1}$) | $P\text{-}PO_4^-$ (mg P $L^{-1}$) | DOC (mg C $L^{-1}$) | T (ºC) | Conductivity (µS $cm^{-1}$) | DO (mg $L^{-1}$) | pH | PPCPs (ng $L^{-1}$) |
|---|---|---|---|---|---|---|---|---|---|---|
| **Exposure** | | | | | | | | | | |
| 0% | 1.21 ± 0.16 | 0.17 ± 0.32 | 0.002 ± 0.003 | 0.13 ± 0.19 | 1.18 ± 0.11 | 22.1 ± 0.64 | 226.1 ± 4.04 | 8.70 ± 0.36 | 8.35 ± 0.26 | 0.0 ± 0.0 |
| 14% | 4.33 ± 0.87 | 0.56 ± 0.35 | 1.04 ± 0.89 | 0.04 ± 0.07 | 2.94 ± 0.43 | 21.7 ± 0.19 | 400.4 ± 53.45 | 9.12 ± 0.27 | 8.42 ± 0.31 | 1666.61 ± 778.01 |
| 29% | 4.63 ± 1.23 | 2.85 ± 1.51 | 3.76 ± 2.64 | 0.09 ± 0.07 | 4.89 ± 0.65 | 20.2 ± 0.35 | 586.1 ± 105.18 | 9.13 ± 0.49 | 8.28 ± 0.26 | 3795.58 ± 1063.58 |
| 43% | 7.16 ± 3.21 | 4.20 ± 2.90 | 5.88 ± 4.99 | 0.37 ± 0.22 | 6.72 ± 0.87 | 19.7 ± 0.30 | 768.0 ± 146.28 | 8.71 ± 0.61 | 8.11 ± 0.27 | 6043.73 ± 1077.78 |
| 58% | 9.35 ± 4.22 | 7.20 ± 4.63 | 6.59 ± 5.33 | 0.62 ± 0.32 | 8.60 ± 1.36 | 20.3 ± 0.18 | 930.0 ± 192.88 | 8.21 ± 1.14 | 8.06 ± 0.38 | 8455.26 ± 2584.82 |
| 72% | 12.77 ± 5.86 | 7.05 ± 5.25 | 8.69 ± 7.70 | 0.94 ± 0.37 | 10.65 ± 1.77 | 20.5 ± 0.17 | 1106.9 ± 243.89 | 7.69 ± 1.49 | 8.07 ± 0.50 | 10465.29 ± 2014.71 |
| 86% | 14.22 ± 7.13 | 7.87 ± 6.02 | 9.33 ± 7.65 | 0.98 ± 0.49 | 11.34 ± 1.69 | 21.7 ± 0.13 | 1203.3 ± 275.52 | 7.24 ± 1.69 | 8.08 ± 0.57 | 11635.55 ± 2136.44 |
| 100% | 18.58 ± 5.71 | 5.44 ± 4.48 | 12.02 ± 10.29 | 1.21 ± 0.50 | 13.42 ± 2.07 | 22.0 ± 0.25 | 1368.6 ± 313.05 | 6.89 ± 1.62 | 8.02 ± 0.51 | 14663.08 ± 3633.01 |
| **Recovery** | | | | | | | | | | |
| 0% | 1.09 ± 0.21 | 0.005 ± 0.006 | 0.002 ± 0.003 | 0.004 ± 0.004 | 1.80 ± 0.21 | 20.9 ± 0.70 | 290.9 ± 41.79 | 8.92 ± 0.56 | 8.32 ± 0.31 | 0.0 ± 0.0 |
| 14% | 0.82 ± 0.29 | 0.002 ± 0.0004 | 0.002 ± 0.002 | 0.003 ± 0.002 | 1.94 ± 0.28 | 20.8 ± 0.69 | 283.7 ± 41.10 | 9.15 ± 0.51 | 8.43 ± 0.32 | |
| 29% | 0.77 ± 0.34 | 0.004 ± 0.004 | 0.002 ± 0.002 | 0.01 ± 0.009 | 1.80 ± 0.17 | 19.4 ± 0.89 | 290.8 ± 37.30 | 9.38 ± 0.55 | 8.47 ± 0.36 | |
| 43% | 0.91 ± 0.35 | 0.003 ± 0.001 | 0.003 ± 0.004 | 0.03 ± 0.03 | 1.94 ± 0.16 | 19.2 ± 0.94 | 302.6 ± 33.89 | 9.39 ± 0.62 | 8.48 ± 0.28 | |
| 58% | 0.95 ± 0.46 | 0.004 ± 0.002 | 0.004 ± 0.003 | 0.05 ± 0.04 | 1.95 ± 0.25 | 19.2 ± 0.98 | 302.6 ± 33.89 | 9.39 ± 0.62 | 8.48 ± 0.28 | |
| 72% | 1.16 ± 0.41 | 0.004 ± 0.001 | 0.003 ± 0.003 | 0.05 ± 0.04 | 1.93 ± 0.16 | 19.8 ± 0.88 | 314.4 ± 36.34 | 9.31 ± 0.69 | 8.51 ± 0.26 | |
| 86% | 0.98 ± 0.33 | 0.003 ± 0.002 | 0.003 ± 0.003 | 0.05 ± 0.04 | 2.10 ± 0.28 | 20.8 ± 0.60 | 312.4 ± 39.91 | 9.05 ± 0.58 | 8.51 ± 0.21 | |
| 100% | 1.16 ± 0.38 | 0.005 ± 0.003 | 0.003 ± 0.002 | 0.06 ± 0.05 | 1.93 ± 0.20 | 20.9 ± 0.73 | 316.7 ± 39.96 | 9.00 ± 0.63 | 8.49 ± 0.23 | 435.37 ± 123.48 |

In order to assess the ecological risk that the micropollutants in the WWTP effluent might pose to biofilms, pharmaceutical concentrations were transformed into toxic-units (TU) (Sprague, 1970) by dividing them by the acute toxicity values reported for algae ($EC_{50}$, 50% effective concentration) previously reported in the literature (Kuzmanovic et al., 2015; Lucas et al., 2016) (Table S4). The compounds BP1, BP4, lamotrigine, lormetazepam, oxazepam, and temazepam were not included in the risk assessment due to the lack of data. Individual TUs were subsequently aggregated under the 'concentration addition' assumption which is commonly accepted as a first tier approach for the overall risk (Backhaus and Faust, 2012). Resulting total TU of about $6\times10^{-3}$ were clearly dominated by the two macrolide antibiotics erythromycin and clarithromycin (42% and 27% of the total TU), with reported $EC_{50}$ (algae) of 46 and 20 µg $L^{-1}$ respectively, followed by the antihypertensive drug valsartan (13.5 %).

The PCA performed with the variables of the exposure phase identified all the PPCPs families accounting for the pollution in the first axis (77.5% of the total variance). This axis grouped together the conductivity, DOC, PCPs, pharmaceuticals (antibiotics, psychiatric drugs, ß-blockers, non-steroidal anti-inflammatory drugs, antihypertensive), contrast agents, and nitrate. The second PCA axis (15.6% of the total variance) identified the oxidation-reduction ranges that defined the progressive effluent contribution; dissolved oxygen concentration was located on the lower end of the axis and opposite to the ammonium concentration (Figure S2a). PCA scores ranked treatments by increasing effluent concentration, and separated well sampling days (Figure S2b and c).

The second PCA, using recovery phase data, included all chemical variables except the PPCPs. The PC1 (35.1% of the variance) had positive coefficients for conductivity and oxygen and negatively correlated with phosphate. The PC2 (25.1% of the variability) separated ammonium, organic matter, and nitrate from nitrite (Figure S3a). Overall, PCA scores showed a homogenization between treatments, and samples were mostly grouped by sampling date (Figure S3b and c).

*3.2.Effects of varying WWTP effluent content on biofilm variables*

Maximum biofilm biomass (AFDM) during the exposure phase occurred at medium diluted to undiluted treatments with the maximum growth observed for the 72% treatment ($37.4 \pm 16.5$ mg $cm^{-2}$) (Table 2). Data fitted on a linear increasing model during the first days but progressed towards a hump-shape quadratic model (Table 3 and Figure S4).

**Table PII 2**. Structural (AFDW, F0, Chl-*a*) and functional ($Y_{eff}$, APA, LAP) biofilm variables measured during the exposure and recovery phases. Mean values (± standard deviation) of three sampling campaigns during the exposure phase, n=9, and four samplings campaigns during the recovery phase, n=12. AFDM, Ash-free dry mass; F0, basal fluorescence; $Y_{eff}$, photosynthetic efficiency; APA, Alkaline phosphatase activity; LAP, Leucine-aminopeptidase activity.

| Treatment | AFDM (mg $cm^{-2}$) | F0 (relative units) | Chl-*a* (µg $cm^{-2}$) | $Y_{eff}$ (relative units) | APA (nmol MUF $cm^{-2}$ $h^{-1}$) | LAP (nmol AMC $cm^{-2}$ $h^{-1}$) |
|---|---|---|---|---|---|---|
| **Exposure** | | | | | | |
| 0% | 16.76 ± 5.70 | 622.56 ± 107.35 | 4.60 ± 2.66 | 272.70 ± 23.85 | 72.41 ± 47.16 | 148.92 ± 75.78 |
| 14% | 22.73 ± 6.72 | 1149.67 ± 94.23 | 12.23 ± 4.05 | 416.00 ± 57.45 | 34.48 ± 31.37 | 312.42 ± 121.81 |
| 29% | 22.65 ± 7.68 | 1396.17 ± 196.95 | 14.76 ± 4.16 | 450.19 ± 58.93 | 45.03 ± 35.31 | 387.35 ± 115.77 |
| 43% | 26.91 ± 10.79 | 1238.50 ± 116.08 | 18.49 ± 7.00 | 465.11 ± 50.22 | 32.88 ± 27.74 | 290.11 ± 64.77 |
| 58% | 26.54 ± 10.43 | 1196.00 ± 179.17 | 15.26 ± 4.52 | 444.26 ± 92.00 | 48.85 ± 37.63 | 342.82 ± 133.64 |
| 72% | 37.38 ± 16.53 | 1154.61 ± 103.64 | 18.75 ± 6.28 | 491.26 ± 51.90 | 40.05 ± 21.72 | 347.34 ± 146.05 |
| 86% | 26.98 ± 5.84 | 1220.50 ± 218.24 | 18.90 ± 4.11 | 421.85 ± 97.03 | 21.50 ± 21.00 | 396.43 ± 118.07 |
| 100% | 27.12 ± 2.33 | 1033.00 ± 1180.80 | 15.65 ± 10.07 | 435.74 ± 73.51 | 44.38 ± 33.19 | 398.67 ± 247.83 |
| **Recovery** | | | | | | |
| 0% | 19.18 ± 6.06 | 695.28 ± 112.71 | 3.72 ± 2.20 | 245.53 ± 47.94 | 109.46 ± 29.72 | 256.70 ± 139.28 |
| 14% | 24.51 ± 4.86 | 1268.56 ± 224.33 | 10.97 ± 4.13 | 309.75 ± 73.96 | 91.45 ± 25.53 | 405.32 ± 244.63 |
| 29% | 28.86 ± 9.72 | 1232.53 ± 201.47 | 12.61 ± 4.78 | 358.53 ± 86.18 | 62.63 ± 34.24 | 451.59 ± 249.06 |
| 43% | 32.83 ± 16.05 | 1195.58 ± 190.53 | 12.26 ± 5.90 | 365.03 ± 76.51 | 65.52 ± 47.32 | 318.91 ± 104.54 |
| 58% | 33.53 ± 11.47 | 1004.69 ± 206.33 | 10.69 ± 4.84 | 365.00 ± 47.07 | 76.40 ± 51.58 | 324.26 ± 61.52 |
| 72% | 27.52 ± 9.26 | 1024.64 ± 184.40 | 12.16 ± 5.98 | 374.78 ± 56.36 | 65.13 ± 47.17 | 376.85 ± 195.41 |
| 86% | 20.93 ± 7.68 | 926.11 ± 127.51 | 9.42 ± 5.38 | 391.56 ± 61.64 | 50.34 ± 27.23 | 323.03 ± 166.43 |
| 100% | 23.42 ± 13.64 | 942.19 ± 129.30 | 9.25 ± 6.53 | 380.83 ± 48.17 | 50.92 ± 39.02 | 359.06 ± 250.37 |

AFDM first followed a cubic model during the recovery phase, later peaked at the 58% treatment (33.5 ± 11.5 mg $cm^{-2}$) (Table 2), and finally progressed towards a quadratic model, where the hump remained below the control to reach a subsidy-stress pattern (Figure S4).

Chlorophyll-*a* content was rather constant (ca. 4 µg $cm^{-2}$) in the unpolluted treatment, and increasing WWTP effluent concentration resulted in growing chl-*a* content. Values ranged from 12.2 (± 4.0) µg $cm^{-2}$ in the treatment 14% to 18.9 (± 4.1) µg $cm^{-2}$ in the treatment 86%. At the 100% treatment the average chl-*a* concentration was lower (15.7 µg $cm^{-2}$) than the precedent treatment, but highly variable as well (SD =10.1 µg $cm^{-2}$) (Table 2). The chl-*a* data could be fitted to a quadratic model, showing inhibition at the higher effluent and not levelling off with respect to the unpolluted treatment. In the recovery phase, chl-*a* data fitted a cubic model though later fitted to a quadratic model (Figure S5).

The basal fluorescence (F0) remained unchanged in the unpolluted channels (622.6 – 695.3). Effluents caused a quadratic model (Table 3 and Figure S6), characteristic of a subsidy-stress response (Figure S6), with the F0 peaking at low and medium diluted treatments. The 100% treatment had quite lower values with respect to the other treatments, but also high variability (1033.0 ± 1180.8) (Table 2). The F0 peaked in treatments previously exposed to lower levels of contamination during the recovery phase, and data fitted to cubic to quadratic models (Figure S6).

As for the $Y_{eff}$ values, little change was observed (272.7 – 245.5) in the unpolluted channel (Table 2). The photosynthetic efficiency quickly responded to the WWTP effluents. This variable followed a quadratic model (Table 3 and Figure S7) during the exposure phase, the medium diluted treatments having the higher values (491.3 ± 51.9, 72% treatment) while the most polluted showed the lowest activity. In the recovery phase, data fitted best to an increasing linear model (Table 3 and Figure S7), having the maximum peak of activity (391.6 ± 61.6) at the 86% treatment (Table 2).

The extracellular enzyme activities APA and LAP showed different patterns of response. In the unpolluted treatment APA remained within the range of 72.4-109.5 nmol $cm^{-2}$ $h^{-1}$. Values decreased linearly at the beginning of the exposure (Table 2) but increased in the 100% treatment allowing to fit the quadratic model at the end of the exposure (day 29) (Table 3 and Figure S8). In the recovery phase APA activity incremented (e.g. 91.5 ±

25.5 nmol $cm^{-2}$ $h^{-1}$, 14% treatment), fitting first (day 35) a quadratic model, and shifting later to a linear pattern that moved to a cubic model at the end of the recovery (day 56) (Table 3 and Figure S8). Regarding LAP activity, the unpolluted treatment had the lowest values (148.9 - 256.7 nmol $cm^{-2}$ $h^{-1}$) (Table 2). LAP gradually changed from quadratic to cubic model, the activity being higher in the medium diluted and undiluted treatments. LAP achieved maximum values at the 29% treatment (451.6 ± 249.1 nmol $cm^{-2}$ $h^{-1}$) (Table 2) during the recovery phase, contributing towards a quadratic model and suggesting a subsidy-stress effect (Table 3 and Figure S9).

A total of 20 algal genera were identified, belonging to four different algal groups (Ochrophyta, diatoms; Rhodophyta, red algae; Chlorophyta, green algae), as well as to Cyanobacteria. Biofilms in the 0% treatment showed dominance of diatoms and low abundance of green algae in both phases of the experiment. By the end of the exposure (day 29), diatoms remained the most abundant in the 100% treatments whereas green algae were the most abundant in the 14% to 86% treatments, and cyanobacteria experienced a decrease from 29% treatment to the 100% treatment. Regarding the genera composition, pollution-tolerant taxa such as the diatom *Nitzschia*, the green alga *Scenedesmus* or the cyanobacteria *Aphanocapsa*, increased with higher effluent concentration, while diversity decreased. In the recovery phase (day 49), there was an increase of cyanobacteria abundance in the treatments from 14% to 72%, notably by *Aphanocapsa*, while the abundance remained low in treatments 86% and 100%. Regarding taxa proportion there was no variation between the end of the exposure phase and the recovery (Table S5).

**Table PII 3**. Best-fit selected models of biofilm variables (see Supplementary Material for Figures S4 to S9). The exposure phase includes from day 15 to 29, and the recovery phase goes from day 35 to 56. $Y_{eff}$, photosynthetic efficiency; APA, Alkaline phosphatase activity; LAP, Leucine-Aminopeptidase activity; F0, basal fluorescence; AFDM, Ash-free dry mass; Chl-*a*, chlorophyll-*a*. RSE, Residual Standard Error; $R^2$, coefficient of determination.

| | | **AFDM** | **Chl-*a*** | **F0** | **Yeff** | **APA** | **LAP** |
|---|---|---|---|---|---|---|---|
| | Best fit | LINEAR | LINEAR | N/A | QUADRATIC | LINEAR | QUADRATIC |
| | Shape | increasing | increasing | | concave | decreasing | concave |
| **Day 15** | RSE | 8.21 | 3.41 | | 56.29 | 7.16 | 68.32 |
| | $R^2$ | 0.38 | 0.70 | | 0.53 | 0.15 | 0.54 |
| | p-value | 0.11 | 0.19 | | 0.83 | 0.02 | 0.09 |
| | Best fit | N/A | QUADRATIC | QUADRATIC | QUADRATIC | LINEAR | QUADRATIC |
| | Shape | | concave | concave | concave | decreasing | concave |
| **Day 22** | RSE | | 3.13 | 212.41 | 35.57 | 19.94 | 43.45 |
| | $R^2$ | | 0.79 | 0.63 | 0.88 | 0.60 | 0.74 |
| | p-value | | 0.98 | 0.67 | 0.72 | 0.59 | 0.41 |
| | Best fit | QUADRATIC | QUADRATIC | QUADRATIC | QUADRATIC | QUADRATIC | CUBIC |
| | Shape | concave | concave | concave | concave | convex | increasing |
| **Day 29** | RSE | 3.53 | 3.98 | 115.99 | 41.06 | 22.14 | 76.74 |
| | $R^2$ | 0.76 | 0.58 | 0.72 | 0.74 | 0.37 | 0.87 |
| | p-value | 0.24 | 0.76 | 0.43 | 0.26 | 0.41 | 0.39 |
| | Best fit | CUBIC | CUBIC | CUBIC | LINEAR | QUADRATIC | CUBIC |
| | Shape | increasing | increasing | increasing | increasing | convex | increasing |
| **Day 35** | RSE | 5.89 | 2.74 | 101.20 | 42.09 | 19.58 | 97.16 |
| | $R^2$ | 0.70 | 0.82 | 0.93 | 0.30 | 0.80 | 0.66 |
| | p-value | 0.74 | 0.52 | 0.61 | 0.77 | 0.20 | 0.77 |
| | Best fit | QUADRATIC | QUADRATIC | QUADRATIC | LINEAR | LINEAR | LINEAR |
| | Shape | concave | concave | concave | increasing | decreasing | decreasing |
| **Day 42** | RSE | 1.97 | 3.75 | 207.26 | 43.58 | 12.27 | 132.75 |
| | $R^2$ | 0.90 | 0.30 | 0.28 | 0.37 | 0.64 | 0.02 |
| | p-value | 0.10 | 0.05 | 0.69 | 0.89 | 0.76 | 0.29 |
| | Best fit | QUADRATIC | QUADRATIC | QUADRATIC | LINEAR | LINEAR | QUADRATIC |
| | Shape | concave | concave | concave | increasing | decreasing | concave |
| **Day 49** | RSE | 4.34 | 2.34 | 146.77 | 18.75 | 8.96 | 34.53 |
| | $R^2$ | 0.61 | 0.70 | 0.47 | 0.86 | 0.79 | 0.49 |
| | p-value | 0.33 | 0.64 | 0.66 | 0.98 | 0.53 | 0.17 |
| | Best fit | QUADRATIC | QUADRATIC | QUADRATIC | LINEAR | CUBIC | QUADRATIC |
| | Shape | concave | concave | concave | increasing | decreasing | concave |
| **Day 56** | RSE | 6.32 | 3.17 | 178.45 | 34.57 | 21.55 | 40.47 |
| | $R^2$ | 0.54 | 0.63 | 0.23 | 0.80 | 0.75 | 0.77 |
| | p-value | 0.94 | 0.23 | 0.49 | 0.22 | 0.98 | 0.07 |

*3.3.Interaction of biofilm and chemical variables*

An RDA was performed for the exposure phase to evaluate the effects of the chemical variables on the biofilm variables. The total variation of biofilm variables accounting for the environmental variables reached 52.2% ($R_{adj}^2$=0.522). After the forward selection procedure, the parsimonious model significantly explained about 52% ($R_{adj}^2$=0.518) of the variance, and included ammonium, non-steroidal anti-inflammatory drugs (NSAIDs), and oxygen as explanatory variables. The first RDA axis defined a range of chemical contamination while the second axis synthesized the variability in oxygen concentration, which mostly affected LAP activity and $Y_{eff}$, while chl-*a* and APA seemed to be unaffected (Figure 2a).

Regarding the recovery phase, the total variance explained by a second RDA model was about 66.3% ($R_{adj}^2$=0.663). The most parsimonious model included only conductivity and phosphate concentration as explanatory variables. This model explained about 60.3% of the variance ($R_a^2$=0.601). The biofilm variables followed the same pattern as that during the exposure phase: LAP activity was the most affected by the chemical variables, while chl-*a* remained unaffected (Figure 2b).

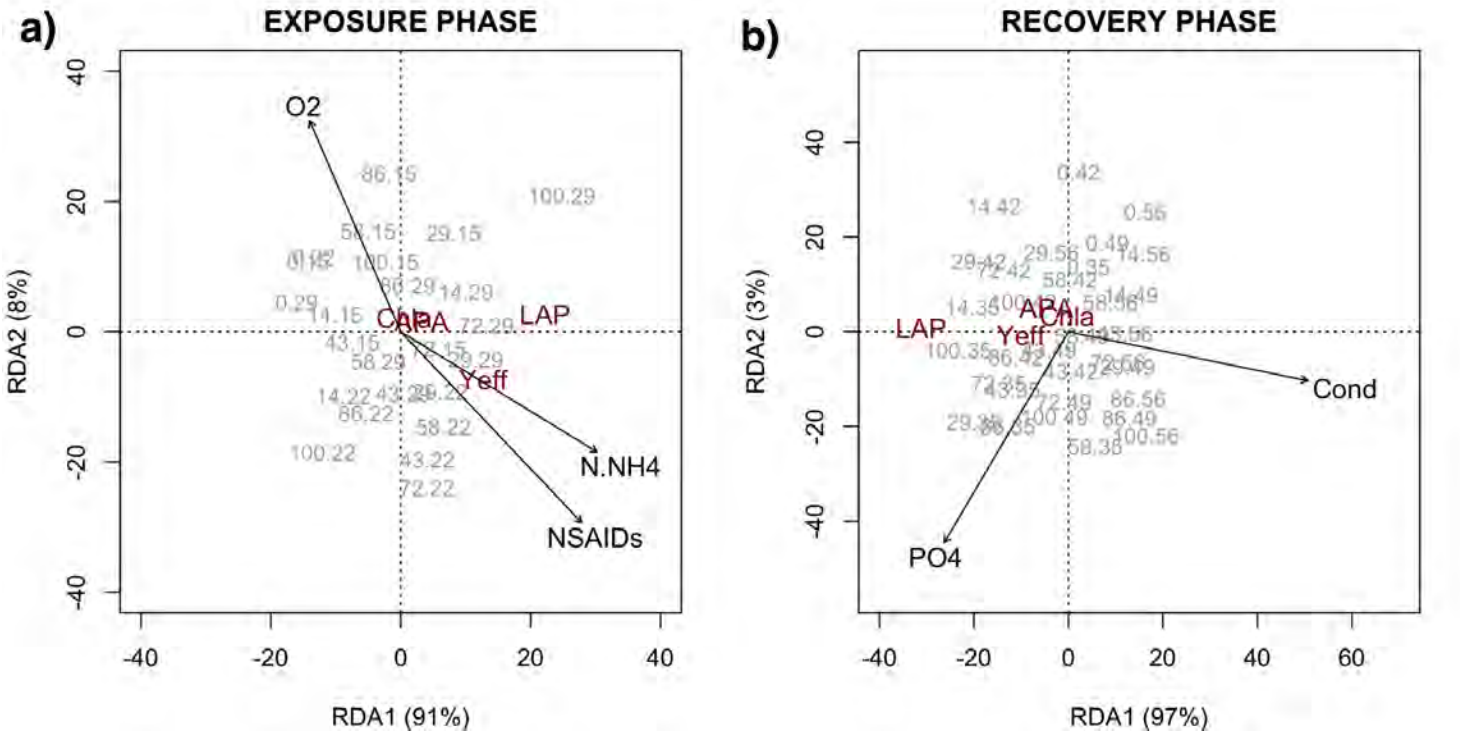


**Figure PII 2**. Redundancy Discriminant Analysis (RDA) at (a) exposure (b) recovery phases. Each RDA include biofilm metrics (Chl-a, LAP, APA and $Y_{eff}$), and physicochemical variables and organic micropollutants (black arrows). Scores (in grey) indicate treatments (first number) and samplings days (second number).

## 4. **Discussion**

Following the treatment of sewage waters in WWTPs, effluents are returned to the fluvial systems. Depending on the dilution capacity of the receiving water bodies, influenced by seasonal variation of the water flow, discharges of treated effluents may constitute a significant proportion of the water flow (Brooks et al., 2006; Drury et al., 2013). This might potentially alter the quality of the water, causing undesirable effects such as eutrophication, and might pose risk to ecosystems and downstream water uses (Brooks, 2018). The European Community Directive 91/271/EEC regulates the quality of WWTP effluent by defining maximum concentrations of organic load (BOD5, COD), suspended solids and nutrients (N, P) that could be discharged into freshwater ecosystems. These limits vary slightly with the population equivalent of the WWTP; in our study, the analytical characterization of the effluent used (Table 1) showed particularly high levels for total nitrogen (ca. 36 mg $L^{-1}$ N). On the other hand, according to the Water Framework Directive (Directive 2000/60/EC), the chemical status of the freshwater waterbodies must fulfil the environmental quality standards for the list of priority substances (Directive 2013/39) (European commision, 2013). WWTP effluents are one of the most relevant point sources of both nutrients and anthropogenic contaminants to river ecosystems (Daughton and Ternes, 1999; Marti et al., 2004; Mijangos et al., 2018; Petrovic et al., 2002). The mixture of chemical compounds occurring in sewage effluents may act either as enhancer (subsidy) or as inhibitor (stress) of biological activity. On one hand, certain concentrations of nutrients and dissolved organic carbon may stimulate the metabolism and the growth of bacteria and primary producers (Carey and Migliaccio, 2009). On the other hand, excessive amount of nutrients alongside anthropogenic contaminants which have not been completely removed during sewage treatment may have adverse effects on aquatic organisms, since these remain chronically exposed. Harmful effects of organic toxicants include diverse endpoints such as endocrine disruption (i.e. feminization of male fish) (Jobling et al., 1998), antibiotic resistances, mutagenicity, bioaccumulation, and metabolism alteration (Huerta et al., 2015; Mijangos et al., 2018). Several studies have shown that the presence of PPCPs can negatively affect river biofilms by altering the structural and functional attributes of algae and microbial communities (Corcoll et al., 2014; Proia et al., 2013). Owing to their continuous release into freshwaters they need to be regarded as pseudo-persistent organic contaminants (Daughton and Ternes, 1999).

In this study, we used a mesocosm facility as an alternative to field studies to identify causative effects on the biofilm properties of a progressive amount of effluent in the loaded water. This approach was designed to simulate the hydrological situation encountered in river systems downstream the outlet of the WWTP. The mesocosm setup combines rigorous control over all environmental conditions with realistic exposure scenarios; the proportion of effluent we used mimicked those occurring in worldwide urban rivers receiving WWTP discharges (Carey and Migliaccio, 2009; Drury et al., 2013; Ekka et al., 2006; Grizzetti et al., 2017; Rice and Westerhoff, 2017). We focused on biofilms for being the first receivers of sewage effluents because of their position at the interface between water and sediments (Sabater et al., 2007). Organisms may respond to the continuous arrival of effluents (exposure phase), which may finally cease and give way to the return of previous conditions (recovery situation).

*Biofilms responses to WWTP effluent exposure*

The effluents caused visible effects on the general biogeochemistry of the channels. As one of the apparent effects, the use of undiluted WWTP effluent resulted in a decrease in the oxygen concentration, associated with hypoxic or anoxic episodes during the night. This effluent produced clear signs of eutrophication, common in highly polluted rivers (Smith, 2003), which in our channels was evidenced by the biomass accrual and increase of chl-*a* content and basal fluorescence with increasing effluent content in the water. The respiration of the biofilm biomass, as well as the heterotrophs consumption of dissolved organic carbon, could be attributed to the reduction of the dissolved oxygen (Martí et al., 2010).

However, many of the responses observed in the biofilms did not show their maxima at the highest exposure scenario of undiluted WWTP effluent treatment. One of the hypotheses we aimed to test in this study was that biofilms exposed to sewage effluent would mostly follow a humped-back subsidy-stress pattern, where chemicals would subsidize biofilm activities up to certain threshold to subsequently cause stress. Odum et al.(1979) proposed the ‘subsidy-stress’ hypothesis indicating that depending on the concentration, a substance could either enhance (subsidize) or depress (stress) the response. The effluents contained both nutrients in excess and organic microcontaminants, with likely opposing effects. The nutrient concentrations in the channels receiving WWTP effluent from the 29 to 100% exceeded boundaries to

eutrophic systems of 700 µg $L^{-1}$ N and 60 µg $L^{-1}$ P (Dodds, 2007). The measured PPCPs concentrations of the undiluted WWTP effluent treatment also showed very high concentrations. Overall, the measured biofilm variables did not follow a general linear pattern or a hump-shaped pattern, but the patterns of response differed between variables and also changed over time.

Total PPCPs concentrations reached maximum values between 1.7 and 14.7 µg/L, within the range found in rivers receiving sewage effluents (Luo et al., 2014; Mandaric et al., 2018; Osorio et al., 2012; Verlicchi et al., 2012). The concentrations of the PPCPs in the treatment under undiluted conditions declined between water renewals, probably as the combine effect of adsorption to the artificial stream materials, partitioning into the sediments (da Silva et al., 2011), photodegradation (Boreen et al., 2004; Piram et al., 2008), and the biotic transformation (Corcoll et al., 2015). Our RDA results identified the non-steroidal anti-inflammatory drugs (NSAIDs) as one of the organic microcontaminants most significantly affecting the biofilm functional variables during the exposure phase. NSAIDs which include drugs like diclofenac and ibuprofen are commonly found in sewage impacted waters (Acuña et al., 2015a), due to their widespread use as non-prescription drugs (Reemtsma et al., 2006).

Regarding the risk assessment, TUs were calculated on the basis of short-term exposures (acute toxicities), but chronic thresholds would be more appropriate in order to estimate effects caused by the expected continuous exposure in the environment. As such data are largely not available, scaling factors have been proposed. Although, some authors suggested a ratio for acute to chronic of 5 for algae (Ahlers et al., 2006; Kuzmanovic et al., 2016; Malaj et al., 2014) a more conservative estimations applying a factor of 1000 is often used. Altogether, the TU threshold for chronic toxicity effects may be set in the range TU = 1/ 5 to 1/1000. In our mesocosm experiment, the total TU value for the channel exposed to undiluted WWTP effluent was $6\times10^{-3}$, which lies at the lower end of this range thus suggesting potential long-term ecological effects caused by the effluent exposure.

The responses of chl-*a*, basal fluorescence, and AFDM followed similar patterns. Biofilm biomass accrual responded slowly to effluent exposure. During the first two weeks, biofilm biomass increase linearly but when the exposure time growth became inhibited in the channels with high WWTP effluent concentration (quadratic pattern of response).

By contrast biomass accrual was consistently enhanced in biofilms impacted by medium levels of effluent concentration. Larger biofilm thickness may result in increased storage of organic materials within the biofilm (Dodds et al., 1999), as well as in decreased diffusion between the biofilm and the water column (Flemming et al., 2016); it is likely that these two properties confer higher resistance to change to the biofilms inhabiting the channels with higher effluent proportion. In particular, the autotrophic biomass (chlorophyll-*a*) decrease was not described by the most important explanatory variables (dissolved oxygen, NSAIDs concentration, or ammonium concentration); growth saturation after nutrient enrichment (Bushong and Bachman, 1989; Ribot et al., 2015) may be associated to this apparent lack of sensitivity.

Recently described in a companion paper, the structural response of biofilm cannot be separated from the adaptation of its community composition (Romero et al., 2019). The bacterial community structure exhibited abrupt changes when exposed at above 50% of WWTP effluent concentration. In our study, green algae grew considerably under low and medium dilution of WWTP effluent concentration, reflecting their stimulation under high nitrogen concentration (Domingues et al., 2011), while cyanobacteria decreased under high pollution stress. Overall, the highest proportion of pollution-tolerant taxa occurred under higher effluent concentrations. Diatoms (e.g. *Nitzschia*), green algae (e.g. *Scenedesmus*), and cyanobacteria (*Aphanocapsa*) responded by shifting towards these tolerant taxa, in the manner already observed elsewhere (Sabater et al., 2016b; Stevenson et al., 2010; Tornés et al., 2007; Walsh et al., 2005). It is well known that chemical exposure favors the replacement of sensitive species by tolerant ones (Corcoll et al., 2012b).

While structural changes occurred and were observed after a longer time period, functional variables displayed a fast response to effluent exposure. Photosynthetic efficiency is known to quickly respond to pollution stress (Sabater et al., 2016a; Schmitt-Jansen and Altenburger, 2008). This variable consistently followed a smooth hump-shaped pattern. Extracellular enzyme activities responded quickly to changes in nutrient availability. The APA, which is expressed or inhibited by the availability of inorganic phosphate (Chróst and Overbeck, 1990; Proia et al., 2012; Romaní et al., 2012), mostly followed a linear decreasing model, but by the end of the exposure the activity followed a consistent U-shaped model, where the channels with high concentration of wastewater effluent had the highest APA activity. We speculate that biofilm ability to take inorganic

phosphorus may be impaired due to the presence of contaminants, and as the demand for P could not be accounted from the water column, APA could get enhanced as a result of internal biofilm cycling (Bott et al., 1984; Romaní et al., 2012). LAP activity was the most sensitive biofilm variables; LAP activity on low and medium diluted treatments was enhanced, but limited at high concentration of WWTP effluent (quadratic response). After three weeks of exposure, channels fed with undiluted WWTP effluent experienced an increase in LAP activity which could be the result of higher biofilm biomass and higher biofilm complexity (Romani et al., 2004). Previous studies reported that high peptidase activity (LAP) was related to high levels of nutrient content and algal production (Montuelle and Volat, 1998).

*Biofilm responses in the recovery phase*

The replacement of initial conditions in all channels created uniformity of the physico-chemical parameters. Dissolved oxygen concentration and conductivity, however, were not completely homogeneous, indicating an incomplete recovery. This probably reflected legacy effects affecting the biofilms. In this experimental phase, structural biofilm variables mostly exhibited a hump-shaped response, while the functional variables experienced mostly linear responses. In general, the biofilms previously exposed to undiluted wastewater effluent maintained a high stress level, despite the return to non-polluted conditions.

Structural biofilm variables during the recovery phase did not present relevant differences with those from the exposure phase. In our experimental design, we avoided the lack of non-polluted organisms by adding newly colonized cobblestones to the head of all channels. Still, the algal composition did not show significant changes during the last days of the exposure phase, stressing that overall, the structural variables responded slowly to changes of water impairment. The treatments previously subjected to a medium dilution of wastewater effluent took higher distance from the unpolluted treatment and experienced the lowest recoveries.

Biofilm biomass (AFDM) during recovery followed subsidy-stress dynamics. Although chl-*a* and F0 in the undiluted treatments approached unpolluted treatment values without suffering stress, the presence of several genera confirmed the evidence that the system did not return to initial conditions. The inability of the biofilms to recover was probably

mediated by the legacy of nutrients and pollutants retained within their matrices, or cells (Battin et al., 2003; Corcoll et al., 2015; Huerta et al., 2016).

On the other hand, functional variables responded quickly once the exposure phase was terminated and showed the highest recovery rates in these channels having received WWTP effluent at high dilution. Photosynthetic efficiency exhibited the most pronounced linear recovery response. APA presented a hump-shaped response, the medium diluted treatments showing the higher biofilm biomass as well as the highest demand for phosphorus. Finally, LAP activity was one of the most impacted variable: it displayed a humped-back subsidy-stress pattern once the excess of nutrient input ended.

## 5. Conclusions

Our results indicated that WWTP effluent acted predominantly as subsidizers rather than inhibitor although this pattern changed with increasing proportion of WWTP effluent in the channels. In this case the structure and function of biofilms were compromised by reduced biofilm biomass or photosynthetic efficiency in the most contaminated treatments. Responses were complex, with non-linear patterns characterizing most treatment scenarios, while no clear pattern appeared for several variables. Besides, WWTP effluents produced long lasting and persistent effects on biofilm communities, this being evident by the incomplete recovery when the unpolluted-state conditions were restored. Our results indicate that the effects caused by WWTP effluent discharges on biofilm structure and function respond to the chemical pressure only in part, and that the proper biofilm dynamics (changes in community composition, increase in thickness) imprint particular response pathways, which change through time.

## Acknowledgments

This study has been financially supported by the EU FP7 project GLOBAQUA [Grant Agreement No. 603629] and by the Generalitat de Catalunya [Consolidated Research Groups: 2017 SGR 01404−Water and Soil Quality Unit]. NM thanks SCIEX for generously providing the loaned instrument. Authors are grateful to Vicenç Acuña, Maria Casellas, Ferran Romero and Olatz Pereda for their support and advice during the experiment, and to Peter Eichhorn for his critical reading of the manuscript.

# Supplementary information

## Paper II. The response patterns of stream biofilms to urban sewage change with exposure time and dilution

Laia Sabater-Liesa[a], Nicola Montemurro[a], Carme Font[b], Antoni Ginebreda[a*], Juan David González-Trujillo[b], Natalia Mingorance[b], Sandra Pérez[a], Damià Barceló[a,b]

[a]Department of Environmental Chemistry, IDAEA-CSIC, Jordi Girona 18-26, Barcelona, Spain

[b]ICRA, Carrer Emili Grahit 101, Girona, Spain

*corresponding author

Methods (continuation of section *2.3 Pharmaceuticals and Personal Care Products (PPCPs) analysis*)

1. *Chemicals, reagents, and solutions*

Analytical reference standards of the analyzed pharmaceuticals and personal care products (80 compounds, Table S1) were of high purity (mostly 90%) and were obtained from Sigma Aldrich (St. Luis, MO, U.S). Isotopically labeled compounds (32 compounds, Table S1) were purchased from Cerilliant, Alsachim (Illkirch-Graffenstaden, France), or Toronto Research Chemicals (Toronto, ON, Canada).

LC-MS grade acetonitrile (ACN) (≥99.9%), methanol (MeOH) (≥99.9%), ethyl acetate (EtAc) (≥99.9%) dimethyl sulfoxide (DMSO) (≥99.9%), and HPLC water were purchased from Merck (Darmstadt, Germany). Formic acid (≥96%, ACS reagent) and ammonium acetate were supplied by Sigma-Aldrich. Glass microfiber filter GF/F 0.7 µm, nylon membrane filter 0.45 µm, and PTFE syringe filters (13 mm, 0.45 µm) were purchased from Whatman (Little Chalfort, UK).

Individual stock standard solutions (concentration of 1000 µg $mL^{-1}$) were prepared in either 100% methanol, 100% DMSO, 1 N NaOH–methanol (80:20, v/v), or 100% HPLC water depending on the solubility of each compound. Working solutions mixture of analytes and/or the isotopically labeled compounds mixture (2 µg $mL^{-1}$), for analysis and calibration purposes, were prepared by diluting adequate volumes of the individual stock solutions with MeOH. All the solutions were stored at -20 °C.

2. *Sample preparation*

The extraction of the target analytes from WWTP effluent samples was adapted from Zonja (2015). Briefly, the collected samples were filtrated under vacuum conditions through a glass microfiber filter GF/F 0.7 µm and a nylon membrane filter 0.45 µm placed in series both from Whatman, (UK). Sample volume for the extraction was 500 mL. Samples were spiked with a mix of different labeled compounds at a concentration of 100 ng $L^{-1}$. The pH was adjusted to 6.8 - 7.1. Blanks were prepared with 500 mL of HPLC water and spiked with the same internal standard mixture. Solid phase extraction was performed by Oasis HLB (500mg) cartridges (Waters Corporation, Milford, MA, US). The cartridges were conditioned with 5 mL of methanol/ethyl acetate (1:1) mixture and 5 mL of Milli-Q water. After samples were passed through the cartridges, 5 mL of Milli-Q water was passed to wash them and they were dried under air flow. Then, the cartridges were eluted with 3x3mL of MeOH/EtAc (1:1) and the extracts were evaporated under a gentle stream of nitrogen at 24 ºC using a TurboVap® LV (Biotage AB, Uppsala, Sweden). Once evaporated to dryness, the extracts were re-dissolved in 1000 µL of the initial mobile phase conditions (ACN/water – 3:97) and filtered through a 0.45 µm PTFE syringe filters (Whatman, UK). The filtrate was transferred to a 2-mL vial for the analysis.

3. *Liquid Chromatography (LC) separation*

LC separation was performed using a SCIEX ExionLC™ AD system (Sciex, Redwood City, CA, U.S.) with a Acquity® UPLC BEH C18 column (100 mm x 2.1 mm i.d., 1.7 µm particle size, Waters Corporation, Milford, MA, US), maintained at 40 °C in the column oven. A fast elution of 10 min was carried out using a binary linear range composed of 5 mM ammonium acetate, 0.1% formic acid in water (A) and 0.1% formic acid in acetonitrile (B). The flow rate of 0.6 mL/min, the injection volume was 5 µL, and the auto-sampler temperature was maintained at 8 °C.

4. *MS and MS/MS conditions*

The SCIEX X500R QTOF system (Sciex, Redwood City, CA, U.S.) with Turbo V™ source and Electrospray Ionization (ESI) and operating in positive polarity was used for detection of analytes and labeled compound. Any drift in the mass accuracy of the SCIEX Q-TOF was automatically corrected and maintained throughout batch acquisition by infusion of Reserpine reference standard (C33H40N2O9, m/z 609.28066), with the TwinSprayer making use of the Calibrant Delivery System, an independent path embedded in the analytical sprayer probe. Calibration was running every 5 samples during the batch acquisition.

High resolution data were acquired using the SWATH acquisition mode workflow consisting of a single TOF-MS experiment over a m/z range from 100 to 950 Da with an accumulation time of 100 ms (AT), followed by 10 MS/MS experiments with variable Q1

windows (30 to 900 m/z, 30ms AT) and using a Collision Energy (CE) of 35V with an energy spread of ±15V. The source conditions for the system were optimized as follow. Ion Spray Voltage was set to 5500 V; source temperature and nitrogen gas flows (Atomizing gas, GS1 and Auxiliary gas, GS2) were set to 550° C and 60 psi, respectively. Curtain gas was set to 35 psi and, Declustering Potential (DP) was set to 80 V.

All data were acquired and processed using SCIEX OS software version 1.3. High confidence identification was based on unique fragment ions ant their ion ratios as well as HR-MS/MS library searching using high resolution spectral libraries supplied by SCIEX. Five main confidence criteria were used for positive identification determination, which were Mass Error, Fragment Mass Error, Retention Time Error, Isotope Ratio, and Library Score.

**Table PII S1**. List of analyzed target pharmaceuticals and personal care products.

| Therapeutic class | Compound | Isotope-labelled standard |
|---|---|---|
| Analgesics and anti-inflammatories | Acetaminophen | Acetaminophen d4 |
| | Acetylsalicylic acid | Acetaminophen d4 |
| | Codeine | Codeine d3 |
| | Diclofenac | Diclofenac d4 |
| | Ibuprofen | Iboprufen d3 |
| | Indomethacin | Indomethacin d4 |
| | Ketoprofen | Diclofenac d4 |
| | Naproxen | Naproxen d3 |
| | Meclofenamic acid | Meclofenamic acid d4 |
| | Propyphenazone | Carbamazepine d10 |
| Anti-hypertensives | Amlodipine | Carbamazepine d10 |
| | Diltiazem | Carbamazepine d10 |
| | Valsartan | Valsartan d3 |
| | Verapamil | Carbamazepine d10 |
| Anticoagulants | Warfarin | Carbamazepine d10 |
| Antimicrobial agents | Furazolidone | Venlafaxine d6 |
| | Triclocarban | Diclofenac d4 |
| Anaesthetics | Ketamine | Carbamazepine d10 |
| | Midazolam | Midazolam 13C6 |
| | Zolpidem | Carbamazepine d10 |
| Lipid regulators | Bezafibrate | Bezafibrate d4 |
| | Clofibric acid | Diclofenac d4 |
| | Fenofibrate | Fenofibrate d6 |
| | Gemfibrozil | Gemfibrozil d6 |
| Psychiatric drugs and stimulants | Bromazepam | Lorazepam d4 |
| | Carbamazepine | Carbamazepine d10 |
| | Chlorpromazine | Carbamazepine d10 |
| | Citalopram | Lorazepam d4 |
| | Diazepam | Lorazepam d4 |
| | Fluoxetine | Carbamazepine d10 |
| | Lamotrigine | Lamotrigine 13C3 |
| | Lorazepam | Lorazepam d4 |
| | Lormetazepam | Lorazepam d4 |
| | Mephedrone | Metoprolol d7 |
| | Oxazepam | Lorazepam d4 |
| | Oxcarbazepine | Carbamazepine d10 |
| | Paroxetine | Paroxetine d4 |
| | Sertaline | Sertraline d3 |
| | Temazepam | Lorazepam d4 |
| | Venlafaxine | Venlafaxine d6 |

| Therapeutic class | Compound | Isotope-labelled standard |
|---|---|---|
| Opioids and drugs of abuse | Cocaine | Cocaine d3 |
| | Methadone | Methadone d3 |
| Anti-ulcer agents | Lansoprazole | Carbamazepine d10 |
| | Omeprazole | Carbamazepine d10 |
| Histamine H1 receptor antagonists | Loratadine | Diclofenac d4 |
| Corticosteroids | Dexamethasone | Carbamazepine d10 |
| β-blockers | Atenolol | Atenolol d7 |
| | Carazolol | Venlafaxine d6 |
| | Metoprolol | Metoprolol d7 |
| | Propranolol | Metoprolol d7 |
| | Sotalol | Sotalol d6 |
| Antibiotics | Tetracycline | Carbamazepine d10 |
| | Azythromycin | Venlafaxine d6 |
| | Clarithromycin | Carbamazepine d10 |
| | Erythromycin | Erythromycin-13C d3 |
| | Sulfadiazine | Sulfadiazine d4 |
| | Sulfaguanidine | Sulfadiazine d4 |
| | Sulfamerazine | Sulfadiazine d4 |
| | Sulfamethazine | Sulfamethazine d4 |
| | Sulfathiazole | Sulfadiazine d4 |
| | Sulfamethoxazole | Sulfamethoxazole d4 |
| | Sulfamethoxine | Sulfadiazine d4 |
| | Sulfapyridine | Sulfadiazine d4 |
| | Nalidixic acid | Carbamazepine d10 |
| | Pipemidic acid | Codeine d3 |
| | Ciprofloxacin | Carbamazepine d10 |
| | Enrofloxacin | Codeine d3 |
| | Flumequine | Carbamazepine d10 |
| | Amoxicillin | Codeine d3 |
| | Cefalexin | Codeine d3 |
| | Chloramphenicol | Carbamazepine d10 |
| | Trimethoprim | Trimethoprim d3 |
| Diuretics | Furosemide | Furosemide d5 |
| Contrast agents | Iopamidol | Iopamidol d3 |
| | Iopromide | Iopromide d3 |
| | Iohexol | Iohexol d5 |
| Antiprotozoal | Metronidazole | Cocaine d3 |
| Personal Care Products | Benzotriazole | Codeine d3 |
| | Benzoresorcinol (BP1) | Oxybenzone D5 |
| | Bis(2,4-dihydroxyphenyl)methanone (BP2) | Oxybenzone D5 |

**Table PII S2**. Mean values (± standard deviation) of the chloride concentration during the exposure phase (n=9).

| **Treatment** | Concentration (mg $L^{-1}$) |
|---|---|
| 0% | 17.29 ± 7.84 |
| 14% | 41.87 ± 6.38 |
| 29% | 71.77 ± 13.63 |
| 43% | 102.59 ± 0.96 |
| 58% | 135.75 ± 34.99 |
| 72% | 163.97 ± 34.20 |
| 86% | 180.55 ± 38.61 |
| 100% | 198.13 ± 42.04 |

**Table PII S3**. Concentrations of PPCPs and total concentration by therapeutic class measured in the streams treated with 100% wastewater effluent. Mean values (± standard deviation) of 10 sampling campaigns, n= 30.

| **Therapeutic class** | **Compound** | **ng $L^{-1}$** (± SD) | **Total** (ng $L^{-1}$) |
|---|---|---|---|
| ß-Blockers | Atenolol | 984.85 ± 246.87 | **984.85** |
| Antibiotics | Azithromycin | 111.39 ± 94.14 | **417.73** |
| | Clarithromycin | 77.05 ± 29.28 | |
| | Erythromycin | 51.47 ± 66.50 | |
| | Sulfamethoxazole | 129.29 ± 91.60 | |
| | Trimethoprim | 48.52 ± 65.26 | |
| Psychiatric drugs | Carbamazepine | 63.55 ± 10.70 | **534.53** |
| | Citalopram | 18.11 ± 11.00 | |
| | Lamotrigine | 36.47 ± 19.11 | |
| | Lormetazepam | 44.26 ± 11.24 | |
| | Oxazepam | 99.47 ± 24.45 | |
| | Temazepam | 44.80 ± 12.76 | |
| | Venlafaxine | 227.88 ± 44.29 | |
| NSAIDs | Diclofenac | 606.53 ± 154.72 | **1779.90** |
| | Indomethacin | 4.85 ± 5.68 | |
| | Ketoprofen | 332.87 ± 103.28 | |
| | Naproxen | 835.66 ± 420.13 | |
| Antihyperthensives | Diltiazem | 12.63 ± 5.76 | **3214.22** |
| | Valsartan | 3201.59 ± 1120.30 | |
| Contrast agents | Iopromide | 9792.44 ± 8615.15 | **9792.44** |
| PCPs | Benzotriazole | 2412.50 ± 940.31 | **2740.32** |
| | BP1 | 62.80 ± 33.08 | |
| | BP4 | 265.02 ± 185.80 | |

**Table PII S4**. Toxicological data of studied compounds for algae. Toxic units (TU) of measured concentrations of compounds (µg $L^{-1}$) in the water phase are based on acute toxicity values ($EC_{50}$). TU = concentration compound (µg $L^{-1}$) / $EC_{50}$ algae (µg $L^{-1}$).

| Therapeutic group | Compounds | $EC_{50}$ (µg $L^{-1}$) | TU |
|---|---|---|---|
| ß-Blockers | Atenolol | 190000 [1] | 5.18E-06 |
| Antibiotics | Azithromycin | 1874 [1] | 5.94E-05 |
| | Clarithromycin | 46 [1] | 1.68E-03 |
| | Erythromycin | 20 [1] | 2.57E-03 |
| | Sulfamethoxazole | 1900 [1] | 6.80E-05 |
| | Trimethoprim | 16000 [1] | 3.03E-06 |
| Psychiatric drugs | Carbamazepine | 85000 [1] | 7.48E-07 |
| | Citalopram | 360 [1] | 5.03E-05 |
| | Lamotrigine | / | / |
| | Lormetazepam | / | / |
| | Oxazepam | / | / |
| | Temazepam | / | / |
| | Venlafaxine | 635 [1] | 3.59E-04 |
| NSAIDs | Diclofenac | 14500 [1] | 4.18E-05 |
| | Indomethacin | 18000 [1] | 2.69E-07 |
| | Ketoprofen | 164000 [1] | 2.03E-06 |
| | Naproxen | 137944 [1] | 6.06E-06 |
| Antihyperthensives | Diltiazem | 40590 [2] | 3.11E-07 |
| | Valsartan | 3865 [1] | 8.28E-04 |
| Contrast agents | Iopromide | 256000 [2] | 3.83E-05 |
| PCPs | Benzotriazole | 5904 [1] | 4.09E-04 |
| | BP1 | / | / |
| | BP4 | / | / |

[1](Kuzmanovic et al., 2015) Table S2 and ref. cit. [2] (Lucas et al., 2016) Table S1and ref. cit.

**Table PII S5**. Relative abundance of the four main algal groups at the exposure phase (day 29) and at the recovery phase (day 49).

| TREATMENT | | Diatoms | Rodophyta | Clorophyta | Cyanobacteria |
|---|---|---|---|---|---|
| 0% | Day29 | 0.61 | 0.07 | 0.13 | 0.19 |
| | Day 49 | 0.55 | 0.02 | 0.19 | 0.24 |
| 14% | Day29 | 0.11 | 0.01 | 0.69 | 0.19 |
| | Day 49 | 0.17 | 0.01 | 0.51 | 0.31 |
| 29% | Day29 | 0.11 | 0.00 | 0.86 | 0.02 |
| | Day 49 | 0.17 | 0.02 | 0.56 | 0.26 |
| 43% | Day29 | 0.18 | 0.03 | 0.70 | 0.09 |
| | Day 49 | 0.17 | 0.02 | 0.44 | 0.38 |
| 58% | Day29 | 0.26 | 0.07 | 0.56 | 0.10 |
| | Day 49 | 0.09 | 0.02 | 0.40 | 0.49 |
| 72% | Day29 | 0.19 | 0.02 | 0.73 | 0.06 |
| | Day 49 | 0.17 | 0.01 | 0.46 | 0.36 |
| 86% | Day29 | 0.31 | 0.01 | 0.62 | 0.06 |
| | Day 49 | 0.22 | 0.00 | 0.74 | 0.04 |
| 100% | Day29 | 0.55 | 0.01 | 0.37 | 0.07 |
| | Day 49 | 0.49 | 0.07 | 0.36 | 0.07 |

**Figure PII S1**. Correlation and linear regression analysis of chloride.

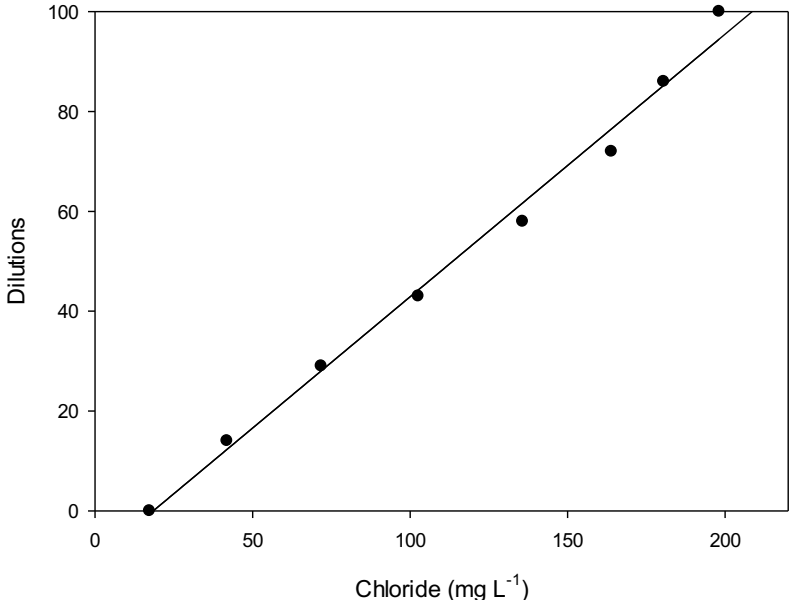

**Figure PII S2**. Principal component analysis of physico-chemical variables at exposure phase (a) PCA loadings (b) PCA scores per treatments and (c) PCA scores per sampling dates

a)

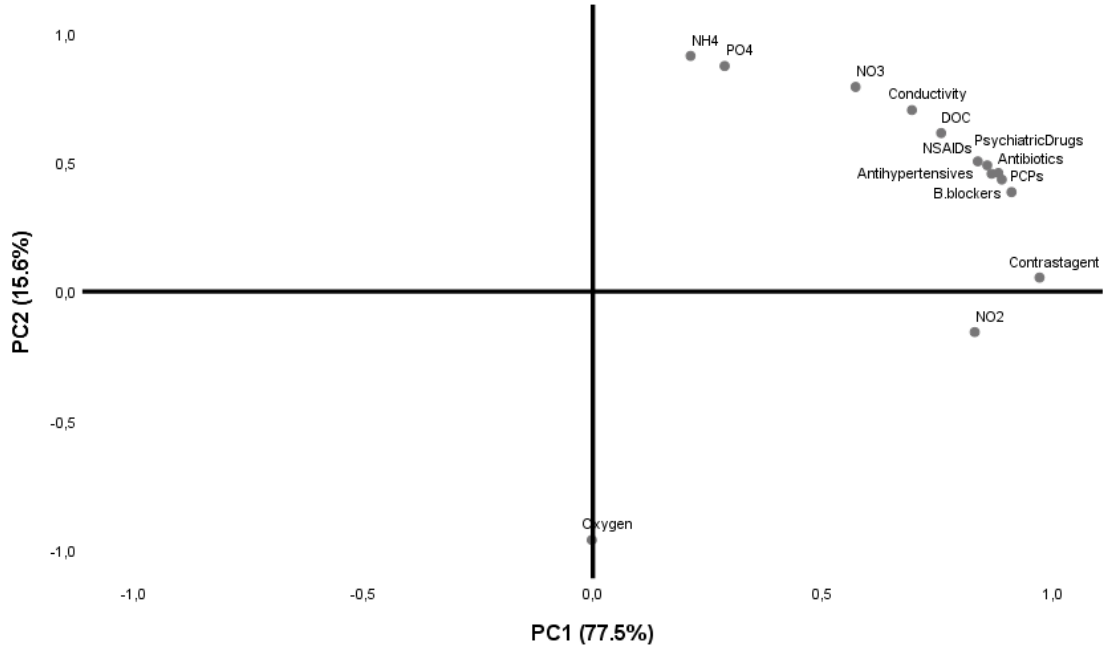


b)

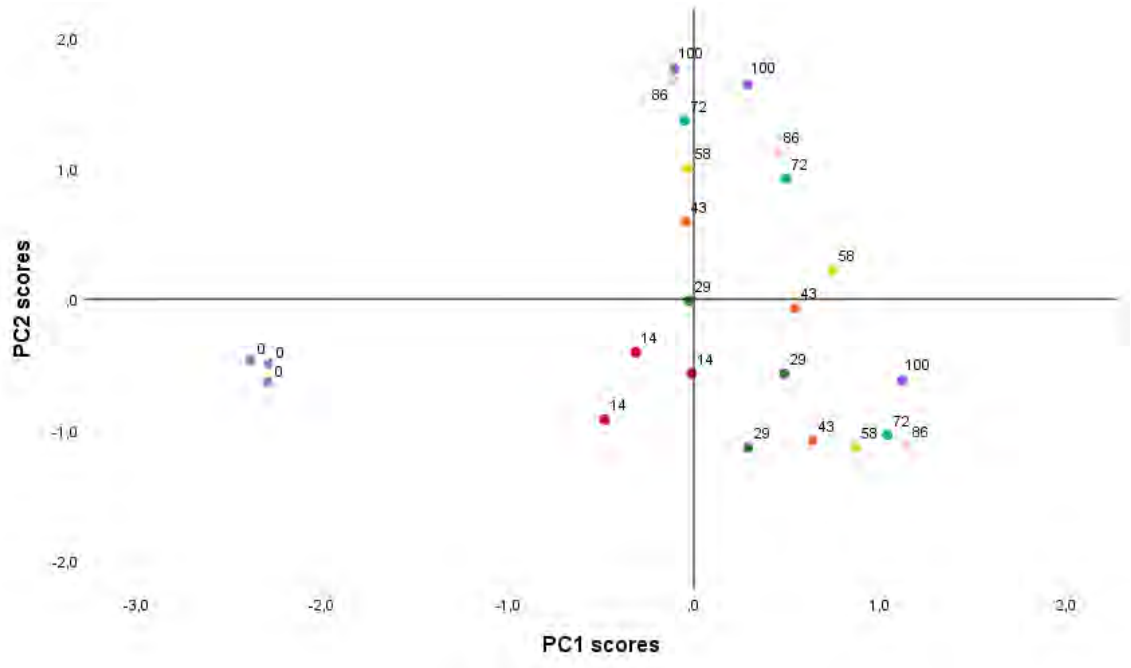


c)

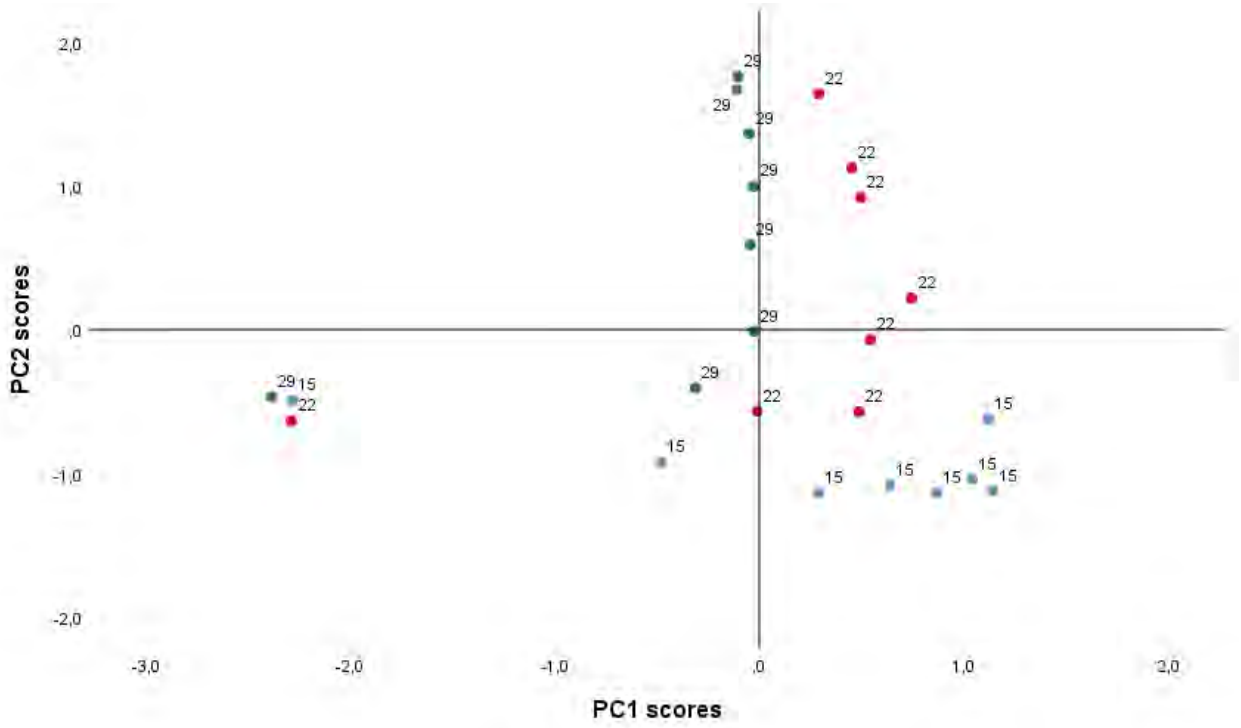
PC2 scores
PC1 scores
2,0
1,0
,0
-1,0
-2,0
-3,0
-2,0
-1,0
,0
1,0
2,0
29
22
15

**Figure PII S3**. Principal component analysis of physico-chemical variables at recovery phase (a) PCA loadings (b) PCA scores per treatments and (c) PCA scores per sampling dates

a)

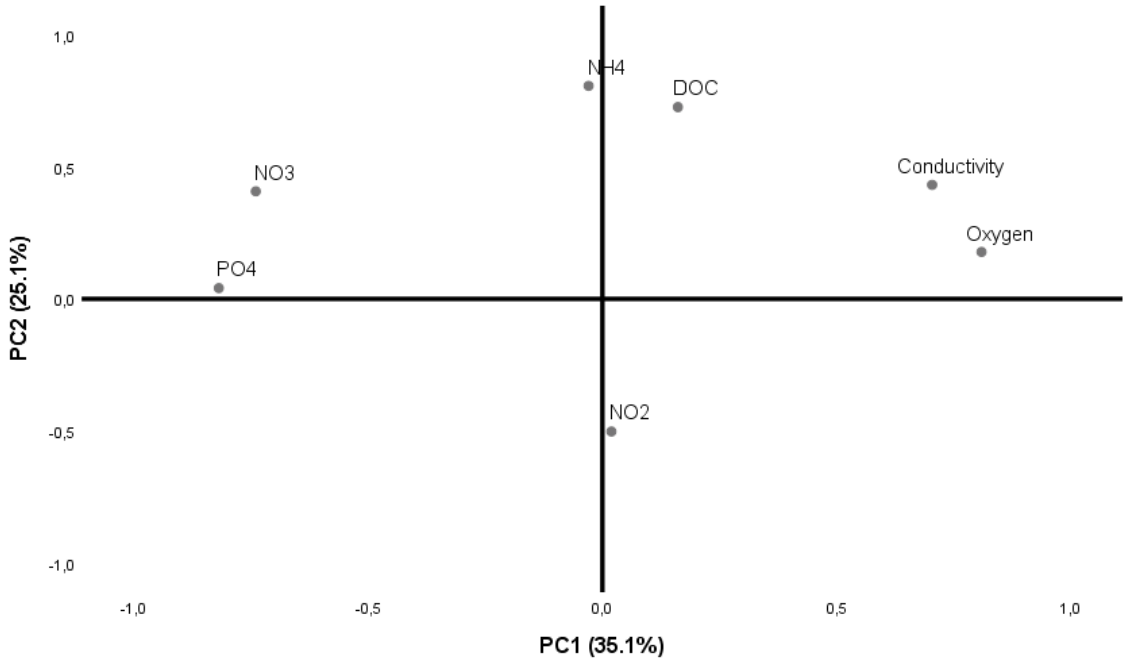


b)

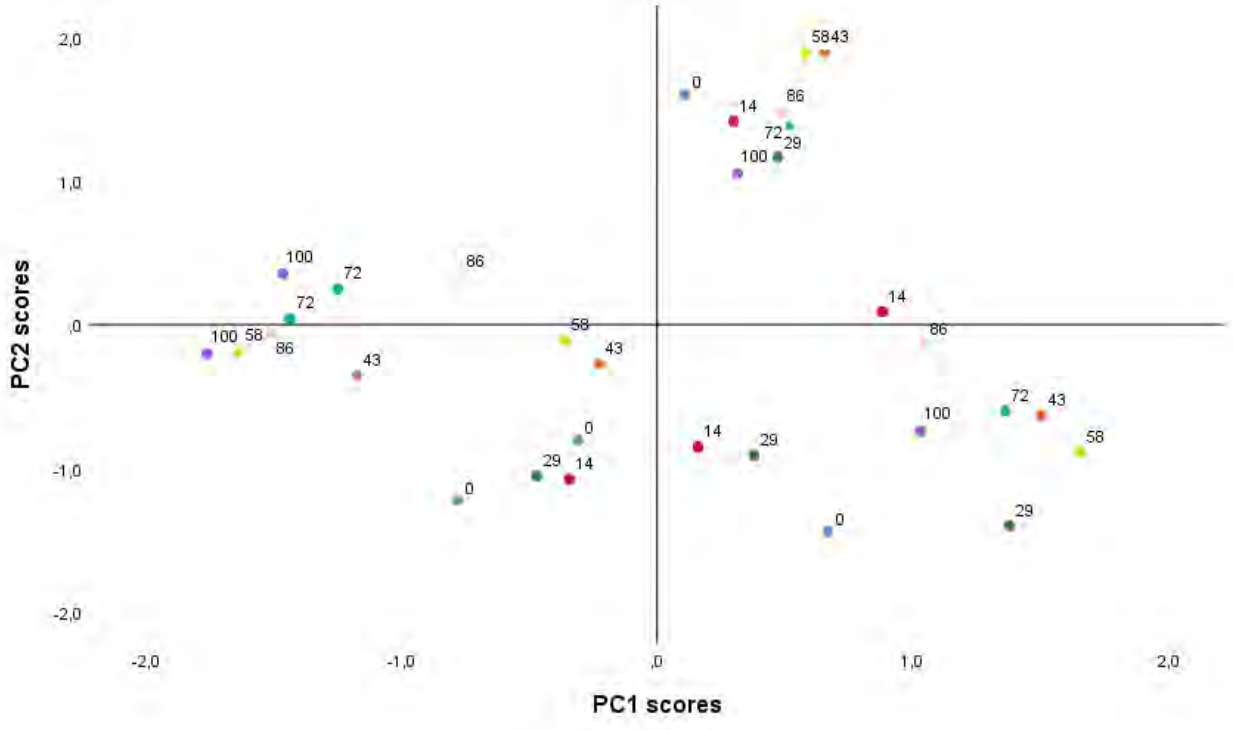

c)

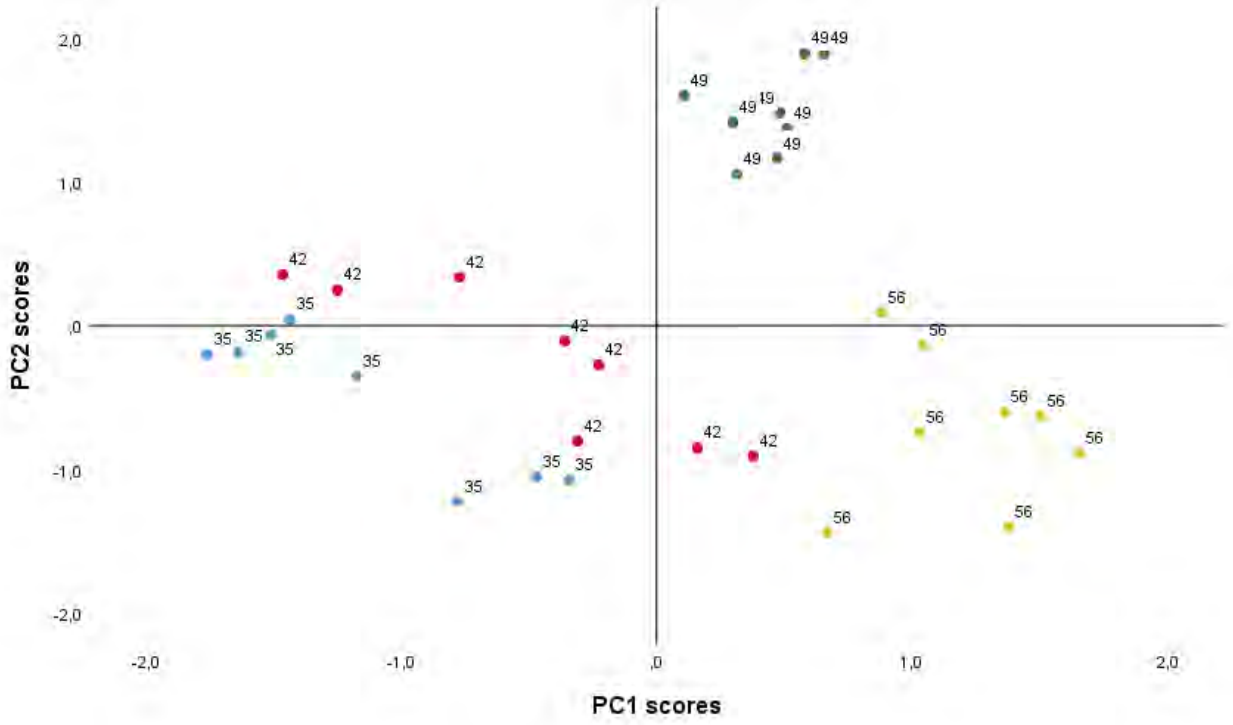

**Figure PII S4**. Models for ash-free dry mass (AFDM) at the exposure phase (days 15 and 29) and the recovery phase (days 35, 42, 49 and 56)

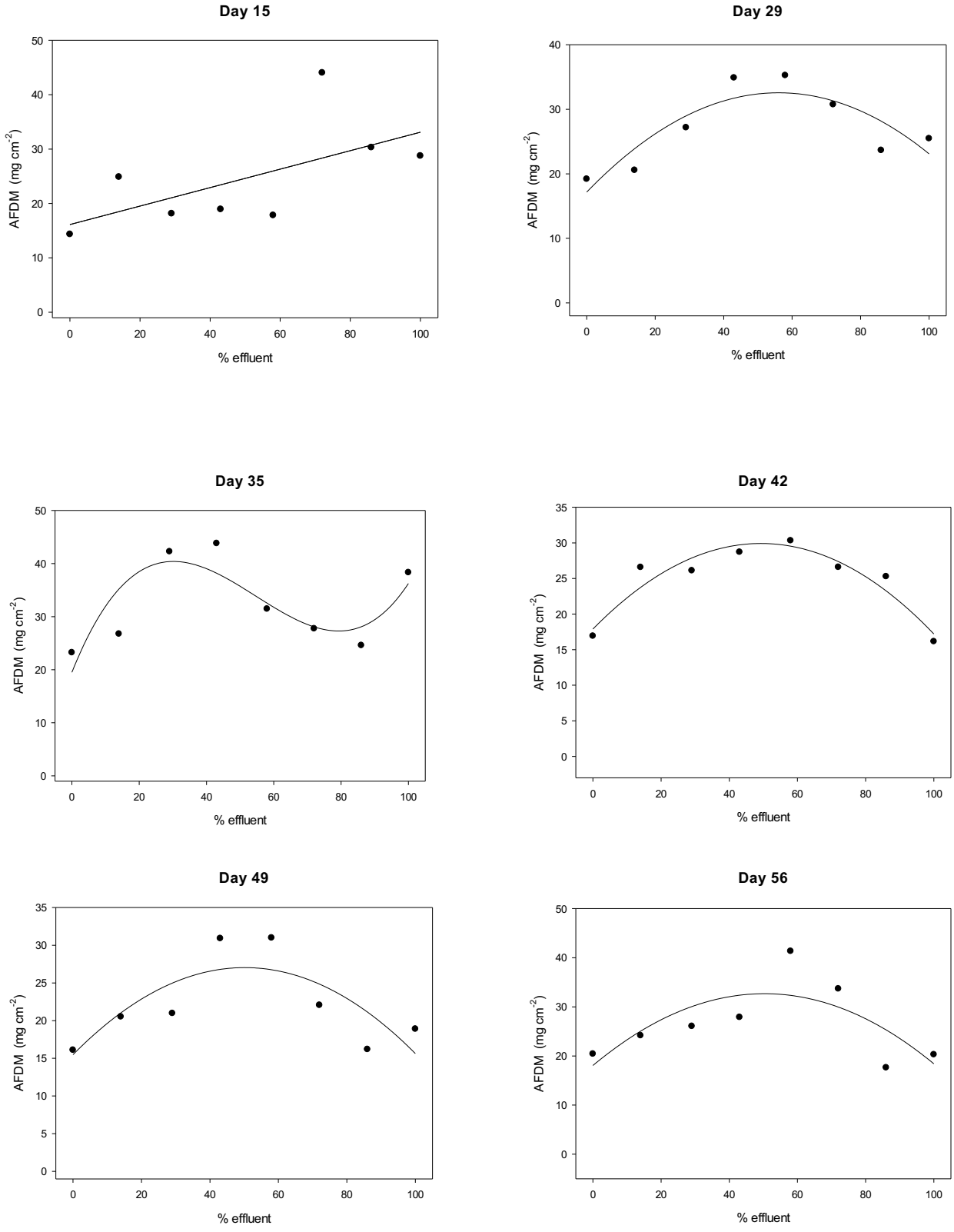

**Figure PII S5**. Models for chlorophyll-a concentration at the exposure phase (days 15, 22 and 29) and the recovery phase (days 35, 42, 49 and 56)

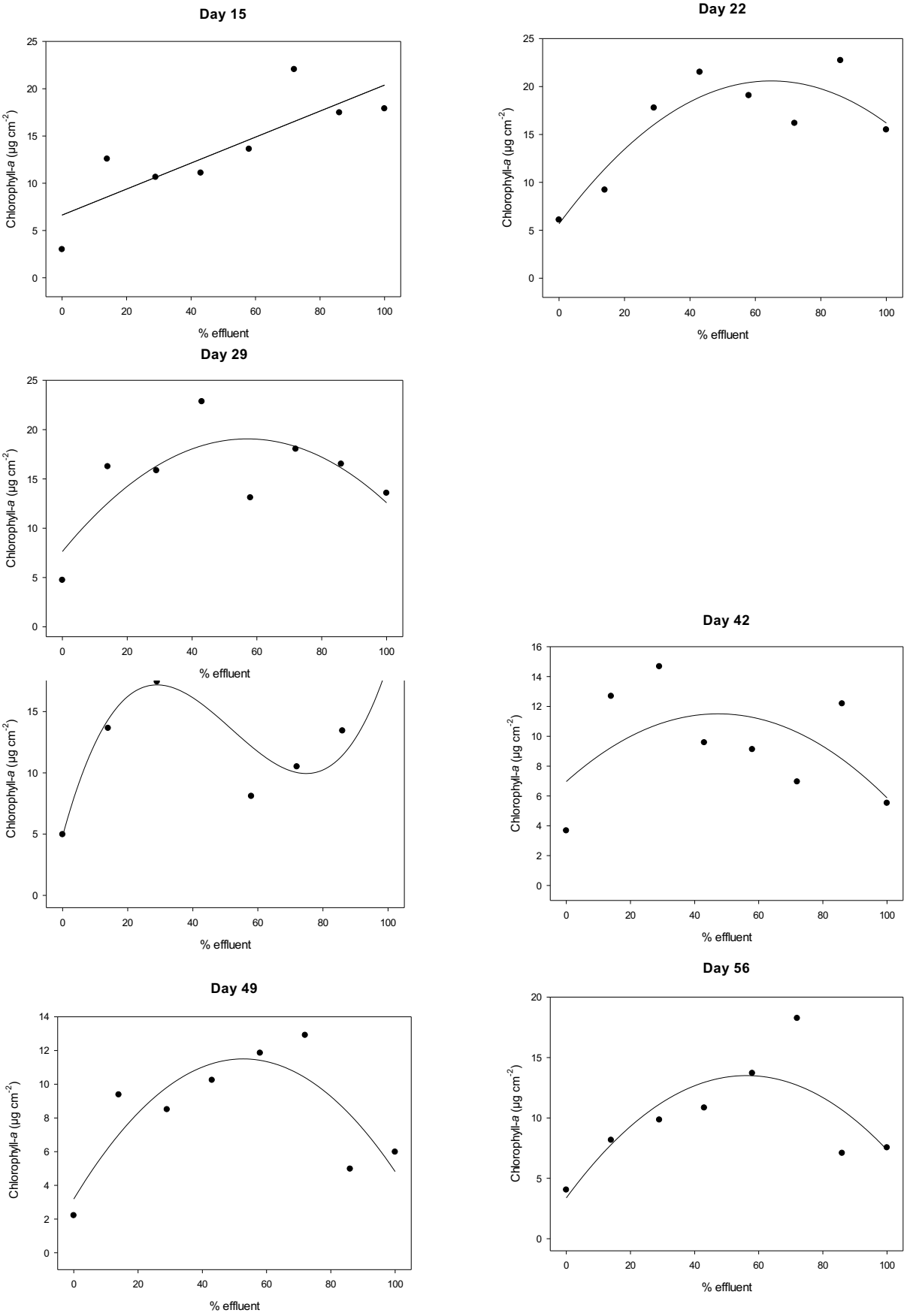

**Figure PII S6**. Models for basal fluorescence (F0) at the exposure phase (days 22 and 29) and the recovery phase (days 35, 42, 49 and 56)

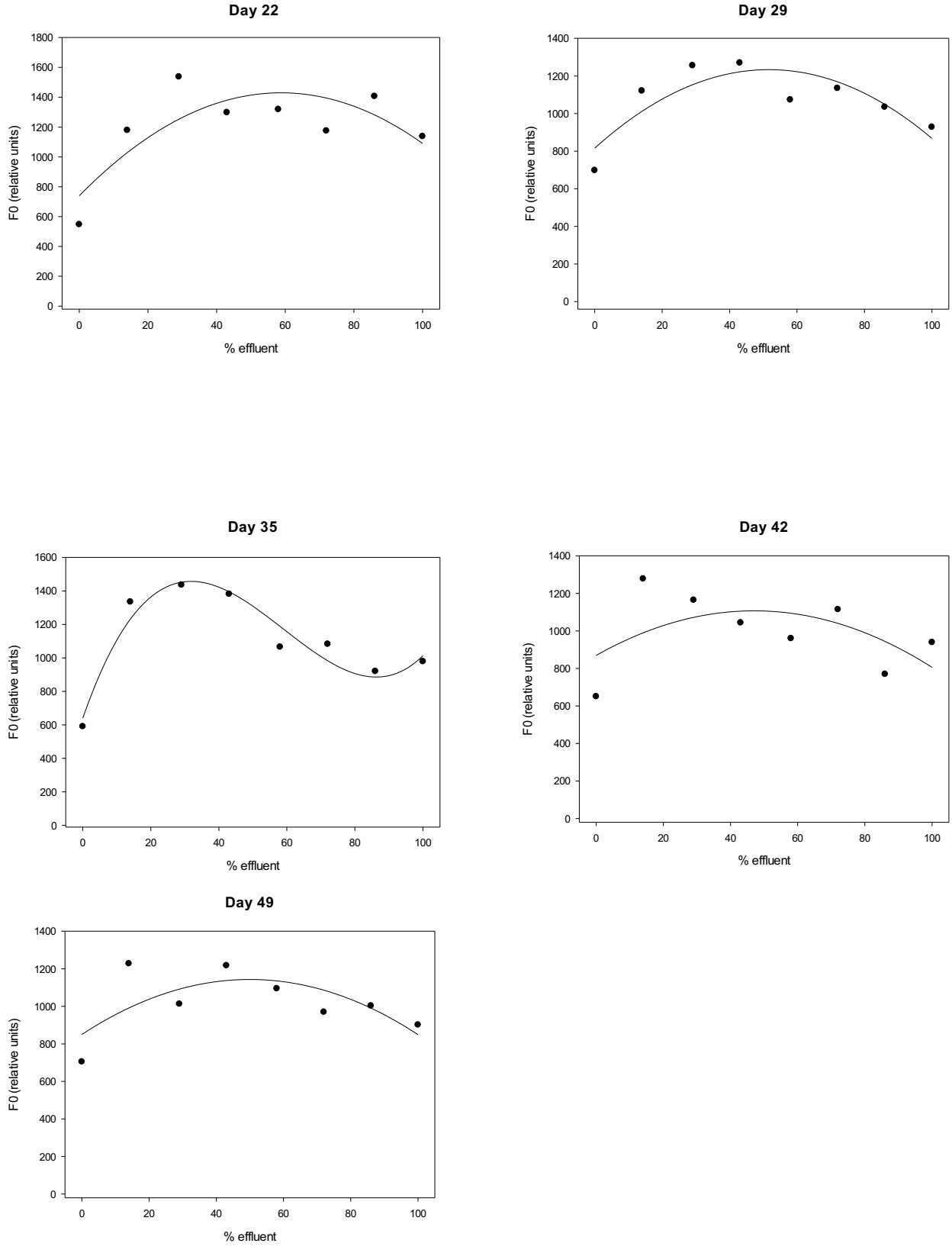

**Figure PII S7**. Models for photosynthetic efficiency ($Y_{eff}$) at the exposure phase (days 15, 22 and 29) and the recovery phase (days 35, 42, 49 and 56)

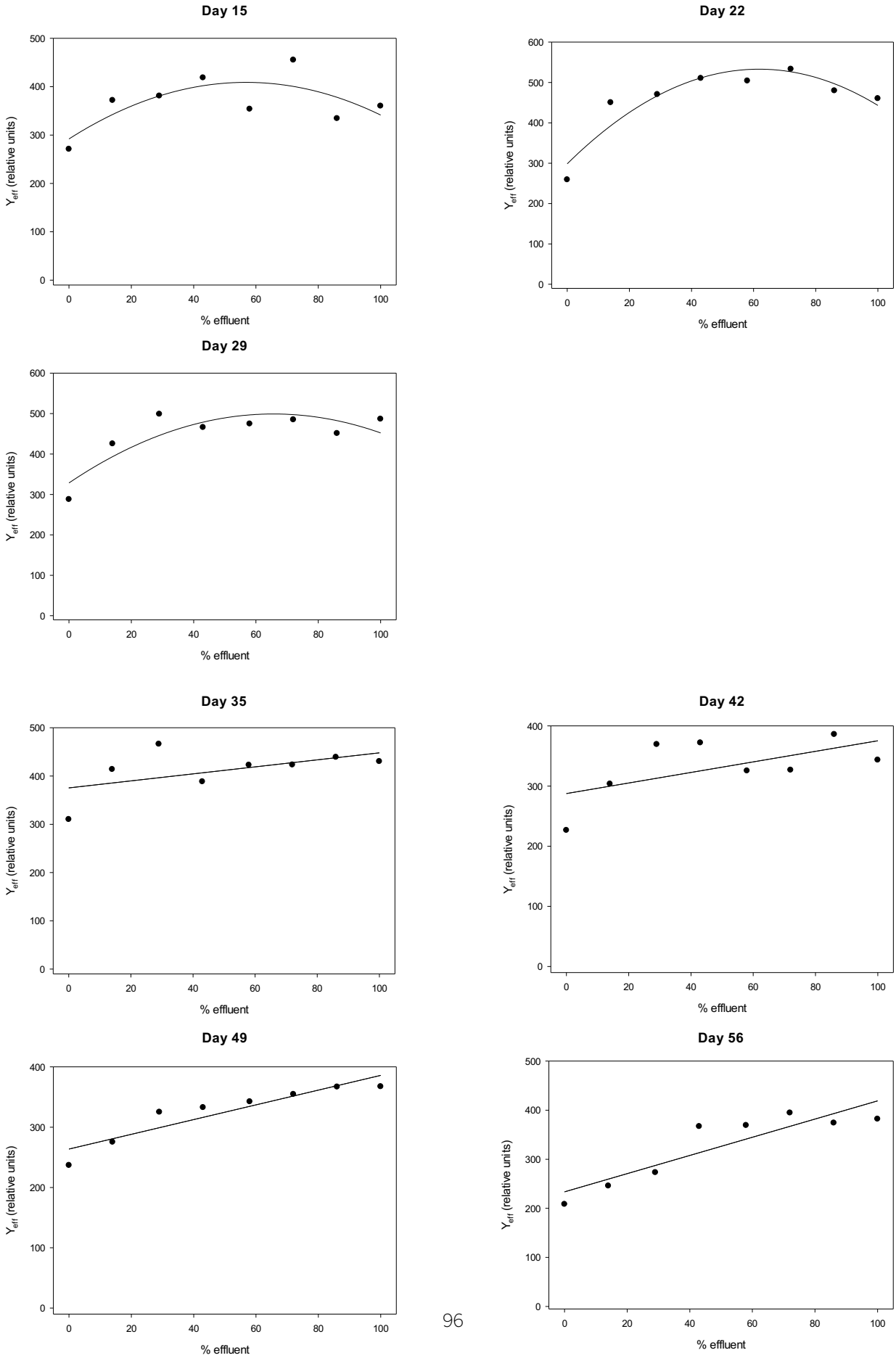

**Figure PII S8**. Models for alkaline phosphatase activity (APA) at the exposure phase (days 15 , 22 and 29) and the recovery phase (days 35, 42, 49 and 56)

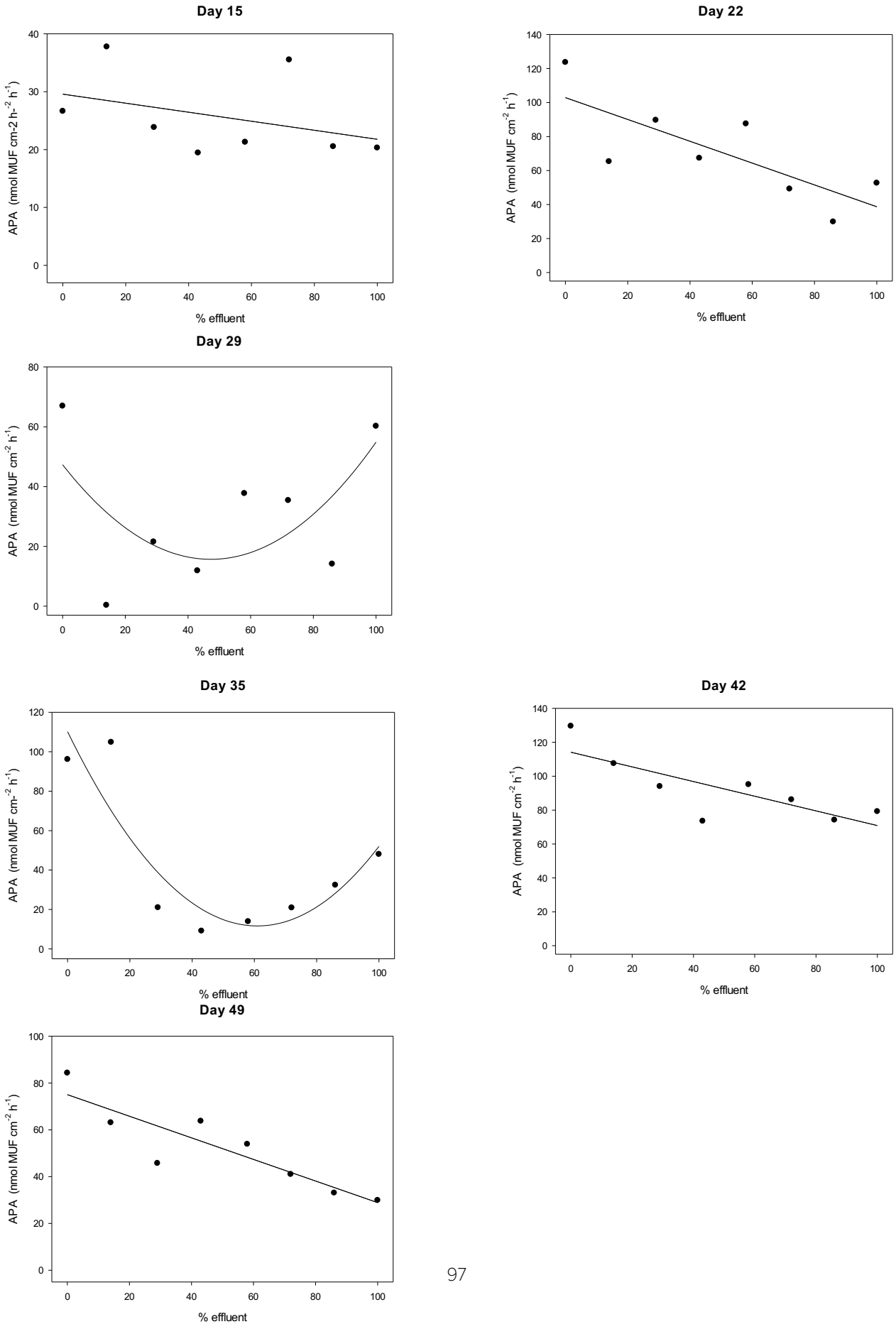

**Figure PII S9**. Models for leucine-aminopeptidase activity (LAP) at the exposure phase (days 15, 22 and 29) and the recovery phase (days 35, 42, 49 and 56)

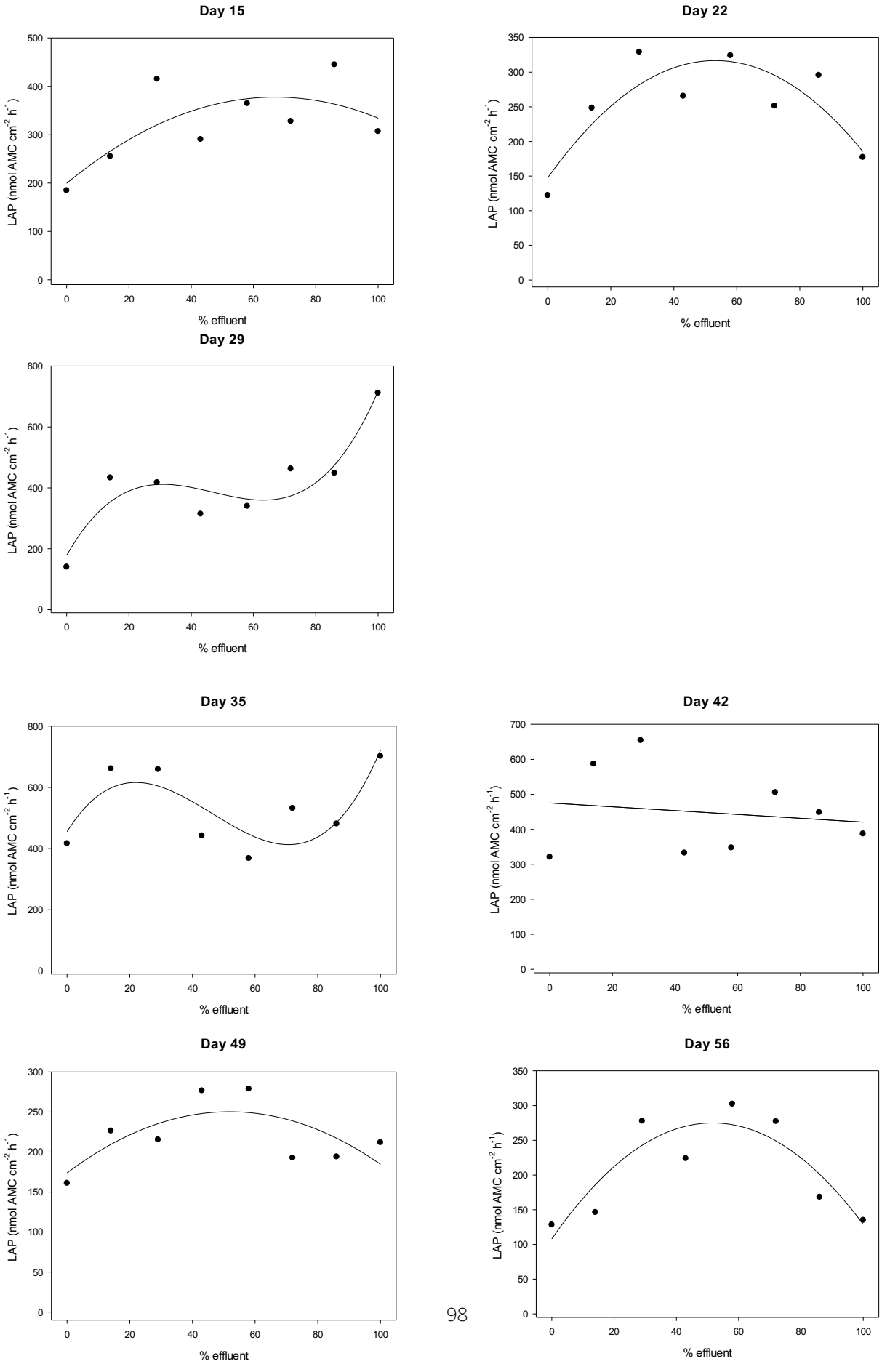

# Paper III

## Retrospective mass spectrometric analysis of wastewater-fed mesocosms to assess the degradation of drugs and their human metabolites

Laia Sabater-Liesa, Nicola Montemurro, Antoni Ginebreda, Damià Barceló, Peter Eichhorn, Sandra Pérez. Journal of Hazardous Materials; (2020)

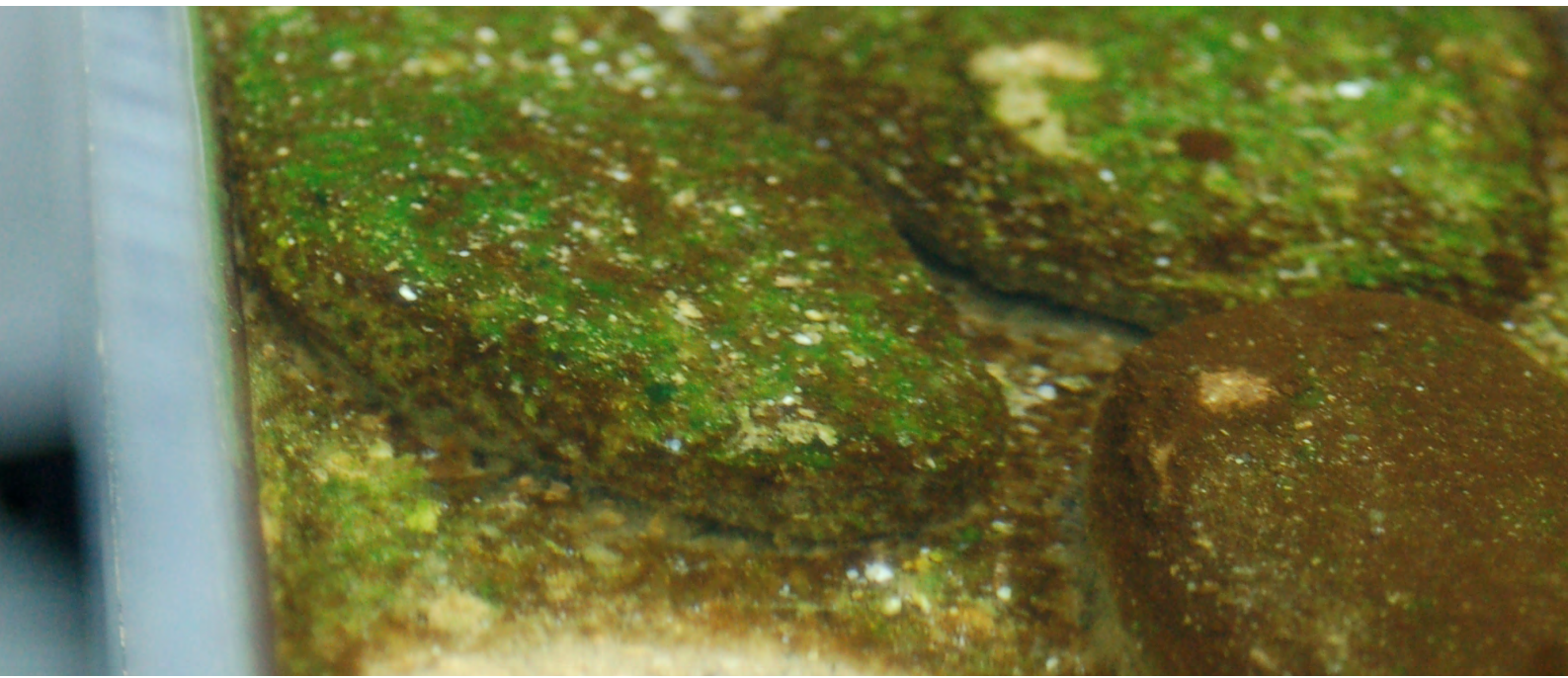

# Paper III. Retrospective mass spectrometric analysis of wastewater-fed mesocosms to assess the degradation of drugs and their human metabolites

Laia Sabater-Liesa[1], Nicola Montemurro[1*], Antoni Ginebreda[1], Damià Barceló[1], Peter Eichhorn[1], Sandra Pérez[1]

[1]ENFOCHEM, Department of Environmental Chemistry, IDAEA-CSIC, Jordi Girona 18-26, 08034 Barcelona, Spain

*corresponding author

## Abstract

Temporary rivers become dependent on wastewater effluent for base flows, which severely impacts river ecosystems through exposure to elevated levels of nutrients, dissolved organic matter, and organic micropollutants. However, biodegradation processes occurring in these rivers can be enhanced by wastewater bacteria/biofilms. Here, we evaluated the attenuation of pharmaceuticals and their human metabolites performing retrospective analysis of 120 compounds (drugs, their metabolites and transformation products) in mesocosm channels loaded with wastewater effluents twice a week for a period of 31 days. Eighteen human metabolites and seven biotransformation products were identified with high level of confidence. Compounds were classified into five categories. Type-A: recalcitrant drugs and metabolites (diclofenac, carbamazepine and venlafaxine); Type-B: degradable drugs forming transformation products (TPs) (atenolol, sitagliptin, and valsartan); Type-C: drugs for which no known human metabolites or TPs were detected (atorvastain, azithromycin, citalopram, clarithromycin, diltiazem, eprosartan, fluconazole, ketoprofen, lamotrigine, lormetazepam, metformin, telmisartan, and trimethoprim); Type-D: recalcitrant drug metabolites (4-hydroxy omeprazole sulfide, erythro/threo-hydrobupropion, and zolpidem carboxylic acid); Type-E: unstable metabolites whose parent drug was not detectable (norcocaine, benzolylecgonine, and erythromycin A enol ether). Noteworthy was the valsartan acid formation from valsartan with transient formation of TP-336.

**Keywords**: Mesoscosm, pharmaceuticals, natural attenuation, human metabolites, transformation products.

## Introduction

Organic micropollutants such as pharmaceuticals are frequently detected in surface waters downstream from wastewater treatment plants (WWTP) where, they are not completely removed from the waste stream (Murray et al., 2010; Ternes, 1998). At the discharge point, WWTP effluents are mixed and diluted with river discharge. Under high anthropogenic pressure or during dry periods they can constitute nearly the entire flow of the receiving water body in rivers. A larger fraction of WWTP effluent in the river translates into a low dilution ratio (Rice and Westerhoff, 2017) and thus elevated concentrations of sewage-borne contaminants (Boxall et al., 2004; Luo et al., 2014). This is the case of temporary waterways which cease to flow at some point in space and time along their course.

Once drugs, in unchanged form or as metabolites, are released into the aquatic environment, they can undergo natural attenuation processes such as dilution, sorption, photolysis, or biotransformation. The individual contribution of each of these processes to the overall dissipation from the water column is influenced by the properties of the pharmaceuticals as well as by the biological, physicochemical, and hydrological parameters of the river (Kümmerer, 2009; Kunkel and Radke, 2008; Writer et al., 2013). Biotransformation can be brought about by the action of microorganisms (bacteria and/or fungi) (Osorio et al., 2016; Tran et al., 2013), cyanobacteria and microalgae (Subashchandrabose et al., 2011) present in the aquatic systems where, they transform pharmaceutical compounds and their human metabolites into transformation products (TPs) (Längin et al., 2008; Zonja et al., 2015). Monitoring human metabolites and TPs in water bodies is of great interest to understand the fate of anthropogenic organic compounds in the environment because metabolites and TPs can potentially resist to further degradation and exhibit enhanced mobility in comparison to their precursor substance (Cwiertny et al., 2014; Evgenidou et al., 2015; Kümmerer, 2009; Mompelat et al., 2009). Thus, identification and quantification of TPs is crucial to assess the overall impact on freshwater ecosystems (Helbling et al., 2010) and they help understand the processes involved in the removal of chemical compounds (Matamoros et al., 2016; Zonja et al., 2015).

The characterization of TPs is generally performed at laboratory-scale in batch reactors spiked with a known concentration of the parent compound (Helbling et al., 2010; Pérez

and Barceló, 2008). Once the identity of TPs are elucidated, the subsequent step usually consists of demonstrating their presence in real samples (Kern et al., 2010). Few studies aiming at TP detection have been performed in mesocosms with native water. Some of them evaluated the fate of few pharmaceuticals without detecting their TPs (Li et al., 2015; Serra-Compte et al., 2019; Subirats et al., 2018). In our previous studies in a mesocosm experiment with artificial streams, where biofilms were exposed to WWTP effluent for a period of one month, using targeted high-resolution mass spectrometry (HRMS) we detected and quantified 20 drugs belonging to six therapeutic groups (β-blockers, antibiotics, psychiatric drugs, nonsteroidal anti-inflammatory drugs, antihypertensives, and contrast agents) (Sabater-Liesa et al., 2019) with concentrations ranging from 18 to 9792 ng/L. On the basis of these findings, we hypothesized the occurrence of degradation of some of these pharmaceuticals and the possible presence of their TPs in water.

In general, the analysis of TPs in environmental samples is challenging due to their structural diversity and complexity of the matrix, as well as the low concentrations at which they occur. In recent years, liquid chromatography coupled to HRMS has been increasingly applied for suspect screening (SS) of environmental samples (Hollender et al., 2019). The main advantage of using these HRMS-suspect screening techniques is the detection of substances potentially present in the samples without the need to rely on authentic standards which are sometimes not available for metabolites and TPs (Hannemann et al., 2016). Furthermore, one advantage of full-MS HR data is the ability to retrospectively interrogate them for the presence of specific molecular ions or fragment ions of discrete compounds that had not been included in the initial list of target analytes. HRMS data recorded over a wide m/z range on a properly calibrated instrument obviates the need for re-injecting the samples (Alygizakis et al., 2018). Indeed, HR hybrid mass systems, such as time-of-flight (ToF) mass spectrometers offer a greater wealth of data because these systems allow to generate structural information for any analyte that is amenable to ionization under the operational conditions of the instrument. Indeed, the retrospective approach with post-acquisition processing is not limited to the analysis of a few individual classes of compounds and can be applied to other ionized analytes of interest (Peña-Herrera et al., 2020). The retrospective analysis has been widely used for tracking extensive lists of pharmaceuticals, and their metabolites/TPs in surface waters and wastewater, although without further distinction between their origin (Alygizakis et

al., 2018; Bijlsma and Loeschcke, 2013; Boix et al., 2016; Campos-Mañas et al., 2019; Gago-Ferrero et al., 2015; Hernández et al., 2011; Krauss et al., 2010). For instance, the chemical structures of several human drug metabolites are identical to those of TPs of microbial origin (Radjenović et al., 2008).

In this context, we set out (1) to use mesocosms loaded with native WWTP effluent to examine the course of degradation of pharmaceuticals which had emerged in preceding suspect analyses and (2) to determine whether TPs formed in the channels could be differentiated from human metabolites already present in the wastewater effluent used to feed the channels. For this purpose, we created a list of compounds comprising TPs previously reported in the literature as well as known human metabolites to screen the mesocosm samples by means of retrospective HRMS analysis.

## 2. Materials and methods

### *2.1 Reagents*

LC-MS grade acetonitrile (≥99.9%), methanol (≥99.9%), ethyl acetate (≥99.9%), dimethyl sulfoxide (≥99.9%), and HPLC water were purchased from Merck (Darmstadt, Germany). Formic acid (≥96%, ACS reagent) and ammonium acetate were supplied by Sigma-Aldrich. Glass microfiber filter GF/F 0.7 μm, nylon membrane filter 0.45 μm, and PTFE syringe filters (13 mm, 0.45 μm) were purchased from Whatman (Little Chalfort, UK).

Analytical reference standards, isotopically labeled compounds, as well as individual stock solutions and work mixtures preparation were reported in detail elsewhere (Sabater-Liesa et al., 2019).

### *2.2. Experimental conditions and water sampling*

We performed the work in the Experimental Streams Facility of the Catalan Institute for Water Research (ICRA, Girona, Spain). Six artificial streams (3 treatments + 3 controls) consisted of methacrylate channels (length, 200 cm; width, 10 cm; and depth, 10 cm), and were filled with 5 L of fine sediment and cobblestones extracted from an unpolluted segment of the Llémena River (Sant Esteve de Llémena, NE Spain). Water was maintained under continuous recirculation at a flow of 50 mL $s^{-1}$. Day-night cycles were simulated with LED lights and defined as 10 h daylight (09:00-19:00 h) and 14 h darkness (19:00-09:00 h). The emission pattern was close to that of PAR, and complemented with

some UV on the lower part of the band. Biofilms were first acclimated to non-contaminated water (rainwater) for 14 days with sampling collection on day 14 (control sample). Over the following 31 days, three artificial streams received WWTP effluent obtained from the municipal WWTP of Quart (Girona, Spain). Water was transported in plastic tanks to the laboratory and transferred to the channels, and it was replaced twice a week with fresh WWTP effluent with a total of nine water renewals. Seven hundred fifty-mL samples were collected from the mesocosms at the beginning and the end of each cycle. Samples were stored at -20 ºC until analysis. Detailed information regarding sampling and methodology are described in detail in Sabater-Liesa et al.(2019).

*2.3 Sample treatment and LC-HRMS workflow*

The following suspect screening workflow consisted of a retrospective analysis of the samples previously analyzed and described in (Sabater-Liesa et al., 2019) and extracted by adapting a previously validated method reported elsewhere (Zonja et al., 2015). Briefly, 500 mL-samples were concentrated by using solid-phase extraction on 500-mg Oasis HLB cartridges (Waters, Milford, MA, US). The cartridges were eluted with 3x3 mL methanol/ethyl acetate (1:1) and reconstituted in 20 % acetonitrile.LC separation was performed using a SCIEX ExionLC™ AD system (Sciex, Redwood City, CA, U.S.) with an Acquity® UPLC BEH C18 column (100 mm x 2.1 mm i.d., 1.7 µm particle size (Waters), maintained at 40 °C. The mobile phases were (A) 5 mM ammonium acetate, 0.1% formic acid and (B) 0.1% formic acid in acetonitrile (B). Compounds were separated with a linear gradient started with 3% of B for 0.1 min and increased to 98 % in 7 min, kept constant at 98 % for 1.4 min and finally brought back to initial conditions in the following 90 s. The flow rate was 0.6 mL/min, the injection volume was 5 µL, and the auto-sampler temperature was maintained at 8 °C. A SCIEX X500R QTOF system (Sciex, Redwood City, CA) was used for data acquisition employing SWATH acquisition workflow which consisted of an MS scan over an m/z range from 100 to 950 with an accumulation time (AT) of 100 ms followed by ten MS/MS experiments with variable Q1 windows (m/z 30 to 900, 30 ms AT) and recorded using a collision energy of 35 V with an energy spread of ±15 V. The instrument provided a resolving power (FWHM) of 31,000 at m/z 132.9049 and 44,000 at m/z 829.5395 with a mass error of 0.2 ppm.

In this work, compound detection and identification was carried out according to the workflow depicted in Figure 1. The files were processed by Sciex OS 1.6 software. The

total ion chromatograms were automatically deconvoluted to generate extracted ion chromatograms of concrete m/z values. Then, a two-step data processing approach was employed to detect and identify suspected metabolites and TPs. The TPs were prioritized using scientific search engines (Web of Science and Science Direct) and by consulting peer-reviewed publications and original publications cited in review articles considering the last 15 years (Beretsou et al., 2016; Boix et al., 2016; Eichhorn et al., 2005; Gröning et al., 2007; Gros et al., 2014; Helbling et al., 2010; Hermes et al., 2018; Jelic et al., 2012; Jewell et al., 2016; Kosjek et al., 2012; Llorca et al., 2015; Osorio et al., 2014; Pérez et al., 2006; Pérez and Barceló, 2008; Quintana et al., 2005; Schulz et al., 2008; Terzic et al., 2011; Xu et al., 2016). An exact mass compound database which included 105 related TPs already reported in literature taking into account the positive confirmation of the presence of the 15 target compounds previously detected in Sabater-Liesa (2019) in the same waters was generated (Table S1). Whereas, additional parent compounds and related metabolites were manually searched in the integrated SCIEX NIST-2017 spectral library, the most commonly encountered compounds in surface water by consulting the most recent peer-reviewed publications (aus der Beek et al., 2016; Beretsou et al., 2016; Henning et al., 2019; Hermes et al., 2018; Jewell et al., 2016; Luo et al., 2014). Of the more than 17,000 compounds included in the library, 351 compounds were selected including 122 new parent compounds and 229 metabolites. The full list, including the molecular formulas, the exact mass, the exact masses of the molecular ion $[M + H]^+$, the most abundant fragment ion for each compound, and the SMILES code (where possible) are shown in Table S2. After loading the databases into the software, the monoisotopic masses and their isotopic distributions, and the mass spectra (fragment ions, only for NIST list) were used to retrieve tentative candidates. For metabolites with structural isomers, when a molecular formula was detected, only the most probable isomers were considered for the assessment of the identity of the compound according to the literature. In this case, the high confidence identification of the formed metabolites and TPs in the mesocosm study was based on the use of characteristic fragmentation obtained during the SWATH acquisition.

HRMS experimental data are ideally matched against an MS/MS spectra libraries considering both molecular and fragment ions in the search algorithm. To optimize searching and identification with HRMS data, the criteria used for the reduction of features included a minimum peak area and height (Intensity ≥1000 cps), a minimum

peak width of three points, a mass accuracy threshold of ±5 ppm on the monoisotopic peaks, the presence of a reasonable isotopic pattern (Intensity ≥1000 cps), a mass accuracy threshold of 5 ppm on the monoisotopic peaks and a fragment mass accuracy of ± 5 ppm or in any case <10 ppm (where possible). Additional confidence criteria for the identification of the suspects were the presence of a similar pattern of chromatographic retention time during batch experiments (Triplicates. retention time delta of 0.03 min), their absence in the blank and the control samples.

The Library search is performed by selecting the "Smart Confirmation Search" algorithm for potential matches. To save time, this algorithm initially will look for potential candidates by name in the library and then for spectrum in case of mismatch. The Maximal number of hits was set to 5 with a Library Hit Score >70%, and the Formula Finder Score >50% and it was verified using free online chemical database ChemSpider connected with the analytical SCIEX O.S. 1.6 software. This score is obtained from the result of the search algorithm and from the isotopic profile of the experimental acquisition of TOF-MS. The selected Formula Finder criteria were Man-made compounds, Max elements ($C_{49}$ $H_{80}$ $Br_2$ $Cl_5$ $F_6$ $I_3$ $N_{10}$ $O_{16}$ P $S_3$ Si), and Mass tolerance 5 ppm. The Formula Finder Score can be used as an additional confidence criterion; however, a high formula search score does not necessarily mean that the candidate generated is the one identified by formula search as there are often several formulas that match within a few ppm of mass error. If an unknown peak does not have a library match, the software will use the formula search algorithm to predict a potential chemical formula based on the accurate TOF-MS mass data (mass error, elemental composition, number of hits). In case a peak has a library match, the proposed formula will match the compound formula for the MS/MS library.

Furthermore, the matching of the acquired spectra with the commercial library was evaluated considering three additional parameters provided by the software: fit value (Fit), reverse fit value (rFit) and purity factor (Purity). According to Matraszek-Zuchowska et al. (2016), the Fit and rFit values describe the similarity between the acquired spectrum and that contained in the reference library. Specifically, the Fit value provides information on the similarity of the spectrum of the reference library with the spectrum acquired by the machine, while the rFit value reflects the similarity of the fragments of the acquired spectrum with those in the reference spectrum. For a positive finding, fit must be greater than 50% while rfit values must present a score close to 100.

The degree of matching (fragmentation similarity) is given by the combination of both the Fit and rFit values through the Purity value which considers the peaks equal between the experimental spectrum and the library.

To identify the most probable structures, the fragmentation information, if available, was verified using the ChemSpider service (Pence and Williams, 2010). The level of confidence for the identification of the detected compounds was determined according to the proposed levels reported by Schymanski (2014), where level 1 match up to confirmed structures (if reference standard is available), level 2a to probable structures by library spectrum match, level 2b to probable structures by diagnostic evidence, level 3 to tentative candidate(s), level 4 to unequivocal molecular formulas, and level 5 to exact mass (*m/z*) of interest.

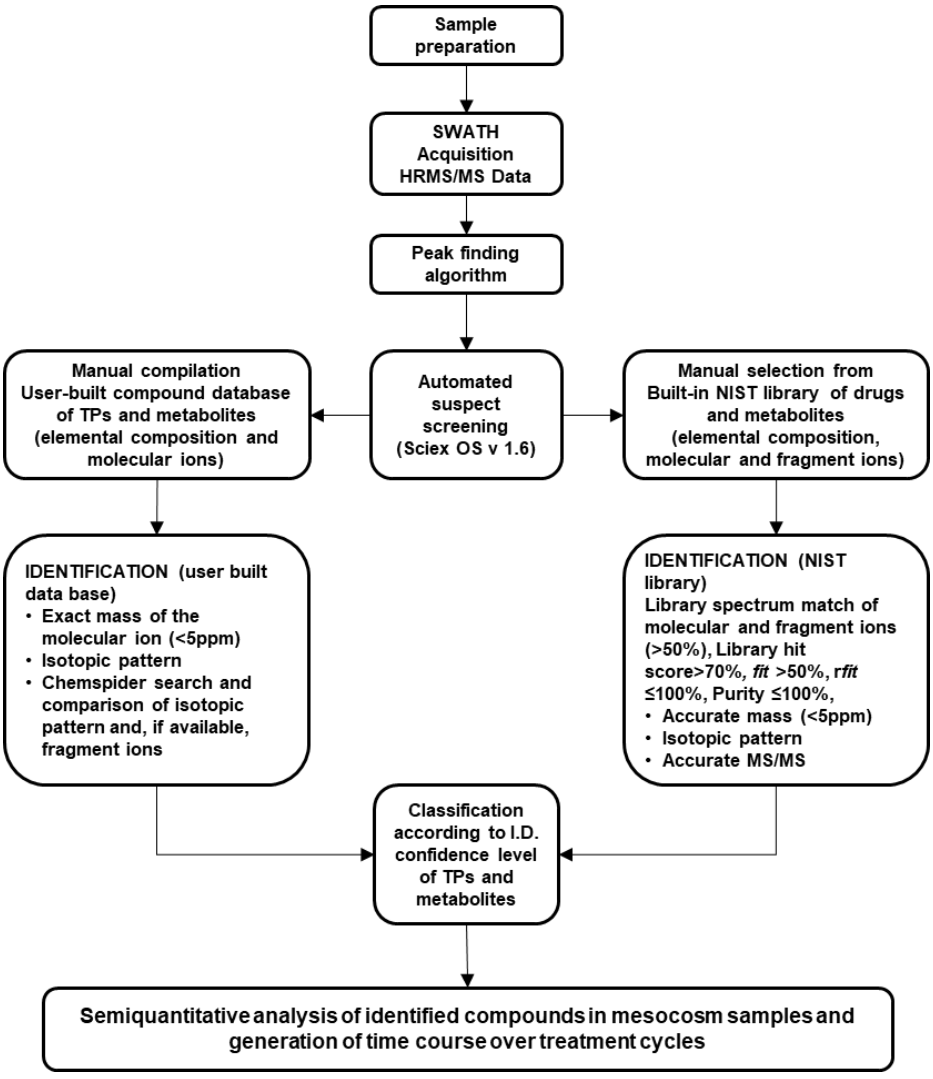


**Figure PIII 1.** Analytical workflow of suspect screening process

## 3. Results and discussion

### *3.1 QA/QC procedures*

According to the previous study (Sabater et al. 2019), all samples were spiked with a mix of 32 different labeled compounds at a concentration of 100 ng $L^{-1}$. Acclimated rainwater from control channels was used as a control, whereas blanks were prepared with 500 mL of HPLC water and spiked with the same internal standard mixture. In addition, the calibration of the instrument by infusing a standard solution of reserpine ($C_{33}H_{40}N_2O_9$, m/z 609.28066) was injected every 5 samples in positive mode during the batch acquisition.

### *3.2 Screening for metabolites and TPs*

We explored the potential presence of known drug metabolites and TPs reported in the literature and those collected in the NIST library by suspect screening (Figure 1). For the SS workflow using the NIST library, compounds of interest were manually searched in the database via the search tool. The list that is generated containing the name of the compound, the mass of the precursor ion, the mass of the most abundant ion and the chemical formula (Tab. S2) is then transferred into the process method. The Library search is performed by selecting the "Smart Confirmation Search" algorithm for potential matches. This algorithm will initially filter the possible candidates by name and then by spectrum in case of mismatch. After processing was complete, the results were sorted by fit values.

A list of possible formulas is determined according to the accurate mass of precursor ion, the average MS/MS mass accuracy of matching fragments, as well as its distinct isotopic pattern based on its molecular formula. Proposed formulas are scored based on the best mass accuracy and high hit count. In case the accurate mass of the detected peak and the Formula Finder function are not enough to generate the expected chemical formula for that peak, it is possible to start an online session with the extensive ChemSpider database using candidate formulae and acquired MS/MS spectra to find candidate structures by matching in silico fragmentation pattern to predict candidate structures (Fig. S2).

In the case of the user-built database, only the mass of the precursor ion and the chemical formula was added to the list. If there is no match in the spectral library, the software will use the Formula Finder algorithm and the Chemspider hit count to try to predict a potential

chemical formula based only on the accurate mass TOF MS data (mass error, elemental composition, hit count).

In total, 40 compounds were detected using both suspect screening lists. Fifteen compounds could be confirmed by using analytical standards (confidence level 1), 20 were confirmed by a matching MS/MS spectrum retrieved in either the NIST or Chemspider libraries (confidence level 2a). Library Hit Scores were higher than 70 %, Fit were higher than 50% with rFit and Purity close to 100 % for most of the cases (Table 1). Whereas the other five compounds turned up after comparison of the molecular ion peaks in the deconvoluted TIC against the user-built database containing the chemical formulae (confidence level 2b, amenable retention time and isotopic pattern).

Sixty-four substances were rejected on the basis of retention time or poor MS/MS spectrum match. If no NIST library MS/MS spectra was found (see Fig. S6A for atenolol-acid), the tentative identification was based on similarity between the observed fragment ions of the compounds and those ions reported in the ChemSpider database. As shown in Figure S6A, for the peak m/z 268.1543, the software automatically generated the molecular formula $C_{14}H_{21}NO_4$ with a mass error of below 5 ppm for all samples. However, no compound is associated with this formula in the commercial library. A ChemSpider session was opened to try to justify the Formula Finder result matching the proposed elemental composition and isotope pattern. Hence, a list of compounds with identical chemical formula was retrieved with the ranking according to the number of PubMed citations (Fig S6B). Scrolling through the panel of compounds proposed by the software (upper left panel in Fig S6B), the ChemSpider ID 56653 corresponded to the compound CY1634360, that is precisely the acid atenolol, as evidenced by the structure shown in the lower left panel of the same figure. Matching fragment ions were indicated in blue in the upper right panel, whereas, in the lower right panel (Fig S6B) all the experimental fragments are listed. For example, the fragment $[M + H]^+$ 191.0703 has been associated with the molecular formula $C_{11}H_{11}O_3^+$. By highlighting this fragment, the portion of the molecule corresponding to this mass is marked in the lower left panel. A larger number of matching fragment ions indicated a higher likelihood of correct assignment.

When no TP with matching elemental composition was found in the NIST and ChemSpider database, other criteria were used to increase the confidence in the

identification of the suspect such as fragmentation and spectral similarity with its parent compound. For TPs without library mass spectra or a feedback in the ChemSpider database such as Valsartan-TP336 (Figure 1), the identification confidence was not as high as in the cases where MS/MS library matching was available. The exact mass fit with the theoretical isotopic distribution generating the formula $C_{19}H_{21}N_5O$ with an associated Score of 93% and a mass error of 2 ppm. The spectrum of the tentatively identified metabolite (Figure S3A) had the peaks m/z 207.0917 and 235.0978 in common with valsartan (m/z 207.0912 and 235.0975, Fig. S3B), indicating that two dealkylations have occurred. These results are supported by the fact that previous studies also detected these substances and a similar elution order between the TP and the parent compound was reported. Furthermore, the presence of both compounds, the parent (valsartan) and the final TP (valsartan acid) positively detected in the samples can indicate the presence of the degradation intermediate as reported by (Helbling et al., 2010).

*3.2. Occurrence of human metabolites and TPs in the mesocosm*

In addition to the 15 detected drugs, 18 human metabolites and seven TPs were found in the mesocosms fed with treated wastewater. The detected TPs were: atenolol-acid (Radjenović et al., 2008; Xu et al., 2016), valsartan-TP336 (VLS-TP336) and the second-generation TP valsartan acid (VLS-acid) (Helbling et al., 2010), sitagliptin-TP449 (STG-TP449) (Henning et al., 2019), 4'-hydroxy-diclofenac (4'OH-DCF) (Kosjek et al., 2008), 1-(2,6-dichlorophenyl)-2-indolinone (DCF-lactam), 2-[(2,6-dichlorophenyl)amino] benzoic acid (DCF-BA) (Jewell et al., 2016; Kosjek et al., 2008) (Table 1).

**Table PIII 1** – Drug and metabolites/transformation products detected in water samples from mesocosm

| Drug | Metabolite/transformation product | Human MTB | Microbial TP | Formula Finder Score | Library Search Fit/rFit/Purity | RT (min) | Confidence level*** |
|---|---|---|---|---|---|---|---|
| | ***TYPE-A: detection of parent & MTB - no evidence for transformation in mesocosm*** | | | | | | |
| **Carbamazepine (CBZ)** | | | | 90.6 | 99.2/88.6/86.2 | 2.78 | 1 |
| | Carbamazepine-10,11-epoxide | X | | 94.6 | 81.8/99.9/81.5 | 2.58 | 2a |
| | 10,11-Dihydro-10-hydroxycarbamazepine | X | | 84.5 | 100/100/100 | 2.8 | 2a |
| **Diazepam (DZP)** | | | | 88.5 | 72/83.9/38.8 | 4.55 | 2a |
| | Nordiazepam | X | | 91.1 | 87.6/96.4/76.4 | 4.12 | 2a |
| | Oxazepam (OZP) | X | | 90.1 | 100/83.3/83.3 | 3.77 | 1 |
| | Temazepam | X | | 94.1 | 100/89.1/89.1 | 4.14 | 1 |
| **Nordiazepam (NDZP)** | Oxazepam | X | | 90.1 | 100/83.3/83.3 | 3.77 | 1 |
| **Temazepam (TMZ)** | Oxazepam | X | | 90.1 | 100/83.3/83.3 | 3.77 | 1 |
| **Diclofenac (DCF)** | | | | 89.8 | 100/97.6/97.6 | 4.99 | 1 |
| | 4´-Hydroxy-diclofenac (4'-OH-DCF) | X | X | 96.7 | 97.1/94.4/92.2 | 4.15 | 2a |
| | 1-(2,6-Dichlorophenyl)-2-indolinone (DCF-lactam) | | X* | 86.7 | -/-/-** | 4.97 | 2b |
| | 2-[(2,6-Dichlorophenyl)amino]benzoic acid (DCF-BA) | | X* | 92.3 | -/-/-** | 4.98 | 2b |
| **Venlafaxine (VFX)** | | | | 88.2 | 93.6/65.2/41.8 | 2.98 | 1 |
| | O-desmethyl-venlafaxine (O-DVFX) | X | | 86.5 | 99.9/93.1/93.0 | 2.33 | 2a |
| | N-desmethyl-venlafaxine (N-DVFX) | X | | 84.4 | 100/100/100 | 2.55 | 2a |
| | N,O-didesmethyl-venlafaxine (N,O-dDVFX) | X | | 81.5 | 85.3/96.3/73.0 | 2.33 | 2a |
| | ***TYPE-B: detection of parent & TP - evidence for transformation in mesocosm*** | | | | | | |
| **Atenolol (ATL)** | | | | 89.4 | 98.3/94.4/91.4 | 1.38 | 1 |
| | Atenolol-acid (ATL-acid) | X | X | 94.8 | -/-/-** | | 2b |
| **Sitagliptin (STG)** | | | | 93.2 | 98.8/99.5/98.2 | 2.8 | 2a |
| | Sitagliptin TP449 (STG-TP449) | | X | 87.5 | -/-/-** | 3.43 | 2b |
| **Valsartan (**VLS**)** | | | | 89.7 | 97.4/78.1/67.3 | 4.48 | 1 |
| | Valsartan-TP336 (VLS-TP336) | | X | 93.0 | -/-/-** | 3.75 | 2b |
| | Valsartan acid (VLS acid) | | X | 86.6 | 100/95.9/95.9 | 3.05 | 1 |
| **Drug** | **Metabolite/transformation product** | **Human MTB** | **Microbial TP** | **Formula Finder** | **Library Search Fit/rFit/Purity** | **RT (min)** | **Confidence level*** ** |

| | | | Score | | | |
|---|---|---|---|---|---|---|
| | ***TYPE-C: only detection of parent compounds*** | | | | | |
| **Atorvastatin (ATV)** | | | 78.6 | 98.3/96.7/93.8 | 4.05 | 2a |
| **Azythromycin (AZY)** | | | 92.2 | 87.2/32.4/92.0 | 3.95 | 1 |
| **Citalopram (CLT)** | | | 86.2 | 100/96.7/96.7 | 3.44 | 1 |
| **Clarithromycin (CTP)** | | | 87.5 | 98.1/59.3/51.0 | 3.97 | 1 |
| **Dialtiazem (DTZ)** | | | 92.7 | 84.3/94.5/66.2 | 3.52 | 1 |
| **Eprosartan (EPS)** | | | 94.2 | 85.0/95.5/69.8 | 3.08 | 2a |
| **Fluconazole (FLZ)** | | | 92.4 | 99.8/99.8/99.6 | 2.44 | 2a |
| **Ketoprofen (KTF)** | | | 83.9 | 100/98.9/98.9 | 4.23 | 1 |
| **Lamotrine (LMG)** | | | 96.8 | 93.2/63.3/39.4 | 2.46 | 1 |
| **Lormetazepam (LMZ)** | | | 92.5 | 99.7/72.1/70.5 | 4.27 | 1 |
| **Metformin (MTF)** | | | 87.3 | 99.9/74.1/73.9 | 0.47 | 2a |
| **Telmisartan (TLS)** | | | 87.9 | 100/100/100 | 4.33 | 2a |
| **Trimethoprim (TMP)** | | | 89.1 | 100/79.3/79.3 | 2.05 | 1 |
| **Atorvastatin (ATV)** | | | 78.6 | 98.3/96.7/93.8 | 4.05 | 2a |
| **Azythromycin (AZY)** | | | 92.2 | 87.2/32.4/92.0 | 3.95 | 1 |
| **Citalopram (CLT)** | | | 86.2 | 100/96.7/96.7 | 3.44 | 1 |
| **Clarithromycin (CTP)** | | | 87.5 | 98.1/59.3/51.0 | 3.97 | 1 |
| | ***TYPE D: only detection of MTB- no evidence for transformation in mesocosm*** | | | | | |
| **Bupropion** | Erythro/threo-Hydrobupropion (HB) | X | 91.2 | 96.4/92.2/84.9 | 2.96 | 2a |
| **Zolpidem** | Zolpidem phenyl-4-carboxylic acid (ZPD-CA) | X | 81.8 | 100/99.0/99.0 | 2.08 | 2a |
| ***TYPE E: only detection of MTB - evidence for transformation in mesocosm*** | | | | | | |
| **Cocaine** | Benzoylecgonine (BLG) | X | 89.7 | 100/97.9/97.9 | 2.16 | 2a |
| | Norcocaine (NCC) | X | 91.4 | 93.8/99.0/99.0 | 3.08 | 2a |
| **Erythromycin A** | Erythromycin A enol ether (EAEE) | X | 90.2 | 85.4/38.3/34.0 | 3.96 | 2a |
| **Omeprazol** | 4-Hydroxy omeprazole sulfide (4-OH-OMZ) | X | 87.5 | 96.1/98.8/94.8 | 2.6 | 2a |

* Compounds already present in the wastewater samples

**Compounds not contained in the user-built database. The OS software is unable to calculate Fit, rFit, and Purity values for these compounds.

***Schymanski et al., 2014, 1: confirmed with reference standard; 2a: probable structures by library spectrum match; 2b: probable structure by diagnostic evidence; 3: tentative candidate; 4: unequivocal molecular formula; 5:exact mass (m/z) of interest

Regarding the abundance-time profiles of the detected drugs, metabolites and TPs in samples collected at the start and end of each cycle, the compounds can be classified into four categories as shown in Figure 2. Type-A: drugs with measurable levels of both parent and metabolites neither of which display significant concentration changes over the experimental duration (CBZ, DZP, DCF, and VFX); Type-B: drugs showing lower concentrations in the samples collected at the end of each cycle with concomitant (intermittent) increase of TP levels (ATL, STG and VLS); Type-C: parent compounds which were detected in the streams but no human metabolites or TPs were detected in the samples (ATV, AZY, CLT, CTP, DTZ, EPS, FLZ, KTF, LMG, LMZ, MTF, TLS and TMP ); Type-D: drug metabolites with similar levels before and after treatment whose parents were not detectable (ZPD-CA, HB); Type-E: unstable metabolites whose parent drugs was not detectable in either start or end samples (NCC, BLG, EAEE, 4-OH-OMZ sulf).

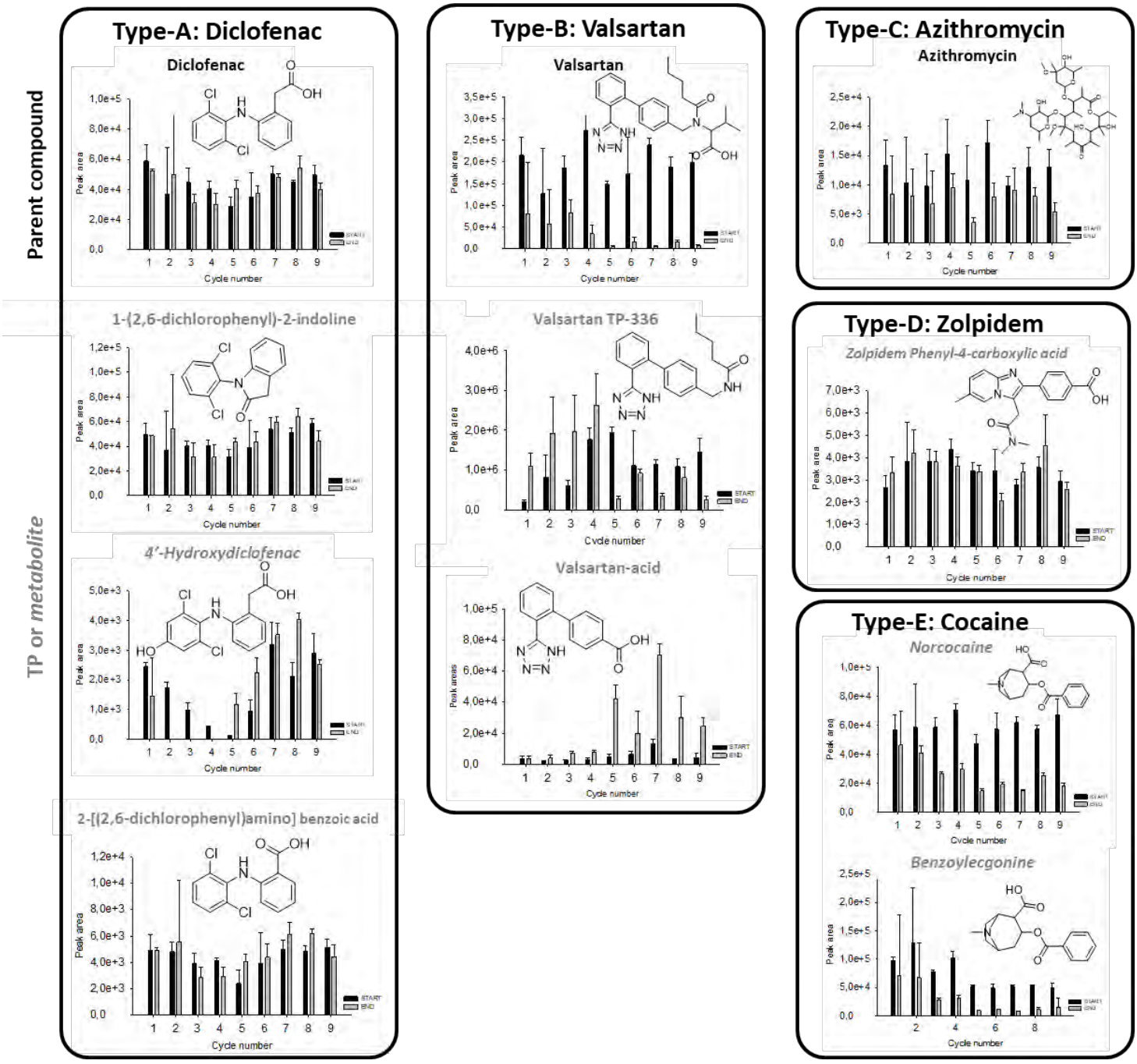


**Figure PIII 2**. Classification of drugs based on degradability and detected metabolites and TPs

With CBZ and DCF the type-A group comprises two substances that are among those drugs most thoroughly studied in the environment with respect to occurrence, persistence to biodegradation, and advanced wastewater treatment techniques for enhanced removal (Jelic et al., 2012; Jewell et al., 2016; Pérez and Barceló, 2008). As much as CBZ persists in the mesocosm, so do its two metabolites: neither the epoxide nor the 10,11-dihydro-10-hydroxy exhibit a clear trend towards elimination over the course of the mesocosm experiments. As far as DCF and its two metabolites DCF-lactam and DCF-BA are concerned, the time profiles are very similar without substantial differences in the start and end samples over the nine treatment cycles. The profile of 4′-OH-DCF, in turn, is a typical in so far as on the one hand its start levels fluctuate largely over the course of the experiment while on the other hand the start-end ratio varies substantially over time. Although of speculative nature, the former observation may be related to the source of this oxidative biotransformation product. It is described to be excreted into human urine not only in free form but also as glucuronide conjugate (Stierlin et al., 1979). The inherent susceptibility of this species to hydrolysis might explain why its levels in the start samples vary so widely. Partial hydrolysis of the conjugate might have occurred in the WWTP or during transport of the effluent samples to the experimental facilities. Moreover 4′-OH-DCF is also a TP formed during the degradation of diclofenac in batch reactors (Kosjek et al., 2008). With regards to VFX as the fourth compound in this group, the abundance-time profiles of the parent compound and its mono- or didemethylated derivates, which are key intermediates in the metabolic pathway in humans, display similar patterns with only minor variations in the Start-end ratios. What appears to be a trend of slightly lower VFX levels in the end samples from the forth through the ninth cycle does not translate into markedly higher abundances of the N-demethyl and O-demethyl metabolites as one might have expected in case the microbial metabolism proceeded in analogy to that in humans. However, it must be considered that the absolute abundances of these three entities being at least 20-fold lower for the parent drug. Taking into consideration that the basic amine as the preferred site of protonation during electrospray ionization is conserved among them, it is reasonable to assume that the absolute abundances can be used as a suitable estimate of the relative concentrations. Hence, demethylation of VXF is unlikely to translate into higher levels of the O- and N-demethyl derivatives. Furthermore, any formation of the two latter metabolites might be compensated for by subsequent conversion into the didesmethyl intermediate, assuming that the metabolic reactions followed those taking place in the human liver. Similar results were obtained in

batch experiments amended with wastewater for O-DVFX, and O,N-dDVFX. However, in the latter work, N-DVFX was formed in the batch reactors because they detected that its concentrations increased until the end of the experiment (Kern et al., 2010). Further compound that it falls in the Type-A is DZP with unchanged abundance between start and end samples (Figure 3). The same wholes true for TMZ, NDZP and OZP (Seddon et al., 1989). While the two former compounds are known to be human metabolites originating from hydroxylation and N-demethylation respectively, OZP is both a prescription drug itself and the metabolite of diazepam as shown in Figure 3. This means the source of its occurrence in the start samples is likely a combination of human diazepam metabolism and therapeutic treatment with OZP.

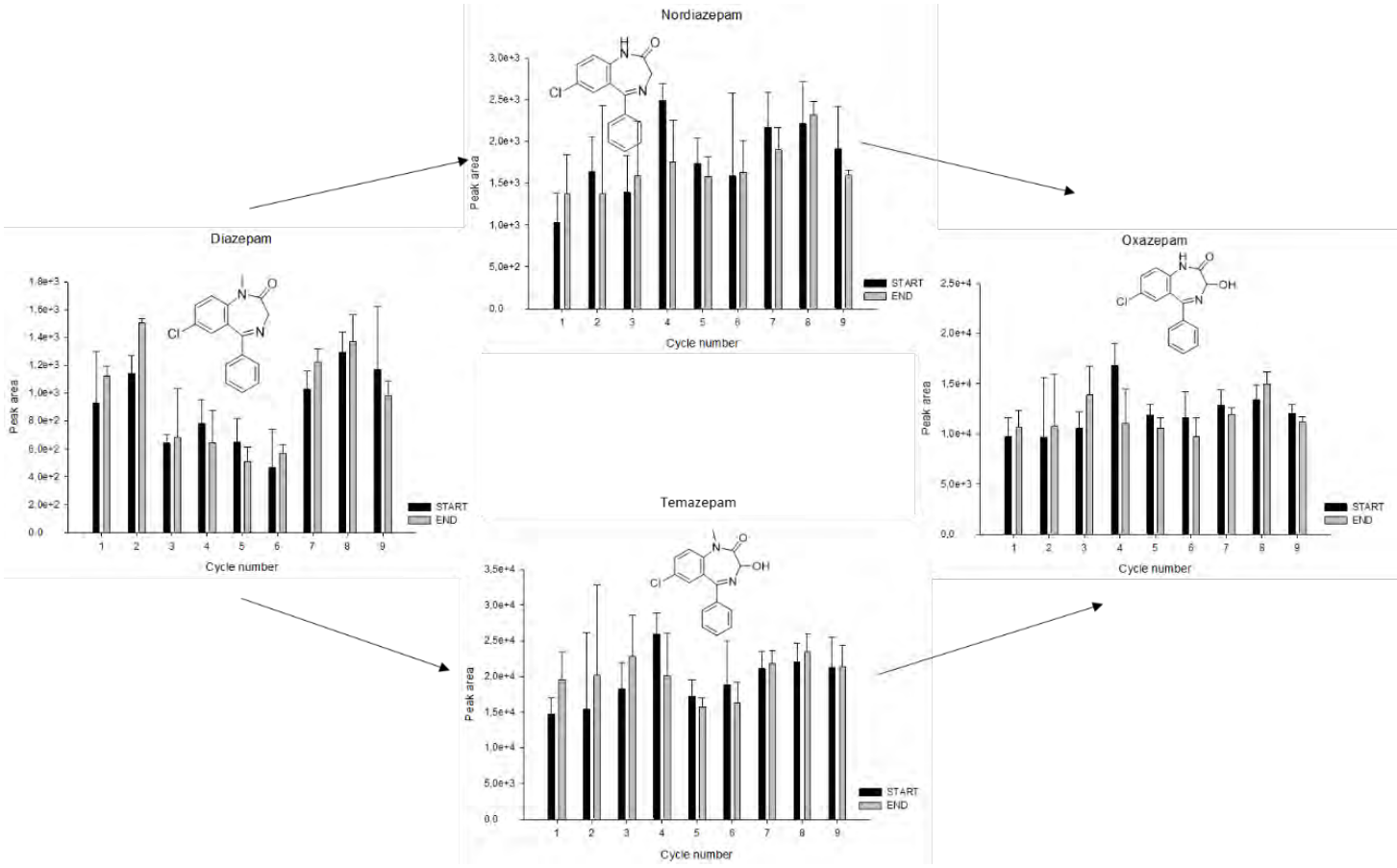


**Figure PIII 3**. Human metabolism of diazepam and intensities of detected metabolites in the channels

As for ATL, STG and VLS as the three Type-B compounds, they exhibit signs of biotransformation in the artificial streams. The substantial decrease of the start-end ratios

of ATL is paralleled by concomitant release of atenolol-acid (Radjenović et al., 2008), which arises from hydrolysis of the primary amide, in all but the samples from cycle 1 (Figure 4). ATL-acid is also a human metabolite originated from metoprolol (Kern et al., 2010). STG is partially degraded to its acetylated TP (STG-TP449) (Figure 4) which was detected in the influents and effluents of pilot- and full-scale WWTPs (Henning et al., 2019). VLS, in turn, displays a more differentiated pattern with the formation of a first-generation (VLS-TP336) and a second-generation transformation product (VLS-acid) Figure 2. When the data is plotted as the ratios of start-to-end samples instead of absolute abundances as in Figure 2, it becomes apparent that the ratio for VLS-TP336 increases over time while that of VLS-acid decreases (see trendlines in Figure 5). This trend is an indicator of an adaptive process of the degrading microbial community whose ability to dealkylate the amide group in VLS is enhanced upon continuous exposure to this substrate. On the other hand, the negative slope of the trendline of VLS-acid is suggestive of accumulation in the system, i. e. it is not subject to further degradation. While O-desmethyl-VLS was reported to occur in a highly impacted stream, coming from the degradation of VLS and its glucuronide (Writer et al., 2013), in our study it was not detected.

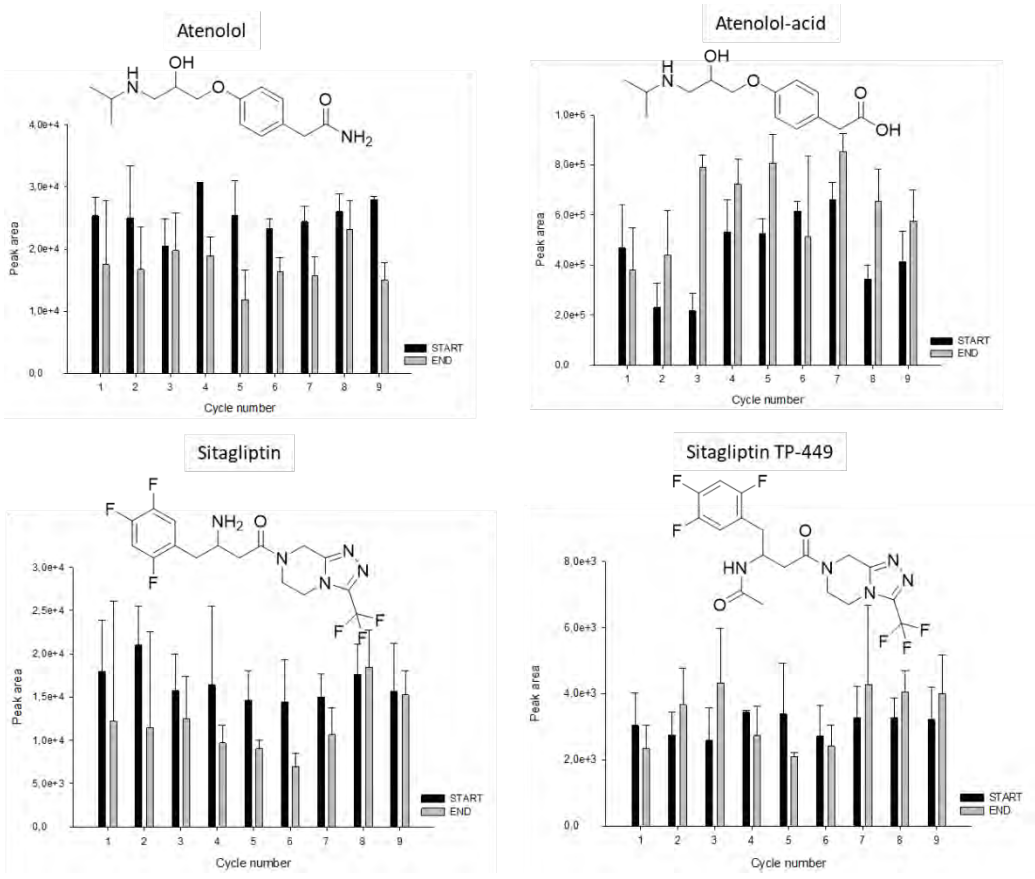


**Figure PIII 4**. Profiles of atenolol and sitagliptin and their TPs in stream channels

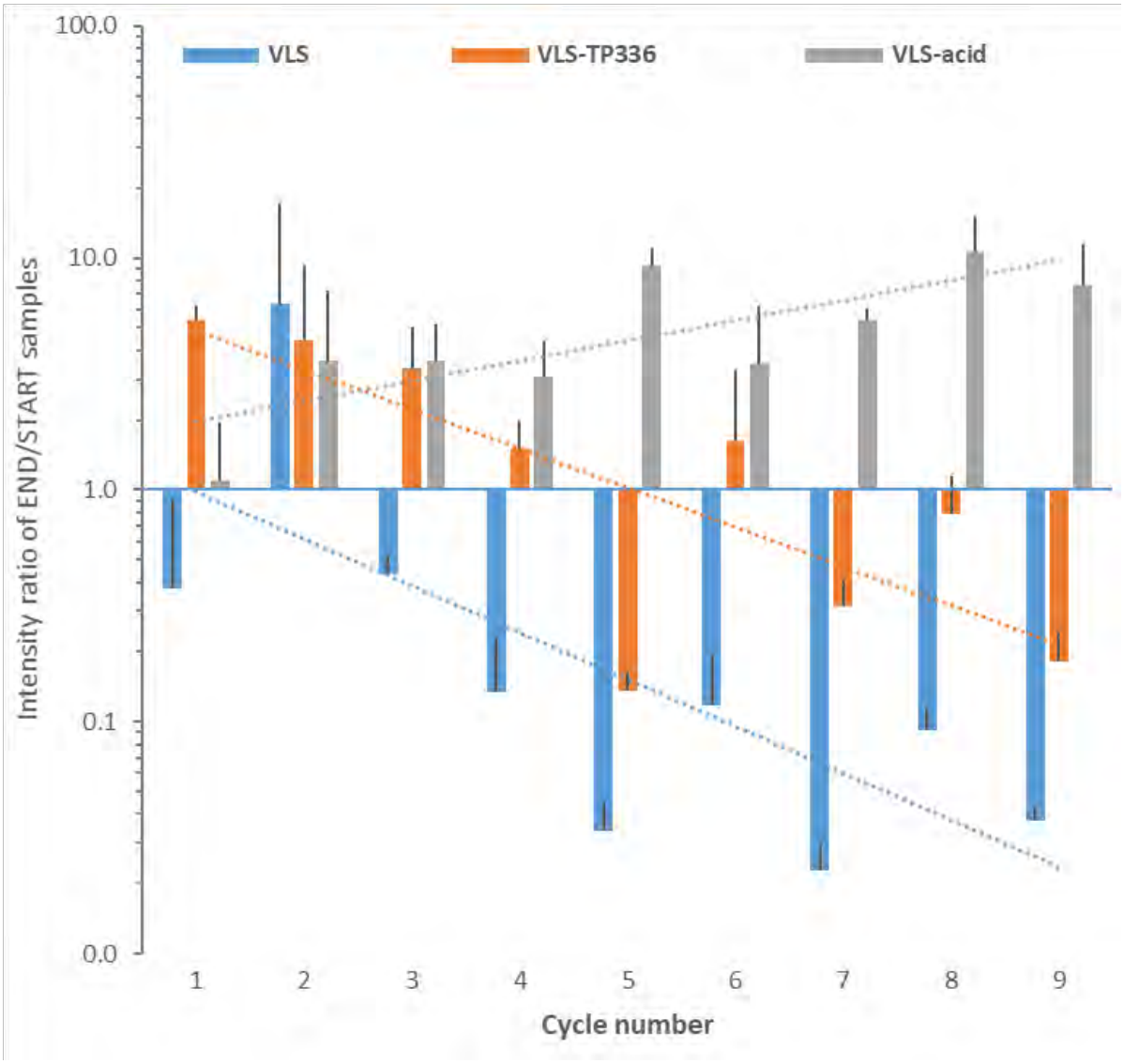


**Figure PIII 5**. Ratio of end-to start samples for valsartan and its TPs and trend lines

Type-C include 13 drugs for which nor human metabolites nor postulated TPs were detected in any of the samples (see Table 1). However, several of them (AZY, CLT, CTP) show clear signs of dissipation suggesting removal by biotransformation. The search for known TPs (Table S1) was negative.

The Type-D compounds include ZPD-CA and HB whose parent drugs, zolpidem and bupropion, respectively, could not be detected in any of start samples (not surprisingly, they were also absent in the end samples). This observation is in agreement with the extensive conversion of both pharmaceuticals in the human liver, following efficient

intestinal absorption, leading to only a very small fraction of the administered dose to be excreted unaltered (Connarn et al., 2017; Pichard et al., 1995). The concentrations of both metabolites in the start and end samples remain rather stable over the 9 cycles suggesting their recalcitrance to further metabolic reactions by the microbial community residing in the artificial streams. However, in another studies which they screened HB in real streams, this compound was degraded with a half-life of 7.9 h (Writer et al., 2013).

The Type-E compounds include NCC, BLG, EAEE and 4-OH-OMZ sulf. These parent compounds are highly metabolized. Their human metabolites are degraded in the mesocosm. Further TPs of the human metabolites were not detected.

## 4. Conclusions

Mesocosm experiments performed in artificial indoor channels fed with native wastewater, combined with HRMS analysis and suspect-screening data processing, provide a useful method for a realistic study of the fate of compounds potentially recalcitrant in wastewater treatment plants. Our findings are particularly relevant for rivers with low dilution capacity as those found in the Mediterranean area, which are often subjected to severe seasonal fluctuations. Indeed, our experiments, performed using water renewal cycles of 3-4 days, for a total of 30 days, highlight the recalcitrance of most of the compounds detected in the wastewater used to feed the channels.

The application of suspect-screening methods revealed the presence of human drug metabolites and TPs in the treated wastewater and allowed to follow up their fate during the duration of the experiments, thus enabling their classification into five categories according to their detectability and changes of abundance over time. The majority of pharmaceuticals detected in the mesocosms water, exhibited either negligible or very limited removal over the course of the nine treatment cycles. A notable exception were drugs and human metabolites that are amenable to hydrolysis, namely atenolol, benzoylecgonine and norcocaine. The only pathway with clear evidence for acclimation upon repeat renewal of the wastewater was the oxidative degradation of VLS: the conversion of its first-generation TP (VLS TP336) became more efficient over time leading to the formation of VLS acid, which turned out to be quite resistant to further degradation.

If exposure assessment focuses exclusively on the parent compounds, human drug metabolites and persistent TPs may go unnoticed. In this context, receiving waters may best be defined as a complex mixture of xenobiotics comprising intact parent compounds, metabolites and TPs whose activities may have ecological implications. This can be useful in the context of the WFD, and daughter directives, in the characterization of river basin specific pollutants, and delimitation of mixing areas affected by discharges

**Acknowledgments**

This study has been financially supported by the EU through the PRIMA project (INWAT 201980E121). This work was supported by the Spanish Ministry of Science and Innovation (Project CEX2018-000794-S). The authors also acknowledge SCIEX for providing the loan instrument LC/HRMS QTOF X500R. The EU is not liable for any use that may be made of the information contained therein.

Supplementary information

# Retrospective mass spectrometric analysis of wastewater-fed mesocosms to assess the degradation of drugs and their human metabolites

Laia Sabater-Liesa[1], Nicola Montemurro[1*], Antoni Ginebreda[1], Damià Barceló[1], Peter Eichhorn[1], and Sandra Pérez[1]

[1]ENFOCHEM, Department of Environmental Chemistry, IDAEA-CSIC, Jordi Girona 18-26, 08034 Barcelona, Spain

*corresponding author

**Table PIII S1**. User-built database for suspect list screening of TPs

| Substance | | Monoisotopic mass | $[M+H]^+$ | Chemical Formula | SMILES | Reference |
|---|---|---|---|---|---|---|
| Atenolol | | 266.1630 | 267.1708 | C14H22N2O3 | CC(C)NCC(COc1ccc(cc1)CC(=O)N)O | |
| | Atenolol-acid | 267.1465 | 268.1543 | C14H21NO4 | CC(C)NCC(COc1ccc(cc1)CC(=O)O)O | (Radjenović et al., 2008) |
| | Hydroxy-atenolol | 269.1543 | 270.1621 | C14H22N2O4 | CC(C)NCC(COC1=CC=C(C=C1)C(C(=O)N)O)O | (Hermes et al., 2018) |
| | Atenolol-TP117 | 117.1148 | 118.1226 | C6H15NO | CC(CNC(C)C)O | (Xu et al., 2016) |
| | Atenolol-TP167 | 167.0941 | 168.1019 | C9H13NO2 | OC(CN)COC1=CCH=CH2C=C1 | (Xu et al., 2016) |
| Azithromycin | | 748.5085 | 749.5163 | C38H72N2O12 | CC[C@@H]1[C@@]([C@@H]([C@H](N(C[C@@H](C[C@@]([C@@H]([C@H]([C@@H]([C@H](C(=O)O1)C)O[C@H]2C[C@@]([C@H]([C@@H](O2)C)O)(C)OC)C)O[C@H]3[C@@H]([C@H](C[C@H](O3)C)N(C)C)O)(C)O)C)C)O)(C)O | |
| | Azithromycin-TP | 828.4749 | 829.4827 | C38H73N2O15P | C[C@@H]([C@]([C@H]1C)([H])O[C@H]2C[C@@](C)(OC)[C@@H](O)[C@H](C)O2)[C@@]([C@](C)(O)C[C@@H](C)CN(C)[C@H](C)[C@@H](O)[C@](C)(O)[C@@H](CC)OC1=O)([H])O[C@@H]3O[C@H](C)C[C@H](N(C)C)[C@H]3OP(O)(O)=O | (Terzic et al., 2011) |

| Substance | | Monoisotopic mass | $[M+H]^+$ | Chemical Formula | SMILES | Reference |
|---|---|---|---|---|---|---|
| Carbamazepine | | 236.0945 | 237.1023 | C15H12N2O | c1ccc2c(c1)C=Cc3ccccc3N2C(=N)O | |
| | Acridine | 179.0730 | 180.0808 | C13H9N | c1ccc2c(c1)cc3ccccc3n2 | (Jelic et al., 2012) |
| | Acridone | 195.0679 | 196.0757 | C13H9NO | c1ccc2c(c1)c(=O)c3ccccc3[nH]2 | (Jelic et al., 2012) |
| | 9-carboxylic acid-acridine | 223.0633 | 224.0711 | C14H9NO2 | OC(=O)C1=C2C=CC=CC2=NC2=C1C=CC=C2 | (Hermes et al., 2018) |
| | 2-Hydroxy-CBZ | 252.0894 | 253.0972 | C15H12N2O2 | c1ccc2c(c1)C=Cc3cc(ccc3N2C(=N)O)O | (Hermes et al., 2018) |
| | 3-Hydroxy-CBZ | 252.0894 | 253.0972 | C15H12N2O2 | c1ccc2c(c1)C=Cc3ccc(cc3N2C(=O)N)O | (Hermes et al., 2018) |
| | Oxacarbazepine (Trileptan) | 252.0894 | 253.0972 | C15H12N2O2 | c1ccc2c(c1)CC(=O)c3ccccc3N2C(=O)N | ChemSpider |
| | 10-Hydroxy-CBZ | 254.1050 | 255.1128 | C15H14N2O2 | NC(=O)N1c2ccccc2CC(O)c3ccccc13 | (Hermes et al., 2018) |
| | Carbamazepine-o-quinone | 266.0687 | 267.0765 | C15H10N2O3 | c1ccc2c(c1)ccc-3cc(=O)c(=O)cc3n2C(=O)N | ChemSpider |
| | 11-Keto Oxcarbazepine | 266.0687 | 267.0765 | C15H10N2O3 | c1ccc2c(c1)c(=O)c(=O)c3ccccc3n2C(=O)N | ChemSpider |
| | 10-Methoxycarbamazepine | 266.1050 | 267.1128 | C16H14N2O2 | COC1=Cc2ccccc2N(c3c1cccc3)C(=O)N | ChemSpider |
| | 2,3-Dihydroxycarbamazepine | 268.0843 | 269.0921 | C15H12N2O3 | c1ccc2c(c1)C=Cc3cc(c(cc3N2C(=O)N)O)O | ChemSpider |
| | 10,11-Dihydroxy-CBZ | 270.0999 | 271.1077 | C15H14N2O3 | O=C(N)N3c1ccccc1C(\O)=C(\O)c2c3cccc2 | (Jelic et al., 2012) |
| | 10-Bromocarbamazepine | 314.0050 | 315.0128 | C15H11BrN2O | c1ccc2c(c1)C=C(c3ccccc3N2C(=O)N)Br | ChemSpider |
| | Carbamazepine benzoquinone | 344.1156 | 345.1234 | C21H16N2O3 | C1=CC=C2C(=C1)C=CC3=CC(=O)C(=O)C=C3N2C(=O)N | ChemSpider |
| | Carbamazepine nicotinamide | 358.1425 | 359.1503 | C21H18N4O2 | c1ccc2c(c1)C=Cc3ccccc3N2C(=O)N.c1cc(cnc1)C(=O)N | (Hermes et al., 2018) |
| | Carbamazepine-10,11-dibromo- | 393.9311 | 394.9389 | C15H12Br2N2O | c1ccc2c(c1)C(C(c3ccccc3N2C(=O)N)Br)Br | ChemSpider |
| | Carbamazepine glucuronide | 412.1265 | 413.1343 | C21H20N2O7 | c1ccc2c(c1)C=Cc3ccccc3N2C(=O)NC4[C@@H]([C@H]([C@@H]([C@H](O4)C(=O)O)O)O)O | ChemSpider |
| | 2-Hydroxy-CBZ Glucuronide | 428.1215 | 429.1293 | C21H20N2O8 | O=C(N)[NH]1C2=C(C=CC=C2)C=C(O[C6H9O6])C3=C1C=CC=C3 | ChemSpider |
| | 3-Hydroxy-CBZ Glucuronide | 428.1215 | 429.1293 | C21H20N2O8 | O=C(N)[NH]1C2=C(C=CC=C2)C(O[C6H9O6])=CC3=C1C=CC=C3 | ChemSpider |

| Substance | | Monoisotopic mass | $[M+H]^+$ | Chemical Formula | SMILES | Reference |
|---|---|---|---|---|---|---|
| Citalopram | | 324.3990 | 325.4068 | C20H21FN2O | CN(C)CCCC1(c2ccc(cc2CO1)C#N)c3ccc(cc3)F | |
| | Citalopram-TP329 | 328.1582 | 329.1660 | C19H21FN2O2 | FC(C=C1)=CC=C1C(OC2)(CCCNC)C3=C2C=C(C(N)=O)C=C3 | (Beretsou et al., 2016) |
| | Citalopram-TP330 | 329.1422 | 330.1500 | C19H20FNO3 | FC(C=C1)=CC=C1C(OC2)(CCCNC)C3=C2C=C(C(O)=O)C=C3 | (Beretsou et al., 2016) |
| | Citalopram-TP339 | 338.1425 | 339.1503 | C20H19FN2O2 | FC(C=C1)=CC=C1C(OC2=O)(CCCN(C)C)C3=C2C=C(C#N)C=C3 | (Beretsou et al., 2016) |
| | Citalopram-TP341 | 340.1582 | 341.1660 | C20H21FN2O2 | FC(C=C1)=CC=C1C(OC2)(CCC[N+](C)([O-])C)C3=C2C=C(C#N)C=C3 | (Beretsou et al., 2016) |
| | Citalopram-TP343 | 342.1738 | 343.1816 | C20H23FN2O2 | FC(C=C1)=CC=C1C(OC2)(CCCN(C)C)C3=C2C=C(C(N)=O)C=C3 | (Beretsou et al., 2016) |
| | Citalopram-TP344 | 343.1578 | 344.1656 | C20H22FNO3 | FC(C=C1)=CC=C1C(OC2)(CCCN(C)C)C3=C2C=C(C(O)=O)C=C3 | (Beretsou et al., 2016) |
| | Citalopram-TP355 | 354.1374 | 355.1452 | C20H19FN2O3 | FC(C=C1)=CC=C1C(OC2=O)(CCC[N+](C)([O-])C)C3=C2C=C(C#N)C=C3 | (Beretsou et al.. 2016) |
| | Citalopram-TP357 | 356.1531 | 357.1609 | C20H21FN2O3 | FC(C=C1)=CC=C1C(OC2=O)(CCCN(C)C)C3=C2C=C(C(N)=O)C=C3 | (Beretsou et al.. 2016) |
| | Citalopram-TP359 | 358.1687 | 359.1765 | C20H23FN2O3 | FC(C=C1)=CC=C1C(OC2)(CCC[N+](C)([O-])C)C3=C2C=C(C(N)=O)C=C3 | (Beretsou et al.. 2016) |
| | Citalopram-TP360 | 359.1528 | 360.1606 | C20H22FNO4 | FC(C=C1)=CC=C1C(OC2)(CCC[N+](C)([O-])C)C3=C2C=C(C(O)=O)C=C3 | (Beretsou et al.. 2016) |

| Substance | | Monoisotopic mass | $[M+H]^+$ | Chemical Formula | SMILES | Reference |
|---|---|---|---|---|---|---|
| Diclofenac | | 295.0167 | 296.0245 | C14H11Cl2NO2 | ClC1=C(NC2=CC=CC=C2CC(O)=O)C(Cl)=CC=C1 | |
| | Diclofenac-TP225 | 225.0790 | 226.0868 | C14H11NO2 | O=C1CC2=CC=CC=C2N1C3=CC(O)=CC=C3 | (Jewell et al.. 2016) |
| | Diclofenac-TP243 | 242.9854 | 243.9932 | C10H7Cl2NO2 | ClC1=C(NC#CC#C)C(Cl)=CC=C1.O=O.[HH] | (Jewell et al.. 2016) |
| | Diclofenac-TP259 | 259.0400 | 260.0478 | C14H10NO2Cl | ClC1=CC=C(O)C=C1N2C3=CC=CC=C3CC2=O | (Jewell et al.. 2016) |
| | Diclofenac-TP273 | 272.9959 | 274.0037 | C11H9Cl2NO3 | [C5H5O3]NC1=C(Cl)C=CC=C1Cl | (Jewell et al.. 2016) |
| | Diclofenac-TP275 | 275.0349 | 276.0427 | C14H10ClNO3 | ClC1=CC(C=C/C1=N\C2=CC=CC=C2CC(O)=O)=O | (Jewell et al.. 2016) |
| | 1-(2.6-Dichlorophenyl)-2-indolinone (DCF-lactam) | 277.0061 | 278.0139 | C14H9Cl2NO | ClC1=C(N2C3=CC=CC=C3CC2=O)C(Cl)=CC=C1 | (Hermes et al.. 2018) |
| | 2-[(2.6-Dichlorophenyl)amino]benzoic acid (DCF-BA) | 281.0010 | 282.0088 | C13H9Cl2NO2 | ClC1=C(NC2=CC=CC=C2C(O)=O)C(Cl)=CC=C1 | (Jewell et al.. 2016) |
| | Diclofenac-TP285 | 284.9959 | 286.0037 | C12H9Cl2NO3 | ClC1=C(/N=C\C=C/C(CC(O)=O)=O)C(Cl)=CC=C1 | (Jewell et al.. 2016) |
| | Diclofenac-TP287 | 287.0116 | 288.0194 | C12H11Cl2NO3 | [C6H7O3]NC1=C(Cl)C=CC=C1Cl | (Jewell et al.. 2016) |
| | Diclofenac-TP293a | 293.0010 | 294.0088 | C14H9Cl2NO2 | ClC1=C(N2C3=CC=C(O)C=C3CC2=O)C(Cl)=CC=C1 | (Jewell et al.. 2016) |
| | Diclofenac-TP293b | 293.0010 | 294.0088 | C14H9Cl2NO2 | ClC1=C(N2C3=CC=CC=C3CC2=O)C(Cl)=CC(O)=C1 | (Jewell et al.. 2016) |
| | Diclofenac-TP297 | 296.9959 | 298.0037 | C13H9Cl2NO3 | ClC1=C(NC2=CC=CC=C2C(O)=O)C(Cl)=CC(O)=C1 | (Jewell et al.. 2016) |
| | 4HDQI | 308.9959 | 310.0037 | C14H9Cl2NO3 | OC(=O)Cc1ccccc1Nc2c(Cl)cc(O)cc2Cl | (Jewell et al.. 2016) |
| | 5HDQI | 308.9959 | 310.0037 | C14H9Cl2NO3 | ClC(C=CC=C1Cl)=C1/N=C(C(CC(O)=O)=O)=C2)\C=CC2=O | (Jewell et al.. 2016) |
| | Diclofenac-TP324 | 324.0068 | 325.0146 | C14H10Cl2N2O3 | ClC1=C(NC2=CC=CC=C2CC(ON=O)=O)C(Cl)=CC=C1 | (Pérez and Barceló. 2008) |
| | Diclofenac-TP340 | 340.0018 | 341.0096 | C14H10Cl2N2O4 | ClC1=CC=CC(Cl)=C1NC2=CC=C([N+]([O-])=O)C=C2CC(O)=O | (Pérez and Barceló. 2008) |
| | Diclofenac-TP343a | 343.0014 | 344.0092 | C14H11Cl2NO5 | [C8H7O5]NC1=C(Cl)C=CC=C1Cl | (Jewell et al.. 2016) |
| | Diclofenac-TP343b | 343.0014 | 344.0092 | C14H11Cl2NO5 | [C8H7O5]NC1=C(Cl)C=CC=C1Cl | (Jewell et al.. 2016) |
| | Diclofenac-TP391a | 390.9684 | 391.9762 | C14H11Cl2NO6S | ClC1=C(NC2=CC=C(OS(=O)([O-])=O)C=C2CC(O)=O)C(Cl)=CC=C1 | (Jewell et al.. 2016) |
| | Diclofenac-TP391b | 390.9684 | 391.9762 | C14H11Cl2NO6S | ClC1=C(NC2=CC=CC=C2CC(O)=O)C(Cl)=CC(OS(=O)([O])=O)=C1 | (Jewell et al.. 2016) |

| Substance | | Monoisotopic mass | $[M+H]^+$ | Chemical Formula | SMILES | Reference |
|---|---|---|---|---|---|---|
| Erythromycin | | 733.4612 | 734.4690 | C37H67NO13 | CC[C@@H]1[C@@]([C@@H]([C@H](C(=O)[C@@H](C[C@@]([C@@H]([C@H]([C@@H]([C@H](C(=O)O1)C)O[C@H]2C[C@@]([C@H]([C@@H](O2)C)O)(C)OC)C)O[C@H]3[C@@H]([C@H](C[C@H](O3)C)N(C)C)O)(C)O)C)C)O)(C)O | |
| | Erythromycin-TP704 | 703.4501 | 704.4579 | C36H66NO12 | C[C@@H]([C@@H]([C@H](C(O[C@@H]([C@H](C)[C@H](O)[C@@H](C)C1=O)CC)=O)C)O[C@H]2C[C@]([C@@H](O)[C@H](C)O2)(O)C)[C@H]([C@](C)(O)C[C@H]1C)O[C@H](O[C@@H](C[C@@H]3N(C)C)C)[C@@H]3O | (Llorca et al.. 2015) |
| | Erythromycin-TP718 | 717.4658 | 718.4736 | C37H68NO12 | C[C@@H]([C@@H]([C@H](C(O[C@@H]([C@H](C)[C@H](O)[C@@H](C)C1=O)CC)=O)C)O[C@H]2C[C@]([C@@H](O)[C@H](C)O2)(OC)C)[C@H]([C@](C)(O)C[C@H]1C)O[C@H](O[C@@H](C[C@@H]3N(C)C)C)[C@@H]3O | (Llorca et al.. 2015) |
| | Erythromycin-TP720 | 719.4450 | 720.4528 | C36H66NO13 | C[C@@H]([C@@H]([C@H](C(O[C@@H]([C@@]([C@H](O)[C@@H](C)C1=O)(C)O)CC)=O)C)O[C@H]2C[C@]([C@@H](O)[C@H](C)O2)(O)C)[C@H]([C@](C)(O)C[C@H]1C)O[C@H](O[C@@H](C[C@@H]3N(C)C)C)[C@@H]3O | (Llorca et al.. 2015) |
| | Erythromycin-TP734 | 734.4685 | 735.4763 | C37H68NO13 | C[C@@H]([C@@H]([C@H](C(O[C@@H]([C@@]([C@H](O)CC)(C)O)CC)=O)C)O[C@H]1C[C@]([C@@H](O)[C@H](C)O1)(OC)C)[C@H]([C@@H](C)/C=C(C)/C(O)=O)O[C@H](O[C@@H](C[C@@H]2N(C)C)C)[C@@H]2O | (Llorca et al.. 2015) |
| | Erythromycin-TP748 | 747.4401 | 748.4479 | C37H66NO14 | C[C@@H]([C@@H]([C@H](C(O[C@@H]([C@@]([C@H](O)[C@@H](C)C1=O)(C)O)CC)=O)C=O)O[C@H]2C[C@]([C@@H](O)[C@H](C)O2)(OC)C)[C@H]([C@](C)(O)C[C@H]1C)O[C@H](O[C@@H](C[C@@H]3N(C)C)C)[C@@H]3O | (Llorca et al.. 2015) |
| | Erythromycin-TP750 | 749.4556 | 750.4634 | C37H68N O14 | C[C@@H]([C@@H]([C@H](C(O[C@@H]([C@@]([C@H](O)[C@@H](C)C1=O)(C)O)CC)=O)CO)O[C@H]2C[C@]([C@@H](O)[C@H](C)O2)(OC)C)[C@H]([C@](C)(O)C[C@H]1C)O[C@H](O[C@@H](C[C@@H]3N(C)C)C)[C@@H]3O | (Llorca et al.. 2015) |
| | Erythromycin-TP752 | 751.4713 | 752.4791 | C37H70NO14 | C[C@@H]([C@@H]([C@H](C(O[C@@H]([C@@]([C@H](O)CC)(C)O)CC)=O)C)O[C@H]1C[C@]([C@@H](O)[C@H](C)O1)(OC)C)[C@H]([C@](C)(O)C[C@@H](C)C(O)=O)O[C@H](O[C@@H](C[C@@H]2N(C)C)C)[C@@H]2O | (Llorca et al.. 2015) |

| Substance | | Monoisotopic mass | $[M+H]^+$ | Chemical Formula | SMILES | Reference |
|---|---|---|---|---|---|---|
| Iopromide | | 790.8697 | 791.8775 | C18H24I3N3O8 | CN(CC(CO)O)C(=O)c1c(c(c(c(c1I)NC(=O)COC)I)C(=O)NCC(CO)O)I | |
| | Iopromide-TP451 | 451.0235 | 452.0313 | C14H19O6N3I | O=C(N)C1=C(I)C(C(NCC(O)CO)=O)=CC(NC(COC)=O)=C1 | (Gros et al.. 2014) |
| | Iopromide-TP465 | 465.0392 | 466.0470 | C15H21O6N3I | O=C(NC)C1=C(I)C(C(NCC(O)CO)=O)=CC(NC(COC)=O)=C1 | (Gros et al.. 2014) |
| | Iopromide-TP525A | 525.0603 | 526.0681 | C17H25O8N3I | O=C(NCC(O)CO)C1=C([H])C(C(NCC(O)CO)=O)=C(I)C(NC(COC)=O)=C1[H] | (Gros et al.. 2014) |
| | Iopromide-TP577 | 576.9202 | 577.9280 | C14H18O6N3I2 | O=C(N)C1=C(I)C(C(NCC(O)CO)=O)=C(I)C(NC(COC)=O)=C1 | (Gros et al.. 2014) |
| | Iopromide-TP643 | 642.7962 | 643.8040 | C12H12I3N3O4 | IC1=C(NC(COC)=O)C(I)=C(C(N)=O)C(I)=C1C(NC)=O | (Schulz et al.. 2008) |
| | Iopromide-TP651 | 650.9569 | 651.9647 | C17H24O8N3I2 | O=C(NCC(O)CO)C1=C(I)C(C(NCC(O)CO)=O)=C(I)C(NC(COC)=O)=C1 | (Gros et al.. 2014) |
| | Iopromide-TP665 | 664.9726 | 665.9804 | C18H26O8N3I2 | O=C(N(C)CC(O)CO)C1=C(I)C(C(NCC(O)CO)=O)=C(I)C(NC(COC)=O)=C1 | (Gros et al.. 2014) |
| | Iopromide-TP681 | 680.9677 | 681.9755 | C18H26O9N3I2 | O=C(N(C)CC(O)CO)C1=C(I)C(C(NCC(O)CO)=O)=C(I)C(NC(COC)=O)=C1O | (Gros et al.. 2014) |
| | Iopromide-TP701 | 700.8017 | 701.8095 | C14H14I3N3O6 | IC1=C(NC(COC)=O)C(I)=C(C(N)=O)C(I)=C1C(N(C)CC(O)=O)=O | (Schulz et al.. 2008) |
| | Iopromide-TP729 | 728.7966 | 729.8044 | C15H14I3N3O7 | IC1=C(NC(COC)=O)C(I)=C(C(N)=O)C(I)=C1C(N(C)CC(C(O)=O)=O)=O | (Schulz et al.. 2008) |
| | Iopromide-TP731 | 730.8122 | 731.8200 | C15H16I3N3O7 | IC1=C(NC(COC)=O)C(I)=C(C(N)=O)C(I)=C1C(N(C)CC(O)C(O)=O)=O | (Schulz et al.. 2008) |
| | Iopromide-TP759 | 758.8072 | 759.8150 | C16H16I3N3O8 | IC1=C(NC(COC)=O)C(I)=C(C(NCCCO)=O)C(I)=C1C(N(C)CCCO)=O | (Pérez et al.. 2006) |
| | Iopromide-TP805 | 804.8490 | 805.8563 | C18H22I3N3O9 | IC1=C(NC(COC)=O)C(I)=C(C(NCC(O)CO)=O)C(I)=C1C(N(C)CC(O)C(O)=O)=O | (Pérez et al.. 2006) |
| | Iopromide-TP819 | 818.8283 | 819.8361 | C18H20I3N3O10 | IC1=C(NC(COC)=O)C(I)=C(C(NCC(O)C(O)=O)=O)C(I)=C1C(N(C)CC(O)C(O)=O)=O | (Pérez et al.. 2006) |

| Substance | | Monoisotopic mass | $[M+H]^+$ | Chemical Formula | SMILES | Reference |
|---|---|---|---|---|---|---|
| Ketoprofen | | 254.0943 | 255.1021 | C16H14O3 | CC(c1cccc(c1)C(=O)c2ccccc2)C(=O)O | |
| | 3-(Keto-carboxymethyl)hydratropic acid | 220.0377 | 221.0455 | C11H10O5 | O=C(C(C1=CC=CC(C(C(O)=O)=O)=C1)C)O | (Quintana et al.. 2005) |
| | 3-(Hydroxy-carboxymethyl)hydratropic acid | 222.0534 | 223.0612 | C11H12O5 | CC(C1=CC(=CC=C1)C(C(=O)O)O)C(=O)O | (Quintana et al.. 2005) |
| Lamotrigine | | 255.0079 | 256.0157 | C9H7Cl2N5 | c1cc(c(c(c1)Cl)Cl)c2c(nc(nn2)N)N | |
| | 5-desamino-5 oxo-2,5 dihydro lamotrigine | 255.9919 | 256.9997 | C9H6Cl2N4O | C1=CC(=C(C(=C1)Cl)Cl)C2=NN=C(NC2=O)N | (Hannemann et al.. 2016) |
| Oxazepam | | 286.0509 | 287.0587 | C15H11ClN2O2 | c1ccc(cc1)C2=NC(C(=Nc3c2cc(cc3)Cl)O)O | |
| | Oxazepam-TP271 | 270.0560 | 271.0638 | C15H11ClN2O | ClC1=CC(C(C2=CC=CC=C2)=NC(O)=CN3)=C3C=C1 | (Kosjek et al., 2012) |
| Sitagliptin | | 407.1181 | 408.1259 | C16H15F6N5O | c1c(c(cc(c1F)F)F)C[C@H](CC(=O)N2CCn3c(nnc3C(F)(F)F)C2)N | |
| | Sitagliptin-TP176 | 173.99234 | 175.00014 | C7HF3O2 | FC1=C(F)C=C(C(O)=O)C(F)=C1 | (Henning et al.. 2019) |
| | Sitagliptin-TP190 | 188.00799 | 189.01579 | C8H3F3O2 | FC1=C(F)C=C(CC(O)=O)C(F)=C1 | (Henning et al.. 2019) |
| | Sitagliptin-TP192 | 192.06176 | 193.06956 | C6H7F3N4 | FC(F)(F)C1=NN=C2CNCCN21 | (Henning et al.. 2019) |
| | Sitagliptin-TP406 | 406.08592 | 407.09372 | C16H12F6N4O2 | FC1=C(F)C=C(CC(CC(N2CCN3C(C2)=NN=C3C(F)(F)F)=O)=O)C(F)=C1 | (Henning et al.. 2019) |
| | Sitagliptin-TP408 | 408.10157 | 409.10937 | C16H14F6N4O2 | FC1=C(F)C=C(C[C@@H](O)CC(N2CCN3C(C2)=NN=C3C(F)(F)F)=O)C(F)=C1 | (Henning et al.. 2019) |
| | Sitagliptin-TP435 | 435.11247 | 436.12027 | C17H15F6N5O2 | FC1=C(F)C=C(C[C@@H](NC=O)CC(N2CCN3C(C2)=NN=C3C(F)(F)F)=O)C(F)=C1 | (Henning et al.. 2019) |
| | Sitagliptin-TP449 | 449.12812 | 450.13592 | C18H17F6N5O2 | FC1=C(F)C=C(C[C@@H](NC(C)=O)CC(N2CCN3C(C2)=NN=C3C(F)(F)F)=O)C(F)=C1 | (Henning et al.. 2019) |
| | Sitagliptin-TP505 | 505.11795 | 506.12575 | C20H17F6N5O4 | FC1=C(F)C=C(C[C@@H](NC(/C=C/C(O)=O)=O)CC(N2CCN3C(C2)=NN=C3C(F)(F)F)=O)C(F)=C1 | (Henning et al.. 2019) |
| | Sitagliptin-TP507 | 507.1336 | 508.1414 | C20H19F6N5O4 | FC1=C(F)C=C(C[C@@H](NC(CCC(O)=O)=O)CC(N2CCN3C(C2)=NN=C3C(F)(F)F)=O)C(F)=C1 | (Henning et al.. 2019) |

| Substance | | Monoisotopic mass | $[M+H]^+$ | Chemical Formula | SMILES | Reference |
|---|---|---|---|---|---|---|
| Sulfamethoxazole | | 253.0521 | 254.0599 | C10H11N3O3S | Cc1cc(no1)NS(=O)(=O)c2ccc(cc2)N | |
| | Sulfanilamide | 172.0307 | 173.0385 | C6H8N2O2S | c1cc(ccc1N)S(=O)(=O)N | ChemSpider |
| | Sulfanilic-acid | 173.0147 | 174.0225 | C6H7NO3S | c1cc(ccc1N)S(=O)(=O)O | ChemSpider |
| | 4-nitro-SMX | 283.0263 | 284.0341 | C10H9N3O5S | O=S(C1=CC=C([N+]([O-])=O)C=C1)(NC2=NOC(C)=C2)=O | (Nödler et al.. 2012) |
| Trimethoprim | | 290.1379 | 291.1457 | C14H18N4O3 | COc1cc(cc(c1OC)OC)Cc2c[nH]c(=N)[nH]c2=N | |
| | 3-desmethyl-TMP | 276.1222 | 277.1300 | C13H16N4O3 | COc1cc(Cc2cc(N)nc(N)n2)cc(O)c1OC | (Hermes et al.. 2018) |
| | 5-(2,4,5-Trimethoxy)-2,4-pyrimidinediamnine | 304.1172 | 305.1250 | C14H16N4O4 | COc1cc(cc(OC)c1OC)C(=O)c2cnc(N)nc2N | (Hermes et al.. 2018) |
| | Trimethoprim-TP306 | 306.1328 | 307.1406 | C14H18N4O4 | NC1=NC(N)=NC=C1C(O)C2=CC(OC)=C(OC)C(OC)=C2 | (Eichhorn et al.. 2005) |
| | Trimethoprim-TP324 | 324.1434 | 325.1512 | C14H21N4O5 | NC1NC(N)=NC(C1(O)CC2=CC(OC)=C(OC)C(OC)=C2)=O | (Eichhorn et al.. 2005) |
| Valsartan | | 435.5188 | 436.5266 | C24H29N5O3 | CCCCC(=O)N(Cc1ccc(cc1)c2ccccc2c3[nH]nnn3)[C@@H](C(C)C)C(=O)O | |
| | Valsartan-TP252 | 251.1171 | 252.1249 | C14H13N5 | NCC1=CC=C(C2=CC=CC=C2C3=NN=NN3)C=C1 | (Helbling et al., 2010) |
| | Valsartan-acid | 266.0799 | 267.0877 | C14H10N4O2 | OC(=O)c1ccc(cc1)c2ccccc2c3nnn[nH]3 | (Hermes et al.. 2018) |
| | Valsartan-TP336 | 335.1746 | 336.1824 | C19H21N5O | CCCCC(NCC1=CC=C(C2=CC=CC=C2C3=NN=NN3)C=C1)=O | (Helbling et al.. 2010) |
| Venlafaxine | | 277.4018 | 278.4096 | C17H27NO2 | CN(C)CC(c1ccc(cc1)OC)C2(CCCCC2)O | |
| | Venlafaxine-TP258 | 257.1780 | 258.1858 | C17H24NO | CN(C)CC(C1=CC=CC=C1)C2=CC(OC)C=CC2 | (Boix et al.. 2016) |
| | Venlafaxine-TP264 | 263.1886 | 264.1964 | C16H26NO2 | CN(C)CC(C1=CC=C(O)C=C1)C2(O)CCCCC2 | (Boix et al., 2016) |
| | Venlafaxine-TP274 | 273.1729 | 274.1807 | C17H24NO2 | CN(C)CC(C1=CC=C(O)C=C1)C2=CC(OC)C=CC2 | (Boix et al., 2016) |
| | Venlafaxine-TP292 | 291.1835 | 292.1913 | C17H26NO3 | OC1(CC(CCC1)=O)C(C2=CC=C(OC)C=C2)CN(C)C | (Boix et al., 2016) |
| | Venlafaxine-N-Oxide | 293.1991 | 294.2069 | C17H27NO3 | COc1ccc(cc1)C(C[N+](C)(C)[O-])C2(O)CCCCC2 | (Hermes et al.. 2018) |
| | Venlafaxine-TP294 | 293.1991 | 294.2069 | C17H28NO3 | OC1(CC(O)CCC1)C(C2=CC=C(OC)C=C2)CN(C)C | (Boix et al., 2016) |

**Table PIII S2**. Suspect list of metabolites from the database NIST 2017 (SCIEX)

| Compound | | Monoisotopic mass | Precursor (Q1) [M+H]+ | Fragment (Q3) [M+H]+ | Chemical Formula | Retention time | SMILES |
|---|---|---|---|---|---|---|---|
| 2,4-Dihydroxyphenyl (phenyl)methanone | | 214.0625 | 215.0703 | 137.0238 | C13H10O3 | 4.25 | C1=CC=C(C=C1)C(=O)C2=C(C=C(C=C2)O)O |
| 5-Benzoyl-4-hydroxy-2-methoxybenzenesulfonic acid | | 308.0349 | 309.04274 | 53.0025 | C14H12O6S | 1.17 | COc1cc(O)c(cc1S(O)(=O)=O)C(=O)c2ccccc2 |
| Aceprometazine | | 326.14476 | 327.15256 | 86.0963 | C19H22N2OS | 3.16 | CC(CN1c2ccccc2Sc3c1cc(cc3)C(=O)C)N(C)C |
| Acetaminophen | | 151.0628 | 152.0706 | 107.0373 | C8H9NO2 | 0.97 | CC(=O)Nc1ccc(cc1)O |
| | 3-Hydroxyacetaminophen | 167.0577 | 168.0655 | 108.0444 | C8H9NO3 | 0.57 | CC(=O)Nc1ccc(c(c1)O)O |
| | 3-Cysteinylacetaminophen | 270.0669 | 271.0747 | 182.0280 | C11H14N2O4S | 2.28 | CC(=O)Nc1ccc(c(c1)SC[C@@H](C(=O)O)N)O |
| | Acetaminophen sulfate | 231.0196 | 232.0274 | 152.0698 | C8H9NO5S | 0.97 | CC(=O)Nc1ccc(cc1)OS(=O)(=O)O |
| | S-Methyl-3-thioacetaminophen | 197.0505 | 198.0583 | 108.0443 | C9H11NO2S | 2.12 | CC(=O)Nc1ccc(c(c1)SC)O |
| Alprazolam | | 308.0824 | 309.0902 | 281.0712 | C17H13ClN4 | 8.23 | Cc1nnc2n1-c3ccc(cc3C(=NC2)c4ccccc4)Cl |
| | 4-Hydroxyalprazolam | 324.0773 | 325.08507 | 298.0751 | C17H13ClN4O | 3.87 | Cc1nnc2n1-c3ccc(cc3C(=NC2O)c4ccccc4)Cl |
| | alfa-Hydroxyalprazolam | 324.0773 | 325.0851 | 297.0659 | C17H13ClN4O | 3.28 | C1C2=NN=C(N2C3=C(C=C(C=C3)Cl)C(=N1)C4=CC=CC=C4)CO |
| Amitriptyline | | 277.1825 | 278.1903 | 91.0540 | C20H23N | 2.68 | CN(C)CCC=C1c2ccccc2CCc3c1cccc3 |
| Atipamezole | | 212.1308 | 213.13862 | 183.0914 | C14H16N2 | 1.83 | CCC1(Cc2ccccc2C1)c3cnc[nH]3 |

| Compound | | Monoisotopic mass | Precursor (Q1) [M+H]+ | Fragment (Q3) [M+H]+ | Chemical Formula | Retention time | SMILES |
|---|---|---|---|---|---|---|---|
| Atorvastatin | | 558.2525 | 559.2603 | 262.1028 | C33H35FN2O5 | 3.36 | CC(C)c1c(c(c(n1CC[C@H](C[C@H](CC(=O)O)O)O)c2ccc(cc2)F)c3ccccc3)C(=O)Nc4ccccc4 |
| | 2-Hydroxyatorvastatin lactone | 556.2368 | 557.24463 | 537.2178 | C33H33FN2O5 | 2.54 | CC(C)C1=C(C(=C(N1CCC2CC(CC(=O)O2)O)C3=CC=C(C=C3)F)C4=CC=CC=C4)C(=O)NC5=CC=CC=C5O |
| | 4-Hydroxyatorvastatin lactone | 556.23683 | 557.24463 | 537.2178 | C33H33FN2O5 | 2.54 | O=C(C1=C(C(C)C)N(CC[C@H](C[C@@H](O)C2)OC2=O)C(C3=CC=C(F)C=C3)=C1C4=CC=CC=C4)NC5=CC=C(O)C=C5 |
| | Defluoroatorvastatin | 540.2619 | 541.2697 | 422.2317 | C33H36N2O5 | 5.29 | O=C(C1=C(C(C)C)N(CC[C@@H](O)C[C@@H](O)CC(O)=O)C(C2=CC=CC=C2)=C1C3=CC=CC=C3)NC4=CC=CC=C4 |
| | O-Hydroxyatorvastatin | 574.2474 | 575.25519 | 440 | C33H35FN2O6 | 0.42 | CC(C)c1c(c(c(n1CC[C@H](C[C@H](CC(=O)O)O)O)c2ccc(cc2)F)c3ccccc3)C(=O)Nc4ccccc4O |
| Azithromycin | | 748.5080 | 749.5158 | 83.0495 | C38H72N2O12 | 3.96 | CC[C@@H]1[C@@]([C@@H]([C@H](N(C[C@@H](C[C@@]([C@@H]([C@H]([C@@H]([C@H](C(=O)O1)C)O[C@H]2C[C@@]([C@H]([C@@H](O2)C)O)(C)OC)C)O[C@H]3[C@@H]([C@H](C[C@H](O3)C)N(C)C)O)(C)O)C)C)O)(C)O |
| Benzotriazole | | 119.0478 | 120.0556 | 65.0382 | C6H5N3 | 2.03 | C1=CC2=NNN=C2C=C1 |
| | 2-(2-Hydroxy-5-methylphenyl)benzotriazole | 225.0897 | 226.09749 | 120.0555 | C13H11N3O | 2.34 | CC1=CC(=C(C=C1)O)N2N=C3C=CC=CC3=N2 |
| | 1H-Benzotriazole-5-carboxylic acid. 1-(1-methylethyl) | 205.0846 | 206.0924 | 164.0451 | C10H11N3O2 | 2.56 | CC(C)N1C2=C(C=C(C=C2)C(=O)O)N=N1 |
| Bromazepam | | 315.0002 | 316.008 | 182.0836 | C14H10BrN3O | 2.36 | c1ccnc(c1)C2=NCC(=O)Nc3c2cc(cc3)Br |
| | 3-Hydroxybromazepam | 330.9951 | 332.0029 | 286.9817 | C14H10BrN3O2 | 2.75 | c1ccnc(c1)C2=NC(C(=O)Nc3c2cc(cc3)Br)O |
| | Flubromazepam | 331.9955 | 333.00333 | 183.9753 | C15H10BrFN2O | 2.72 | c1ccc(c(c1)C2=NCC(=O)Nc3c2cc(cc3)Br)F |

| Compound | | Monoisotopic mass | Precursor (Q1) [M+H]+ | Fragment (Q3) [M+H]+ | Chemical Formula | Retention time | SMILES |
|---|---|---|---|---|---|---|---|
| Budesonide | | 430.2350 | 431.24282 | 413.2312 | C25H34O6 | 3.97 | CCCC1O[C@@H]2C[C@H]3[C@@H]4CCC5=CC(=O)C=C[C@@]5([C@H]4[C@H](C[C@@]3([C@@]2(O1)C(=O)CO)C)O)C |
| | 6.alpha-Hydroxybudesonide | 446.2299 | 447.23773 | 339.158 | C25H34O7 | 3.51 | CCCC1O[C@@H]2C[C@H]3[C@@H]4C[C@@H](C5=CC(=O)C=C[C@@]5([C@H]4[C@H](C[C@@]3([C@@]2(O1)C(=O)CO)C)O)C)O |
| Buprofezin | | 305.15566 | 306.16346 | 57.0697 | C16H23N3OS | 1.91 | CC(C)N1/C(=N/C(C)(C)C)/SCN(C1=O)c2ccccc2 |
| Bupropion | | 239.1072 | 240.11497 | 131.072 | C13H18ClNO | 2.56 | CC(C(=O)c1cccc(c1)Cl)NC(C)(C)C |
| | Erythro/threo-Hydrobupropion | 241.1228 | 242.13062 | 168.0572 | C13H20ClNO | 2.97 | CC(C(C1=CC(=CC=C1)Cl)O)[NH2+]C(C)(C)C |
| Caffeine | | 194.0799 | 195.0877 | 138.0655 | C8H10N4O2 | 1.77 | Cn1cnc2c1c(=O)n(c(=O)n2C)C |
| | beta-Hydroxyethyltheophylline | 224.0904 | 225.0982 | 124.0507 | C9H12N4O3 | 1,45 | CN1C2=C(C(=O)N(C1=O)C)N(C=N2)CCO |
| | 1,3,9-Trimethylxanthine | 194.0799 | 195.0877 | 138.0728 | C8H10N4O2 | 1,77 | Cn1cnc2c1n(c(=O)n(c2=O)C)C |
| | 1,3-Dimethyluracil | 140.0581 | 141.0659 | 56.0493 | C6H8N2O2 | 0,43 | Cn1ccc(=O)n(c1=O)C |
| | 1,3-Dimethyluric acid | 196.0591 | 197.0669 | 57.0445 | C7H8N4O3 | 1,16 | Cn1c2c(c(=O)n(c1=O)C)[nH]c(=O)[nH]2 |
| | 1,7-Dimethyluric acid | 196.0591 | 197.0669 | 140.0453 | C7H8N4O3 | 1,37 | Cn1c2c([nH]c1=O)[nH]c(=O)n(c2=O)C |
| | 1-Methyluric acid | 182.0435 | 183.0513 | 126.0295 | C6H6N4O3 | 1,37 | Cn1c(=O)c2c([nH]c(=O)[nH]2)[nH]c1=O |
| | 1-Methylxanthine | 166.0486 | 167.0564 | 110.0348 | C6H6N4O2 | 0,71 | Cn1c(=O)c2c([nH]c1=O)nc[nH]2 |
| | 3-Methyluric acid | 182.0435 | 183.0513 | 57.0444 | C6H6N4O3 | 1,16 | Cn1c2c(c(=O)[nH]c1=O)[nH]c(=O)[nH]2 |
| | 3-Methylxanthine | 166.0486 | 167.0564 | 124.0499 | C6H6N4O2 | 0,75 | Cn1c2c(c(=O)[nH]c1=O)[nH]cn2 |
| | 5-Acetylamino-6-amino-3-methyluracil | 198.0748 | 199.0826 | 181.0714 | C7H10N4O3 | 1,45 | CC(=O)Nc1c([nH]c(=O)n(c1=O)C)N |

| Compound | | Monoisotopic mass | Precursor (Q1) [M+H]+ | Fragment (Q3) [M+H]+ | Chemical Formula | Retention time | SMILES |
|---|---|---|---|---|---|---|---|
| Caffeine (cont.) | 5-Acetylamino-6-formylamino-3-methyluracil | 226.0697 | 227.0775 | 185.0673 | C8H10N4O4 | 2,79 | CC(=O)Nc1c([nH]c(=O)n(c1=O)C)NC=O |
| | 7-Methyluric acid | 182.0435 | 183.0513 | 69.0241 | C6H6N4O3 | 1,53 | Cn1c2c([nH]c(=O)[nH]c2=O)[nH]c1=O |
| | 7-Methylxanthine | 166.0486 | 167.0564 | 84.9600 | C6H6N4O2 | 0,36 | Cn1cnc2c1c(=O)[nH]c(=O)[nH]2 |
| | 8-Chlorotheophylline | 214.0252 | 215.0330 | 158.0116 | C7H7ClN4O2 | 7,53 | Cn1c2c(c(=O)n(c1=O)C)[nH]c(n2)Cl |
| | Paraxanthine | 180.0642 | 181.0720 | 124.0506 | C7H8N4O2 | 1,45 | Cn1cnc2c1c(=O)n(c(=O)[nH]2)C |
| | Tetramethyluric acid | 224.0904 | 225.0982 | 153.0534 | C9H12N4O3 | 1.5 | Cn1c2c(n(c1=O)C)n(c(=O)n(c2=O)C)C |
| | Theobromine | 180.0642 | 181.0720 | 138.0658 | C7H8N4O2 | 1.22 | Cn1cnc2c1c(=O)[nH]c(=O)n2C |
| | Theophylline | 180.0642 | 181.0720 | 124.0510 | C7H8N4O2 | 1.45 | Cn1c2c(c(=O)n(c1=O)C)nc[nH]2 |
| Candesartan cilexetil | | 610.2535 | 611.26126 | 207.0884 | C33H34N6O6 | 0.71 | CCOc1nc2cccc(c2n1Cc3ccc(cc3)c4ccccc4c5[nH]nnn5)C(=O)OC(C)OC(=O)OC6CCCCC6 |
| Carbamazepine | | 236.0944 | 237.1022 | 194.0949 | C15H12N2O | 2.79 | c1ccc2c(c1)C=Cc3ccccc3N2C(=N)O |
| | Carbamazepine-10,11-epoxide | 252.0894 | 253.0972 | 180.0798 | C15H12N2O2 | 2.58 | c1ccc2c(c1)C3C(O3)c4ccccc4N2C(=O)N |
| | 10,11-Dihydro-10-hydroxycarbamazepine | 254.1050 | 255.1128 | 194.0965 | C15H14N2O2 | 2.79 | c1ccc2c(c1)CC(c3ccccc3N2C(=O)N)O |
| | cis-10,11-Dihydroxy-10,11-dihydrocarbamazepine | 270.0999 | 271.1077 | 180.0802 | C15H14N2O3 | 2.58 | C1=CC=C2C(=C1)C(C(C3=CC=CC=C3N2C(=O)N)O)O |
| Cetirizine | | 388.1549 | 389.16265 | 201.0467 | C21H25ClN2O3 | 3.81 | c1ccc(cc1)C(c2ccc(cc2)Cl)N3CCN(CC3)CCOCC(=O)O |
| | rac-Cetirizine N-oxide | 404.1498 | 405.15756 | 201.0466 | C21H25ClN2O4 | 3.15 | C1C[N+](CCN1C(C2=CC=CC=C2)C3=CC=C(C=C3)Cl)(CCOCC(=O)O)[O-] |

| Compound | | Monoisotopic mass | Precursor (Q1) [M+H]+ | Fragment (Q3) [M+H]+ | Chemical Formula | Retention time | SMILES |
|---|---|---|---|---|---|---|---|
| Chlordiazepoxide | | 299.0820 | 300.08982 | 227.0494 | C16H14ClN3O | 2.34 | CNC1=Nc2ccc(cc2C(=[N+](C1)[O-])c3ccccc3)Cl |
| | Norchlordiazepoxide | 285.0664 | 286.07417 | 268.0604 | C15H12ClN3O | 2.00 | c1ccc(cc1)C2=[N+](CC(=Nc3c2cc(cc3)Cl)N)[O-] |
| Chlorpromazine | | 318.0952 | 319.10302 | 86.0982 | C17H19ClN2S | | CN(C)CCCN1C2=CC=CC=C2SC3=C1C=C(C=C3)Cl |
| Chlorpropamide | | 276.0330 | 277.04082 | 139.0059 | C10H13ClN2O3S | 4.26 | CCCNC(=O)NS(=O)(=O)c1ccc(cc1)Cl |
| Ciprofloxacin | | 331.1327 | 332.1405 | 288.1502 | C17H18FN3O3 | 3.11 | c1c2c(cc(c1F)N3CCNCC3)n(cc(c2=O)C(=O)O)C4CC4 |
| | Desethyleneciprofloxacin | 305.1171 | 306.1249 | 288.1140 | C15H16FN3O3 | 1.2 | c1c2c(cc(c1F)NCCN)n(cc(c2=O)C(=O)O)C3CC3 |
| | N-formyl ciprofloxacin | 359.1276 | 360.1354 | 342.1242 | C18H18FN3O4 | 1.5 | OC(=O)C1=CN(C2CC2)c3cc(N4CCN(CC4)C=O)c(F)cc3C1=O |
| | Ciprofloxacin Piperazinyl-N4-sulfate | 411.0895 | 412.0973 | 366.0923 | C17H18FN3O6S | 2.99 | c1c2c(cc(c1F)N3CCN(CC3)S(=O)(=O)O)n(cc(c2=O)C(=O)O)C4CC4 |
| Citalopram | | 324.1633 | 325.17107 | 109.0448 | C20H21FN2O | 3.45 | CN(C)CCCC1(c2ccc(cc2CO1)C#N)c3ccc(cc3)F |
| | Didesmethylcitalopram | 296.1320 | 297.1398 | 109.0442 | C18H17FN2O | 1.79 | c1cc(ccc1[C@]2(c3ccc(cc3CO2)C#N)CCCN)F |
| | Desmethylcitalopram | 310.1476 | 311.1554 | 109.0443 | C19H19FN2O | 1.79 | CNCCCC1(c2ccc(cc2CO1)C#N)c3ccc(cc3)F |
| Clarithromycin | | 747.4764 | 748.4842 | 158.1174 | C38H69NO13 | 3.96 | CC[C@@H]1[C@@]([C@@H]([C@H](C(=O)[C@@H](C[C@@]([C@@H]([C@H]([C@@H]([C@H](C(=O)O1)C)O[C@H]2C[C@@]([C@H]([C@@H](O2)C)O)(C)OC)C)O[C@H]3[C@@H]([C@H](C[C@H](O3)C)N(C)C)O)(C)OC)C)C)O)(C)O |
| Clobenzepam | | 315.1133 | 316.12112 | 271.0636 | C17H18ClN3O | 3.78 | CN(C)CCN1c2ccc(cc2Nc3ccccc3C1=O)Cl |
| Clofibrate | | 242.0705 | 243.07825 | 59.05 | C12H15ClO3 | 2.22 | CCOC(=O)C(C)(C)Oc1ccc(cc1)Cl |
| | Clofibric acid acyl-beta-D-glucuronide | 390.0712 | 391.0790 | 213.0322 | C16H19ClO9 | 2.35 | CC(C)(C(=O)O[C@H]1[C@@H]([C@H]([C@@H]([C@H](O1)C(=O)O)O)O)O)Oc2ccc(cc2)Cl |

| Compound | | Monoisotopic mass | Precursor (Q1) [M+H]+ | Fragment (Q3) [M+H]+ | Chemical Formula | Retention time | SMILES |
|---|---|---|---|---|---|---|---|
| Clonazepam | | 315.0406 | 316.0484 | 270.0562 | C15H10ClN3O3 | 4.03 | c1ccc(c(c1)C2=NCC(=O)Nc3c2cc(cc3)[N+](=O)[O-])Cl |
| | 7-Aminoclonazepam | 285.0664 | 286.07417 | 121.0759 | C15H12ClN3O | 2.98 | c1ccc(c(c1)C2=NCC(=O)Nc3c2cc(cc3)N)Cl |
| | Methylclonazepam | 329.0562 | 330.064 | 284.0000 | C16H12ClN3O3 | 2.22 | CN1c2ccc(cc2C(=NCC1=O)c3ccccc3Cl)[N+](=O)[O-] |
| | Trimethylsilyl clonazepam | 387.0801 | 388.0879 | 342.0000 | C18H18ClN3O3Si | 8.24 | C[Si](C)(C)N1c2ccc(cc2C(=NCC1=O)c3ccccc3Cl)[N+](=O)[O-] |
| Clotiazepam | | 318.0588 | 319.06664 | 291.0000 | C16H15ClN2OS | 4.03 | CCc1cc2c(s1)N(C(=O)CN=C2c3ccccc3Cl)C |
| Clozapine | | 326.1293 | 327.1371 | 270.079 | C18H19ClN4 | | CN1CCN(CC1)C2=Nc3cc(ccc3Nc4c2cccc4)Cl |
| | Norclozapine | 312.1137 | 313.12145 | 270.0801 | C17H17ClN4 | 4.84 | c1ccc2c(c1)C(=Nc3cc(ccc3N2)Cl)N4CCNCC4 |
| Cocaine | | 303.1465 | 304.15433 | 182.1153 | C17H21NO4 | 2.76 | CN1[C@H]2CC[C@@H]1[C@H]([C@H](C2)OC(=O)c3ccccc3)C(=O)OC |
| | 4-Fluorotropacocaine | 263.1316 | 264.1394 | 124.1122 | C15H18FNO2 | 3.79 | CN1C2CCC1CC(C2)OC(=O)c3ccc(cc3)F |
| | 3',4',5'-Trimethoxytropacocaine | 335.1728 | 336.1806 | 124.1121 | C18H25NO5 | 1.67 | CN1C2C(OC)CC1C(C(C2OC)OC(C3=CC=CC=C3)=O)OC |
| | 3',4',5'-Trimethoxycocaine | 393.1782 | 394.1860 | 182.1176 | C20H27NO7 | 2.45 | CN1C2CCC1C(C(C2)OC(C3=CC(OC)=C(OC)C(OC)=C3)=O)C(OC)=O |
| | Benzoylecgonine | 289.1309 | 290.1387 | 168.1008 | C16H19NO4 | 2.16 | CN1[C@H]2CC[C@@H]1[C@H]([C@H](C2)OC(=O)c3ccccc3)C(=O)O |
| | Cocaethylene | 317.1622 | 318.16998 | 196.1334 | C18H23NO4 | 4.04 | CCOC(=O)[C@@H]1[C@H]2CC[C@H](N2C)C[C@@H]1OC(=O)c3ccccc3 |
| | Hydroxybenzoylecgonine | 305.1258 | 306.1336 | 168.1000 | C16H19NO5 | 2.16 | O=C([C@H]1[C@H](C[C@]2(N([C@]1([H])CC2)C)O)OC(C3=CC=CC=C3)=O)O |
| | Isopropylcocaine | 331.1778 | 332.1856 | 105.0417 | C19H25NO4 | 5.93 | COC(C(C(C1)OC(C2=CC=CC=C2)=O)C3CCC1N3CC(C)C)=O |
| | m-Hydroxycocaine | 319.1415 | 320.1493 | 182.1206 | C17H21NO5 | 2.76 | CN1[C@H]2CC[C@@H]1[C@H]([C@H](C2)OC(=O)c3cccc(c3)O)C(=O)OC |
| | m-Hydroxybenzoylecgonine | 305.1258 | 306.1336 | 137.0247 | C16H19NO5 | 2 | CN1[C@H]2CC[C@@H]1[C@H]([C@H](C2)OC(=O)c3cccc(c3)O)C(=O)O |
| | Methylecgonine | 199.1203 | 200.12812 | 182.1175 | C10H17NO3 | 0.44 | CN1[C@H]2CC[C@@H]1[C@H]([C@H](C2)O)C(=O)OC |

| | | | | | | | |
|---|---|---|---|---|---|---|---|
| Cocaine (cont.) | N-Formylnornicotine | 176.0944 | 177.10224 | 80.0493 | C10H12N2O | 0.75 | c1cc(cnc1)C2CCCN2C=O |
| | Norcocaine | 289.1309 | 290.1387 | 136.0759 | C16H19NO4 | 3.09 | COC(=O)[C@@H]1[C@H]2CC[C@H](N2)C[C@@H]1OC(=O)c3ccccc3 |
| | Norcocaine Desmethyl | 275.1152 | 276.12303 | | C15H17NO4 | 2.18 | O=C(C1=CC=CC=C1)O[C@@H](C[C@H]2N[C@@H]3CC2)[C@@H]3C(O)=O |
| | p-Fluorococaine | 321.1371 | 322.1449 | 182.1175 | C17H20FNO4 | 2.76 | CN1C2CCC1C(C(C2)OC(=O)c3ccc(cc3)F)C(=O)OC |
| | Tropacocaine | 245.1411 | 246.1489 | 124.1121 | C15H19NO2 | 3.79 | CN1[C@@H]2CC[C@H]1C[C@@H](C2)OC(=O)c3ccccc3 |
| | trans-Cinnamoylcocaine | 329.1622 | 330.1700 | 182.1176 | C19H23NO4 | 2.72 | CN1C2CCC1C(C(C2)OC(=O)/C=C/c3ccccc3)C(=O)OC |
| | trans-3,4,5-Trimethoxycinnamoylcocaine | 419.1939 | 420.2017 | 221.0809 | C22H29NO7 | 8.23 | COC(C(C(C1)OC(C2=CC=CC=C2)=O)C3CCC1(OC)N3C(OC)(OC)C(/C=C/C4=CC=CC=C4)=O)=O |
| Codeine | | 299.1516 | 300.15942 | 152.0618 | C18H21NO3 | 1.67 | CN1CC[C@]23c4c5ccc(c4O[C@H]2[C@H](C=C[C@H]3[C@H]1C5)O)OC |
| | 6-Acetylcodeine | 341.1622 | 342.1700 | 152.0621 | C20H23NO4 | 2.31 | CC(=O)O[C@H]1C=C[C@H]2[C@H]3Cc4ccc(c5c4[C@]2([C@H]1O5)CCN3C)OC |
| | 6-Monocetylcodeine | 341.1622 | 342.1700 | 225.0918 | C20H23NO4 | 3.89 | COC1=C2O[C@@H]3[C@]45C2=C(C=C1)C[C@@H](N(CC5)C)[C@]4([H])C=C[C@]3(CCCCCCCCCCCCCCCC)O |
| | Codeine glucuronide | 475.1837 | 476.1915 | 300.1564 | C24H29NO9 | 5.96 | CN1CC[C@]23c4c5ccc(c4O[C@H]2[C@H](C=C[C@H]3[C@H]1C5)O[C@H]6[C@@H]([C@H]([C@@H]([C@H](O6)C(=O)O)O)O)O)OC |
| | Dihydrocodeine | 301.1673 | 302.1751 | 199.0756 | C18H23NO3 | 3.74 | CN1CC[C@]23c4c5ccc(c4O[C@H]2[C@H](CC[C@H]3[C@H]1C5)O)OC |
| | Methylcodeine | 313.1673 | 314.1751 | 58.0649 | C19H23NO3 | 2.99 | CN1CC[C@]23c4c5ccc(c4O[C@H]2[C@H](C=C[C@H]3[C@H]1C5)OC)OC |
| | Norcodeine | 285.1360 | 286.1438 | 152.0619 | C17H19NO3 | 1.58 | COc1ccc2c3c1O[C@@H]4[C@]35CCN[C@H](C2)[C@@H]5C=C[C@@H]4O |
| | O6, N-Diacetylnorcodeine | 369.1571 | 370.1649 | 86.0598 | C21H23NO5 | 2.71 | O[C@@H](C=C1)[C@@]2(C(C)=O)[C@@]3([C@]1([H])[C@@](N(C(C)=O)CC3)([H])C4)C5=C4C=CC(OC)=C5O2 |
| Demoxepam | | 286.05038 | 287.05818 | 105.0365 | C15H11ClN2O2 | 2.16 | c1ccc(cc1)C2=c3cc(ccc3=NC(=O)CN2O)Cl |

| Compound | | Monoisotopic mass | Precursor (Q1) [M+H]+ | Fragment (Q3) [M+H]+ | Chemical Formula | Retention time | SMILES |
|---|---|---|---|---|---|---|---|
| Dexamethasone | | 392.1994 | 393.20718 | 147.08 | C22H29FO5 | 3.67 | C[C@@H]1C[C@H]2[C@@H]3CCC4=CC(=O)C=C[C@@]4([C@]3([C@H](C[C@@]2([C@]1(C(=O)CO)O)C)O)F)C |
| | 17-Oxodexamethasone | 332.1783 | 333.1861 | 171.0833 | C20H25FO3 | 2.88 | CC1CC2C3CCC4=CC(=O)C=CC4(C3(C(CC2(C1=O)C)O)F)C |
| | 17-beta-Carboxy-17-alpha-formyloxydexamethasone | 406.1786 | 407.1864 | 377.1760 | C22H27FO6 | 1.76 | C[C@@H]1C[C@H]2[C@@H]3CCC4=CC(=O)C=C[C@]4(C)[C@@]3(F)[C@@H](O)C[C@]2(C)[C@@]1(OC=O)C(=O)O |
| | 6-beta-Hydroxydexamethasone | 408.1943 | 409.2021 | 227.1068 | C22H29FO6 | 4.3 | C[C@@H]1CC2C3C[C@@H](O)C4=CC(=O)C=C[C@]4(C)[C@@]3(F)[C@@H](O)C[C@]2(C)[C@@]1(O)C(=O)CO |
| | | | | | | | C[C@@H]1CC2C3C[C@H](C4=CC(=O)C=C[C@@]4([C@]3([C@H](C[C@@]2([C@]1(C(=O)CO)O)C)O)F)C)O |
| | Dexamethasone phosphate | 472.1657 | 473.1735 | 91.0539 | C22H30FO8P | 2.58 | C[C@@H]1C[C@H]2[C@@H]3CCC4=CC(=O)C=C[C@@]4([C@]3([C@H](C[C@@]2([C@]1(C(=O)COP(=O)(O)O)O)C)O)F)C |
| | Dexamethasone-3,20-bisethoximes | 478.2838 | 479.2916 | 459.0000 | C26H39FN2O5 | 2.39 | CCON=C1C=CC2(C(=C1)CCC3C2(C(CC4(C3CC(C4(C(=NOCC)CO)O)C)C)O)F)C |
| Diazepam | | 284.0711 | 285.07892 | 193 | C16H13ClN2O | 4.55 | CN1c2ccc(cc2C(=NCC1=O)c3ccccc3)Cl |
| | Nordiazepam | 270.0555 | 271.0633 | 140.0256 | C15H11ClN2O | 4.12 | c1ccc(cc1)C2=NCC(=Nc3c2cc(cc3)Cl)O |
| | N-Ethylnordiazepam | 298.0868 | 299.0946 | 242.0000 | C17H15ClN2O | 0.8 | CCN1c2ccc(cc2C(=NCC1=O)c3ccccc3)Cl |
| Diclofenac | | 295.0162 | 296.02396 | 214.0419 | C14H11Cl2NO2 | 4.99 | c1ccc(c(c1)CC(=O)O)Nc2c(cccc2Cl)Cl |
| | 4'-Hydroxydiclofenac | 311.0111 | 312.0189 | 266.0144 | C14H11Cl2NO3 | 8.24 | c1ccc(c(c1)CC(=O)O)Nc2c(cc(cc2Cl)O)Cl |
| | 5-Hydroxydiclofenac | 311.0111 | 312.0189 | 266.0138 | C14H11Cl2NO3 | 8.24 | c1cc(c(c(c1)Cl)Nc2ccc(cc2CC(=O)O)O)Cl |
| | S-Diclofenac | 502.9637 | 503.9715 | 214.0428 | C23H15Cl2NO2S3 | 2.39 | C1=CC=C(C(=C1)CC(=O)OC2=CC=C(C=C2)C3=CC(=S)SS3)NC4=C(C=CC=C4Cl)Cl |
| | Diclofenac-S-acyl-glutathione | 584.0894 | 585.0972 | 438.0000 | C24H26Cl2N4O7S | 2.99 | O=C(CC1=C(NC2=C(Cl)C=CC=C2Cl)C=CC=C1)SCC(NC(CCC(N)C(O)=O)=O)C(NCC(O)=O)=O |
| Diethylcarbamazine | | 199.1679 | 200.17574 | 100.0754 | C10H21N3O | 4.02 | CCN(CC)C(=O)N1CCN(CC1)C |

| Compound | | Monoisotopic mass | Precursor (Q1) [M+H]+ | Fragment (Q3) [M+H]+ | Chemical Formula | Retention time | SMILES |
|---|---|---|---|---|---|---|---|
| Diltiazem | | 414.1608 | 415.1686 | 178.0378 | C22H26N2O4S | 3.52 | CC(=O)OC1C(Sc2ccccc2N(C1=O)CCN(C)C)c3ccc(cc3)OC |
| | O-Desacetyl-N-desmethyldiltiazem | 358.1346 | 359.1424 | 58.0648 | C19H22N2O3S | 1.5 | CNCCN1C2=CC=CC=C2SC(C(C1=O)O)C3=CC=C(C=C3)OC |
| | Desacetyldiltiazem | 372.1502 | 373.1580 | 178.0318 | C20H24N2O3S | 2.59 | CN(C)CCN1c2ccccc2S[C@H]([C@H](C1=O)O)c3ccc(cc3)OC |
| | N-Desmethyldiltiazem | 400.1452 | 401.1530 | 178.0320 | C21H24N2O4S | 3.52 | CC(=O)O[C@@H]1[C@@H](Sc2ccccc2N(C1=O)CCNC)c3ccc(cc3)OC |
| Dopamine | | 153.0785 | 154.08626 | 137.0602 | C8H11NO2 | | c1cc(c(cc1CCN)O)O |
| | 5-Hydroxydopamine | 169.0734 | 170.08117 | 153.0541 | C8H11NO3 | 0.71 | c1c(cc(c(c1O)O)O)CCN |
| | 6-Hydroxydopamine | 169.0734 | 170.08117 | 153.0547 | C8H11NO3 | 0.71 | c1c(c(cc(c1O)O)O)CCN |
| Dutasteride | | 528.2206 | 529.22842 | 105.0552 | C27H30F6N2O2 | 3.99 | C[C@]12CC[C@H]3[C@H]([C@@H]1CC[C@@H]2C(=O)Nc4cc(ccc4C(F)(F)F)C(F)(F)F)CC[C@@H]5[C@@]3(C=CC(=O)N5)C |
| Enalapril | | 376.1993 | 377.2071 | 114.0561 | C20H28N2O5 | 1.91 | CCOC(=O)[C@H](CCc1ccccc1)N[C@@H](C)C(=O)N2CCC[C@H]2C(=O)O |
| Enalaprilat | | 348.1680 | 349.1758 | 114.0563 | C18H24N2O5 | 1.91 | C[C@@H](C(=O)N1CCC[C@H]1C(=O)O)N[C@@H](CCc2ccccc2)C(=O)O |
| | Enalaprilat butyl tert-butyl diester | 460.2932 | 461.301 | 262.1794 | C26H40N2O5 | 4.64 | O=C([C@H]1N(CCC1)C([C@@H](N[C@@H](CCC2=CC=CC=C2)C(OC(C)(C)CCCCC)=O)C)=O)OC(C)(C)CCCCC |
| | Enalaprilat tert-butyl ester | 404.2306 | 405.2384 | 329.1501 | C22H32N2O5 | 2.52 | C[C@@H](C(=O)N1CCC[C@H]1C(=O)OC(C)(C)C)N[C@@H](CCc2ccccc2)C(=O)O |
| Eprosartan | | 424.1452 | 425.15295 | 135.0439 | C23H24N2O4S | 1.82 | CCCCc1ncc(n1Cc2ccc(cc2)C(=O)O)C=C(Cc3cccs3)C(=O)O |

| Compound | | Monoisotopic mass | Precursor (Q1) [M+H]+ | Fragment (Q3) [M+H]+ | Chemical Formula | Retention time | SMILES |
|---|---|---|---|---|---|---|---|
| Erythromycin | | 733.4607 | 734.46852 | 83.0489 | C37H67NO13 | 3.96 | CC[C@@H]1[C@@]([C@@H]([C@H](C(=O)[C@@H](C[C@@]([C@@H]([C@H]([C@@H]([C@H](C(=O)O1)C)O[C@H]2C[C@@]([C@H]([C@@H](O2)C)O)(C)OC)C)O[C@H]3[C@@H]([C@H](C[C@H](O3)C)N(C)C)O)(C)O)C)O)(C)O |
| | Anhydroerythromycin | 715.4502 | 716.4580 | 558.0000 | C37H65NO12 | | CC[C@@H]1C2([C@@H]([C@H](C3(O2)[C@@H](CC(O3)([C@@H]([C@H]([C@@H]([C@H](C(=O)O1)C)OC4CC(C(C(O4)C)O)(C)OC)C)OC5C(C(CC(O5)C)N(C)C)O)C)C)O)C |
| | Erythromycin A enol ether | 715.4502 | 716.4580 | 158.1172 | C37H65NO12 | 3.96 | CC[C@@H]1[C@@]([C@@H]([C@H](C2=C(C[C@@](O2)([C@@H]([C@H]([C@@H]([C@H](C(=O)O1)C)O[C@H]3C[C@@]([C@H]([C@@H](O3)C)O)(C)OC)C)O[C@H]4[C@@H]([C@H](C[C@H](O4)C)N(C)C)O)C)C)O)(C)O |
| | Erythromycin C | 719.4451 | 720.4529 | 576.0000 | C36H65NO13 | 3.61 | CC[C@@H]1[C@@]([C@@H]([C@H](C(=O)[C@@H](C[C@@]([C@@H]([C@H]([C@@H]([C@H](C(=O)O1)C)O[C@H]2C[C@@]([C@H]([C@@H](O2)C)O)(C)O)C)O[C@H]3[C@@H]([C@H](C[C@H](O3)C)N(C)C)O)(C)O)C)O)(C)O |
| | Erythromycin F | 749.4556 | 750.4634 | 592.0000 | C37H67NO14 | 8.34 | CC[C@@H]1[C@@]([C@@H]([C@H](C(=O)[C@@H](C[C@@]([C@@H]([C@H]([C@@H]([C@H](C(=O)O1)CO)O[C@H]2C[C@@]([C@H]([C@@H](O2)C)O)(C)OC)C)O[C@H]3[C@@H]([C@H](C[C@H](O3)C)N(C)C)O)(C)O)C)O)(C)O |
| | Erythromycylamine | 734.4924 | 735.5002 | 158.1171 | C37H70N2O12 | 3.96 | CC[C@@H]1[C@@]([C@@H]([C@H]([C@H]([C@@H](C[C@@]([C@@H]([C@H]([C@@H]([C@H](C(=O)O1)C)O[C@H]2C[C@@]([C@H]([C@@H](O2)C)O)(C)OC)C)O[C@H]3[C@@H]([C@H](C[C@H](O3)C)N(C)C)O)(C)O)C)N)C)O)(C)O |
| | N-Demethylerythromycin | 719.4451 | 720.45287 | 144.1019 | C36H65NO13 | 3.86 | CC[C@@H]1[C@@]([C@@H]([C@H](C(=O)[C@@H](C[C@]([C@@H]([C@H]([C@@H]([C@H](C(=O)O1)C)O[C@H]2C[C@@]([C@H]([C@@H](O2)C)O)(C)OC)C)O[C@H]3[C@@H]([C@H](C[C@H](O3)C)NC)O)(C)O)C)O)(C)O |

| Compound | | Monoisotopic mass | Precursor (Q1) [M+H]+ | Fragment (Q3) [M+H]+ | Chemical Formula | Retention time | SMILES |
|---|---|---|---|---|---|---|---|
| Erythromycin (cont.) | Pseudoerythromycin A enol ether | 715.4502 | 716.45795 | 158.1174 | C37H65NO12 | 3.96 | CC[C@H]([C@](C)([C@H]1[C@H](C2=C(C[C@@](O2)([C@@H]([C@H]([C@@H]([C@H](C(=O)O1)C)O[C@H]3C[C@@]([C@H]([C@@H](O3)C)O)(C)OC)C)O[C@H]4[C@@H]([C@H](C[C@H](O4)C)N(C)C)O)C)C)O)O |
| Famotidine | | 337.04441 | 338.05221 | 189.0263 | C8H15N7O2S3 | 3.31 | c1c(nc(s1)N=C(N)N)CSCCC(=NS(=O)(=O)N)N |
| | Famotidine acid methyl ester | 274.05529 | 275.06309 | 155.0382 | C9H14N4O2S2 | 5.66 | COC(=N)CCSCC1=CSC(=N1)N=C(N)N |
| Fenofibrate | | 360.1123 | 361.12011 | 233.0362 | C20H21ClO4 | 6.38 | CC(C)OC(=O)C(C)(C)Oc1ccc(cc1)C(=O)c2ccc(cc2)Cl |
| | Fenofibric acid | 318.0654 | 319.0732 | | C17H15ClO4 | 4.87 | CC(C)(C(=O)O)Oc1ccc(cc1)C(=O)c2ccc(cc2)Cl |
| Fenoldopam | | 305.0814 | 306.08915 | 107.0491 | C16H16ClNO3 | | c1cc(ccc1C2CNCCc3c2cc(c(c3Cl)O)O)O |
| Fipronil | | 435.9382 | 436.94598 | 157.0123 | C12H4Cl2F6N4OS | 6.58 | c1c(cc(c(c1Cl)n2c(c(c(n2)C#N)S(=O)C(F)(F)F)N)Cl)C(F)(F)F |
| | Fipronil desulfinyl | 387.9712 | 388.979 | 143.0074 | C12H4Cl2F6N4 | 4.24 | c1c(cc(c(c1Cl)n2c(c(c(n2)C#N)C(F)(F)F)N)Cl)C(F)(F)F |
| | Fipronil sulfide | 419.9433 | 420.95107 | 316.9857 | C12H4Cl2F6N4S | 2.27 | c1c(cc(c(c1Cl)n2c(c(c(n2)C#N)SC(F)(F)F)N)Cl)C(F)(F)F |
| | Fipronil sulfone | 451.9331 | 452.9409 | 319.9826 | C12H4Cl2F6N4O2S | 2.79 | c1c(cc(c(c1Cl)n2c(c(c(n2)C#N)S(=O)(=O)C(F)(F)F)N)Cl)C(F)(F)F |
| Fluconazole | | 306.1035 | 307.11134 | 70.0401 | C13H12F2N6O | 2.44 | c1cc(c(cc1F)F)C(Cn2cncn2)(Cn3cncn3)O |
| Flunitrazepam | | 313.0858 | 314.09355 | 183.0601 | C16H12FN3O3 | 2.65 | CN1c2ccc(cc2C(=NCC1=O)c3ccccc3F)[N+](=O)[O-] |
| | 7-Aminodesmethylflunitrazepam | 269.0959 | 270.10372 | 121.0757 | C15H12FN3O | 4.57 | c1ccc(c(c1)C2=NCC(=O)Nc3c2cc(cc3)N)F |
| | N-Desmethylflunitrazepam | 299.0701 | 300.0779 | 254.0848 | C15H10FN3O3 | 2.92 | c1ccc(c(c1)C2=NCC(=O)Nc3c2cc(cc3)[N+](=O)[O-])F |
| | Norflunitrazepam | 299.0701 | 300.0779 | 278.0561 | C15H10FN3O3 | 3.11 | c1ccc(c(c1)C2=NCC(=O)Nc3c2cc(cc3)[N+](=O)[O-])F |

| Compound | | Monoisotopic mass | Precursor (Q1) [M+H]+ | Fragment (Q3) [M+H]+ | Chemical Formula | Retention time | SMILES |
|---|---|---|---|---|---|---|---|
| Flurazepam | | 387.1508 | 388.15864 | 315.0691 | C21H23ClFN3O | 3.82 | CCN(CC)CCN1c2ccc(cc2C(=NCC1=O)c3ccccc3F)Cl |
| | 2-Hydroxyethylflurazepam | 332.0723 | 333.08006 | 109.0446 | C17H14ClFN2O2 | 3.45 | c1ccc(c(c1)C2=NCC(=O)N(c3c2cc(cc3)Cl)CCO)F |
| | Desalkylflurazepam | 288.0461 | 289.05385 | 140.026 | C15H10ClFN2O | 3.36 | c1ccc(c(c1)C2=NCC(=O)Nc3c2cc(cc3)Cl)F |
| Fluticasone propionate | | 500.1839 | 501.19171 | 91.054 | C25H31F3O5S | 2.58 | CCC(=O)O[C@@]1([C@@H](C[C@@H]2[C@@]1(C[C@@H]([C@]3([C@H]2C[C@@H](C4=CC(=O)C=C[C@@]43C)F)F)O)C)C)C(=O)SCF |
| Fluoxetine | | 309.1335 | 310.1413 | 44.0000 | C17H18F3NO | 4.71 | CNCCC(c1ccccc1)Oc2ccc(cc2)C(F)(F)F |
| | Desmethylfluoxetine | 295.1179 | 296.1257 | 134.0966 | C16H16F3NO | 1.65 | c1ccc(cc1)C(CCN)Oc2ccc(cc2)C(F)(F)F |
| | Norfluoxetine | 295.1179 | 296.1257 | 134.0962 | C16H16F3NO | 1.65 | c1ccc(cc1)C(CCN)Oc2ccc(cc2)C(F)(F)F |
| Gabapentin | | 171.1254 | 172.13321 | 55.0173 | C9H17NO2 | 1.66 | C1CCC(CC1)(CC(=O)O)CN |
| | Gabapentin related bis-nitrile | 148.0995 | 149.10732 | 81.0694 | C9H12N2 | 0,18 | C1CCC(CC1)(CC#N)C#N |
| | Gabapentin related compound A | 153.1148 | 154.12264 | 95.0838 | C9H15NO | 3 | C1CCC2(CC1)CC(=O)NC2 |
| | Gabapentin related compound B | 167.0941 | 168.10191 | 123.033 | C9H13NO2 | 2,24 | C1CCC(CC1)(CC(=O)O)C#N |
| | Gabapentin related compound D | 307.2142 | 308.22202 | 290.2119 | C18H29NO3 | 5,6 | C1CCC2(CC1)CC(=O)N(C2)CC3(CCCCC3)CC(=O)O |
| | Gabapentin related compound E | 186.0887 | 187.09649 | 141.0922 | C9H14O4 | 1,46 | C1CCC(CC1)(CC(=O)O)C(=O)O |
| Gallopamil | | 484.2932 | 485.301 | 165.0909 | C28H40N2O5 | 3.91 | CC(C)C(CCCN(C)CCc1ccc(c(c1)OC)OC)(C#N)c2cc(c(c(c2)OC)OC)OC |
| Irbesartan | | 428.2319 | 429.23974 | 207.0916 | C25H28N6O | 4.47 | CCCCC1=NC2(CCCC2)C(=O)N1Cc3ccc(cc3)c4ccccc4c5[nH]nnn5 |

| Compound | | Monoisotopic mass | Precursor (Q1) [M+H]+ | Fragment (Q3) [M+H]+ | Chemical Formula | Retention time | SMILES |
|---|---|---|---|---|---|---|---|
| Ibuprofen | | 206.1302 | 207.13796 | 161.133 | C13H18O2 | 4.88 | CC(C)Cc1ccc(cc1)C(C)C(=O)O |
| | 2-Hydroxyibuprofen | 222.1251 | 223.1329 | 177.1282 | C13H18O3 | 5.26 | O=C(O)C(c1ccc(cc1)CC(O)(C)C)C |
| | Carboxyibuprofen | 236.1043 | 237.1121 | 163.0753 | C13H16O4 | 3.21 | O=C(O)C(c1ccc(cc1)CC(C(=O)O)C)C |
| | Ibuprofen-beta-D-glucuronide | 382.1622 | 383.1700 | 113.0246 | C19H26O8 | 1.97 | CC(C)CC1=CC=C(C=C1)C(C)C(=O)O[C@@H]2[C@@H]([C@@H]([C@H](C(O2)C(=O)O)O)O)O |
| Indomethacin | | 357.0763 | 358.08406 | 312.079 | C19H16ClNO4 | 2.4 | Cc1c(c2cc(ccc2n1C(=O)c3ccc(cc3)Cl)OC)CC(=O)O |
| | Indomethacin morpholinylamide | 426.1341 | 427.1419 | 138.9955 | C23H23ClN2O4 | 6.58 | Cc1c(c2cc(ccc2n1C(=O)c3ccc(cc3)Cl)OC)CC(=O)N4CCOCC4 |
| | Indomethacin heptyl ester | 455.1858 | 456.1936 | 138.9953 | C26H30ClNO4 | 6.58 | CCCCCCCOC(=O)CC1=C(N(C2=C1C=C(C=C2)OC)C(=O)C3=CC=C(C=C3)Cl)C |
| | N-(2-Phenylethyl)indomethacinamide | 460.1549 | 461.1627 | 139.0023 | C27H25ClN2O3 | 6.58 | Cc1c(c2cc(ccc2n1C(=O)c3ccc(cc3)Cl)OC)CC(=O)NCCc4ccccc4 |
| | N-(3-Pyridyl)indomethacinamide | 433.1188 | 434.1266 | 138.9954 | C24H20ClN3O3 | 6.58 | Cc1c(c2cc(ccc2n1C(=O)c3ccc(cc3)Cl)OC)CC(=O)Nc4cccnc4 |
| | N-(4-Acetamidophenyl)indomethacinamide | 489.1450 | 490.1528 | 138.9950 | C27H24ClN3O4 | 6.58 | Cc1c(c2cc(ccc2n1C(=O)c3ccc(cc3)Cl)OC)CC(=O)Nc4ccc(cc4)NC(=O)C |
| Iohexol | | 820.8798 | 821.8876 | 301.931 | C19H26I3N3O9 | 0.38 | CC(=O)N(CC(CO)O)c1c(c(c(c(c1I)C(=O)NCC(CO)O)I)C(=O)NCC(CO)O)I |
| Ketamine | | 237.0915 | 238.0993 | 125.0149 | C13H16ClNO | 2.28 | CNC1(CCCCC1=O)c2ccccc2Cl |
| | Dehydronorketamine | 221.0602 | 222.0680 | 177.0467 | C12H12ClNO | 3.83 | c1ccc(c(c1)C2(CCC=CC2=O)N)Cl |
| | Norketamine | 223.0759 | 224.0837 | 125.0149 | C12H14ClNO | 1.24 | c1ccc(c(c1)C2(CCCCC2=O)N)Cl |

| Compound | | Monoisotopic mass | Precursor (Q1) [M+H]+ | Fragment (Q3) [M+H]+ | Chemical Formula | Retention time | SMILES |
|---|---|---|---|---|---|---|---|
| Ketoprofen | | 254.0938 | 255.10157 | 105.036 | C16H14O3 | 4.24 | CC(c1cccc(c1)C(=O)c2ccccc2)C(=O)O |
| | Dihydroketoprofen | 256.1094 | 257.1172 | 193.1000 | C16H16O3 | 2.79 | CC(c1cccc(c1)C(c2ccccc2)O)C(=O)O |
| | Ketoprofen-beta-D-glucuronide | 430.1259 | 431.1337 | 113.0246 | C22H22O9 | 2.83 | COC(=O)C1C(C(C(C(O1)OC2=CC3=C(CC(CO3)C4=CC=C(C=C4)O)C=C2)O)O)O |
| Lamotrigine | | 255.0073 | 256.01513 | 43 | C9H7Cl2N5 | 3.51 | c1cc(c(c(c1)Cl)Cl)c2c(nc(nn2)N)N |
| Levomepromazine | | 328.1604 | 329.16821 | 284 | C19H24N2OS | 2.22 | CC(CN1c2ccccc2Sc3c1cc(cc3)OC)CN(C)C |
| | Norlevomepromazine | 314.1448 | 315.15256 | 86.0963 | C18H22N2OS | 2.33 | CC(CNC)CN1C2=CC=CC=C2SC3=C1C=C(C=C3)OC |
| Levofloxacin | | 361.1433 | 362.15106 | 316.147 | C18H20FN3O4 | 1.92 | C[C@H]1COc2c3n1cc(c(=O)c3cc(c2N4CCN(CC4)C)F)C(=O)O |
| Levothyroxine | | 776.6862 | 777.69397 | 126.9052 | C15H11I4NO4 | 2.75 | c1c(cc(c(c1I)Oc2cc(c(c(c2)I)O)I)I)C[C@@H](C(=O)O)N |
| Loratadine | | 382.1443 | 383.15208 | 337.1102 | C22H23ClN2O2 | 4.92 | CCOC(=O)N1CCC(=C2c3ccc(cc3CCc4c2nccc4)Cl)CC1 |
| | 2-Hydroxymethylloratadine | 412.1549 | 413.1627 | 367.1211 | C23H25ClN2O3 | 2.73 | CCOC(=O)N1CCC(=C2C3=C(CCC4=C2N=C(C=C4)CO)C=C(C=C3)Cl)CC1 |
| | 4-Hydroxymethylloratadine | 412.1549 | 413.1627 | 367.1212 | C23H25ClN2O3 | 2.73 | CCOC(=O)N1CCC(=C2C3=C(CCC4=C(C=CN=C42)CO)C=C(C=C3)Cl)CC1 |
| | Descarboethoxyloratadine | 310.1232 | 311.1310 | 259.0000 | C19H19ClN2 | 2.7 | c1cc2c(nc1)C(=C3CCNCC3)c4ccc(cc4CC2)Cl |
| Lorazepam | | 320.0114 | 321.01921 | 283.0283 | C15H10Cl2N2O2 | 8.23 | c1ccc(c(c1)C2=NC(C(=Nc3c2cc(cc3)Cl)O)O)Cl |
| | Delorazepam | 304.0165 | 305.0243 | 140.0262 | C15H10Cl2N2O | 3.36 | c1ccc(c(c1)C2=NCC(=O)Nc3c2cc(cc3)Cl)Cl |
| | Bis(trimethylsilyl) lorazepam | 464.0905 | 465.0983 | 341.0000 | C21H26Cl2N2O2Si2 | 0.14 | C[Si](C)(C)N1c2ccc(cc2C(=NC(C1=O)O[Si](C)(C)C)c3ccccc3Cl)Cl |
| | Lorazepam glucuronide | 496.0435 | 497.0513 | 283.0274 | C21H18Cl2N2O8 | 8.24 | c1ccc(c(c1)C2=NC(C(=O)Nc3c2cc(cc3)Cl)O[C@H]4[C@@H]([C@H]([C@@H]([C@H](O4)C(=O)O)O)O)O)Cl |

| Compound | | Monoisotopic mass | Precursor (Q1) [M+H]+ | Fragment (Q3) [M+H]+ | Chemical Formula | Retention time | SMILES |
|---|---|---|---|---|---|---|---|
| Lormetazepam | | 334.0271 | 335.03486 | 289.029 | C16H12Cl2N2O2 | 4.28 | CN1c2ccc(cc2C(=NC(C1=O)O)c3ccccc3Cl)Cl |
| | Trimethylsilyl lormetazepam | 406.0666 | 407.0744 | 289.0000 | C19H20Cl2N2O2Si | 0.38 | CN1c2ccc(cc2C(=NC(C1=O)O[Si](C)(C)C)c3ccccc3Cl)Cl |
| Losartan | | 422.1617 | 423.16946 | 405 | C22H23ClN6O | 0.81 | CCCCc1nc(c(n1Cc2ccc(cc2)c3ccccc3c4[nH]nnn4)CO)Cl |
| | Losartancarboxaldehyde | 420.1460 | 421.15381 | 207.0919 | C22H21ClN6O | 4.47 | CCCCC1=NC(=C(N1CC2=CC=C(C=C2)C3=CC=CC=C3C4=NNN=N4)C=O)Cl |
| | N1-Losartanyllosartan | 826.3133 | 827.32109 | 207.0919 | C44H44Cl2N12O | 1.27 | CCCCC1=NC(=C(N1CC2=CC=C(C=C2)C3=CC=CC=C3C4=NNN=N4)CN5C(=NN=N5)C6=CC=CC=C6C7=CC=C(C=C7)CN8C(=NC(=C8CO)Cl)CCCC)Cl |
| Mandipropamid | | 411.1232 | 412.13101 | 328.1099 | C23H22ClNO4 | 2.81 | COC1=C(C=CC(=C1)CCNC(=O)C(C2=CC=C(C=C2)Cl)OCC#C)OCC#C |
| Medazepam | | 270.0919 | 271.09965 | 242 | C16H15ClN2 | 3.66 | CN1CCN=C(c2c1ccc(c2)Cl)c3ccccc3 |
| Mephedrone | | 177.1148 | 178.12264 | 144.081 | C11H15NO | 2.19 | Cc1ccc(cc1)C(=O)C(C)NC |
| | nor-Mephedrone | 163.0992 | 164.1070 | 146.0964 | C10H13NO | 1.18 | Cc1ccc(cc1)C(=O)C(C)N |
| Metaclazepam | | 392.0286 | 393.03638 | 363.0079 | C18H18BrClN2O | 2.38 | CN1c2ccc(cc2C(=NCC1COC)c3ccccc3Cl)Br |
| Metformin | | 129.1009 | 130.1087 | 71.0602 | C4H11N5 | 0.43 | CN(C)C(=N)NC(=N)N |
| Methiopropamine | | 155.0764 | 156.0842 | 125.0420 | C8H13NS | 0.79 | CC(Cc1cccs1)NC |
| Metoprolol | | 267.1829 | 268.1907 | 74.0604 | C15H25NO3 | 2.52 | CC(C)NCC(COc1ccc(cc1)CCOC)O |
| | alpha-Hydroxymetoprolol | 283.1778 | 284.1856 | 74.0599 | C15H25NO4 | 3.34 | CC(C)NCC(COc1ccc(cc1)C(COC)O)O |
| | Metoprolol acid | 267.1465 | 268.1543 | 222.1499 | C14H21NO4 | 3.09 | CC(C)NCC(COc1ccc(cc1)CC(=O)O)O |
| Metronidazole | | 171.0639 | 172.07167 | 128.0449 | C6H9N3O3 | 1.44 | Cc1ncc(n1CCO)[N+](=O)[O-] |
| | Hydroxymetronidazole | 187.0588 | 188.0666 | 126.0291 | C6H9N3O4 | 1.37 | c1c(n(c(n1)CO)CCO)[N+](=O)[O-] |
| | Benzoylmetronidazole | 275.0901 | 276.0979 | 149.0000 | C13H13N3O4 | 6.11 | Cc1ncc(n1CCOC(=O)c2ccccc2)[N+](=O)[O-] |

| Compound | | Monoisotopic mass | Precursor (Q1) [M+H]+ | Fragment (Q3) [M+H]+ | Chemical Formula | Retention time | SMILES |
|---|---|---|---|---|---|---|---|
| Midazolam | | 325.0777 | 326.0855 | 291.1167 | C18H13ClFN3 | | Cc1ncc2n1-c3ccc(cc3C(=NC2)c4ccccc4F)Cl |
| | 1'-Hydroxymidazolam | 341.0726 | 342.0804 | 140.0498 | C18H13ClFN3O | 2.71 | c1ccc(c(c1)C2=NCc3cnc(n3-c4c2cc(cc4)Cl)CO)F |
| | 1'-Hydroxymidazolam-beta-D-glucuronide | 517.1047 | 518.1125 | 324.0703 | C24H21ClFN3O7 | 8.2 | C1C2=CN=C(N2C3=C(C=C(C=C3)Cl)C(=N1)C4=CC=CC=C4F)COC5C(C(C(C(O5)C(=O)O)O)O)O |
| | 4-Hydroxymidazolam | 341.0726 | 342.0804 | 297.0584 | C18H13ClFN3O | 2.91 | Cc1ncc2n1-c3ccc(cc3C(=NC2O)c4ccccc4F)Cl |
| | Alpha-hydroxymidazolam | 341.0726 | 342.0804 | 324.0705 | C18H13ClFN3O | 0.84 | c1ccc(c(c1)C2=NCc3cnc(n3-c4c2cc(cc4)Cl)CO)F |
| Montelukast | | 585.2099 | 586.21772 | 422.1631 | C35H36ClNO3S | 2.9 | CC(C)(c1ccccc1CC[C@H](c2cccc(c2)/C=C/c3ccc4ccc(cc4n3)Cl)SCC5(CC5)CC(=O)O)O |
| | Montelukast acyl-beta-D-glucuronide | 761.2420 | 762.24981 | 113.0242 | C41H44ClNO9S | 2.85 | O=C(O[C@@H]1O[C@H](C(=O)O)[C@@H](O)[C@H](O)[C@H]1O)CC6(CS[C@@H](c4cccc(\C=C\c2nc3c(cc2)ccc(Cl)c3)c4)CCc5ccccc5C(O)(C)C)CC6 |
| | Montelukast sulfoxide | 601.2048 | 602.21263 | 143.0173 | C35H36ClNO4S | 8.98 | CC(C)(c1ccccc1CCC(c2cccc(c2)/C=C/c3ccc4ccc(cc4n3)Cl)S(=O)CC5(CC5)CC(=O)O)O |
| | Montelukast-1,2-diol | 601.2048 | 602.21263 | 438.1622 | C35H36ClNO4S | 3.45 | CC(C(c1ccccc1CC[C@H](c2cccc(c2)/C=C/c3ccc4ccc(cc4n3)Cl)SCC5(CC5)CC(=O)O)O)O |
| Naproxen | | 230.0938 | 231.10157 | 185.2 | C14H14O3 | 3.5 | CC(c1ccc2cc(ccc2c1)OC)C(=O)O |
| | O-Desmethylnaproxen | 216.0781 | 217.0859 | 171.0800 | C13H12O3 | 1.28 | C[C@@H](c1ccc2cc(ccc2c1)O)C(=O)O |
| Nefopam | | 253.1461 | 254.15394 | 166 | C17H19NO | 2.44 | CN1CCOC(c2ccccc2C1)c3ccccc3 |
| Nicotine | | 162.1152 | 163.1230 | 117.0500 | C10H14N2 | 0.62 | CN1CCCC1c2cccnc2 |
| | 2-Methylnicotine | 176.1308 | 177.13862 | 144.0811 | C11H16N2 | 1.37 | Cc1c(cccn1)C2CCCN2C |
| | 3-trans-Hydroxynorcotinine | 178.0737 | 179.0815 | 80.0493 | C9H10N2O2 | 0.75 | C1C(NC(=O)C1O)C2=CN=CC=C2 |
| | 6-Methylnicotine | 176.1308 | 177.13862 | 146.0961 | C11H16N2 | 1.81 | Cc1ccc(cn1)[C@@H]2CCCN2C |
| | (2S)-Nicotine 1-oxide | 178.1101 | 179.1179 | 84.0805 | C10H14N2O | 0.43 | C[N+]1(CCCC1C2=CN=CC=C2)[O-] |
| | Cotinine | 176.0944 | 177.1022 | 80.0492 | C10H12N2O | 0,75 | CN1C(CCC1=O)c2cccnc2 |
| | Cotinine-N-oxide | 192.0894 | 193.09715 | 96.044 | C10H12N2O2 | 1.16 | O=C2N(C)[C@H](c1c[n+]([O-])ccc1)CC2 |
| | N-Nitrosonornicotine | 177.0897 | 178.09749 | 148.0987 | C9H11N3O | 0.84 | c1cc(cnc1)C2CCCN2N=O |

| Compound | | Monoisotopic mass | Precursor (Q1) [M+H]+ | Fragment (Q3) [M+H]+ | Chemical Formula | Retention time | SMILES |
|---|---|---|---|---|---|---|---|
| Nicotine (cont.) | N'-Nitrosonornicotine N-.beta.-D-glucuronide | 353.1218 | 354.12958 | 120.0682 | C15H19N3O7 | 1.52 | c1cc(c[n+](c1)[C@H]2[C@@H]([C@H]([C@@H]([C@H](O2)C(=O)[O-])O)O)O)[C@@H]3CCCN3N=O |
| | Nicotine N-beta-D-glucuronide | 338.1473 | 339.1551 | 163.1231 | C16H22N2O6 | 4.69 | CN1CCCC1C2=C[N+](=CC=C2)C3C(C(C(C(O3)C(=O)[O-])O)O)O |
| | Norcotinine | 162.07879 | 163.08659 | 80.0498 | C9H10N2O | 0.56 | c1cc(cnc1)C2CCC(=O)N2 |
| | Nornicotine | 148.09952 | 149.10732 | 80.0492 | C9H12N2 | 0.56 | C1CC(NC1)C2=CN=CC=C2 |
| | Metanicotine | 162.11517 | 163.12297 | 130.0654 | C10H14N2 | 2.51 | CNCC/C=C/c1cccnc1 |
| | (R,S)-Norcotinine | 162.0788 | 163.0866 | 80.0492 | C9H10N2O | 0.56 | C1CC(=O)NC1C2=CN=CC=C2 |
| | rac-N'-Nitrosonornicotine 1-N-oxide | 193.0846 | 194.0924 | 147.0917 | C9H11N3O2 | 1.99 | c1cc(c[n+](c1)[O-])C2CCCN2N=O |
| | trans-3'-Hydroxycotinine | 192.0894 | 193.09715 | 80.0491 | C10H12N2O2 | 0.75 | CN1[C@@H](C[C@H](C1=O)O)c2cccnc2 |
| | trans-Nicotine-1'-oxide | 178.1101 | 179.11789 | 132.0807 | C10H14N2O | 0.76 | C[N+]1(CCCC1C2=CN=CC=C2)[O-] |
| Nifedipine | | 346.1160 | 347.12376 | 315 | C17H18N2O6 | 2.75 | CC1=C(C(C(=C(N1)C)C(=O)OC)c2ccccc2[N+](=O)[O-])C(=O)OC |
| | Dehydronifedipine | 344.1003 | 345.10811 | 284.0916 | C17H16N2O6 | 2.34 | Cc1c(c(c(c(n1)C)C(=O)OC)c2ccccc2[N+](=O)[O-])C(=O)OC |
| Nimetazepam | | 295.0952 | 296.10297 | 250.1105 | C16H13N3O3 | 1.93 | CN1c2ccc(cc2C(=NCC1=O)c3ccccc3)[N+](=O)[O-] |
| | 7-Aminonimetazepam | 265.1210 | 266.12879 | 135.0914 | C16H15N3O | 0.94 | CN1C(=O)CN=C(C2=C1C=CC(=C2)N)C3=CC=CC=C3 |
| Nitrazepam | | 281.0795 | 282.08732 | 236.0942 | C15H11N3O3 | 1.64 | c1ccc(cc1)C2=NCC(=Nc3c2cc(cc3)[N+](=O)[O-])O |
| | 7-Aminoflunitrazepam | 283.1116 | 284.11937 | 135.0915 | C16H14FN3O | 3.72 | CN1c2ccc(cc2C(=NCC1=O)c3ccccc3F)N |
| | 7-Aminonitrazepam | 251.1053 | 252.11314 | 121.0759 | C15H13N3O | 2.32 | c1ccc(cc1)C2=NCC(=O)Nc3c2cc(cc3)N |
| Nordiazepam | | 270.0555 | 271.06327 | 140.0256 | C15H11ClN2O | 4.12 | c1ccc(cc1)C2=NCC(=Nc3c2cc(cc3)Cl)O |
| | Trimethylsilyl nordazepam | 342.0950 | 343.10279 | 269 | C18H19ClN2OSi | 0.19 | C[Si](C)(C)N1c2ccc(cc2C(=NCC1=O)c3ccccc3)Cl |
| | N-Ethylnordiazepam | 298.0868 | 299.09457 | 242 | C17H15ClN2O | 0.8 | CCN1c2ccc(cc2C(=NCC1=O)c3ccccc3)Cl |

| Compound | | Monoisotopic mass | Precursor (Q1) [M+H]+ | Fragment (Q3) [M+H]+ | Chemical Formula | Retention time | SMILES |
|---|---|---|---|---|---|---|---|
| Olmesartan medoxomil | | 558.2222 | 559.22996 | 190.0655 | C29H30N6O6 | 4.53 | CCCc1nc(c(n1Cc2ccc(cc2)c3ccccc3c4[nH]nnn4)C(=O)OCc5c(oc(=O)o5)C)C(C)(C)O |
| | Olmesartan medoxomil methyl ether | 572.2378 | 573.24561 | 207.0918 | C30H32N6O6 | 0.71 | CCCc1nc(c(n1Cc2ccc(cc2)c3ccccc3c4n[nH]nn4)C(=O)OCc5c(oc(=O)o5)C)C(C)(C)OC |
| Omeprazole | | 345.1142 | 346.12199 | 198.0000 | C17H19N3O3S | 0.8 | Cc1cnc(c(c1OC)C)CS(=O)c2[nH]c3ccc(cc3n2)OC |
| | 4-(Acetyloxy)omeprazole | 373.1091 | 374.1169 | 184.0421 | C18H19N3O4S | 1.9 | CC1=CN=C(C(=C1OC(=O)C)C)CS(=O)(=O)C2=NC3=C(N2)C=C(C=C3)OC |
| | 4-Desmethoxy-4-nitroomeprazole sulfone | 376.0836 | 377.0914 | 195.0221 | C16H16N4O5S | 2.84 | CC1=CN=C(C(=C1[N+](=O)[O-])C)CS(=O)(=O)C2=NC3=C(N2)C=C(C=C3)OC |
| | 4-Hydroxyomeprazole sulfide | 315.1036 | 316.1114 | 168.0475 | C16H17N3O2S | 2.59 | CC1=CNC(=C(C1=O)C)CSC2=NC3=C(N2)C=C(C=C3)OC |
| | 4-Desmethoxy-4-chloroomeprazole | 349.0647 | 350.0725 | 149.0705 | C16H16ClN3O2S | 2.35 | Cc1cnc(c(c1Cl)C)CS(=O)c2[nH]c3ccc(cc3n2)OC |
| | 5-O-Desmethylomeprazole | 331.0985 | 332.1063 | 297.0564 | C16H17N3O3S | 3.1 | CC1=CN=C(C(=C1OC)C)CS(=O)C2=NC3=C(N2)C=C(C=C3)O |
| | 5-O-Desmethylomeprazole sulfide | 315.1036 | 316.1114 | 165.0120 | C16H17N3O2S | 4.92 | CC1=CN=C(C(=C1OC)C)CSC2=NC3=C(N2)C=C(C=C3)O |
| | 5'-Hydroxyomeprazole | 361.1091 | 362.1169 | 214.0000 | C17H19N3O4S | 1.5 | Cc1c(ncc(c1OC)CO)CS(=O)c2[nH]c3cc(ccc3n2)OC |
| | Omeprazole N-oxide | 361.1091 | 362.1169 | 149.0710 | C17H19N3O4S | 2.35 | CC1=C[N+](=C(C(=C1OC)C)CS(=O)C2=NC3=C(N2)C=CC(=C3)OC)[O-] |
| | Omeprazole sulfide | 329.1193 | 330.1271 | 182.0630 | C17H19N3O2S | 1.88 | CC1=CN=C(C(=C1OC)C)CSC2=NC3=C(N2)C=C(C=C3)OC |
| | Omeprazole sulfone | 361.1091 | 362.1169 | 150.0914 | C17H19N3O4S | 3.14 | Cc1cnc(c(c1OC)C)CS(=O)(=O)c2[nH]c3ccc(cc3n2)OC |
| | Omeprazole sulfone N-oxide | 377.1040 | 378.1118 | 149.0711 | C17H19N3O5S | 2.35 | Cc1c[n+](c(c(c1OC)C)CS(=O)(=O)c2[nH]c3ccc(cc3n2)OC)[O-] |

| Compound | | Monoisotopic mass | Precursor (Q1) [M+H]+ | Fragment (Q3) [M+H]+ | Chemical Formula | Retention time | SMILES |
|---|---|---|---|---|---|---|---|
| Oxazepam | | 286.0504 | 287.05818 | 241.0529 | C15H11ClN2O2 | 3.77 | c1ccc(cc1)C2=NC(C(=Nc3c2cc(cc3)Cl)O)O |
| | Bis(trimethylsilyl) oxazepam | 430.1294 | 431.1372 | 341.0000 | C21H27ClN2O2Si2 | 0.14 | C[Si](C)(C)N1c2ccc(cc2C(=NC(C1=O)O[Si](C)(C)C)c3ccccc3)Cl |
| | Oxazepam glucuronide | 462.0825 | 463.0903 | 285.0431 | C21H19ClN2O8 | 8.25 | c1ccc(cc1)C2=NC(C(=O)Nc3c2cc(cc3)Cl)O[C@H]4[C@@H]([C@H]([C@@H]([C@H](O4)C(=O)O)O)O)O |
| Pantoprazole | | 383.0746 | 384.08241 | 152.071 | C16H15F2N3O4S | 2.31 | COc1ccnc(c1OC)CS(=O)c2[nH]c3ccc(cc3n2)OC(F)F |
| | Pantoprazole sulfide | 367.0797 | 368.0875 | 92.0493 | C16H15F2N3O3S | 3.88 | COc1ccnc(c1OC)CSc2[nH]c3ccc(cc3n2)OC(F)F |
| Paroxetine | | 329.1422 | 330.15 | 192.1187 | C19H20FNO3 | 3.68 | c1cc(ccc1[C@@H]2CCNC[C@H]2COc3ccc4c(c3)OCO4)F |
| | Defluoroparoxetine | 311.1516 | 312.1594 | 70.0648 | C19H21NO3 | 1.6 | C1CNCC(C1C2=CC=CC=C2)COC3=CC4=C(C=C3)OCO4.Cl |
| | Desmethyleneparoxetine | 317.1422 | 318.1500 | 124.0164 | C18H20FNO3 | 2.15 | FC1=CC=C([C@H]2[C@H](COC3=CC(O)=C(O)C=C3)CNCC2)C=C1.Cl |
| | N-Methylparoxetine | 343.1579 | 344.1657 | 84.0807 | C20H22FNO3 | 2.71 | CN1CCC(C(C1)COC2=CC3=C(C=C2)OCO3)C4=CC=C(C=C4)F |
| | Desmethylene paroxetine | 353.1189 | 354.1267 | 192.1173 | C18H21ClFNO3 | 3.89 | C1CNCC(C1C2=CC=C(C=C2)F)COC3=CC(=C(C=C3)O)O.Cl |
| Phenazepam | | 347.9660 | 348.9738 | 183.9763 | C15H10BrClN2O | 0.36 | c1ccc(c(c1)C2=NCC(=O)Nc3c2cc(cc3)Br)Cl |
| | 3-Hydroxyphenazepam | 363.9609 | 364.96869 | 319.9466 | C15H10BrClN2O2 | 0.8 | c1ccc(c(c1)C2=NC(C(=O)Nc3c2cc(cc3)Br)O)Cl |
| Pipamperone | | 375.2317 | 376.23948 | 98.0597 | C21H30N3O2F | 2.75 | c1cc(ccc1C(=O)CCCN2CCC(CC2)(C(=O)N)N3CCCCC3)F |
| Prazepam | | 324.1024 | 325.11022 | 271.0629 | C19H17ClN2O | 2.09 | c1ccc(cc1)C2=NCC(=O)N(c3c2cc(cc3)Cl)CC4CC4 |
| Promethazine | | 284.1342 | 285.142 | 86.0999 | C17H20N2S | 4.26 | CC(CN1c2ccccc2Sc3c1cccc3)N(C)C |
| | Promethazine N-oxide | 300.1291 | 301.1369 | 86.0963 | C17H20N2OS | 2.33 | CC(CN1c2ccccc2Sc3c1cccc3)[N+](C)(C)[O-] |
| | Promethazine sulfoxide | 300.1291 | 301.1369 | 86.0960 | C17H20N2OS | 2.33 | CC(CN1c2ccccc2S(=O)c3c1cccc3)N(C)C |
| Propamocarb | | 188.1520 | 189.15975 | 102.0548 | C9H20N2O2 | 1.32 | CCCOC(=O)NCCCN(C)C |

| Compound | | Monoisotopic mass | Precursor (Q1) [M+H]+ | Fragment (Q3) [M+H]+ | Chemical Formula | Retention time | SMILES |
|---|---|---|---|---|---|---|---|
| Quetiapine | | 383.1662 | 384.17402 | 253.0795 | C21H25N3O2S | 2.63 | c1ccc2c(c1)C(=Nc3ccccc3S2)N4CCN(CC4)CCOCCO |
| | 7-Hydroxyquetiapine | 399.1611 | 400.16894 | 269.0743 | C21H25N3O3S | 2.14 | c1ccc2c(c1)C(=Nc3ccc(cc3S2)O)N4CCN(CC4)CCOCCO |
| | Norquetiapine | 295.1138 | 296.1216 | 210.0376 | C17H17N3S | 1.48 | c1ccc2c(c1)C(=Nc3ccccc3S2)N4CCNCC4 |
| | Quetiapine metabolite (+2O, -2H) | 413.1404 | 414.1482 | 221.1072 | C21H23N3O4S | 2.7 | OCC1OC(OO1)CN2CCN(C3=NC(C=CC=C4)=C4SC5=C3C=CC=C5)CC2 |
| | Quetiapine metabolite/impurity (-46) | 337.1244 | 338.1322 | 210.0361 | C19H19N3OS | 2.71 | O/C=C/N1CCN(C2=NC(C=CC=C3)=C3SC4=C2C=CC=C4)CC1 |
| | Quetiapine metabolite/impurity (-88) | 295.1138 | 296.1216 | 210.0352 | C17H17N3S | 3.41 | C1(C=CC=C2)=C2SC(C=CC=C3)=C3C(N4CCNCC4)=N1 |
| | Quetiapine sulfoxide | 399.1611 | 400.1689 | 221.1073 | C21H25N3O3S | 2.7 | C1CN(CCN1CCOCCO)C2=NC3=CC=CC=C3[S+](C4=CC=CC=C42)[O-] |
| Rac erythro-Dihydrobupropion | | 241.1228 | 242.13062 | 168.0572 | C13H20ClNO | 2.97 | Clc1cc(ccc1)[C@@H](O)[C@@H](NC(C)(C)C)C |
| Ractopamine | | 301.1673 | 302.17507 | 107.049 | C18H23NO3 | 3.54 | CC(CCc1ccc(cc1)O)NCC(c2ccc(cc2)O)O |
| Ranitidine | | 314.1407 | 315.1485 | 176.0481 | C13H22N4O3S | 1.44 | CNC(=C[N+](=O)[O-])NCCSCc1ccc(o1)CN(C)C |
| Rapamycin | | 913.5546 | 914.5624 | 614.0000 | C51H79NO13 | 3.96 | CNC(=C[N+](=O)[O-])NCCSCc1ccc(o1)CN(C)C |
| | 7-O-Demethylrapamycin | 899.5390 | 900.54677 | 864.5234 | C50H77NO13 | 6.68 | C[C@@H]1CCC2C[C@@H](/C(=C/C=C/C=C/[C@H](C[C@H](C(=O)[C@@H]([C@@H](/C(=C/[C@H](C(=O)C[C@H](OC(=O)[C@@H]3CCCCN3C(=O)C(=O)[C@@]1(O2)O)[C@H](C)C[C@@H]4CC[C@H]([C@@H](C4)OC)O)C)/C)O)OC)C)C)/C)OC |
| Rosuvastatin | | 481.1678 | 482.1756 | 133.0462 | C22H28FN3O6S | 2.31 | CC(C)c1c(c(nc(n1)N(C)S(=O)(=O)C)c2ccc(cc2)F)/C=C/[C@H](C[C@H](CC(=O)O)O)O |

| Compound | | Monoisotopic mass | Precursor (Q1) [M+H]+ | Fragment (Q3) [M+H]+ | Chemical Formula | Retention time | SMILES |
|---|---|---|---|---|---|---|---|
| Sertaline | | 305.0733 | 306.08108 | 158.9762 | C17H17Cl2N | 4.10 | CNC1CCC(C2=CC=CC=C12)C3=CC(=C(C=C3)Cl)Cl |
| | Norsertraline | 291.0576 | 292.0654 | 158.9760 | C16H15Cl2N | 4.11 | C1CC(C2=CC=CC=C2C1C3=CC(=C(C=C3)Cl)Cl)N |
| | Sertraline carbamoyl glucuronide | 525.0952 | 526.1030 | 113.0239 | C24H25Cl2NO8 | 2.65 | CN(C1CCC(C2=CC=CC=C12)C3=CC(=C(C=C3)Cl)Cl)C(=O)OC4C(C(C(C(O4)C(=O)O)O)O)O |
| | Sertraline carbamoyl glucuronide methyl ester triacetate | 665.1425 | 666.1503 | 339.0682 | C31H33Cl2NO11 | 2.14 | ](C2=CC=CC=C21)C3=CC(Cl)=C(Cl)C=C3.O=C(OC)[C@@H](O4)[C@@H](OC(C)=O)[C@H](OC(C)=O)[C@@H](OC(C)=O)C4OC(N)=O |
| Sulfadiazine | | 250.0519 | 251.05972 | 156.0108 | C10H10N4O2S | 2.74 | c1cnc(nc1)NS(=O)(=O)c2ccc(cc2)N |
| | N-Acetylsulfadiazine | 292.0625 | 293.0703 | 134.0593 | C12H12N4O3S | 2.95 | CC(=O)Nc1ccc(cc1)S(=O)(=O)Nc2ncccn2 |
| Sulfamerazine | | 264.0676 | 265.07537 | 156.0112 | C11H12N4O2S | 2.74 | Cc1ccnc(n1)NS(=O)(=O)c2ccc(cc2)N |
| | N-Acetylsulfamerazine | 306.0781 | 307.0859 | 134.0596 | C13H14N4O3S | 2.95 | Cc1ccnc(n1)NS(=O)(=O)c2ccc(cc2)NC(=O)C |
| Sulfamethazine | | 278.0832 | 279.09102 | 92.05 | C12H14N4O2S | 2.20 | CC1=CC(=NC(=N1)NS(=O)(=O)C2=CC=C(C=C2)N)C |
| | Desaminosulfamethazine | 263.0723 | 264.0801 | 77.0000 | C12H13N3O2S | 0.56 | Cc1cc(nc(n1)NS(=O)(=O)c2ccccc2)C |
| | N4-Acetylsulfamethazine | 320.0938 | 321.1016 | 134.0592 | C14H16N4O3S | 2.95 | Cc1cc(nc(n1)NS(=O)(=O)c2ccc(cc2)/N=C(\C)/O)C |
| Sulfamethoxazole | | 253.0516 | 254.05939 | 156.0115 | C10H11N3O3S | 2.74 | Cc1cc(no1)NS(=O)(=O)c2ccc(cc2)N |
| | N-Acetylsulfamethoxazole | 295.0622 | 296.0700 | 134.0593 | C12H13N3O4S | 2.95 | Cc1cc(no1)NS(=O)(=O)c2ccc(cc2)NC(=O)C |
| Sulfamethoxypyridazine | | 280.0625 | 281.0703 | 156.0109 | C11H12N4O3S | 2.88 | COc1ccc(nn1)NS(=O)(=O)c2ccc(cc2)N |
| Sulfapyridine | | 249.0567 | 250.06447 | 92.05 | C11H11N3O2S | 1.88 | c1ccnc(c1)NS(=O)(=O)c2ccc(cc2)N |
| | N-Acetylsulfapyridine | 291.0672 | 292.0750 | 134.0596 | C13H13N3O3S | 2.95 | CC(=O)Nc1ccc(cc1)S(=O)(=O)Nc2ccccn2 |
| Telmisartan | | 514.2364 | 515.24415 | 469.2387 | C33H30N4O2 | 5.53 | CCCc1nc2c(cc(cc2n1Cc3ccc(cc3)c4ccccc4C(=O)O)c5nc6ccccc6n5C)C |
| Temazepam | | 300.0660 | 301.07383 | 255.0679 | C16H13ClN2O2 | 4.16 | CN1c2ccc(cc2C(=NC(C1=O)O)c3ccccc3)Cl |
| | Trimethylsilyl temazepam | 372.1056 | 373.1134 | 283.0000 | C19H21ClN2O2Si | 2.71 | CN1c2ccc(cc2C(=NC(C1=O)O[Si](C)(C)C)c3ccccc3)Cl |
| | Temazepam glucuronide | 476.0981 | 477.1059 | 301.0707 | C22H21ClN2O8 | 2.42 | CN1c2ccc(cc2C(=NC(C1=O)O[C@H]3[C@@H]([C@H]([C@@H]([C@H](O3)C(=O)O)O)O)O)c4ccccc4)Cl |

| Compound | | Monoisotopic mass | Precursor (Q1) [M+H]+ | Fragment (Q3) [M+H]+ | Chemical Formula | Retention time | SMILES |
|---|---|---|---|---|---|---|---|
| Tetrazepam | | 288.1024 | 289.11022 | 253.134 | C16H17ClN2O | 2.55 | CN1c2ccc(cc2C(=NCC1=O)C3=CCCCC3)Cl |
| Tolpropamine | | 253.1825 | 254.19033 | 181.1011 | C18H23N | 4.55 | Cc1ccc(cc1)C(CCN(C)C)c2ccccc2 |
| Trimethoprim | | 290.1374 | 291.14517 | 123.067 | C14H18N4O3 | 2.04 | COc1cc(cc(c1OC)OC)Cc2c[nH]c(=N)[nH]c2=N |
| Tripamide | | 369.0909 | 370.0987 | 289.0000 | C16H20ClN3O3S | 4.27 | c1cc(c(cc1C(=O)NN2C[C@H]3[C@@H]4CC[C@@H](C4)[C@H]3C2)S(=O)(=O)N)Cl |
| Valsartan | | 435.2265 | 436.23432 | 235.0975 | C24H29N5O3 | 4.47 | CCCCC(=O)N(Cc1ccc(cc1)c2ccccc2c3[nH]nnn3)[C@@H](C(C)C)C(=O)O |
| | 4-Hydroxyvalsartan | 451.2214 | 452.2292 | 207.0919 | C24H29N5O4 | 4.47 | O=C(O)[C@@H](N(C(=O)CCC(O)C)Cc3ccc(c1ccccc1c2nnnn2)cc3)C(C)C |
| Venlafaxine | | 277.2037 | 278.21146 | 58.0648 | C17H27NO2 | 2.99 | CN(C)CC(c1ccc(cc1)OC)C2(CCCCC2)O |
| | D,L-N,N-Didesmethyl-O-desmethylvenlafaxine | 235.1567 | 236.1645 | 107.0497 | C14H21NO2 | 2.32 | C1CCC(CC1)(C(CN)C2=CC=C(C=C2)O)O.Cl |
| | D,L-N,N-Didesmethylvenlafaxine | 249.1724 | 250.1802 | 121.0643 | C15H23NO2 | 4.57 | NCC(c1ccc(O)cc1)C2(O)CCCCC2 |
| | N,O-Didesmethylvenlafaxine | 249.1724 | 250.1802 | 107.0495 | C15H23NO2 | 2.32 | CNCC(c1ccc(cc1)O)C2(CCCCC2)O |
| | N-Desmethylvenlafaxine | 263.1880 | 264.1958 | 121.0644 | C16H25NO2 | 4.57 | CNCC(c1ccc(cc1)OC)C2(CCCCC2)O |
| | O-Desmethylvenlafaxine | 263.1880 | 264.1958 | 58.0650 | C16H25NO2 | 2.32 | CN(C)CC(C1=CC=C(C=C1)O)C2(CCCCC2)O |
| | rac-N,N-Didesmethyl-O-desmethylvenlafaxine glucuronide | 411.1888 | 412.1966 | 201.1268 | C20H29NO8 | 3.9 | Cl.CNC[C@H](C1=CC=C(O[C@@H]2OC([C@@H](O)C(O)C2O)C(O)=O)C=C1)C1(O)CCCCC1 |
| Verapamil | | 454.2826 | 455.29043 | 165.0954 | C27H38N2O4 | 3.91 | CC(C)C(CCCN(C)CCc1ccc(c(c1)OC)OC)(C#N)c2ccc(c(c2)OC)OC |
| | Desmethylverapamil | 440.2670 | 441.2748 | 151.0745 | C26H36N2O4 | 3.11 | CC(C)C(CCCN(C)CCC1=CC(=C(C=C1)OC)OC)(C#N)C2=CC(=C(C=C2)O)OC |
| | Norverapamil | 440.2670 | 441.2748 | 165.0880 | C26H36N2O4 | 3.91 | CC(C)C(CCCNCCC1=CC(=C(C=C1)OC)OC)(C#N)C2=CC(=C(C=C2)OC)OC |
| Xipamide | | 354.0436 | 355.05138 | 122.0961 | C15H15ClN2O4S | 0.43 | Cc1cccc(c1NC(=O)c2cc(c(cc2O)Cl)S(=O)(=O)N)C |

| Compound | | Monoisotopic mass | Precursor (Q1) [M+H]+ | Fragment (Q3) [M+H]+ | Chemical Formula | Retention time | SMILES |
|---|---|---|---|---|---|---|---|
| Warfarin | | 308.1043 | 309.11214 | 163.0353 | C19H16O4 | 2.96 | CC(=O)CC(c1ccccc1)c2c(=O)c3ccccc3oc2O |
| | 6-Hydroxywarfarin | 324.0993 | 325.1071 | 179.0339 | C19H16O5 | 2.59 | CC(=O)CC(C1=CC=CC=C1)C2=C(C3=C(C=CC(=C3)O)OC2=O)O |
| | 7-Hydroxywarfarin | 324.0993 | 325.1071 | 179.0340 | C19H16O5 | 2.59 | CC(=O)CC(c1ccccc1)c2c(c3ccc(cc3oc2=O)O)O |
| Zolazepam | | 286.1225 | 287.13027 | 138.1021 | C15H15FN4O | 2.59 | Cc1c2c(n(n1)C)N(C(=O)CN=C2c3ccccc3F)C |
| Zolpidem | | 307.1679 | 308.17574 | 235.1228 | C19H21N3O | 3.46 | Cc1ccc(cc1)c2c(n3cc(ccc3n2)C)CC(=O)N(C)C |
| | Zolpidem 6-carboxylic acid | 337.1421 | 338.1499 | 265.0950 | C19H19N3O3 | 2.08 | Cc1ccc(cc1)c2c(n3cc(ccc3n2)C(=O)O)CC(=O)N(C)C |
| | Zolpidem phenyl-4-carboxylic acid | 337.1421 | 338.1499 | 292.1450 | C19H19N3O3 | 2.06 | Cc1ccc2nc(c(n2c1)CC(=O)N(C)C)c3ccc(cc3)C(=O)O |

**Figure PIII S1**. TYPE A: detection of parent & MTB, no evidence for transformation in mesocosm

**a) Carbamazepine**

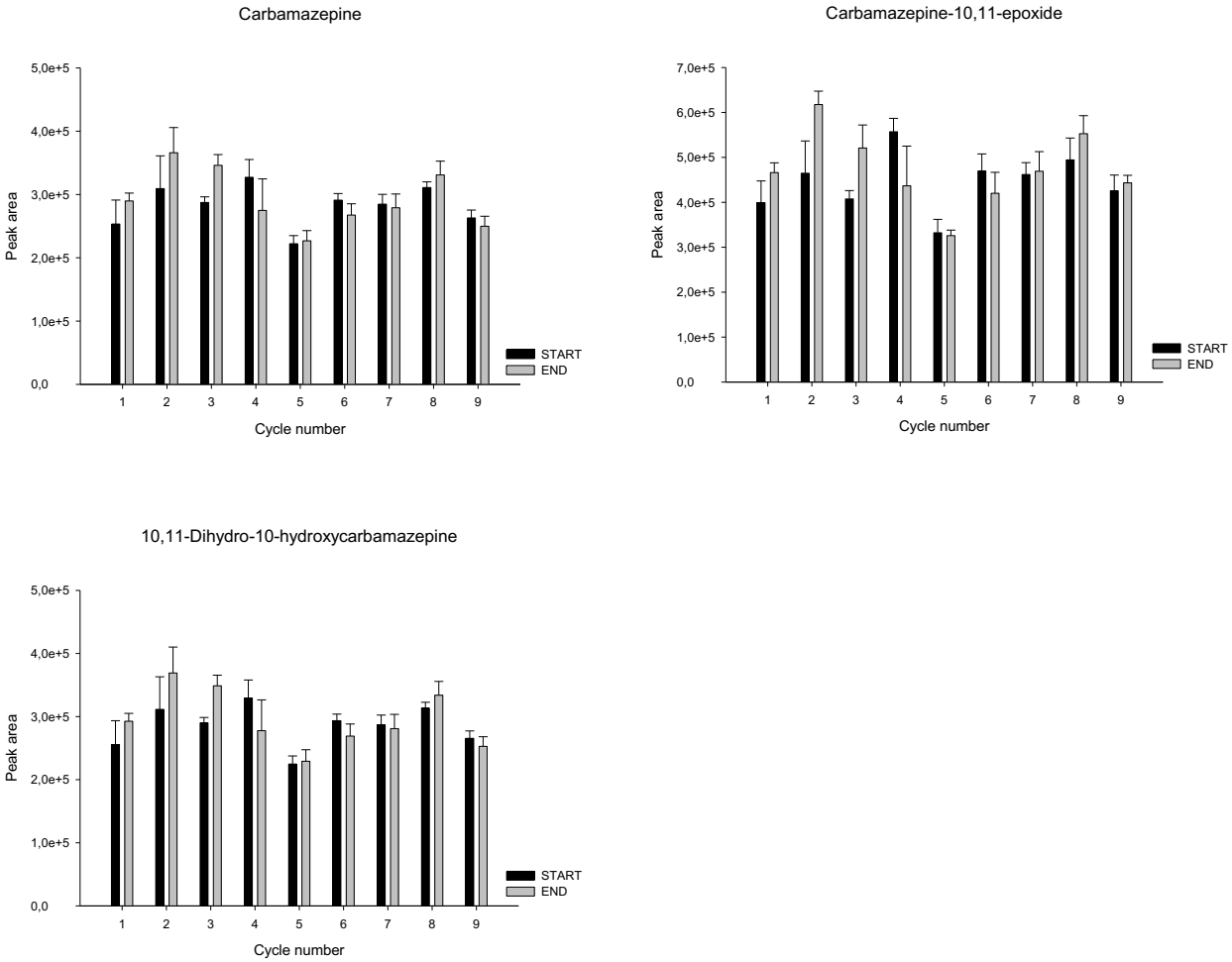

## b) Diclofenac

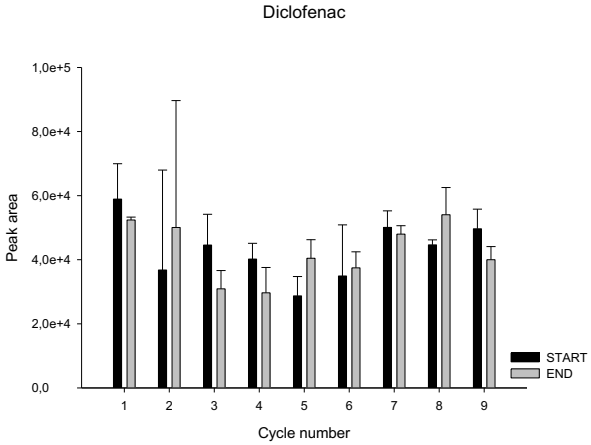


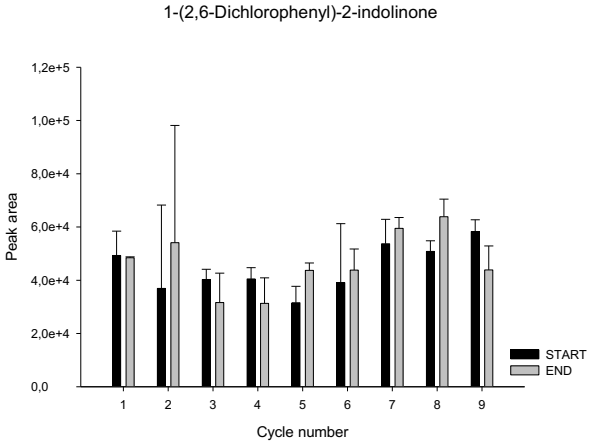


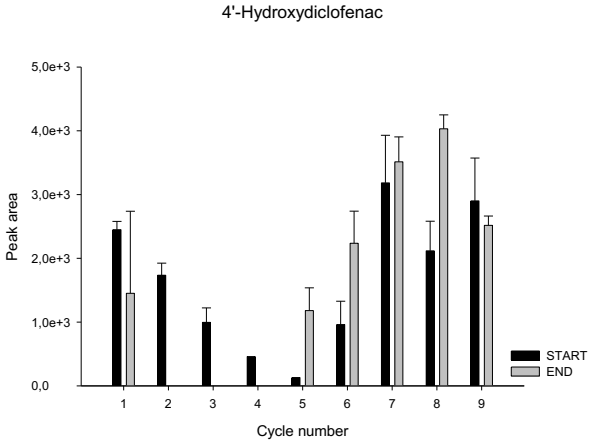


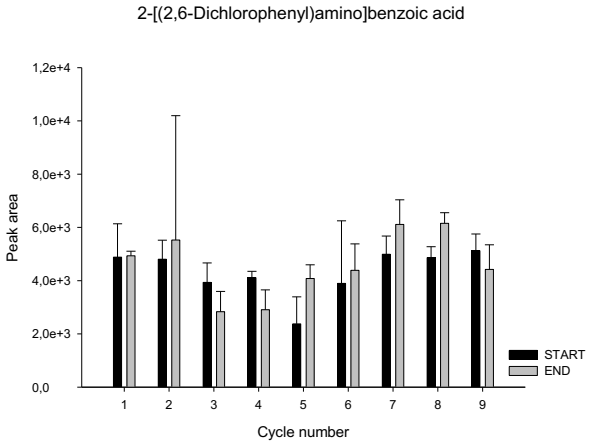

## c) Diazepam

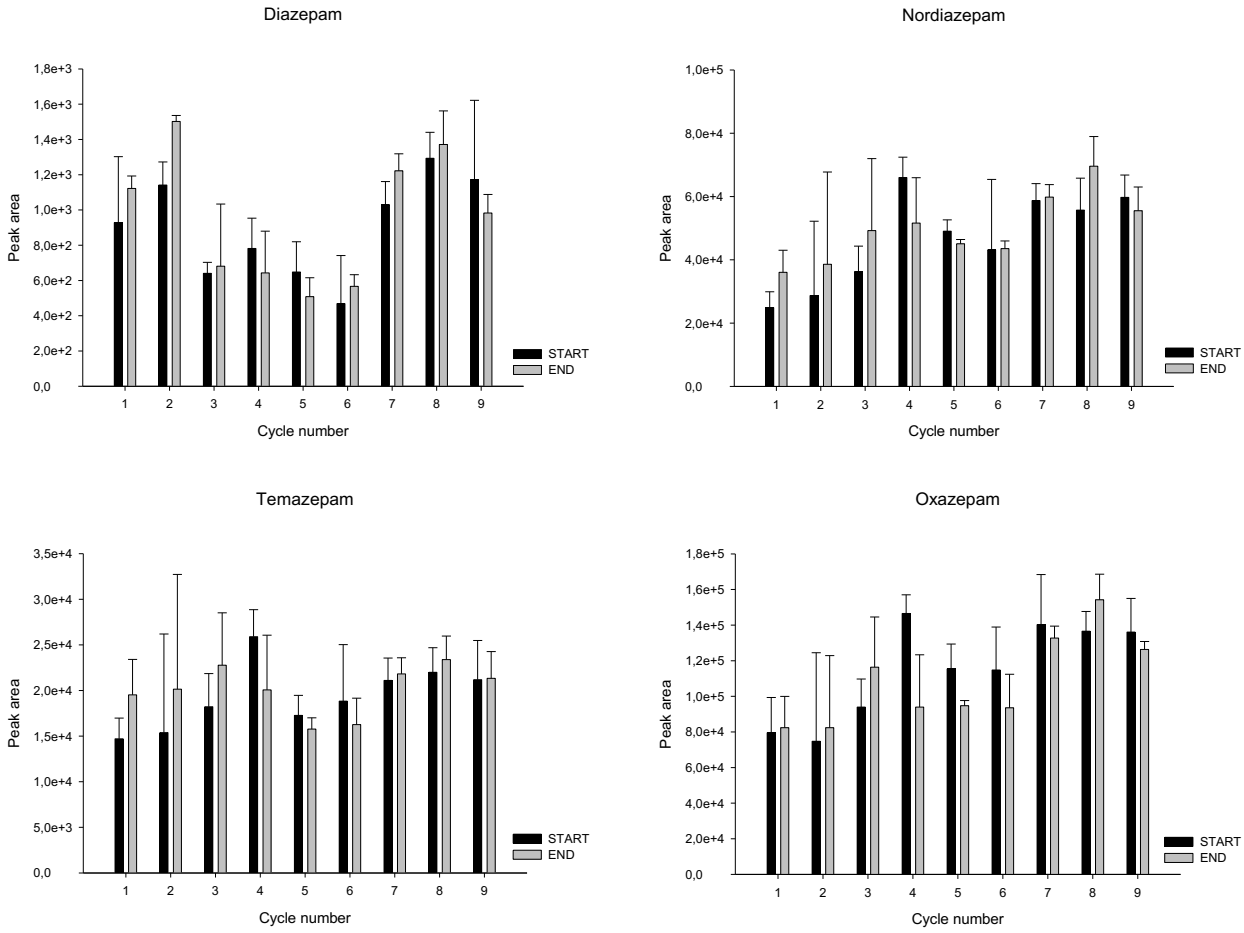
Diazepam
Peak area
1,8e+3
1,6e+3
1,4e+3
1,2e+3
1,0e+3
8,0e+2
6,0e+2
4,0e+2
2,0e+2
0,0
1 2 3 4 5 6 7 8 9
Cycle number
START
END
Nordiazepam
Peak area
1,0e+5
8,0e+4
6,0e+4
4,0e+4
2,0e+4
0,0
1 2 3 4 5 6 7 8 9
Cycle number
START
END
Temazepam
Peak area
3,5e+4
3,0e+4
2,5e+4
2,0e+4
1,5e+4
1,0e+4
5,0e+3
0,0
1 2 3 4 5 6 7 8 9
Cycle number
START
END
Oxazepam
Peak area
1,8e+5
1,6e+5
1,4e+5
1,2e+5
1,0e+5
8,0e+4
6,0e+4
4,0e+4
2,0e+4
0,0
1 2 3 4 5 6 7 8 9
Cycle number
START
END

## d) Venlafaxine

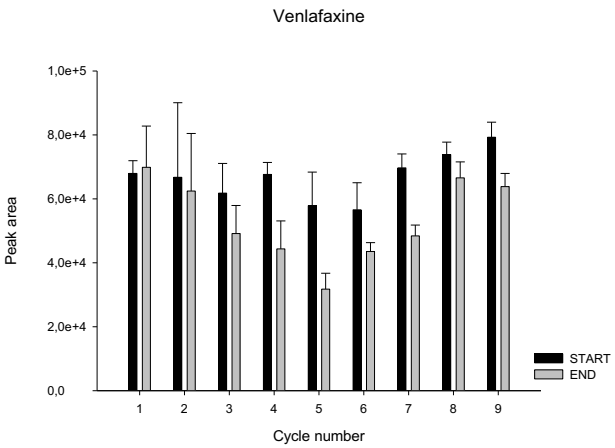


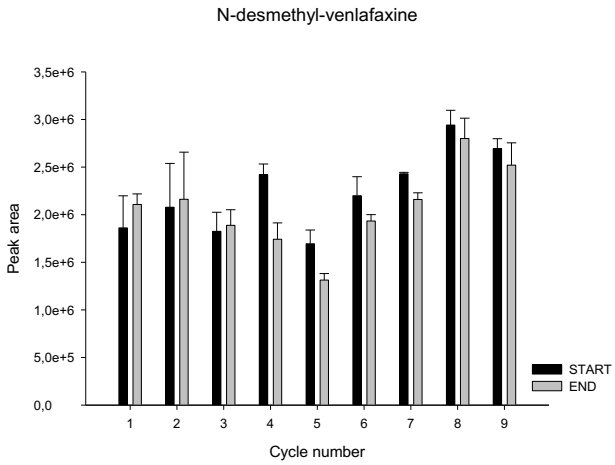


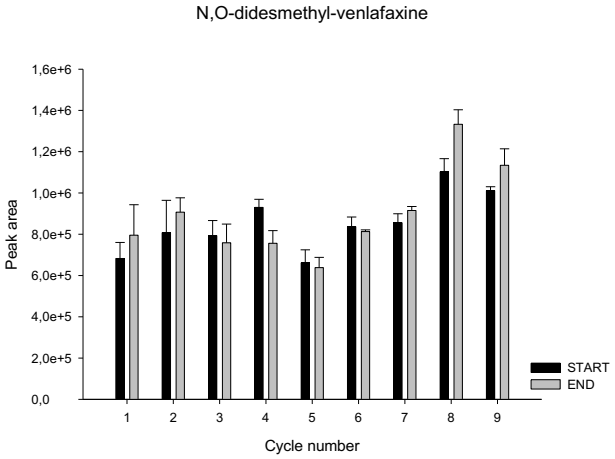


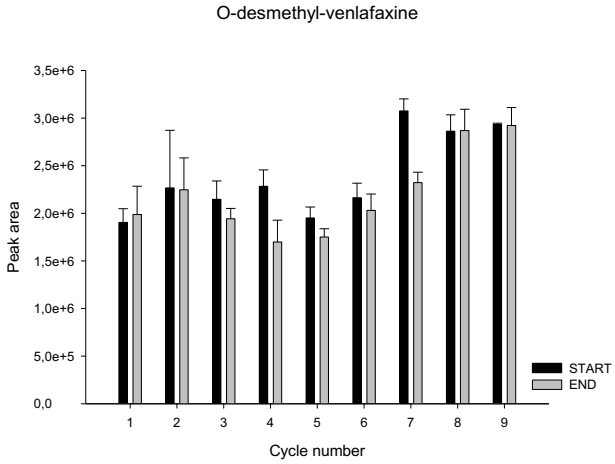

**Figure PIII S2**. TYPE B: detection of parent & TP, evidence for transformation in mesocosm

**a) Atenolol**

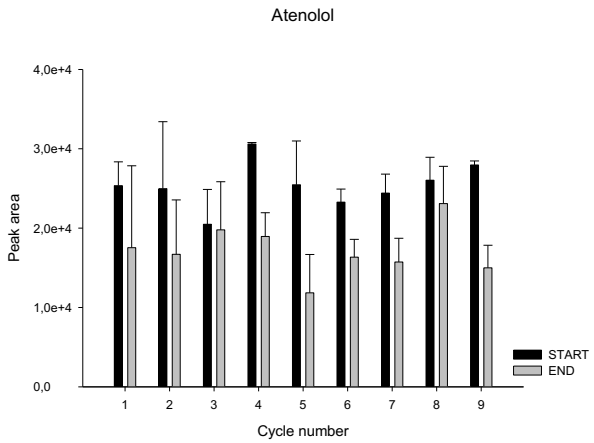


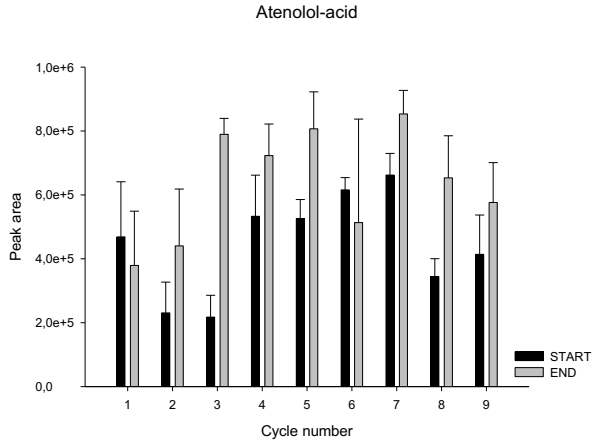


**b) Sitagliptin**

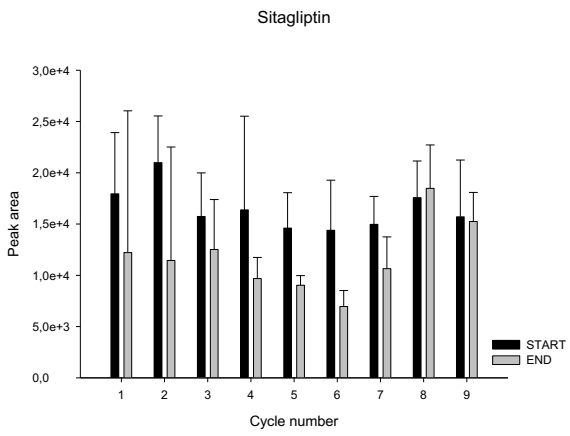


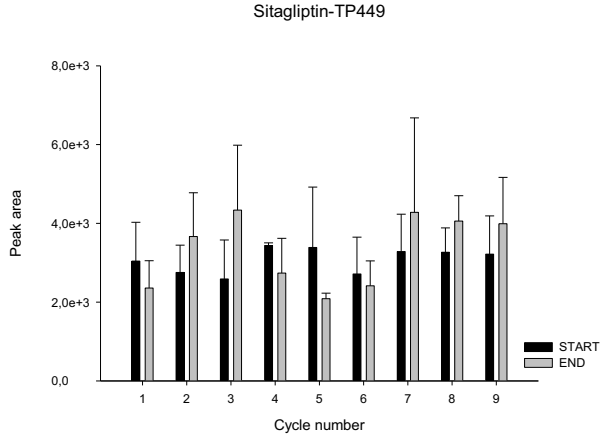

## c) Valsartan

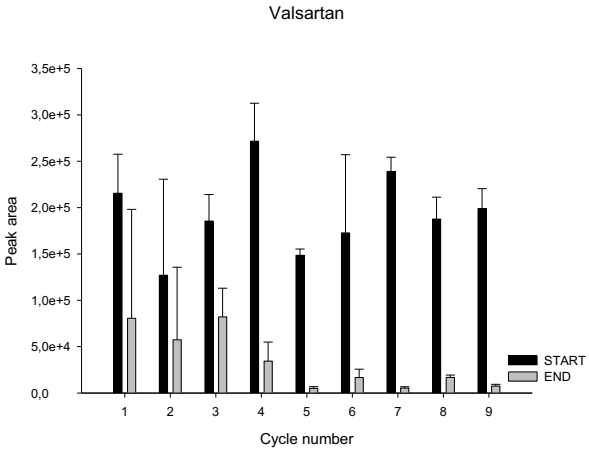
Valsartan
Peak area
3,5e+5
3,0e+5
2,5e+5
2,0e+5
1,5e+5
1,0e+5
5,0e+4
0,0
1 2 3 4 5 6 7 8 9
Cycle number
START
END

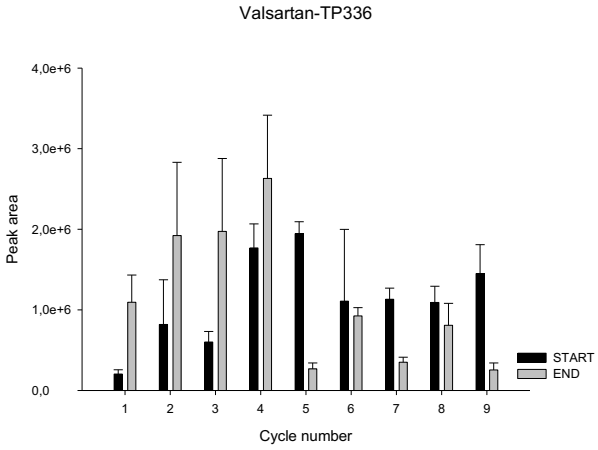
Valsartan-TP336
Peak area
4,0e+6
3,0e+6
2,0e+6
1,0e+6
0,0
1 2 3 4 5 6 7 8 9
Cycle number
START
END

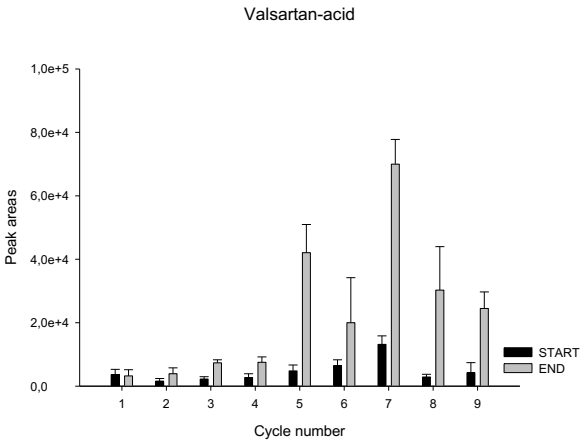
Valsartan-acid
Peak areas
1,0e+5
8,0e+4
6,0e+4
4,0e+4
2,0e+4
0,0
1 2 3 4 5 6 7 8 9
Cycle number
START
END

**Figure PIII S3**. TYPE C: Only detection of parent compounds

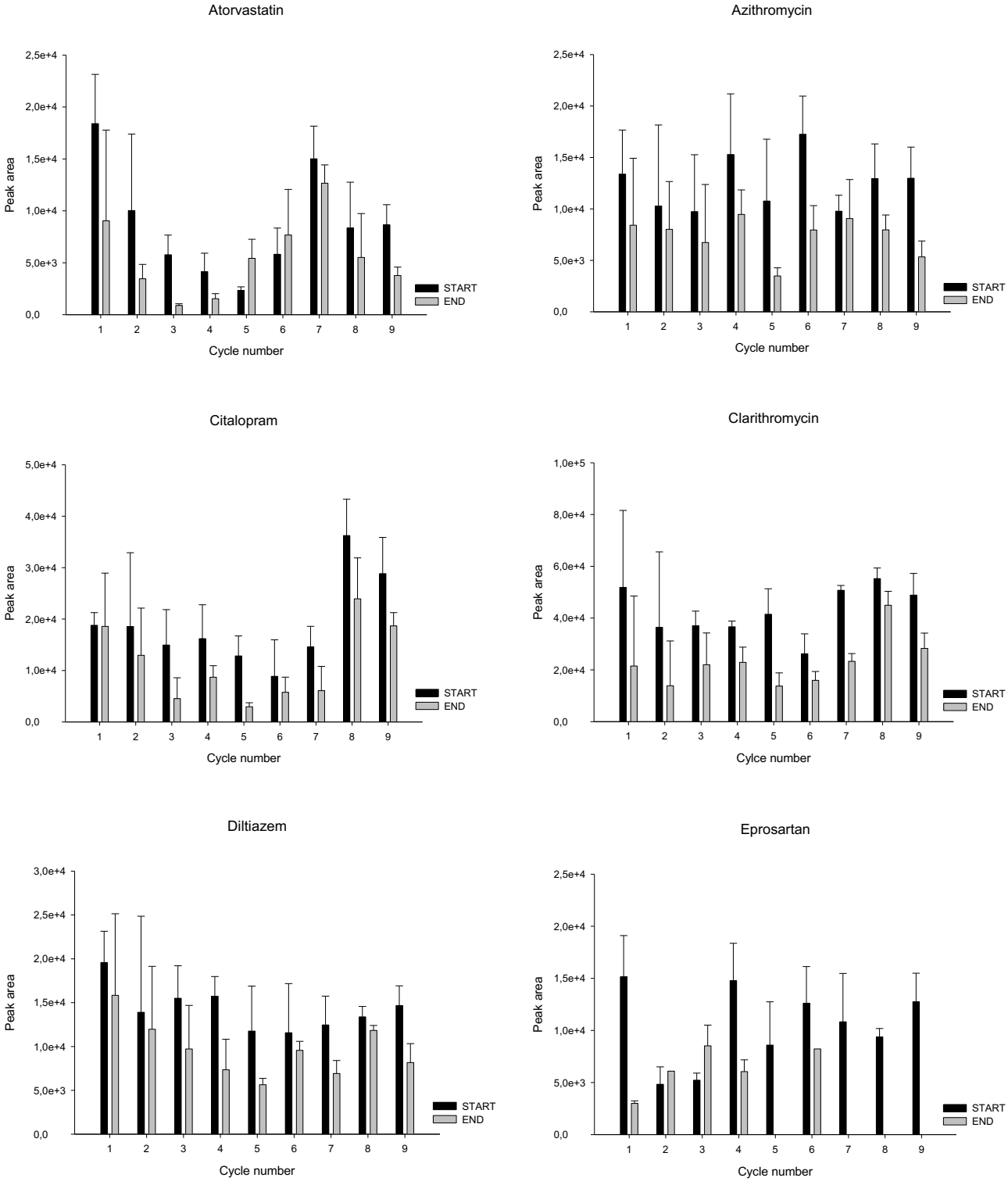

Fluconazole

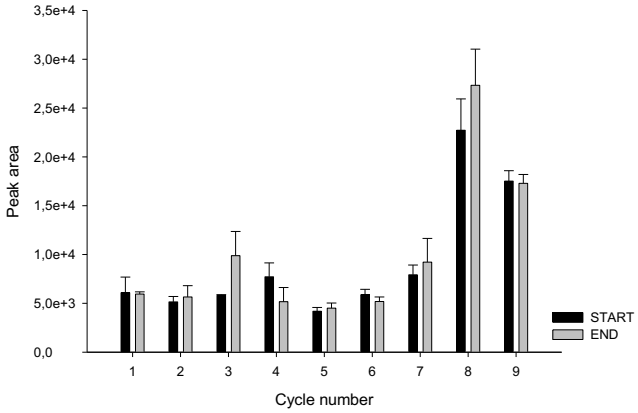


Ketoprofen

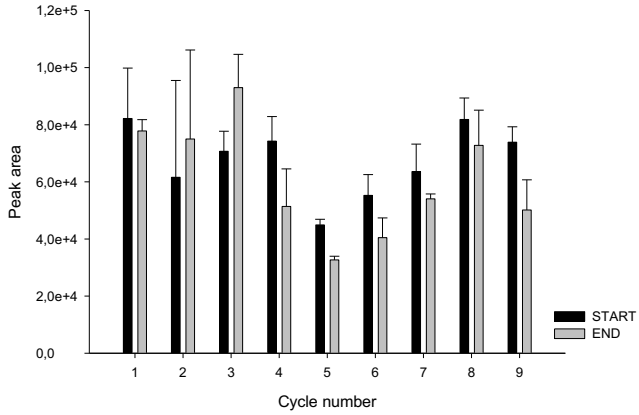


Lamotrigine

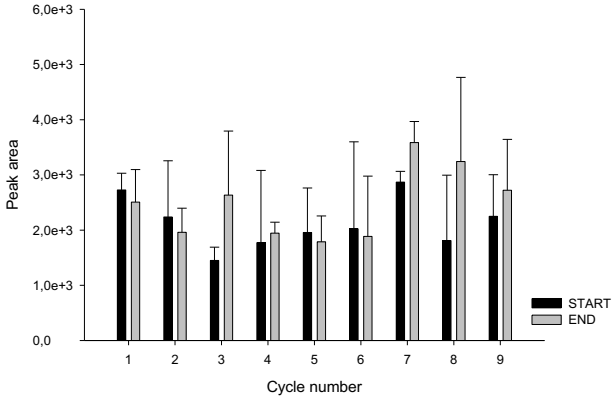


Lormetazepam

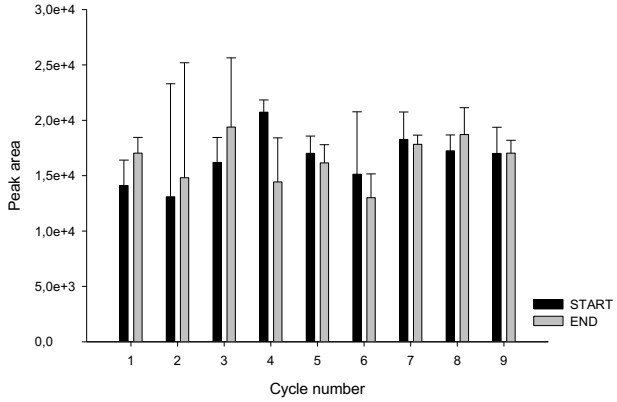


Metformin

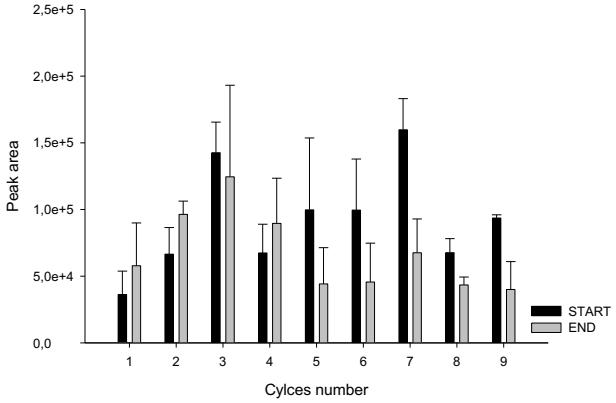


Telmisartan

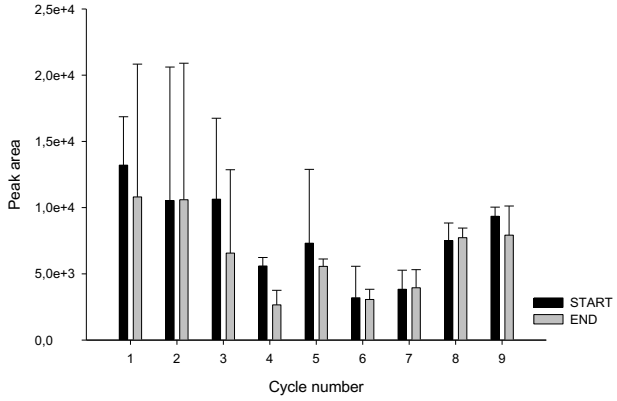


Trimethoprim

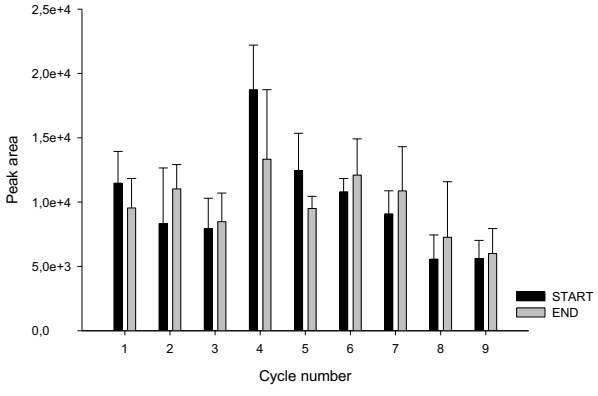

**Figure PIII S4**. TYPE D: only detection of MTB, no evidence for transformation in mesocosm

**a) Bupropion**

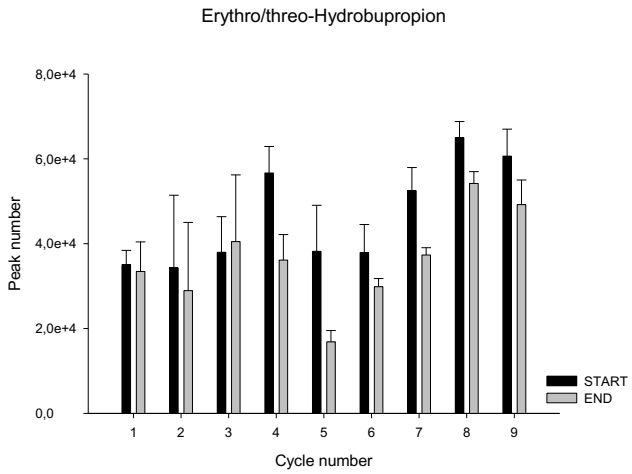


**b) Zolpidem**

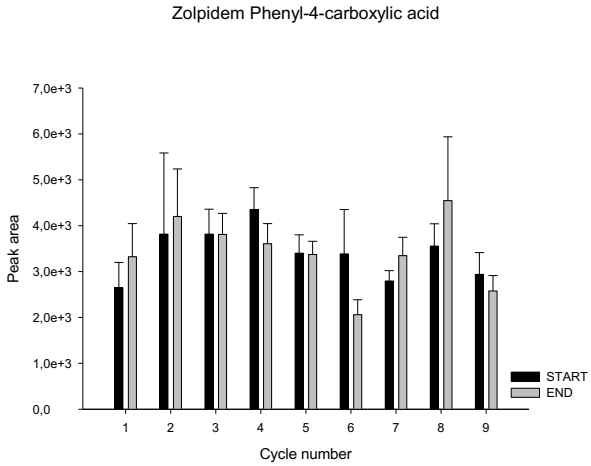

**Figure PIII S5**. TYPE E: only detection of MTB, evidence for transformation in mesocosm

**a) Cocaine**

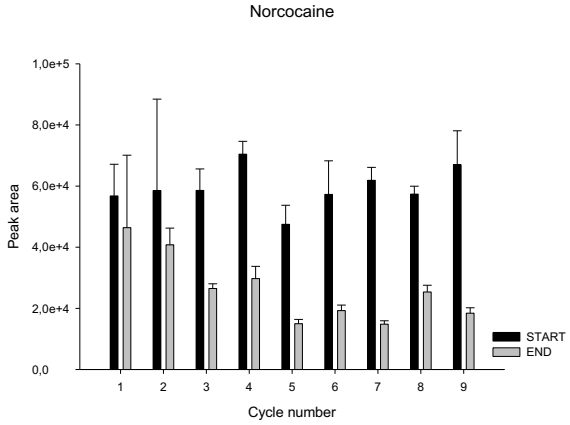


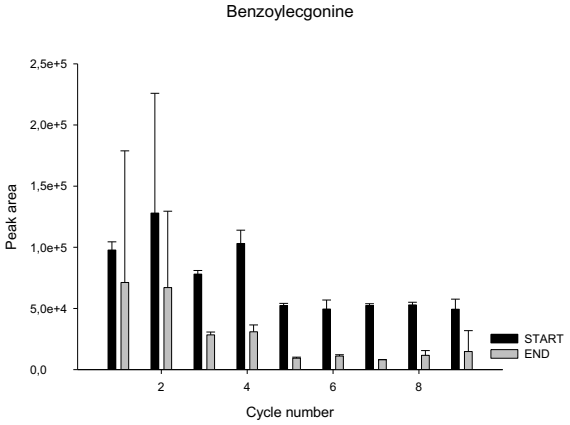


**b) Erythromycin A**

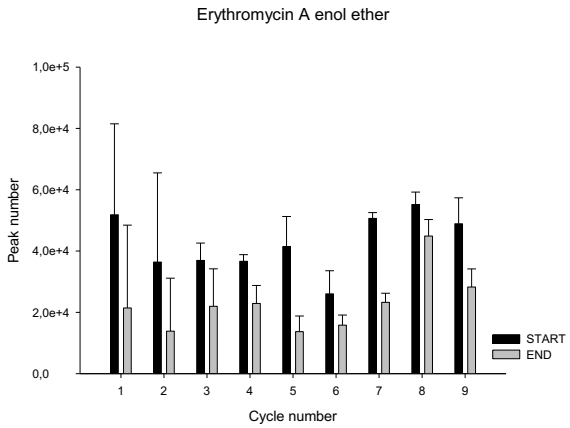


**c) Omeprazol**

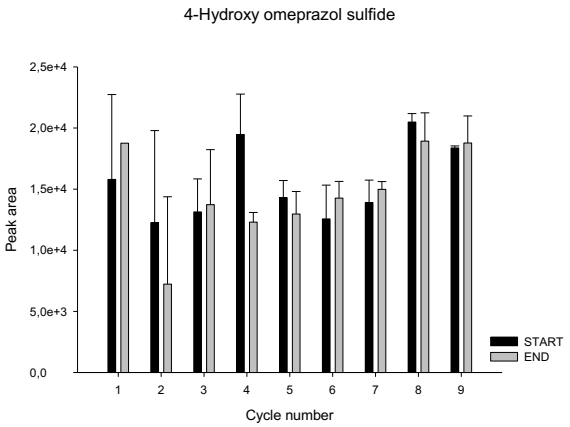

**Figure PIII S6**. Tentative identification of atenolol-acid by querying the ChemSpider database

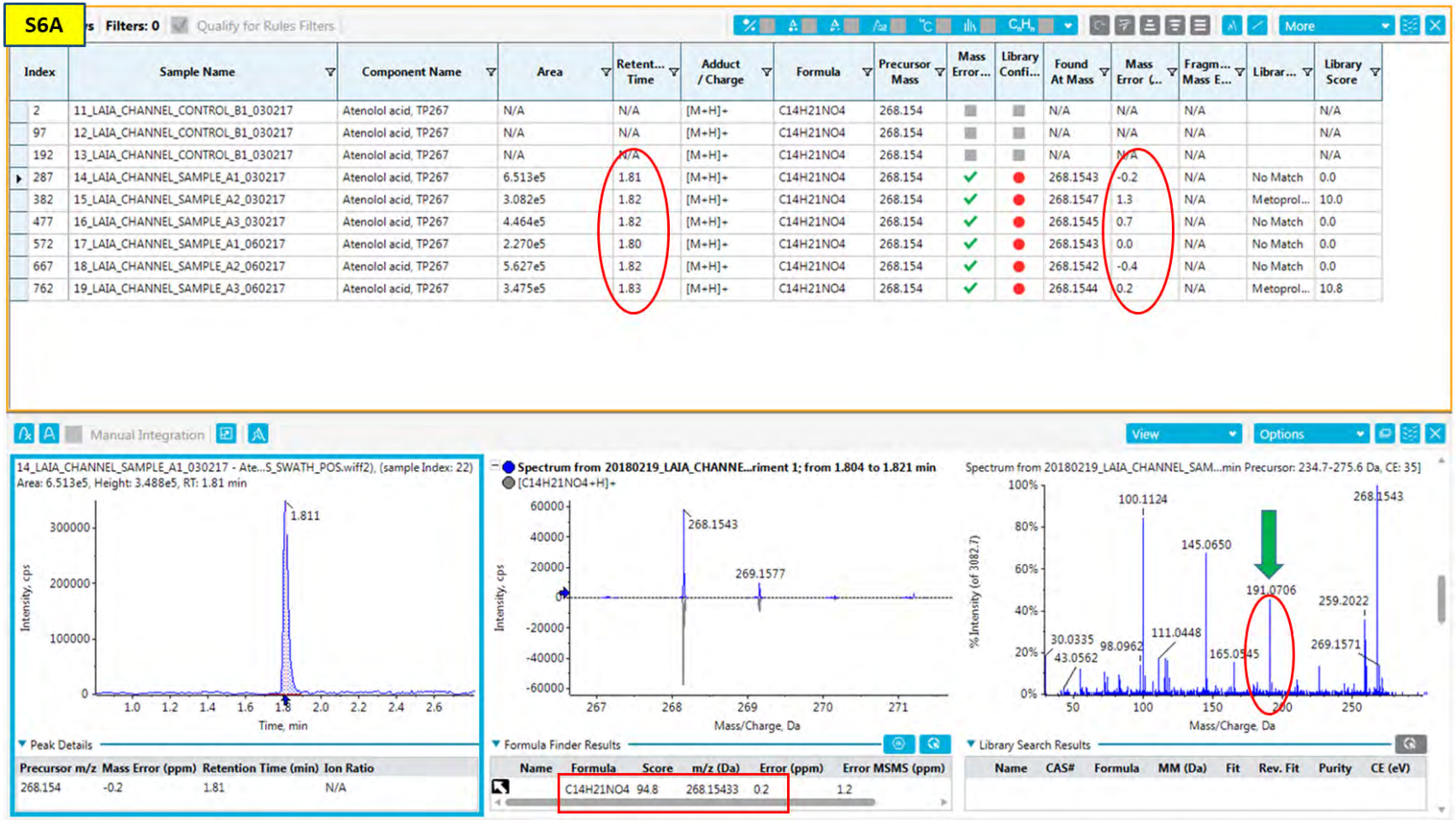

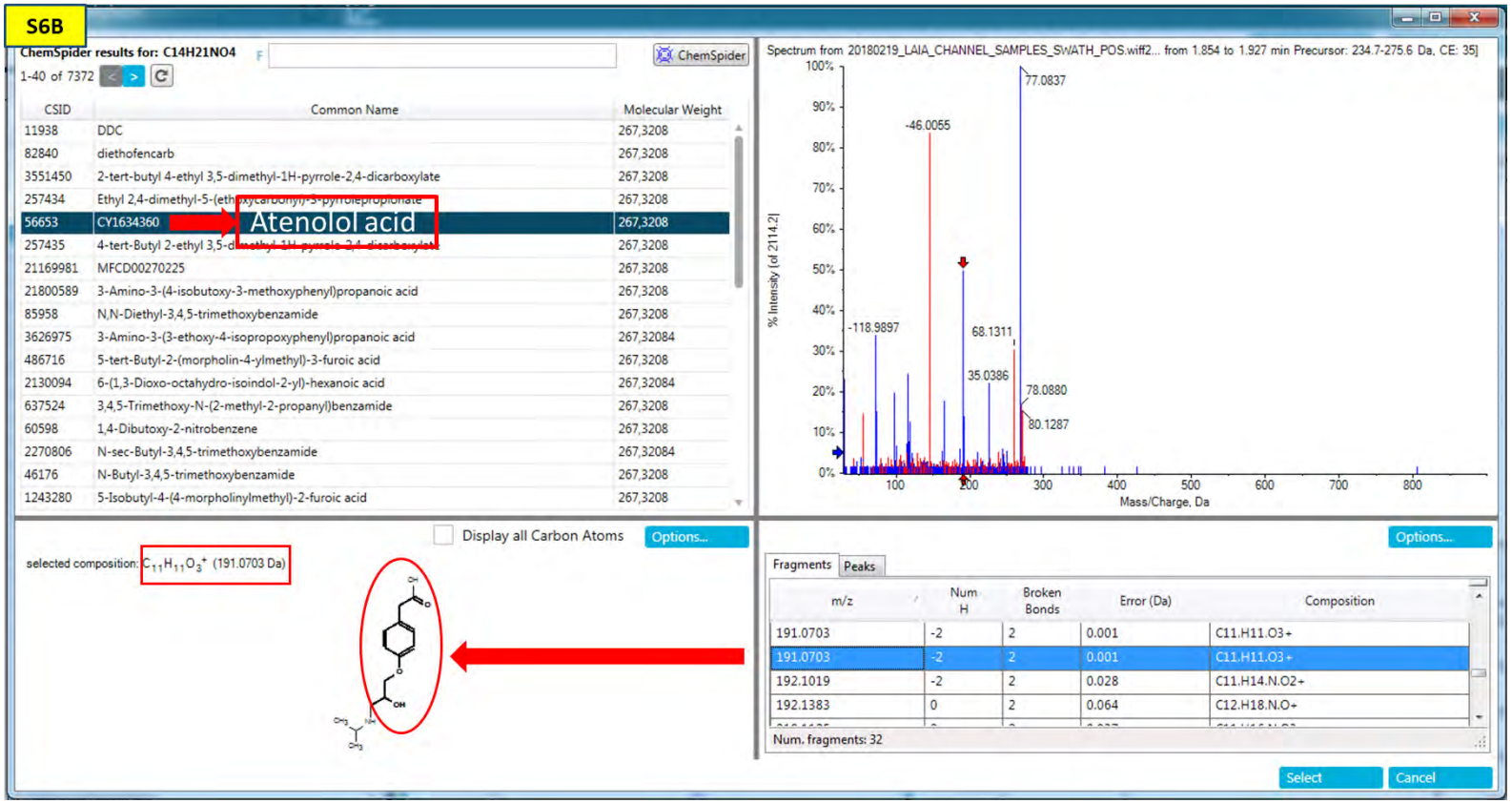


For the peak m/z 268.1543, the software automatically generated the molecular formula C14H21NO4 with a mass error of below 5 ppm for all samples. However, no compound is associated with this formula in the commercial library (Fig. S6A). Nonetheless, it was possible to interrogate Chemspider online database to try to justify the Formula Finder result matching the proposed elemental composition and isotope pattern. Hence, a list of compounds with identical chemical formula was retrieved with the ranking according to the number of PubMed citations (Fig S6B). Scrolling through the panel of compounds proposed by the software (upper left panel), the ChemSpider ID 56653 corresponded to the compound CY1634360, that is precisely the acid atenolol, as evidenced by the structure shown in the lower left panel of the same figure. Matching fragment ions were indicated in blue in the upper right panel, whereas, in the lower right panel all the experimental fragments are listed. For example, the fragment [M + H]+ 191.0703 has been associated with the molecular formula C11H11O3+. By highlighting this fragment, the portion of the molecule corresponding to this mass is marked in the lower left panel. A larger number of matching fragment ions indicated a higher likelihood of correct assignment.

**Figure PIII S7**. Tentative identification of Valsartan-TP336 by the MS/MS spectra. A: Valsartan-TP336; B: Valsartan.

**S7A**

| | Sample Name | Component Name | Area | Retent... Time | Adduct / Charge | Formula | Precursor Mass | Mass Error... | Library Confi... | Found At Mass | Mass Error (... | Fragm... Mass E... | Library Hit | Library Score |
|---|---|---|---|---|---|---|---|---|---|---|---|---|---|---|
| 85 | 11_LAIA_CHANNEL_CONTROL_B1_030217 | VSTp1 | N/A | N/A | [M+H]+ | C19H21N5O | 336.182 | | | N/A | N/A | N/A | | N/A |
| 180 | 12_LAIA_CHANNEL_CONTROL_B1_030217 | VSTp1 | N/A | N/A | [M+H]+ | C19H21N5O | 336.182 | | | N/A | N/A | N/A | | N/A |
| 275 | 13_LAIA_CHANNEL_CONTROL_B1_030217 | VSTp1 | N/A | N/A | [M+H]+ | C19H21N5O | 336.182 | | | N/A | N/A | N/A | | N/A |
| 370 | 14_LAIA_CHANNEL_SAMPLE_A1_030217 | VSTp1 | 1.554e5 | 3.75 | [M+H]+ | C19H21N5O | 336.182 | ✓ | ● | 336.1818 | -0.2 | N/A | No Match | 0.0 |
| 465 | 15_LAIA_CHANNEL_SAMPLE_A2_030217 | VSTp1 | 1.970e5 | 3.76 | [M+H]+ | C19H21N5O | 336.182 | ✓ | ● | 336.1819 | 0.0 | N/A | No Match | 0.0 |
| 560 | 16_LAIA_CHANNEL_SAMPLE_A3_030217 | VSTp1 | 2.597e5 | 3.76 | [M+H]+ | C19H21N5O | 336.182 | ✓ | ● | 336.1821 | 0.7 | N/A | No Match | 0.0 |
| 655 | 17_LAIA_CHANNEL_SAMPLE_A1_060217 | VSTp1 | 9.415e5 | 3.74 | [M+H]+ | C19H21N5O | 336.182 | ✓ | ● | 336.1817 | -0.5 | N/A | No Match | 0.0 |
| 750 | 18_LAIA_CHANNEL_SAMPLE_A2_060217 | VSTp1 | 8.611e5 | 3.76 | [M+H]+ | C19H21N5O | 336.182 | ✓ | ● | 336.1816 | -0.9 | N/A | No Match | 0.0 |
| 845 | 19_LAIA_CHANNEL_SAMPLE_A3_060217 | VSTp1 | 1.482e6 | 3.76 | [M+H]+ | C19H21N5O | 336.182 | ✓ | ● | 336.1810 | -2.7 | N/A | No Match | 0.0 |

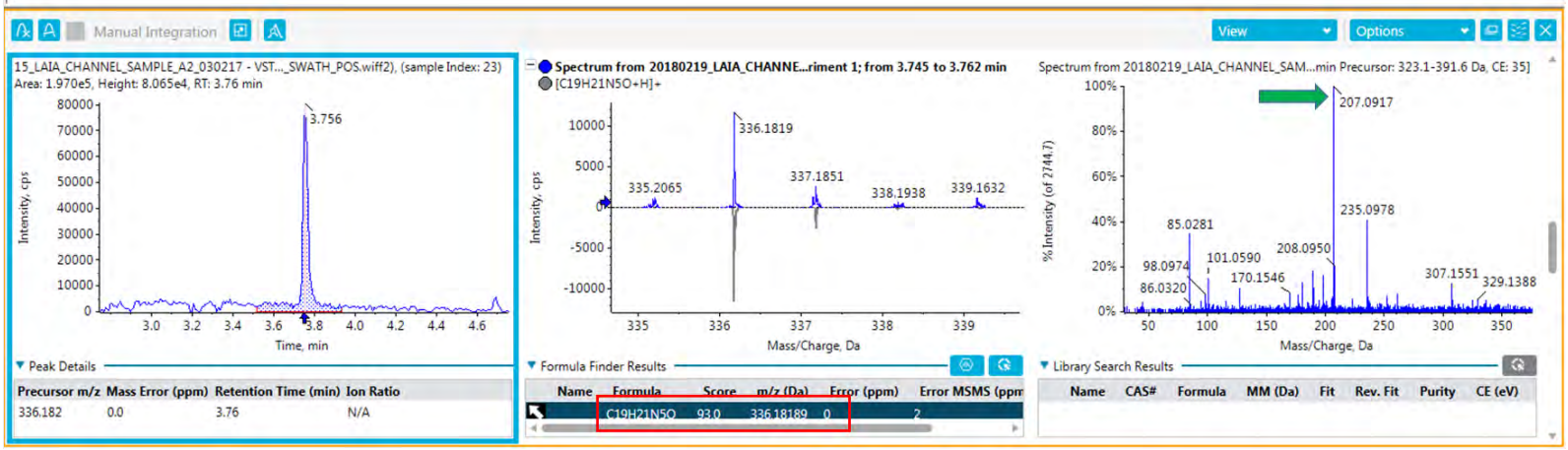

**S7B**

| | Sample Name | Component... | Area | Retent... Time | Adduct / C... | Formula | Precursor Mass | Mass Error... | Frag... Mass... | Library Confi... | Found At Mass | Mass Error (... | Fragm... Mass E... | Library Hit | Library Score |
|---|---|---|---|---|---|---|---|---|---|---|---|---|---|---|---|
| 395 | 11_LAIA_CHANNEL_CONTROL_B1_030217 | Valsartan (NIST) | N/A | N/A | [M+H]+ | C24H29N5O3 | 436.234 | | | | N/A | N/A | N/A | | N/A |
| 824 | 12_LAIA_CHANNEL_CONTROL_B1_030217 | Valsartan (NIST) | N/A | N/A | [M+H]+ | C24H29N5O3 | 436.234 | | | | N/A | N/A | N/A | | N/A |
| 1253 | 13_LAIA_CHANNEL_CONTROL_B1_030217 | Valsartan (NIST) | N/A | N/A | [M+H]+ | C24H29N5O3 | 436.234 | | | | N/A | N/A | N/A | | N/A |
| 1682 | 14_LAIA_CHANNEL_SAMPLE_A1_030217 | Valsartan (NIST) | 2.187e5 | 4.47 | [M+H]+ | C24H29N5O3 | 436.234 | ✓ | ▲ | ✓ | 436.2334 | -2.2 | -6.4 | Valsartan (NIST) | 97.4 |
| 2111 | 15_LAIA_CHANNEL_SAMPLE_A2_030217 | Valsartan (NIST) | 1.720e5 | 4.47 | [M+H]+ | C24H29N5O3 | 436.234 | ✓ | ✓ | ✓ | 436.2341 | -0.5 | -2.8 | Valsartan (NIST) | 97.4 |
| 2540 | 16_LAIA_CHANNEL_SAMPLE_A3_030217 | Valsartan (NIST) | 2.559e5 | 4.47 | [M+H]+ | C24H29N5O3 | 436.234 | ✓ | ✓ | ✓ | 436.2333 | -2.3 | -4.8 | Valsartan (NIST) | 97.3 |
| 2969 | 17_LAIA_CHANNEL_SAMPLE_A1_060217 | Valsartan (NIST) | 2.162e5 | 4.46 | [M+H]+ | C24H29N5O3 | 436.234 | ✓ | ▲ | ✓ | 436.2337 | -1.5 | -5.5 | Valsartan (NIST) | 96.7 |
| 3398 | 18_LAIA_CHANNEL_SAMPLE_A2_060217 | Valsartan (NIST) | 1.666e4 | 4.47 | [M+H]+ | C24H29N5O3 | 436.234 | ✓ | ✓ | ✓ | 436.2345 | 0.3 | 2.2 | Valsartan (NIST) | 88.6 |
| 3827 | 19_LAIA_CHANNEL_SAMPLE_A3_060217 | Valsartan (NIST) | 9.154e3 | 4.48 | [M+H]+ | C24H29N5O3 | 436.234 | ✓ | ✓ | ✓ | 436.2342 | -0.2 | -1.1 | Valsartan (NIST) | 92.7 |
| 4256 | 20_LAIA_CHANNEL_SAMPLE_A1_070217 | Valsartan (NIST) | 7.792e3 | 4.48 | [M+H]+ | C24H29N5O3 | 436.234 | ✓ | ✓ | ● | 436.2342 | -0.4 | 3.3 | No Match | 0.0 |
| 4685 | 21_LAIA_CHANNEL_SAMPLE_A2_070217 | Valsartan (NIST) | 1.821e5 | 4.47 | [M+H]+ | C24H29N5O3 | 436.234 | ✓ | ✓ | ✓ | 436.2330 | -3.1 | -3.0 | Valsartan (NIST) | 96.7 |
| 5114 | 22_LAIA_CHANNEL_SAMPLE_A3_070217 | Valsartan (NIST) | 1.915e5 | 4.47 | [M+H]+ | C24H29N5O3 | 436.234 | ✓ | ▲ | ✓ | 436.2336 | -1.6 | -5.5 | Valsartan (NIST) | 97.2 |
| 5543 | 20_LAIA_CHANNEL_SAMPLE_A1_090217 | Valsartan (NIST) | 1.477e5 | 4.47 | [M+H]+ | C24H29N5O3 | 436.234 | ✓ | ✓ | ✓ | 436.2335 | -1.9 | -4.6 | Valsartan (NIST) | 97.1 |
| 5972 | 21_LAIA_CHANNEL_SAMPLE_A2_090217 | Valsartan (NIST) | 9.792e3 | 4.48 | [M+H]+ | C24H29N5O3 | 436.234 | ✓ | ✓ | ● | 436.2353 | 2.2 | 3.3 | No Match | 0.0 |

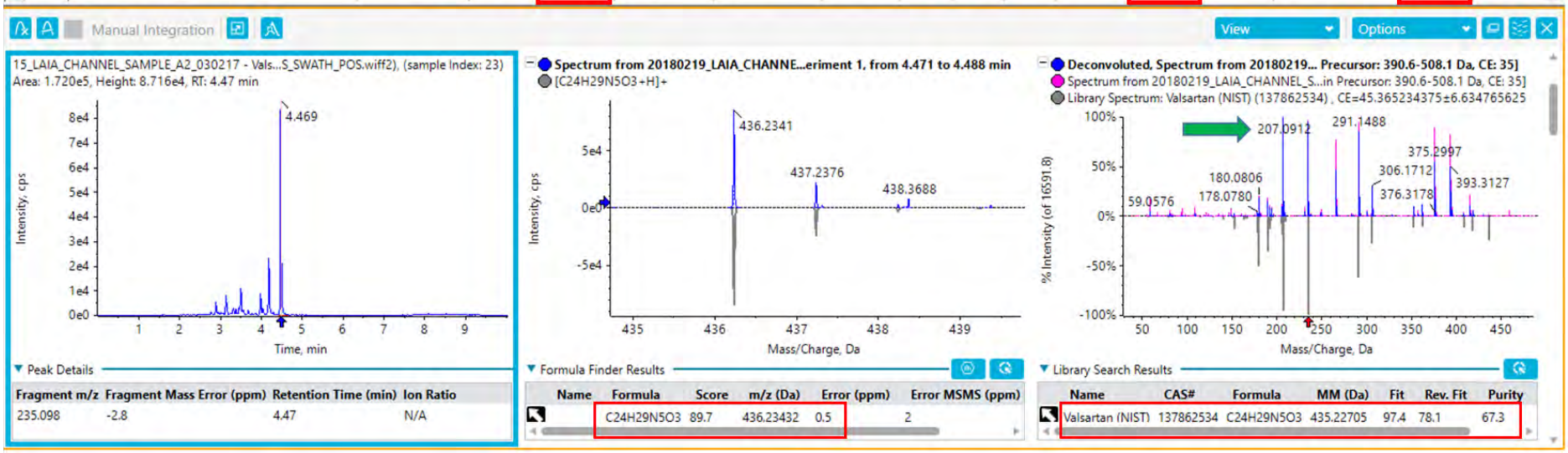

# General discussion

# General discussion

The chemical status of river systems, their changes in time and space, and the biological implications occurring at different scales of analysis, have been the object of this thesis. This general discussion will provide some insights into the complex interactions between chemical and biological compartments, and also some derivations from the results obtained during the thesis.

**Relating aquatic chemistry to biological communities**

In the past, the terms "biological communities" and "chemical quality" were evolved independently, maintaining rather strict academic separation. The study of the biological compartment has classically aimed at understanding how species are structured in populations and communities, and how do they function. The emphasis has been placed on their diversity, composition, distribution, and role in the ecosystem (Leibold and Chase, 2017). Defining the chemicals present in the environment has been a sustained field of study, especially by quantifying concentrations of compounds in different matrices (water, sediment, biota), and improving detection and analysis methods. The reality, though, is that the two fields of knowledge have evolved separately, probably because of the lack of multidisciplinary approaches using both at the same time. Such a perspective is essential given that freshwater biological communities not only are affected by chemicals occurring in the environment but also perform as potential transformers to these substances (Kosjek et al., 2007).

Early studies already observed that the composition and distribution of biological communities were modulated by organic matter, by nutrients in excess, or by heavy metal pollution (Margalef, 1960). This was the foundation of the saprobic system, an early categorization of water bodies affected by sewage, and based on the indicator value of organisms (Sládeček, 1986). "New" (emerging) organic chemicals were not considered at that time, but awareness increased because of obvious implications of some of them on both the human and the ecosystem health (on which the *Silent Spring*, of Rachel Carson (1962) , was particularly significant). This perception quickly joined with the increasingly higher capability to determine chemical substances at the very small concentrations at which they occur in the environment (Krauss et al., 2010). Nowadays, organic microcontaminants cannot be contemplated aside from other pollutants such as nutrients

in excess, or total organic carbon (TOC), all of them being chemical players within the rivers' system.

**Multiple-scale approach: potentialities and limitations**

Connecting chemical occurrences with biological communities demands complete sets of environmental and biological variables, at multiple scales. Field studies provide realistic data, but also have drawbacks regarding the complexity of monitoring stressors, which need to be considered on the relationship between water quality and biological communities. Relating pressures and river quality (chemical, biological) require long-term data, to be complemented with hydromorphological data, and even land-use data, at each sampling site. Drainage networks are affected by infrastructures, which cause them to run artificially, and lose connectivity. This obviously makes difficult establishing accurate longitudinal patterns

Fulfilling the requirements of both good quality and complete data, is often decided at the cost of reducing the number of sampling sites (López-Doval et al., 2012). In the first paper of this Thesis, microcontaminant data were not available for many sites, given the condition of concurring chemical and biological data. This forced to perform the analysis of chemical and biological quality solely considering general variables (nutrients, temperature, conductivity), to be compared with a fraction of the biological communities (phytoplankton). Moreover, temporal data that could cover the dynamics of the river were scarcely available, this forcing to restrict our analysis to a simple spatial approximation (Paper I).

Field-based evidence and laboratory experiments are complementary in nature, and optimally need to be performed conjointly. The two have recognized strengths and weaknesses. Implications derived from field studies are correlational but may not have sufficient statistical power to indicate emerging patterns of ecological structure. Field monitoring and modeling do not provide insight on mechanisms associated with causal relationships. Uncovering these require experiments in the laboratory, where controlled conditions could be imposed. In this thesis, this scale was approached by using a series of artificial indoor streams where physical parameters were easily controlled and manipulated (mesocosms) (Navarro et al., 2000). In this experiment, biofilm variables provided the necessary testing of responses to chemical stressors. Laboratory experiments might shed light on the relevance of the factors tested, though are simplifications of the

real complexity of river systems (Paper II). It is worth recognizing that the statistical power of some of the relationships detected in the Paper II was low; this indicates that several other factors are at play and undermine the relationships searched during the experiments. Laboratory results need to be therefore validated with the corresponding observations from field studies, though results obtained with the two methodologies need to be used cautiously (Sabater and Borrego, 2016).

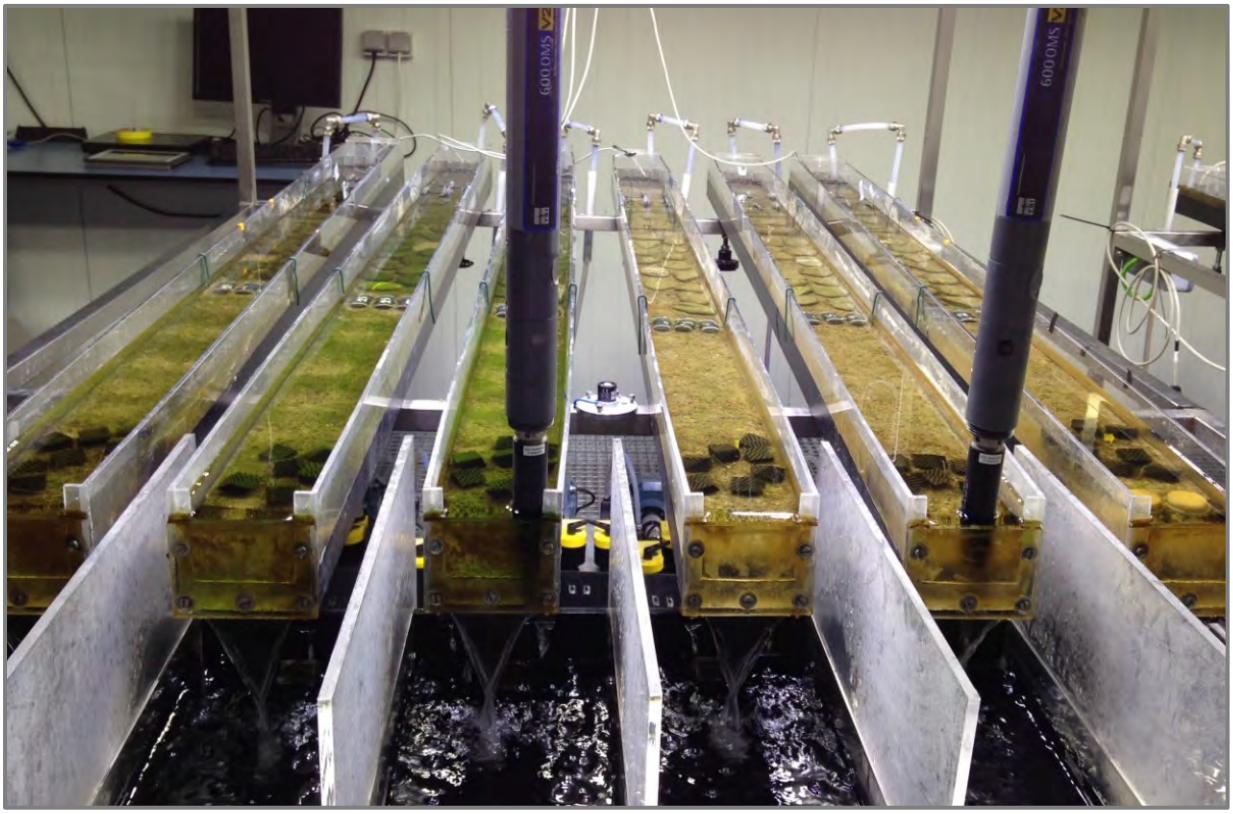

**Figure D1**. Artificial indoor streams at ICRA Facility

The transformation and degradation of organic contaminants in the environment are the ultimate scale regarding the fate of these molecules. Most chemical analytical methods focus on parent target compounds and rarely include metabolites or TPs which derive from them but are environmentally transformed or human metabolized. The concentration of these chemical compounds in some cases can be higher than the original compounds (Paper III). A major limitation to understanding in which manner these TPs contribute to the overall presence of chemicals in the environment is the lack of analytical reference standards, either not commercially available or too expensive (Kern et al., 2009). Thus, the results of laboratory degradation studies may not be representative of actual environmental conditions. However, high-resolution instruments allow identifying

metabolites and TPs that were not previously known to be present in water samples. Performing a retrospective data analysis for compounds not included in a first phase of data processing is a procedure to obtain a more complete list of compounds without proceeding to re-analysis of the samples (re-run). The risk associated with these different compounds, particularly TPs, is usually unknown and so it is the potential effect these might have on the organisms exposed to these compounds. Anyhow, the contribution of human drug metabolites and persistent TPs may go unnoticed when focusing exclusively on the parent compounds. Neglecting the relevance of these compounds may produce biased or incomplete relationships between chemical and biological qualities. This approach can be useful in the context of the WFD, and daughter directives, in the characterization of river basin specific pollutants, and delimitation of mixing areas affected by discharges.

**The relevance of hidden chemical compounds**

Once organic contaminants, in unchanged form or as metabolites, are released into the aquatic environment, can undergo attenuation or transformation processes. As said in the previous section, these compounds may outnumber those usually identified with target LC-MS. Using the MS identified by the retrospective analysis (Paper III) at the beginning and the end of a renewal cycle, a Principal Components Analysis (PCA) was carried out including all detected masses from the mesocosms loaded with native WWTP effluent. The PCA, presented in Figure D2, reveals a clear separation of the mass scores between samples collected at the start and the end of water renewal cycles of 3-4 days, and between these two and the control channels.

Paper III details that roughly twice the number of the parent compounds identified in Paper II with target LC-MS were further detected with retrospective suspect analysis, while other 64 were also detected but could not be identified. Although the observable chemical MS change over time, it can be suggested that most xenobiotics exhibited either negligible or very limited removal as they persist. Other drugs and human metabolites with apparent high removal were hydrolyzed or metabolized by biological communities (to be likely used as carbon or energy sources) (Dantas et al., 2008). Many of these forms persisted but as TPs form or as metabolites, and it is evident from these findings that if exposure assessment focuses exclusively on the parent compounds, human drug metabolites and persistent TPs may go unnoticed.

A lesson to learn from this exercise is that to understand the full picture in the aquatic environments both parent compounds and their degradation products need to be considered. The challenge is identifying and quantifying TPs and metabolites because in most cases these chemical compounds are formed but remain undetected. In paper III, ca. 8000 intense and significant peaks were detected by the retrospective analysis but could be neither identified nor related to any molecule. Data of transformation of organic micropollutants would not only be useful for assessing the potential for exposure to these TPs, but also to understand the environmental fate of the parent compound (Helbling et al., 2010).

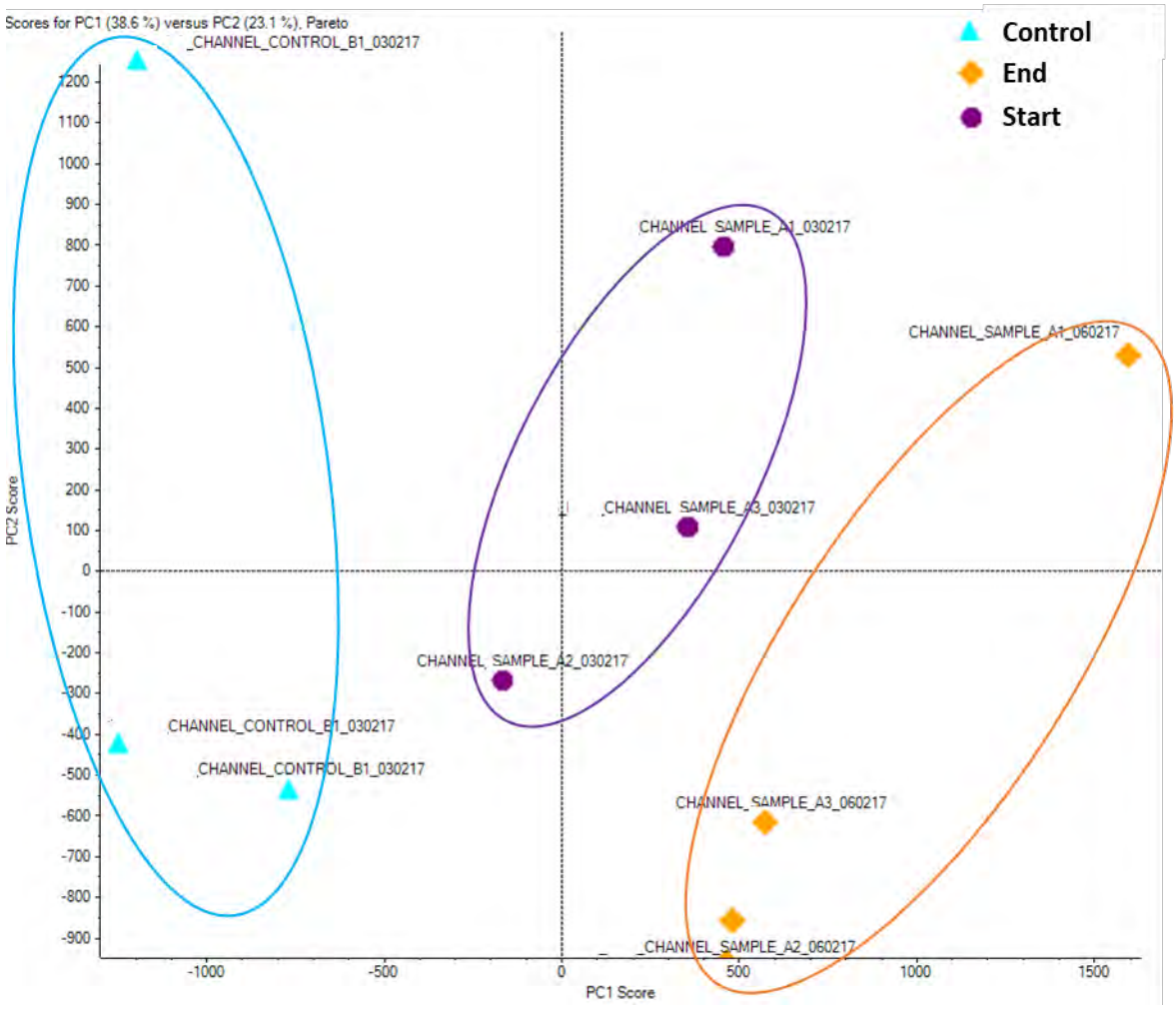


**Figure D2.** Principal component analysis (PCA) scores of samples collected at the start and the end of a water renewal cycle

Finally, the complexity is even higher when we consider that organic microcontaminants in polluted sites co-occur with nutrient enrichment (by phosphorus (P) and nitrogen (N)) or/and heavy metals. The interaction of these thousands of chemicals, and with biological

communities in a river system will ultimately determine whether a given pollutant (mixture) leads to undesirable consequences or alter the quality of the water.

**The relationship between chemical compounds and biological communities**

This Thesis began by stating that water chemical status is crucial to determine the ecological status of river systems, as it determines the composition of the media in which live biological communities (Weigelhofer et al., 2018). A chemical compound may act either as an enhancer (subsidizer) or as an inhibitor (stressor) of biological activities, since certain concentrations of nutrients may stimulate the metabolism and the growth of biological communities, as bacteria and primary producers (Carey and Migliaccio, 2009), or an excessive amount of nutrients or/and microcontaminants may have adverse effects on aquatic organisms, since these remain chronically exposed. In the complex mixtures, as I detailed above, chemicals may then perform as subsidies and stressors at the same time and understanding the outcomes of this is a formidable challenge to be faced in the time to come.

Ones and the others, subsidizers and stressors may cause the rearrangement of the species composition (or of its overall physiological functioning) by replacing stressor-sensitive species by stressor-tolerant others (Blanck et al. 1988). They also affect the physiological state of the cells, by enhancing or depleting their ability to respond to current, past, and future stressors. When this complexity is transferred to the scenario's implications for many co-occurring chemicals in polluted systems, we might face a myriad of direct and indirect paths to be faced by biological communities, with the perspective of a highly complex response.

This complexity was observed in the Ebro river, one of the largest rivers in the Iberian Peninsula, and strongly regulated by dams. This system offers a suitable case study to explore the sensitivity of the river system constrained within the framework of the physical-chemical conditions. In the analysis we conducted in Paper I, the main result was that the longitudinal dynamics of chemical status has a stronger neighboring influence (affecting the contiguous river stretches), this being even more simple than the biological communities which are more complex and results of a mixture of local and neighboring influences. Such an observation indicates that when results obtained at the flask or mesocosm scales aim to be translated to real-sized ecosystems, the physical framework of the system, as well as the complex interactions between chemical and

biological processes need to be fully considered. On the one hand, the physical template imposed by the hierarchical structure of a river network determines that the effects on a given site in the river transfer downstream until the system can attenuate this impact. On the other hand, the biological complexity crosses several temporal and spatial scales, combined with the physical described above, but also involving other smaller scales (site, habitat) that provide a rather heterogeneous picture. Considering all these different aspects is another challenge to be approached in future research.

# Conclusions

# Conclusions

1. The biological (phytoplankton biomass and community structure) and chemical variables (i.e. nutrients) in the regulated river Ebro did not follow identical longitudinal patterns, although the two were tightly related. The chemical status of any given section of the river was highly influenced by the contiguous river stretches. This contrasted to the longitudinal patterns of the biological communities, which were mostly driven by local (segment) influences.

2. A mesocosm experiment performed with different dilutions of real WWTP effluent showed that sewage effluents are sources of nutrients, dissolved organic matter, and anthropogenic contaminants, and perform either as enhancers (subsidizers) or inhibitors (stressors) of biological activities. Biofilms exposed to low-medium effluent concentrations were benefited, but treatments reaching 58% to 100% of WWTP effluent caused the highest effects on biofilms.

3. Continued chemical (i.e. nutrient, organic matter, contaminants) and physical (i.e. temperature, pH, dams) stressors irreversibly affected phytoplankton and biofilm communities. Phytoplankton community in the Ebro could not fully recover after the presence of reservoirs. Biofilms from the mesocosms did not recover their community structure, biomass, or functions after chemical impacts, even after initial conditions were reestablished. Legacy (both in time and space) of physical and chemical stressors affected the recovery of both phytoplankton and biofilm communities. In the two cases, the new environmental conditions favored opportunist organisms and species replacement but complicated a fully recovery of the former structure and function.

4. Changes on biofilm structure and function can be attributed only in part to chemical pressures (nutrients and microcontaminants). The intrinsic biofilm dynamics (changes in community composition and/or increase in thickness)

imprint particular response pathways to potential effects caused by sewage effluent.

5. The application of suspect-screening methods on the pharmaceutical products occurring in sewage waters revealed the presence of undetected human drug metabolites and of transformation products, and allowed to follow up their fate during the duration of the experiments, which had different detection and changes of abundance over time.

6. The most frequently detected pharmaceutical compounds in the mesocosm waters such as carbamazepine, diazepam, diclofenac, and venlafaxine exhibited negligible or very limited removal over the nine treatment cycles. This indicated that these detected compounds had a recalcitrant pattern.

7. Some drugs and human metabolites experienced hydrolysis, as atenolol, benzoylecgonine and norcocaine. The only pathway with clear evidence for acclimation upon repeated renewal of the wastewater was the oxidative degradation of valsartan: the conversion of its first-generation transformation product (VLS TP336) became more efficient over time leading to the formation of VLS acid, which turned out to be quite resistant to further degradation.

# References

# References

Aceña, J., Heuett, N., Gardinali, P., Pérez, S., 2016. Suspect Screening of Pharmaceuticals and Related Bioactive Compounds, Their Metabolites and Their Transformation Products in the Aquatic Environment, Biota and Humans Using LC-HR-MS Techniques. Compr. Anal. Chem. 71, 357–378. https://doi.org/10.1016/bs.coac.2016.02.011

Aceña, J., Rivas, D., Zonja, B., Pérez, S., Barceló, D., 2015a. Liquid chromatography-mass spectrometry: Quantification and confirmation aspects, in: Fast Liquid Chromatography-Mass Spectrometry Methods in Food and Environmental Analysis. pp. 347–377. https://doi.org/10.1142/9781783264940_0009

Aceña, J., Stampachiacchiere, S., Pérez, S., Barceló, D., 2015b. Advances in liquid chromatography - High-resolution mass spectrometry for quantitative and qualitative environmental analysis. Anal. Bioanal. Chem. 407, 6289–6299. https://doi.org/10.1007/s00216-015-8852-6

Acuña, V., Ginebreda, A., Mor, J.R., Petrovic, M., Sabater, S., Sumpter, J., Barceló, D., 2015a. Balancing the health benefits and environmental risks of pharmaceuticals: Diclofenac as an example. Environ. Int. 85, 327–333. https://doi.org/10.1016/j.envint.2015.09.023

Acuña, V., von Schiller, D., García-Galán, M.J., Rodríguez-Mozaz, S., Corominas, L., Petrovic, M., Poch, M., Barceló, D., Sabater, S., 2015b. Occurrence and in-stream attenuation of wastewater-derived pharmaceuticals in Iberian rivers. Sci. Total Environ. 503–504, 133–141. https://doi.org/10.1016/j.scitotenv.2014.05.067

Ahlers, J., Riedhammer, C., Vogliano, M., Ebert, R.U., Kühne, R., Schüürmann, G., 2006. Acute to chronic ratios in aquatic toxicity - Variation across trophic levels and relationship with chemical structure. Environ. Toxicol. Chem. 25, 2937–2945. https://doi.org/10.1897/05-701R.1

Allan, J., Castillo, M., 2007. Stream ecology: structure and function of running waters.

Allan, J.D., 1995. Stream ecology: structure and function of running waters. Stream Ecol. Struct. Funct. Run. waters. https://doi.org/10.1577/1548-8659-125.1.154

Alygizakis, N.A., Samanipour, S., Hollender, J., Ibáñez, M., Kaserzon, S., Kokkali, V., Van Leerdam, J.A., Mueller, J.F., Pijnappels, M., Reid, M.J., Schymanski, E.L., Slobodnik, J., Thomaidis, N.S., Thomas, K. V, 2018. Exploring the Potential of a Global Emerging Contaminant Early Warning Network through the Use of

Retrospective Suspect Screening with High-Resolution Mass Spectrometry. Environ. Sci. Technol. 52, 5135–5144. https://doi.org/10.1021/acs.est.8b00365

Amoros, C., Bornette, G., 2002. Connectivity and biocomplexity in waterbodies of riverine floodplains. Freshw. Biol. 47, 761–776.

Anselin, L., 1995. Local Indicators of Spatial Association—LISA. Geogr. Anal. 27, 93–115. https://doi.org/10.1111/j.1538-4632.1995.tb00338.x

Aristi, I., Casellas, M., Elosegi, A., Insa, S., Petrovic, M., Sabater, S., Acuña, V., 2016. Nutrients versus emerging contaminants-Or a dynamic match between subsidy and stress effects on stream biofilms. Environ. Pollut. 212, 208–215. https://doi.org/10.1016/j.envpol.2016.01.067

Artigas, J., Soley, S., Pérez-Baliero, M.C., Romaní, A.M., Ruiz-González, C., Sabater, S., 2012. Phosphorus use by planktonic communities in a large regulated Mediterranean river. Sci. Total Environ. 426, 180–187.

aus der Beek, T., Weber, F.A., Bergmann, A., Hickmann, S., Ebert, I., Hein, A., Küster, A., 2016. Pharmaceuticals in the environment-Global occurrences and perspectives. Environ. Toxicol. Chem. 35, 823–835. https://doi.org/10.1002/etc.3339

Backhaus, T., Faust, M., 2012. Predictive environmental risk assessment of chemical mixtures: A conceptual framework. Environ. Sci. Technol. 46, 2564–2573. https://doi.org/10.1021/es2034125

Barceló, D., Petrovic, M., 2007. Pharmaceuticals and personal care products (PPCPs) in the environment. Anal. Bioanal. Chem. https://doi.org/10.1007/s00216-006-1012-2

Barceló, D., Sabater, S., 2010. Water quality and assessment under scarcity. Prospects and challenges in Mediterranean watersheds. J. Hydrol. 383, 1–4.

Barret, M., Carrère, H., Latrille, E., Wisniewski, C., Patureau, D., 2010. Micropollutant and sludge characterization for modeling sorption equilibria. Environ. Sci. Technol. 44, 1100–1106. https://doi.org/10.1021/es902575d

Batalla, R.J., Gómez, C.M., Kondolf, G.M., 2004. Reservoir-induced hydrological changes in the Ebro River basin (NE Spain). J. Hydrol. 290, 117–136.

Batalla, R.J., Vericat, D., 2011. An appraisal of the contemporary sediment yield in the Ebro Basin. J Soils Sediments. https://doi.org/DOI 10.1007/s11368-011-0378-8

Battin, T.J., Besemer, K., Bengtsson, M.M., Romani, A.M., Packmann, A.I., 2016. The ecology and biogeochemistry of stream biofilms. Nat Rev Micro 14, 251–263.

Battin, T.J., Kaplan, L.A., Newbold, J.D., Hansen, C.M.E., 2003. Contributions of microbial biofilms to ecosystem processes in stream mesocosms. Nature 426, 439–

442.

Beretsou, V.G., Psoma, A.K., Gago-Ferrero, P., Aalizadeh, R., Fenner, K., Thomaidis, N.S., 2016. Identification of biotransformation products of citalopram formed in activated sludge. Water Res. 103, 205–214. https://doi.org/10.1016/j.watres.2016.07.029

Biggs, B.J.F., 2000. Eutrophication of streams and rivers: dissolved nutrient-chlorophyll relationships for benthic algae. J. North Am. Benthol. Soc. 19, 17–31.

Bijlsma, K., Loeschcke, V., 2013. Environmental stress, adaptation and evolution. Birkhäuser.

Bilger, W., Björkman, O., 1990. Role of the xanthophyll cycle in photoprotection elucidated by measurements of light-induced absorbance changes, fluorescence and photosynthesis in leaves of Hedera canariensis. Photosynth. Res. 25, 173–185. https://doi.org/10.1007/BF00033159

Billen, G., Garnier, J., Hanset, P., 1994. Modelling phytoplnakton development in whole drainage networks: the RIVSTRAHLER model applied to the Seine River system. Hydrobiologia 289, 119–137.

Boix, C., Ibáñez, M., Sancho, J. V., Parsons, J.R., Voogt, P. de, Hernández, F., 2016. Biotransformation of pharmaceuticals in surface water and during waste water treatment: Identification and occurrence of transformation products. J. Hazard. Mater. 302, 175–187. https://doi.org/10.1016/j.jhazmat.2015.09.053

Boreen, A.L., Arnold, W.A., McNeill, K., 2004. Photochemical fate of sulfa drugs in then aquatic environment: Sulfa drugs containing five-membered heterocyclic groups. Environ. Sci. Technol. 38, 3933–3940. https://doi.org/10.1021/es0353053

Bott, T.L., Kaplan, L.A., Kuserk, F.T., 1984. Benthic bacterial biomass supported by streamwater dissolved organic matter. Microb. Ecol. 10, 335–344.

Boxall, A.B.A., Sinclair, C.J., Fenner, K., Kolpin, D., Maund, S.J., 2004. When synthetic chemicals degrade in the environment. Environ. Sci. Technol. https://doi.org/10.1021/es040624v

Brooks, B.W., 2018. Urbanization, environment and pharmaceuticals: Advancing comparative physiology, pharmacology and toxicology. Conserv. Physiol. 6, 79. https://doi.org/10.1093/conphys/cox079

Brooks, T.M., Mittermeier, R.A., da Fonseca, G.A.B., Gerlach, J., Hoffmann, M., Lamoreux, J.F., Mittermeier, C.G., Pilgrim, J.D., Rodrigues, A.S.L., 2006. Global Biodiversity Conservation Priorities. Science (80-. ). 313, 58–61.

Buendia, C., Herrero, A., Sabater, S., Batalla, R.J., 2016. An appraisal of the sediment yield in western Mediterranean river basins. Sci. Total Environ. 572, 538–553. https://doi.org/10.1016/j.scitotenv.2016.08.065

Bunn, S.E., Arthington, A.H., 2002. Basic principles and ecological consequences of altered flow regimes for aquatic biodiversity. Environ. Manage. 30, 492–507.

Bushong, S.J., Bachman, R.W., 1989. In situ nutrient enrichment experiments with periphyton in agricultural streams. Hydrobiologia 178, 1–10.

Campos-Mañas, M.C., Ferrer, I., Antonio, J., Pérez, S., Thurman, E.M., Antonio Sánchez Pérez, J., Agüera, A., 2019. Identification of opioids in surface and wastewaters by LC/QTOF-MS using retrospective data analysis Analysis of Cannabinoids in Hemp Samples View project CONSOLIDER TRAGUA: Treatment and reuse of wastewater for a sustainable management. Quality control and monitoring of priority and emerging contaminants by mass spectrometric methods View project Identification of opioids in surface and wastewaters by LC/QTOF-MS using retrospective data analysis. Sci. Total Environ. 664, 874–884. https://doi.org/10.1016/j.scitotenv.2019.01.389

Carey, R.O., Migliaccio, K.W., 2009. Contribution of Wastewater Treatment Plant Effluents to Nutrient Dynamics in Aquatic Systems: A Review. Environ. Manage. 44, 205–217.

Carson, R., 1962. Silent spring, Houghton Mifflin Company.

Chen, Y., 2013. New Approaches for Calculating Moran's Index of Spatial Autocorrelation. PLoS One 8. https://doi.org/10.1371/journal.pone.0068336

Chróst, R.J., Overbeck, J., 1990. Substrate-ectoenzyme interaction: significance of b-glucosidase activity for glucose metabolism by aquatic bacteria. Arch. Hydrobiol. Beih./Ergebn. Limnol. 34, 93–98.

Chu, B.T.T., Petrovich, M.L., Chaudhary, A., Wright, D., Murphy, B., Wells, G., Poretsky, R., 2018. Metagenomics Reveals the Impact of Wastewater Treatment Plants on the Dispersal of Microorganisms and Genes in Aquatic Sediments. Am Soc Microbiol. https://doi.org/10.1128/AEM

Connarn, J.N., Flowers, S., Kelly, M., Luo, R., Ward, K.M., Harrington, G., Moncion, I., Kamali, M., McInnis, M., Feng, M.R., Ellingrod, V., Babiskin, A., Zhang, X., Sun, D., 2017. Pharmacokinetics and Pharmacogenomics of Bupropion in Three Different Formulations with Different Release Kinetics in Healthy Human Volunteers. AAPS J. 19, 1513–1522. https://doi.org/10.1208/s12248-017-0102-8

Corcoll, N., Acuña, V., Barceló, D., Casellas, M., Guasch, H., Huerta, B., Petrovic, M., Ponsatí, L., Rodríguez-Mozaz, S., Sabater, S., 2014. Pollution-induced community tolerance to non-steroidal anti-inflammatory drugs (NSAIDs) in fluvial biofilm communities affected by WWTP effluents. Chemosphere 112, 185–193. https://doi.org/10.1016/j.chemosphere.2014.03.128

Corcoll, N., Bonet, B., Morin, S., Tlili, A., Leira, M., Guasch, H., 2012a. The effect of metals on photosynthesis processes and diatom metrics of biofilm from a metal-contaminated river: A translocation experiment. Ecol. Indic. 18, 620–631. https://doi.org/10.1016/j.ecolind.2012.01.026

Corcoll, N., Casellas, M., Huerta, B., Guasch, H., Acuna, V., Rodriguez-Mozaz, S., Serra-Compte, A., Barcelo, D., Sabater, S., 2015. Effects of flow intermittency and pharmaceutical exposure on the structure and metabolism of stream biofilms. Sci. Total Environ. 503, 159–170. https://doi.org/10.1016/j.scitotenv.2014.06.093

Corcoll, N., Ricart, M., Franz, S., Sans-Piché, F., Schmitt-Jansen, M., Guasch, H., 2012b. The Use of Photosynthetic Fluorescence Parameters from Autotrophic Biofilms for Monitoring the Effect of Chemicals in River Ecosystems, in: Handbook of Environmental Chemistry. Springer Verlag, pp. 85–115. https://doi.org/10.1007/978-3-642-25722-3_4

Cwiertny, D.M., Snyder, S.A., Schlenk, D., Kolodziej, E.P., 2014. Environmental Designer Drugs: When Transformation May Not Eliminate Risk. Environ. Sci. Technol. 48, 11737–11745. https://doi.org/10.1021/es503425w

da Silva, B.F., Jelic, A., López-Serna, R., Mozeto, A.A., Petrovic, M., Barceló, D., 2011. Occurrence and distribution of pharmaceuticals in surface water, suspended solids and sediments of the Ebro river basin, Spain. Chemosphere 85, 1331–1339. https://doi.org/10.1016/j.chemosphere.2011.07.051

Dakos, V., van Nes, E.H., Donangelo, R., Fort, H., Scheffer, M., 2010. Spatial correlation as leading indicator of catastrophic shifts. Theor. Ecol. 3, 163–174. https://doi.org/10.1007/s12080-009-0060-6

Dale, V.H., Beyeler, S.C., 2001. Challenges in the development and use of ecological indicators. Ecol. Indic. 1, 3–10. https://doi.org/10.1016/s1470-160x(01)00003-6

Dantas, G., Sommer, M.O.A., Oluwasegun, R.D., Church, G.M., 2008. Bacteria subsisting on antibiotics. Science (80-. ). 320, 100–103.

Daughton, C.G., Ternes, T.A., 1999. Pharmaceuticals and personal care products in the environment: Agents of subtle change? Environ. Health Perspect.

https://doi.org/10.1289/ehp.99107s6907

Davis, S.N., Whittemore, D.O., FabrykaMartin, J., 1998. Uses of chloride/bromide ratios in studies of potable water. Gr. Water. Mar Apr 36, 338–350.

Delgadillo-Mirquez, L., Lardon, L., Steyer, J.P., Patureau, D., 2011. A new dynamic model for bioavailability and cometabolism of micropollutants during anaerobic digestion. Water Res. 45, 4511–4521. https://doi.org/10.1016/j.watres.2011.05.047

Delong, M.D., Thorp, J.H., 2006. Significance of instream autotrophs in trophic dynamics of the Upper Mississippi River. Oecologia 147, 76–85.

Directive 2000/60/EC, 2000. Directive 2000/60/EC of the European Parliament and of the Council of 23 October 2000 establishing a framework for Community action in the field of water policy. Off. J. Eur. Parliam. L327, 1–82. https://doi.org/10.1039/ap9842100196

Dodds, W.K., 2007. Trophic state, eutrophication and nutrient criteria in streams. Trends Ecol. Evol. 22, 669–676.

Dodds, W.K., Biggs, B.J.F., Lowe, R.L., 1999. Photosynthesis-irradiance patterns in benthic microalgae: Variations as a function of assemblage thickness and community structure. J. Phycol. 35, 42–53.

Döll, P., Schmied, H.M., 2012. How is the impact of climate change on river flow regimes related to the impact on mean annual runoff? A global-scale analysis. Environ. Res. Lett. 7. https://doi.org/10.1088/1748-9326/7/1/014037

Domingues, R.B., Barbosa, A.B., Sommer, U., Galvão, H.M., 2011. Ammonium, nitrate and phytoplankton interactions in a freshwater tidal estuarine zone: Potential effects of cultural eutrophication. Aquat. Sci. 73, 331–343. https://doi.org/10.1007/s00027-011-0180-0

Drury, B., Rosi-Marshall, E., Kelly, J.J., 2013. Wastewater treatment effluent reduces the abundance and diversity of benthic bacterial communities in urban and suburban rivers. Appl. Environ. Microbiol. 79, 1897–1905. https://doi.org/10.1128/AEM.03527-12

Dudgeon, D., 2010. Prospects for sustaining freshwater biodiversity in the 21st century: linking ecosystem structure and function. Curr. Opin. Environ. Sustain. 2, 422–430.

Dynesius, M., Nilsson, C., 1994. Fragmentation and flow regulation of river systems in the Northern Third of the World. Science (80-. ). 266, 753–762.

Eichhorn, P., Ferguson, P.L., Pérez, S., Aga, D.S., 2005. Application of ion trap-MS with H/D exchange and QqTOF-MS in the identification of microbial degradates of

trimethoprim in nitrifying activated sludge. Anal. Chem. 77, 4176–4184. https://doi.org/10.1021/ac050141p

Eichhorn, P., Pérez, S., Barceló, D., 2012. Time-of-Flight Mass Spectrometry Versus Orbitrap-Based Mass Spectrometry for the Screening and Identification of Drugs and Metabolites: Is There a Winner?, in: Comprehensive Analytical Chemistry. pp. 217–272. https://doi.org/10.1016/B978-0-444-53810-9.00009-2

Ekka, S.A., Haggard, B.E., Matlock, M.D., Chaubey, I., 2006. Dissolved phosphorus concentrations and sediment interactions in effluent-dominated Ozark streams. Ecol. Eng. 26, 375–391. https://doi.org/10.1016/j.ecoleng.2006.01.002

Elosegi, A., Feld, C.K., Mutz, M., von Schiller, D., 2019. Multiple Stressors and Hydromorphological Degradation, in: Multiple Stressors in River Ecosystems. pp. 65–79. https://doi.org/10.1016/b978-0-12-811713-2.00004-2

Ercin, A.E., Hoekstra, A.Y., 2014. Water footprint scenarios for 2050: A global analysis. Environ. Int. 64, 71–82. https://doi.org/10.1016/j.envint.2013.11.019

European commision, 2013. Directive 2013/39/EU of the European Parliament and of the Council of 12 August 2013 amending Directives 2000/60/ECand 2008/105/EC as regards priority substances in the field of water policy. Off. J. Eur. Union 226, 1–17.

Evgenidou, E.N., Konstantinou, I.K., Lambropoulou, D.A., 2015. Occurrence and removal of transformation products of PPCPs and illicit drugs in wastewaters: A review. Sci. Total Environ. https://doi.org/10.1016/j.scitotenv.2014.10.021

Fischer, M., Wang, J., 2011. Spatial data analysis: models, methods and techniques.

Flemming, H.C., Wingender, J., Szewyk, U., Steinberg, P., Rice, S.A., Kjelleberg, S., 2016. Biofilms: an emergent from of bacterial life. Nat. Rev. Microbiol. 14, 563–575.

Friedl, G., Wüest, A., 2002. Disrupting biogeochemical cycles - Consequences of damming. Aquat. Sci. https://doi.org/10.1007/s00027-002-8054-0

Frissell, C.A., Liss, C.E., Warren, C.E., Hurley, M.D., 1986. A Hierarchical Framework for Stream Habitat Classification; Viewing Streams in a Watershed Context. Environ. Manage. 10, 199–214.

Gago-Ferrero, P., Schymanski, E.L., Bletsou, A.A., Aalizadeh, R., Hollender, J., Thomaidis, N.S., 2015. Extended Suspect and Non-Target Strategies to Characterize Emerging Polar Organic Contaminants in Raw Wastewater with LC-HRMS/MS. ACS Publ. 49, 12333–12341. https://doi.org/10.1021/acs.est.5b03454

Gallardo, B., Clavero, M., Sánchez, M.I., Vilà, M., 2016. Global ecological impacts of

invasive species in aquatic ecosystems. Glob. Chang. Biol. 22, 151–163.

Genty, B., Briantais, J.M., Baker, N.R., 1989. The relationship between the quantum yield of photosynthetic electron transport and quenching of chlorophyll fluorescence. Biochim. Biophys. Acta - Gen. Subj. 990, 87–92. https://doi.org/10.1016/S0304-4165(89)80016-9

Ginebreda, A., Sabater-Liesa, L., Rico, A., Focks, A., Barceló, D., 2018. Reconciling monitoring and modeling: An appraisal of river monitoring networks based on a spatial autocorrelation approach - emerging pollutants in the Danube River as a case study. Sci. Total Environ. 618. https://doi.org/10.1016/j.scitotenv.2017.11.020

Giorgi, A.D.N., 1995. Response of periphyton biomass to high phosphorus concentrations in laboratory experiments. Bull. Environ. Contam. Toxicol. 55, 825–832.

Goodwin, P., Jorde, K., Meier, C., Parra, O., 2006. Minimizing environmental impacts of hydropower development: Transferring lessons from past projects to a proposed strategy for Chile. J. Hydroinformatics 8, 253–270. https://doi.org/10.2166/hydro.2006.005

Griffiths, B.S., Philippot, L., 2013. Insights into the resistance and resilience of the soil microbial community. FEMS Microbiol. Rev. 37, 112–129.

Grimm, V., Wissel, C., 1997. Babel, or the ecological stability discussions: An inventory and analysis of terminology and a guide for avoiding confusion. Oecologia. https://doi.org/10.1007/s004420050090

Grizzetti, B., Pistocchi, A., Liquete, C., Udias, A., Bouraoui, F., Van De Bund, W., 2017. Human pressures and ecological status of European rivers. Sci. Rep. 7. https://doi.org/10.1038/s41598-017-00324-3

Gröning, J., Held, C., Garten, C., Claußnitzer, U., Kaschabek, S.R., Schlömann, M., 2007. Transformation of diclofenac by the indigenous microflora of river sediments and identification of a major intermediate. Chemosphere 69, 509–516. https://doi.org/10.1016/j.chemosphere.2007.03.037

Gros, M., Cruz-Morato, C., Marco-Urrea, E., Longrée, P., Singer, H., Sarrà, M., Hollender, J., Vicent, T., Rodriguez-Mozaz, S., Barceló, D., 2014. Biodegradation of the X-ray contrast agent iopromide and the fluoroquinolone antibiotic ofloxacin by the white rot fungus Trametes versicolor in hospital wastewaters and identification of degradation products. Water Res. 60, 228–241. https://doi.org/10.1016/j.watres.2014.04.042

Gros, M., Petrović, M., Barceló, D., 2007. Wastewater treatment plants as a pathway for

aquatic contamination by pharmaceuticals in the ebro river basin (northeast Spain). Environ. Toxicol. Chem. 26, 1553–1562. https://doi.org/10.1897/06-495R.1

Gros, M., Rodríguez-Mozaz, S., Barceló, D., 2012. Fast and comprehensive multi-residue analysis of a broad range of human and veterinary pharmaceuticals and some of their metabolites in surface and treated waters by ultra-high-performance liquid chromatography coupled to quadrupole-linear ion trap tandem. J. Chromatogr. A 1248, 104–121. https://doi.org/10.1016/j.chroma.2012.05.084

Guasch, H., Admiraal, W., Sabater, S., 2003. Contrasting effects of organic and inorganic toxicants on freshwater periphyton. Aquat. Toxicol. 64, 165–175.

Haidvogl, G., 2018. Historic Milestones of Human River Uses and Ecological Impacts, in: Riverine Ecosystem Management. pp. 19–39. https://doi.org/10.1007/978-3-319-73250-3_2

Halling-Sørensen, B., Nors Nielsen, S., Lanzky, P.F., Ingerslev, F., Holten Lützhøft, H.C., Jørgensen, S.E., 1998. Occurrence, fate and effects of pharmaceutical substances in the environment- A review. Chemosphere 36, 357–393. https://doi.org/10.1016/S0045-6535(97)00354-8

Hannemann, M., Zonja, B., Barceló, D., Pérez, S., 2016. HRMS Approaches for Evaluating Transformations of Pharmaceuticals in the Aquatic Environment, in: ACS Symposium Series. American Chemical Society, pp. 25–44. https://doi.org/10.1021/bk-2016-1241.ch003

Helbling, D.E., Hollender, J., Kohler, H.P.E., Singer, H., Fenner, K., 2010. High-throughput identification of microbial transformation products of organic micropollutants. Environ. Sci. Technol. 44, 6621–6627. https://doi.org/10.1021/es100970m

Henning, N., Falås, P., Castronovo, S., Jewell, K.S., Bester, K., Ternes, T.A., Wick, A., 2019. Biological transformation of fexofenadine and sitagliptin by carrier-attached biomass and suspended sludge from a hybrid moving bed biofilm reactor. Water Res. 167. https://doi.org/10.1016/j.watres.2019.115034

Hermes, N., Jewell, K.S., Wick, A., Ternes, T.A., 2018. Quantification of more than 150 micropollutants including transformation products in aqueous samples by liquid chromatography-tandem mass spectrometry using scheduled multiple reaction monitoring. J. Chromatogr. A 1531, 64–73. https://doi.org/10.1016/j.chroma.2017.11.020

Hernández, F., Ibáñez, M., Gracia-Lor, E., Sancho, J. V., 2011. Retrospective LC-QTOF-

MS analysis searching for pharmaceutical metabolites in urban wastewater. J. Sep. Sci. 34, 3517–3526. https://doi.org/10.1002/jssc.201100540

Hillebrand, H., Durselen, C.D., Kirschtel, D., Pollingher, U., Zohary, T., 1999. Biovolume calculation for pelagic and benthic microalgae. J. Phycol. 35, 403–424.

Hollender, J., van Bavel, B., Dulio, V., Farmen, E., Furtmann, K., Koschorreck, J., Kunkel, U., Krauss, M., Munthe, J., Schlabach, M., Slobodnik, J., Stroomberg, G., Ternes, T., Thomaidis, N.S., Togola, A., Tornero, V., 2019. High resolution mass spectrometry-based non-target screening can support regulatory environmental monitoring and chemicals management. Environ. Sci. Eur. 31. https://doi.org/10.1186/s12302-019-0225-x

Holling, C.S., 1973. Resilience and stability of ecological systems. Annu. Rev Ecol Syst 4, 1–23. https://doi.org/10.1146/annurev.es.04.110173.000245

Huerta, B., Jakimska, A., Llorca, M., Ruhí, A., Margoutidis, G., Acuña, V., Sabater, S., Rodriguez-Mozaz, S., Barcelò, D., 2015. Development of an extraction and purification method for the determination of multi-class pharmaceuticals and endocrine disruptors in freshwater invertebrates. Talanta 132, 373–381. https://doi.org/10.1016/j.talanta.2014.09.017

Huerta, B., Rodriguez-Mozaz, S., Nannou, C., Nakis, L., Ruhí, A., Acuña, V., Sabater, S., Barcelo, D., 2016. Determination of a broad spectrum of pharmaceuticals and endocrine disruptors in biofilm from a waste water treatment plant-impacted river. Sci. Total Environ. 540, 241–249.

IPCC, 2014. Climate Change 2014: Synthesis Report. Contribution of Working Groups I, II and III to the Fifth Assessment Report of the Intergovernmental Panel on Climate Change, Ipcc.

Istvánovics, V., Honti, M., Vörös, L., Kozma, Z., 2010. Phytoplankton dynamics in relation to connectivity, flow dynamics and resource availability-the case of a large, lowland river, the Hungarian Tisza. Hydrobiologia 637, 121–141. https://doi.org/10.1007/s10750-009-9991-6

Jackson, R.B., Carpenter, S.R., Dahm, C.N., McKnight, D.M., Naiman, R.J., Postel, S.L., Running, S.W., 2001. Water in a changing world, Issues in Ecology.

Jeffrey, S.W., Humphrey, G.F., 1975. New spectrophotometric equations for determining chlorophylls a, b, and c in higher plants, algae and natural phytoplankton. Biochem. Physiol. Pflanz. 167, 191–194.

Jelic, A., Cruz-Morató, C., Marco-Urrea, E., Sarrà, M., Perez, S., Vicent, T., Petrović,

M., Barcelo, D., 2012. Degradation of carbamazepine by Trametes versicolor in an air pulsed fluidized bed bioreactor and identification of intermediates. Water Res. 46, 955–964. https://doi.org/10.1016/j.watres.2011.11.063

Jelić, A., Gros, M., Petrović, M., Ginebreda, A., Barceló, D., 2012. Occurrence and Elimination of Pharmaceuticals During Conventional Wastewater Treatment, in: Handbook of Environmental Chemistry. Springer Verlag, pp. 1–23. https://doi.org/10.1007/978-3-642-25722-3_1

Jewell, K.S., Falås, P., Wick, A., Joss, A., Ternes, T.A., 2016. Transformation of diclofenac in hybrid biofilm–activated sludge processes. Water Res. 105, 559–567. https://doi.org/10.1016/j.watres.2016.08.002

Jobling, S., Nolan, M., Tyler, C.R., Brighty, G., Sumpter, J.P., 1998. Widespread sexual disruption in wild fish. Environ. Sci. Technol. 32, 2498–2506. https://doi.org/10.1021/es9710870

Johnson, B.L., Richardson, W.B., Naimo, T.J., 1995. Past, present and future concepts in large river ecology. Bioscience 45, 134–141.

Jones, F.H., 1984. The dynamics of suspended algal populations in the lower Wye catchment. Water Res. 18, 25–35. https://doi.org/10.1016/0043-1354(84)90044-7

Kaplan, D., Christiaen, D., Shoshana, A., 1987. Chelating properties of extracellular polysaccharides from Chlorella sp. Appl. Environm. Microbiol. 53, 2953–2956.

Katz, B.G., Eberts, S.M., Kauffman, L.J., 2011. Using Cl/Br ratios and other indicators to assess potential impacts on groundwater quality from septic systems: A review and examples from principal aquifers in the United States. J. Hydrol. 397, 151–166. https://doi.org/10.1016/j.jhydrol.2010.11.017

Kern, S., Baumgartner, R., Helbling, D.E., Hollender, J., Singer, H., Loos, M.J., Schwarzenbach, R.P., Fenner, K., 2010. A tiered procedure for assessing the formation of biotransformation products of pharmaceuticals and biocides during activated sludge treatment. J. Environ. Monit. 12, 2100–2111. https://doi.org/10.1039/c0em00238k

Kern, S., Fenner, K., Singer, H.P., Schwarzenbach, R.P., Hollender, J., 2009. Identification of transformation products of organic contaminants in natural waters by computer-aided prediction and high-resolution mass spectrometry. Environ. Sci. Technol. 43, 7039–7046. https://doi.org/10.1021/es901979h

Köhler, J., 1994. Origin and succession of phytoplankton in a river-lake system (Spree, Germany), in: Phytoplankton in Turbid Environments: Rivers and Shallow Lakes.

Springer Netherlands, pp. 73–83. https://doi.org/10.1007/978-94-017-2670-2_7

Kosjek, T., Heath, E., Petrović, M., Barceló, D., 2007. Mass spectrometry for identifying pharmaceutical biotransformation products in the environment. TrAC - Trends Anal. Chem. 26, 1076–1085. https://doi.org/10.1016/j.trac.2007.10.005

Kosjek, T., Perko, S., Zupanc, M., ZanoŠki Hren, M., Landeka Dragičević, T., Žigon, D., Kompare, B., Heath, E., 2012. Environmental occurrence, fate and transformation of benzodiazepines in water treatment. Water Res. 46, 355–368. https://doi.org/10.1016/j.watres.2011.10.056

Kosjek, T., Žigon, D., Kralj, B., Heath, E., 2008. The use of quadrupole-time-of-flight mass spectrometer for the elucidation of diclofenac biotransformation products in wastewater. J. Chromatogr. A 1215, 57–63. https://doi.org/10.1016/j.chroma.2008.10.111

Krauss, M., Singer, H., Hollender, J., 2010. LC-high resolution MS in environmental analysis: From target screening to the identification of unknowns. Anal. Bioanal. Chem. 397, 943–951. https://doi.org/10.1007/s00216-010-3608-9

Kümmerer, K., 2009. The presence of pharmaceuticals in the environment due to human use - present knowledge and future challenges. J. Environ. Manage. https://doi.org/10.1016/j.jenvman.2009.01.023

Kunkel, U., Radke, M., 2008. Biodegradation of acidic pharmaceuticals in bed sediments: insight from a laboratory experiment. ACS Publ. 42, 7273–7279. https://doi.org/10.1021/es801562j

Kuzmanovic, M., Ginebreda, A., Petrovic, M., Barceló, D., 2016. contaminants of emerging concern in mediterranean watersheds, in: Handbook of Environmental Chemistry. Springer Verlag, pp. 27–45. https://doi.org/10.1007/698_2015_5016

Kuzmanovic, M., Ginebreda, A., Petrovic, M., Barceló, D., 2015. Risk assessment based prioritization of 200 organic micropollutants in 4 Iberian rivers. Sci Total Env. 503–4, 289–299.

Lacorte, S., Barceló, D., al., et, 2006. Pilot survey of a broad range of priority pollutants in sediment and fish from the Ebro river basin (NE Spain). Environm. Poll. 140, 471–482.

Längin, A., Schuster, A., Kümmerer, K., 2008. Chemicals in the environment - The need for a clear nomenclature: Parent compounds, metabolites, transformation products and their elimination. Clean - Soil, Air, Water. https://doi.org/10.1002/clen.200600001

Lawrence, J.R., Swerhone, G.D.W., Wassenaar, L.I., Neu, T.R., 2005. Effects of selected pharmaceuticals on riverine biofilm communities. Can. J. Microbiol. 51, 655–669.

Leibold, M., Chase, J., 2017. Metacommunity Ecology, Volume 59.

Li, H., Calder, C.A., Cressie, N., 2007. Beyond Moran's I: Testing for spatial dependence based on the spatial autoregressive model. Geogr. Anal. 39, 357–375. https://doi.org/10.1111/j.1538-4632.2007.00708.x

Li, Z., Sobek, A., Radke, M., 2015. Flume experiments to investigate the environmental fate of pharmaceuticals and their transformation products in streams. Environ. Sci. Technol. 49, 6009–6017. https://doi.org/10.1021/acs.est.5b00273

Llorca, M., Rodríguez-Mozaz, S., Couillerot, O., Panigoni, K., 2015. Identification of new transformation products during enzymatic. Chemosphere 119, 90–98.

Lobera, G., Muñoz, I., López-Tarazón, J.A., Vericat, D., Batalla, R.J., 2017. Effects of flow regulation on river bed dynamics and invertebrate communities in a Mediterranean river. Hydrobiologia 784, 283–304.

Lock, M., 1993. Attached microbial communities in rivers. Aquat. Microbiol. An Ecol. Approach 113–138.

López-Doval, J.C., De Castro-Català, N., Andrés-Doménech, I., Blasco, J., Ginebreda, A., Muñoz, I., 2012. Analysis of monitoring programmes and their suitability for ecotoxicological risk assessment in four Spanish basins. Sci. Total Environ. 440, 194–203. https://doi.org/10.1016/j.scitotenv.2012.07.035

López-Moreno, J.I., Beguería, S., García-Ruiz, J.M., 2002. Influence of the Yesa reservoir on floods of the Aragón River, central Spanish Pyrenees. Hydrology and Earth System Sciences Discussions, European Geosciences Union.

López-Moreno, J.I., Vicente-Serrano, S.M., Moran-Tejeda, E., Zabalza, J., Lorenzo-Lacruz, J., García-Ruiz, J.M., 2011. Impact of climate evolution and land use changes on water yield in the Ebro Basin. Hydrol. Earth Syst. Sci. 15, 311–322.

Loza, V., Perona, E., Mateo, P., 2014. Specific responses to nitrogen and phosphorus enrichment in cyanobacteria: Factors influencing changes in species dominance along eutrophic gradients. Water Res. 48, 622–631. https://doi.org/10.1016/j.watres.2013.10.014

Lucas, D., Barceló, D., Rodriguez-Mozaz, S., 2016. Removal of pharmaceuticals from wastewater by fungal treatment and reduction of hazard quotients. Sci. Total Environ. 571, 909–915. https://doi.org/10.1016/j.scitotenv.2016.07.074

Luo, Y., Guo, W., Ngo, H.H., Nghiem, L.D., Hai, F.I., Zhang, J., Liang, S., Wang, X.C.,

2014. A review on the occurrence of micropollutants in the aquatic environment and their fate and removal during wastewater treatment. Sci. Total Environ. https://doi.org/10.1016/j.scitotenv.2013.12.065

Malaj, E., von der Ohe, P.C., Grote, M., Kuhne, R., Mondy, C.P., Usseglio-Polatera, P., Brack, W., Schafer, R.B., 2014. Organic chemicals jeopardize the health of freshwater ecosystems on the continental scale. Proc. Natl. Acad. Sci. U. S. A. 111, 9549–9554. https://doi.org/10.1073/pnas.1321082111

Mandaric, L., Celic, M., Marcé, R., Petrovic, M., 2016. Introduction on emerging contaminants in rivers and their environmental risk, in: Handbook of Environmental Chemistry. Springer Verlag, pp. 3–25. https://doi.org/10.1007/698_2015_5012

Mandaric, L., Mor, J.-R., Sabater, S., Petrovic, M., 2018. Impact of urban chemical pollution on water quality in small, rural and effluent-dominated Mediterranean streams and rivers. Sci. Total Environ. 613, 763–772.

Margalef, R., 1960. Ideas for a synthetic approach to the ecology of running waters. Int. Rev. ges. Hydrobiol. 45, 133–153.

Marti, E., Aumatell, J., Godé, L., Poch, M., Sabater, F., 2004. Nutrient Retention Efficiency in Streams Receiving Inputs from Wastewater Treatment Plants. J. Environ. Qual. 33, 285–293. https://doi.org/10.2134/jeq2004.2850

Martí, E., Riera, J.L., Sabater, F., 2010. Effects of wastewater treatment plants on stream nutrient dynamics under water scarcity conditions, in: Sabater, S., Barceló, D. (Eds.), Water Scarcity in the Mediterranean . Springer, pp. 173–195.

Mas-Pla, J., Batalla, R., Cabello, À., Gallart, F., Llorens, P., Pascual, D., Pla, E., Pouget, L., Sànchez, A., Termes, M., Vergonyós, L., 2016. Recursos hidrològics. Tercer Informe Canvi Climàtic a Catalunya. publicacions.iec.cat 1–5.

Matamoros, V., Uggetti, E., García, J., Bayona, J.M., 2016. Assessment of the mechanisms involved in the removal of emerging contaminants by microalgae from wastewater: A laboratory scale study. J. Hazard. Mater. 301, 197–205. https://doi.org/10.1016/j.jhazmat.2015.08.050

Matraszek-Zuchowska, I., Wozniak, B., Posyniak, A., 2016. Comparison of the Multiple Reaction Monitoring and Enhanced Product Ion Scan Modes for Confirmation of Stilbenes in Bovine Urine Samples Using LC–MS/MS QTRAP® System. Chromatographia 79, 1003–1012. https://doi.org/10.1007/s10337-016-3121-1

Mekonnen, M.M., Hoekstra, A.Y., 2016. Sustainability: Four billion people facing severe water scarcity. Sci. Adv. 2. https://doi.org/10.1126/sciadv.1500323

Meybeck, M., 2004. The global change of continental aquatic systems: Dominant impacts of human activities. Water Sci. Technol. 49, 73–83. https://doi.org/10.2166/wst.2004.0420

Meybeck, M., 2003. Global analysis of river systems: from Earth system controls to Anthropocen syndromes. Phyilosophical Trans. R. Soc. B 358, 1935–1955.

Meyer, J.L., Paul, M.J., Taulbee, W.K., 2005. Stream ecosystem function in urbanizing landscapes, in: Journal of the North American Benthological Society. North American Benthological Society, pp. 602–612. https://doi.org/10.1899/04-021.1

Mijangos, L., Ziarrusta, H., Ros, O., Kortazar, L., Fernández, L.A., Olivares, M., Zuloaga, O., Prieto, A., Etxebarria, N., 2018. Occurrence of emerging pollutants in estuaries of the Basque Country: Analysis of sources and distribution, and assessment of the environmental risk. Water Res. 147, 152–163. https://doi.org/10.1016/j.watres.2018.09.033

Mompelat, S., Le Bot, B., Thomas, O., 2009. Occurrence and fate of pharmaceutical products and by-products, from resource to drinking water. Environ. Int. 35, 803–814. https://doi.org/10.1016/j.envint.2008.10.008

Montemurro, N., García-Vara, M., Peña-Herrera, J.M., Llada, J., Barcela, D., Pérez, S., 2018. Conventional and advanced processes for the removal of pharmaceuticals and their human metabolites from wastewater, in: ACS Symposium Series. American Chemical Society, pp. 15–67. https://doi.org/10.1021/bk-2018-1302.ch002

Montuelle, B., Volat, B., 1998. Impact of wastewater treatment plant discharge on enzyme activity in freshwater sediments, in: Ecotoxicology and Environmental Safety. pp. 154–159. https://doi.org/10.1006/eesa.1998.1656

Munn, M.D., Black, R.W., Gruber, S.J., 2002. Response of benthic algae to environmental gradients in an agriculturally dominated landscape. J. North Am. Benthol. Soc. Jun 21, 221–237.

Murray, K.E., Thomas, S.M., Bodour, A.A., 2010. Prioritizing research for trace pollutants and emerging contaminants in the freshwater environment. Environ. Pollut. 158, 3462–3471.

Naiman, R.J., Dudgeon, D., 2011. Global alteration of freshwaters: influences on human and environmental well-being. Ecol. Res. 26, 865–873.

Navarro-Ortega, A., Acuna, V., Bellin, A., Burek, P., Cassiani, G., Choukr-Allah, R., Doledec, S., Elosegi, A., Ferrari, F., Ginebreda, A., Grathwohl, P., Jones, C., Rault, P.K., Kok, K., Koundouri, P., Ludwig, R.P., Merz, R., Milacic, R., Munoz, I.,

Nikulin, G., Paniconi, C., Paunovic, M., Petrovic, M., Sabater, L., Sabater, S., Skoulikidis, N.T., Slob, A., Teutsch, G., Voulvoulis, N., Barcelo, D., 2015. Managing the effects of multiple stressors on aquatic ecosystems under water scarcity. The GLOBAQUA project. Sci. Total Environ. 503, 3–9. https://doi.org/10.1016/j.scitotenv.2014.06.081

Navarro-Ortega, A., Barceló, D., 2010. Persistent Organic Pollutants in Water, Sediments, and Biota in the Ebro River Basin. pp. 139–166. https://doi.org/10.1007/698_2010_77

Navarro, E., Guasch, H., Muñoz, I., Real, M., Sabater, S., 2000. Aplicación de un sistema de canales artificiales en el estudio ecotoxicológico de comunidades microbentónicas. Limnetica 18, 1–14.

Nilsson, C., Catherine, *, Reidy, A., Dynesius, M., Revenga, C., 2005. Fragmentation and Flow Regulation of the World's Large River Systems, SCIENCE.

Nilsson, C., Renofalt, B.M., 2008. Linking flow regime and water quality in rivers: a challenge to adaptive catchment management. Ecol. Soc. 13, 18.

Nödler, K., Licha, T., Barbieri, M., Pérez, S., 2012. Evidence for the microbially mediated abiotic formation of reversible and non-reversible sulfamethoxazole transformation products during denitrification. Water Res. 46, 2131–2139. https://doi.org/10.1016/j.watres.2012.01.028

Noges, P., Argillier, C., Borja, Ã., Garmendia, J.M., Hanganu, J., Kodes, V., Pletterbauer, F., Sagouis, A., Birk, S., 2016. Quantified biotic and abiotic responses to multiple stress in freshwater, marine and ground waters. Sci. Total Environ. 540, 43–52.

Noguera-Oviedo, K., Aga, D.S., 2016. Lessons learned from more than two decades of research on emerging contaminants in the environment. J. Hazard. Mater. https://doi.org/10.1016/j.jhazmat.2016.04.058

Nordström, M.C., Bonsdorff, E., 2017. Organic enrichment simplifies marine benthic food web structure. Limnol. Oceanogr. 62, 2179–2188. https://doi.org/10.1002/lno.10558

Odum, E.P., Finn, J.T., Franz, E.H., 1979. Perturbation Theory and the Subsidy-Stress Gradient. Bioscience 29, 349–352. https://doi.org/10.2307/1307690

Oksanen, J., Blanchet, F.G., Friendly, M., Kindt, R., Legendre, P., Mcglinn, D., Minchin, P.R., O'hara, R.B., Simpson, G.L., Solymos, P., Henry, M., Stevens, H., Szoecs, E., Maintainer, H.W., 2019. Package "vegan" Title Community Ecology Package. Community Ecol. Packag. 2, 1–297.

Osorio, V., Marcé, R., Pérez, S., Ginebreda, A., Cortina, J.L., Barceló, D., 2012. Occurrence and modeling of pharmaceuticals on a sewage-impacted Mediterranean river and their dynamics under different hydrological conditions. Sci. Total Environ. 440, 3–13. https://doi.org/10.1016/j.scitotenv.2012.08.040

Osorio, V., Proia, L., Ricart, M., Perez, S., Ginebreda, A., Cortina, J.L., Sabater, S., Barcelo, D., 2014. Hydrological variation modulates pharmaceutical levels and biofilm responses in a Mediterranean river. Sci. Total Environ. 472, 1052–1061. https://doi.org/10.1016/j.scitotenv.2013.11.069

Osorio, V., Sanchís, J., Abad, J.L., Ginebreda, A., Farré, M., Pérez, S., Barceló, D., 2016. Investigating the formation and toxicity of nitrogen transformation products of diclofenac and sulfamethoxazole in wastewater treatment plants. J. Hazard. Mater. 309, 157–164. https://doi.org/10.1016/j.jhazmat.2016.02.013

Patel, M., Kumar, R., Kishor, K., Mlsna, T., Pittman, C.U., Mohan, D., 2019. Pharmaceuticals of emerging concern in aquatic systems: Chemistry, occurrence, effects, and removal methods. Chem. Rev. https://doi.org/10.1021/acs.chemrev.8b00299

Peña-Herrera, J.M., Montemurro, N., Barceló, D., Pérez, S., 2020. Combining quantitative and qualitative approaches using Sequential Window Acquisition of All Theoretical Fragment-Ion methodology for the detection of pharmaceuticals and related compounds in river fish extracted using a sample miniaturized method. J. Chromatogr. A. https://doi.org/10.1016/j.chroma.2020.461009

Pence, H.E., Williams, A., 2010. Chemspider: An online chemical information resource. J. Chem. Educ. https://doi.org/10.1021/ed100697w

Pérez, S., Barceló, D., 2008. First evidence for occurrence of hydroxylated human metabolites of diclofenac and aceclofenac in wastewater using QqLIT-MS and QqTOF-MS. Anal. Chem. 80, 8135–8145. https://doi.org/10.1021/ac801167w

Pérez, S., Eichhorn, P., Celiz, M.D., Aga, D.S., 2006. Structural characterization of metabolites of the X-ray contrast agent iopromide in activated sludge using ion trap mass spectrometry. Anal. Chem. 78, 1866–1874. https://doi.org/10.1021/ac0518809

Peterson, C.G., Stevenson, R.J., 1992. Resistance and resilience of lotic algal communities: importance of disturbance timing and current. Ecology 73 (4), 1445–1461.

Petraitis, P.S., Latham, R.E., Niesenbaum, R.A., 1989. The maintenance of species diversity by disturbance. Q. Rev. Biol. 64, 393–418. https://doi.org/10.1086/416457

Petrovic, M., Ginebreda, A., Acuña, V., Batalla, R.J., Elosegi, A., Guasch, H., de Alda, M.L., Marcé, R., Muñoz, I., Navarro-Ortega, A., Navarro, E., Vericat, D., Sabater, S., Barceló, D., 2011. Combined scenarios of chemical and ecological quality under water scarcity in Mediterranean rivers. TrAC - Trends Anal. Chem. https://doi.org/10.1016/j.trac.2011.04.012

Petrovic, M., Petrovic, M., Barceló, D., 2007. LC-MS for identifying photodegradation products of pharmaceuticals in the environment. TrAC - Trends Anal. Chem. 26, 486–493. https://doi.org/10.1016/j.trac.2007.02.010

Petrovic, M., Sabater, S., Elosegi, A., Barceló, D., 2016. Emerging contaminants in river ecosystems: Occurrence and effects under multiple stress conditions.

Petrovic, M., Solé, M., López de Alda, M.J., Barceló, D., 2002. Endocrine disruptors in sewage treatment plants, receiving river waters, and sediments: integration of chemical analysis and biological effects on feral carp. Environ. Toxicol. Chem. 21, 2146–2156.

Picard, V., Lair, N., 2005. Spatio-temporal investigations on the planktonic organisms of the Middle Loire (France), during the low water period: biodiversity and community dynamics. Hydrobiologia 551, 69–86.

Pichard, L., Gillet, G., Bonfils, C., Domergue, J., Thenot, J.P., Maurel, P., 1995. Oxidative metabolism of zolpidem by human liver cytochrome P450S. Drug Metab. Dispos. 23, 1253–1262.

Piggott, J.J., Townsend, C.R., Matthaei, C.D., 2016. Reconceptualizing synergism and antagonism among multiple stressors. Ecol. Evol. 5, 1538–1547.

Pimm, S.L., 1984. THE COMPLEXITY AND STABILITY OF ECOSYSTEMS. Nature 307, 321–326. https://doi.org/10.1038/307321a0

Piqué, G., Batalla, R.J., Sabater, S., 2016. Hydrological characterization of dammed rivers in the NW Mediterranean region. Hydrol. Process. 30, 1691–1707. https://doi.org/10.1002/hyp.10728

Piram, A., Salvador, A., Verne, C., Herbreteau, B., Faure, R., 2008. Photolysis of β-blockers in environmental waters. Chemosphere 73, 1265–1271. https://doi.org/10.1016/j.chemosphere.2008.07.018

Pistocchi, A., 2019. An integrated perspective of Multiple Stressors in river ecosystems from the catchment to the continental scale, in: Sabater, S., Elosegi, A., Ludwig, R. (Eds.), Multiple Stressors in River Ecosystems. Elsevier, pp. 353–374.

Posthuma, L., Eijsackers, H.J.P., Koelmans, A.A., Vijver, M.G., 2008. Ecological effects

of diffuse mixed pollution are site-specific and require higher-tier risk assessment to improve site management decisions: A discussion paper. Sci. Total Environ. 406, 503–517. https://doi.org/http://dx.doi.org/10.1016/j.scitotenv.2008.06.065

Prats, J., Val, R., Armengol, J., Dolz, J., 2010. Temporal variability in the thermal regime of the lower Ebro River (Spain) and alteration due to anthropogenic factors. J. Hydrol. 387, 105–118. https://doi.org/10.1016/j.jhydrol.2010.04.002

Proia, L., Osorio, V., Soley, S., Koeck-Schulmeyer, M., Perez, S., Barcelo, D., Romani, A.M., Sabater, S., 2013. Effects of pesticides and pharmaceuticals on biofilms in a highly impacted river. Environ. Pollut. 178, 220–228. https://doi.org/10.1016/j.envpol.2013.02.022

Proia, L., Romaní, A.M., Sabater, S., 2012. Nutrients and light effects on stream biofilms: A combined assessment with CLSM, structural and functional parameters. Hydrobiologia 695, 281–291. https://doi.org/10.1007/s10750-012-1117-x

Quintana, J.B., Weiss, S., Reemtsma, T., 2005. Pathways and metabolites of microbial degradation of selected acidic pharmaceutical and their occurrence in municipal wastewater treated by a membrane bioreactor. Water Res. 39, 2654–2664. https://doi.org/10.1016/j.watres.2005.04.068

Radjenović, J., Pérez, S., Petrović, M., Barceló, D., 2008. Identification and structural characterization of biodegradation products of atenolol and glibenclamide by liquid chromatography coupled to hybrid quadrupole time-of-flight and quadrupole ion trap mass spectrometry. J. Chromatogr. A 1210, 142–153. https://doi.org/10.1016/j.chroma.2008.09.060

Reemtsma, T., Weiss, S., Mueller, J., Petrovic, M., González, S., Barcelo, D., Ventura, F., Knepper, T.P., 2006. Polar pollutants entry into the water cycle by municipal wastewater: A European perspective. Environ. Sci. Technol. 40, 5451–5458. https://doi.org/10.1021/es060908a

Reynolds, C.S., 2006. The ecology of phytoplankton, The Ecology of Phytoplankton. https://doi.org/10.1017/CBO9780511542145

Reynolds, C.S., Descy, J.-P., 1996. The production, biomass and structure of phytoplankton in large rivers. River Syst. 10, 161–187. https://doi.org/10.1127/lr/10/1996/161

Ribot, M., von Schiller, D., Sabater, F., Martí, E., 2015. Biofilm growth and nitrogen uptake responses to increases in nitrate and ammonium availability. Aquat. Sci. 77, 695–707. https://doi.org/10.1007/s00027-015-0412-9

Ricart, M., Guasch, H., Alberch, M., BarcelÃ³, D., Bonnineau, C., Geiszinger, A., FarrÃ©, M., Ferrer, J., Ricciardi, F., RomanÃ-, A.M., 2010. Triclosan persistence through wastewater treatment plants and its potential toxic effects on river biofilms. Aquat. Toxicol. 100, 346–353.

Rice, J., Westerhoff, P., 2017. High levels of endocrine pollutants in US streams during low flow due to insufficient wastewater dilution. Nat. Geosci. 10, 587–591. https://doi.org/10.1038/NGEO2984

Rodriguez-Mozaz, S., Chamorro, S., Marti, E., Huerta, B., Gros, M., Sànchez-Melsió, A., Borrego, C.M., Barceló, D., Balcázar, J.L., 2015a. Occurrence of antibiotics and antibiotic resistance genes in hospital and urban wastewaters and their impact on the receiving river. Water Res. 69, 234–242. https://doi.org/10.1016/j.watres.2014.11.021

Rodriguez-Mozaz, S., Ricart, M., Köck-Schulmeyer, M., Guasch, H., Bonnineau, C., Proia, L., de Alda, M.L., Sabater, S., Barceló, D., 2015b. Pharmaceuticals and pesticides in reclaimed water: Efficiency assessment of a microfiltration-reverse osmosis (MF-RO) pilot plant. J. Hazard. Mater. 282, 165–173. https://doi.org/10.1016/j.jhazmat.2014.09.015

Romani, A.M., 2000. Characterization of extracellular enzyme kinetics in two Mediterranean streams. Arch. Fur Hydrobiol. Apr 148, 99–117.

Romaní, A.M., Amalfitano, S., Artigas, J., Fazi, S., Sabater, S., Timoner, X., Ylla, I., Zoppini, A., 2013. Microbial biofilm structure and organic matter use in mediterranean streams. Hydrobiologia 719, 43–58.

Romaní, A.M., Artigas, J., Ylla, I., 2012. Extracellular Enzymes in Aquatic Biofilms: Microbial Interactions versus Water Quality Effects in the Use of Organic Matter, in: Microbial Biofilms: Current Research and Applications. pp. 153–174.

Romani, A.M., Guasch, H., Munoz, I., Ruana, J., Vilalta, E., Schwartz, T., Emtiazi, F., Sabater, S., 2004. Biofilm structure and function and possible implications for riverine DOC dynamics. Microb. Ecol. 47, 316–328.

Romaní, A.M., Sabater, S., Muñoz, I., 2010. The Physical Framework and Historic Human Influences in the Ebro River, in: Springer Berlin Heidelberg. pp. 1–20. https://doi.org/10.1007/698_2010_66

Romero, F., Sabater, S., Font, C., Balcázar, J.L., Acuña, V., 2019. Desiccation events change the microbial response to gradients of wastewater effluent pollution. Water Res. 151, 371–380. https://doi.org/10.1016/j.watres.2018.12.028

Rosi-Marshall, E.J., Kincaid, D.W., Bechtold, H.A., Royer, T. V., Rojas, M., Kelly, J.J., 2013. Pharmaceuticals suppress algal growth and microbial respiration and alter bacterial communities in stream biofilms. Ecol. Appl. 23, 583–593. https://doi.org/10.1890/12-0491.1

Roura-Carol, M., 2004. Incidència de l'embassament de Mequinensa en el transport de sòlids en suspensió i la qualitat del riu Ebre.

Ruhí, A., Acuña, V., Barceló, D., Huerta, B., Mor, J.-R., Rodríguez-Mozaz, S., Sabater, S., 2016. Bioaccumulation and trophic magnification of pharmaceuticals and endocrine disruptors in a Mediterranean river food web. Sci. Total Environ. 540, 250–259.

Sabater-Liesa, L., Montemurro, N., Font, C., Ginebreda, A., González-Trujillo, J.D., Mingorance, N., Pérez, S., Barceló, D., 2019. The response patterns of stream biofilms to urban sewage change with exposure time and dilution. Sci. Total Environ. 674, 401–411. https://doi.org/https://doi.org/10.1016/j.scitotenv.2019.04.178

Sabater, Sergi, Acuña, V., Batalla, R.J., Borrego, C., Butturini, A., Felip, M., García-Berthou, E., Gascón, S., Marcé, R., Martí, E., Menéndez, M., Muñoz, I., Quintana, X., Sabater, F., 2016a. Ecosistemes Aquàtics Continentals. Tercer informe sobre el canvi climàtic a Catalunya, Institut d'Estudis Catalans and Generalitat de Catalunya.

Sabater, S, Artigas, J., Corcoll, N., Proia, L., Timoner, X., Tornés, E., 2016a. Ecophysiology of river algae, in: River Algae. Springer International Publishing, pp. 197–217. https://doi.org/10.1007/978-3-319-31984-1_9

Sabater, S., Artigas, J., Duran, C., Pardos, M., Romani, A.M., Tornes, E., Ylla, I., 2008. Longitudinal development of chlorophyll and phytoplankton assemblages in a regulated large river (the Ebro River). Sci. Total Environ. 404, 196–206. https://doi.org/10.1016/j.scitotenv.2008.06.013

Sabater, S, Barceló, D., De Castro-Català, N., Ginebreda, A., Kuzmanovic, M., Petrovic, M., Picó, Y., Ponsatí, L., Tornés, E., Muñoz, I., 2016b. Shared effects of organic microcontaminants and environmental stressors on biofilms and invertebrates in impaired rivers. Environ. Pollut. 210, 303–314. https://doi.org/http://dx.doi.org/10.1016/j.envpol.2016.01.037

Sabater, S., Borrego, C., 2016. Application of micro- and mesocosms experiments to pollutant effects in biofilms, in: McGenity, T.J., Timmis, K.N., Nogales Fernández, B. (Eds.), Hydrocarbon and Lipid Microbiology Protocols. Springer Protocols

Handbooks, Heidelberg . https://doi.org/10.1007/8623_2015_170

Sabater, S., Elosegi, A., Dudgeon, D., 2013. River conservation: going against the flow to meet global challenges.

Sabater, S., Elosegi, A., Ludwig, R., 2019. Multiple Stressors in River Ecosystems: Status, Impacts and Prospects for the Future. Elsevier, Oxford.

Sabater, S., Guasch, H., Ricart, M., Romani, A., Vidal, G., Kluender, C., Schmitt-Jansen, M., 2007. Monitoring the effect of chemicals on biological communities. The biofilm as an interface. Anal. Bioanal. Chem. 387, 1425–1434. https://doi.org/10.1007/s00216-006-1051-8

Sabater, S., Romani, A.M., 1996. Metabolic changes associated with biofilm formation in an undisturbed Mediterranean stream. Hydrobiologia 335, 107–113.

Sabater, Sergi, Timoner, X., Borrego, C., Acuña, V., 2016b. Stream biofilm responses to flow intermittency: from cells to ecosystems. Front. Environ. Sci. 4. https://doi.org/10.3389/fenvs.2016.00014

Schmitt-Jansen, M., Altenburger, R., 2008. Community-level microalgal toxicity assessment by multiwavelength-excitation PAM fluorometry. Aquat. Toxicol. 86, 49–58. https://doi.org/10.1016/j.aquatox.2007.10.001

Schreiber, U., Gademann, R., Bird, P., Ralph, P.J., Larkum, A.W.D., Kuhl, M., 2002. Apparent light requirement for activation of photosynthesis upon rehydration of desiccated beachrock microbial mats. J. Phycol. 38, 125–134.

Schulz, M., Löffler, D., Wagner, M., Ternes, T.A., 2008. Transformation of the X-ray contrast medium iopromide in soil and biological wastewater treatment. Environ. Sci. Technol. 42, 7207–7217. https://doi.org/10.1021/es800789r

Schwarzenbach, R.P., Escher, B.I., Fenner, K., Hofstetter, T.B., Johnson, C.A., von Gunten, U., Wehrli, B., 2006. The challenge of micropollutants in aquatic systems. Science (80-. ). 313, 1072–1077. https://doi.org/10.1126/science.1127291

Schymanski, E.L., Jeon, J., Gulde, R., Fenner, K., Ruff, M., Singer, H.P., Hollender, J., 2014. Identifying small molecules via high resolution mass spectrometry: Communicating confidence. Environ. Sci. Technol. https://doi.org/10.1021/es5002105

Seddon, T., Michelle, I., Chenery, R.J., 1989. Comparative drug metabolism of diazepam in hepatocytes isolated from man, rat, monkey and dog. Biochem. Pharmacol. 38, 1657–1665. https://doi.org/10.1016/0006-2952(89)90314-6

Segner, Helmut, Schmitt-Jansen, M., Sabater, S., 2014. Assesing the impact of multiple

stressors on aquatic biota: the receptor's side matters. Environ. Sci. Technol. 48, 7690–7696.

Segner, H, Schmitt-Jansen, M., Sabater, S., 2014. Assessing the Impact of Multiple Stressors on Aquatic Biota: The Receptor's Side Matters. Environ. Sci. Technol. 48, 7690–7696. https://doi.org/10.1021/es405082t

Serôdio, J., Da Silva, J.M., Catarino, F., 1997. Nondestructive tracing of migratory rhythms of intertidal benthic microalgae using in vivo chlorophyll a fluorescence. J. Phycol. 33, 542–553. https://doi.org/10.1111/j.0022-3646.1997.00542.x

Serra-Compte, A., Sánchez-Melsió, Á., Álvarez-Muñoz, D., Barceló, D., Balcázar, J.L., Rodríguez-Mozaz, S., 2019. Exposure to a Subinhibitory Sulfonamide Concentration Promotes the Spread of Antibiotic Resistance in Marine Blue Mussels (Mytilus edulis). Environ. Sci. Technol. Lett. 6, 211–215. https://doi.org/10.1021/acs.estlett.9b00112

Sládeček, V., 1986. Diatoms as Indicators of Organic Pollution. Acta Hydrochim. Hydrobiol. 14, 555–566. https://doi.org/10.1002/aheh.19860140519

Smith, S. V., 1984. Phosphorus versus nitrogen limitation in the marine environment. Limnol. Oceanogr. 29, 1149–1160. https://doi.org/10.4319/lo.1984.29.6.1149

Smith, V.H., 2003. Eutrophication of freshwater and coastal marine ecosystems: A global problem. Environ. Sci. Pollut. Res. https://doi.org/10.1065/espr2002.12.142

Sprague, J.B., 1970. Measurement of pollutant toxicity to fish. II. Utilizing and applying bioassay results. Water Res. https://doi.org/10.1016/0043-1354(70)90018-7

Steffen, W., Crutzen, P.J., Mcneill, J., 2008. The Anthropocene: Are Humans Now Overwhelming the Great Forces of Nature Anthropocene: 1) The Earth System Level View project Plausible and desirable futures in the Anthropocene View project. AMBIO A J. Hum. Enviroment. https://doi.org/10.1579/0044-7447(2007)36[614:TAAHNO]2.0.CO;2

Stevenson, R.J., Pan, Y., Van Dam, H., 2010. Assessing environmental conditions in rivers and streams with diatoms, in: Smol, J.P., Stoermer, E.F. (Eds.), The Diatoms: Applications for the Environmental and Earth Sciences. Cambridge University Press.

Stierlin, H., Faigle, J.W., Sallmann, A., Kung, W., Richter, W.J., Kriemler, H.P., Alt, K.O., Winkler, T., 1979. Biotransformation of diclofenac sodium (voltaren® in animals and in man: I. Isolation and identification of principal metabolites. Xenobiotica 9, 601–610. https://doi.org/10.3109/00498257909042327

Strayer, D.L., Dudgeon, D., 2010. Freshwater biodiversity conservation: recent progress and future challenges. J. N. Am. Benthol. Soc. 29, 344–358.

Strayer, D.L., Dudgeon, David, 2010. Freshwater biodiversity conservation: recent progress and future challenges. journals.uchicago.edu 29, 344–358. https://doi.org/10.1899/08-171.1

Subashchandrabose, S.R., Ramakrishnan, B., Megharaj, M., Venkateswarlu, K., Naidu, R., 2011. Consortia of cyanobacteria/microalgae and bacteria: Biotechnological potential. Biotechnol. Adv. https://doi.org/10.1016/j.biotechadv.2011.07.009

Subirats, J., Timoner, X., Sànchez-Melsió, A., Balcázar, J.L., Acuña, V., Sabater, S., Borrego, C.M., 2018. Emerging contaminants and nutrients synergistically affect the spread of class 1 integron-integrase (intI1) and sul1 genes within stable streambed bacterial communities. Water Res. 138, 77–85. https://doi.org/https://doi.org/10.1016/j.watres.2018.03.025

Sutton, M.A., al., et, 2011. Too much of a good thing. Nature 472, 159–161.

Taylor, S.L., Roberts, S., Walsh, C.J., Hatt, B., 2004. Catchment urbanization and increased benthic algal biomass in streams: linking mechanisms to management. Freshw. Biol. 49, 835–851.

Ternes, T.A., 1998. Occurrence of drugs in German sewage treatment plants and rivers. Water Res. 32, 3245–3260. https://doi.org/10.1016/S0043-1354(98)00099-2

Terzic, S., Senta, I., Matosic, M., Ahel, M., 2011. Identification of biotransformation products of macrolide and fluoroquinolone antimicrobials in membrane bioreactor treatment by ultrahigh-performance liquid chromatography/quadrupole time-of-flight mass spectrometry. Anal. Bioanal. Chem. 401, 353–363. https://doi.org/10.1007/s00216-011-5060-x

Tockner, K., Pennetzdorfer, D., Reiner, N., Schiemer, F., Ward, J. V, 1999. Hydrological connectivity, and the exchange of organic matter and nutrients in a dynamic river-floodplain system (Danube, Austria). Freshw. Biol. 41, 521–535.

Tornés, E., Cambra, J., Gomà, J., Leira, M., Sabater, S., 2007. Indicator taxa of benthic diatom communities: a case study in Mediterranean streams. Ann. Limnol. J. Limnol. 43, 1–11.

Tornes, E., Perez, M.C., Duran, C., Sabater, S., 2014. Reservoirs override seasonal variability of phytoplankton communities in a regulated Mediterranean river. Sci. Total Environ. 475, 225–233. https://doi.org/10.1016/j.scitotenv.2013.04.086

Tran, N.H., Urase, T., Ngo, H.H., Hu, J., Ong, S.L., 2013. Insight into metabolic and

cometabolic activities of autotrophic and heterotrophic microorganisms in the biodegradation of emerging trace organic contaminants. Bioresour. Technol. https://doi.org/10.1016/j.biortech.2013.07.083

Vannote, R.L., Minshall, G.W., Cummins, K.W., Sedell, J.R., Cushing, C.E., 1980. The river continuum concept. Can. J. Fish. Aquat. Sci. 37, 130–137.

Verlicchi, P., Al Aukidy, M., Zambello, E., 2012. Occurrence of pharmaceutical compounds in urban wastewater: Removal, mass load and environmental risk after a secondary treatment-A review. Sci. Total Environ. https://doi.org/10.1016/j.scitotenv.2012.04.028

Vermeulen, J., Whiteoak, K., Nicholls, G., Gerber, F., McAndrew, K., Cherrier, V., Cunningham, E., Kirhensteine, I., Wolters, H., Verweij, W., Schipper, P., 2019. Fitness Check of the Water Framework Directive and the Floods Directive - Final evaluation report.

von Schiller, D., Aristi, I., Ponsati, L., Arroita, M., Acuña, V., Elosegi, A., Sabater, S., 2015. Regulation causes nitrogen cycling discontinuities in Mediterranean rivers. Sci. Total Environ. 540, 168–177. https://doi.org/http://dx.doi.org/10.1016/j.scitotenv.2015.07.017

Vörösmarty, C., Lettenmaier, D., Leveque, C., Meybeck, M., Pahl-Wostl, C., Alcamo, J., Cosgrove, W., Grassl, H., Hoff, H., Kabat, P., Lansigan, F., Lawford, R., Naiman, R., 2004. Humans transforming the global water system. Eos (Washington. DC). 85. https://doi.org/10.1029/2004EO480001

Vorosmarty, C.J., McIntyre, P.B., Gessner, M.O., Dudgeon, D., Prusevich, A., Green, P., Glidden, S., Bunn, S.E., Sullivan, C.A., Liermann, C.R., Davies, P.M., 2010. Global threats to human water security and river biodiversity (vol 467, pg 555, 2010). Nature 468, 334. https://doi.org/10.1038/nature09549

Wagenhoff, A., Lange, K., Townsend, C.R., Matthaei, C.D., 2013. Patterns of benthic algae and cyanobacteria along twin-stressor gradients of nutrients and fine sediment: A stream mesocosm experiment. Freshw. Biol. 58, 1849–1863. https://doi.org/10.1111/fwb.12174

Wagenhoff, A., Townsend, C.R., Phillips, N., Matthaei, C.D., 2011. Subsidy-stress and multiple-stressor effects along gradients of deposited fine sediment and dissolved nutrients in a regional set of streams and rivers. Freshw. Biol. 56, 1916–1936.

Wallach, A.D., Dekker, A.H., Lurgi, M., Montoya, J.M., Fordham, D.A., Ritchie, E.G., 2017. Trophic cascades in 3D: network analysis reveals how apex predators structure

ecosystems. Methods Ecol. Evol. 8, 135–142. https://doi.org/10.1111/2041-210X.12663

Walsh, C.J., Roy, A.H., Feminella, J.W., Cottingham, P.D., Groffman, P., Morgan, R.P., 2005. The urban stream syndrome: current knowledge and the search for a cure. J. North Am. Benthol. Soc. 24, 706–723.

Ward, J. V, Stanford, J.A., 1995. Ecological connectivity in alluvial river ecosystems and its disruption by flow regulation. Regul. Rivers - Res. Manag. 11, 105–119.

Wehr, J.D., Descy, J.P., 1998. Use of phytoplankton in large river management. J. Phycol. Oct 34, 741–749.

Wehr, J.D., Sheath, R.G., Kociolek, J.P., 2015. Freshwater algae of North America: ecology and classification. Elsevier.

Weigelhofer, G., Hein, T., Bondar-Kunze, E., 2018. Phosphorus and Nitrogen Dynamics in Riverine Systems: Human Impacts and Management Options. https://doi.org/10.1007/978-3-319-73250-3_10

Wilson, B.A., Smith, V.H., Denoyelles, F., Larive, C.K., 2003. Effects of three pharmaceutical and personal care products on natural freshwater algal assemblages. Environ. Sci. Technol. 37, 1713–1719.

Writer, J.H., Antweiler, R.C., Ferrer, I., Ryan, J.N., Thurman, E.M., 2013. In-Stream Attenuation of Neuro-Active Pharmaceuticals and Their Metabolites. Environ. Sci. Technol. 47, 9781–9790. https://doi.org/10.1021/es402158t

Xu, Y., Radjenovic, J., Yuan, Z., Ni, B.-J., 2016. Biodegradation of Atenolol by an Enriched Nitrifying Sludge: Products and Pathways A novel method for controlling microbial concrete corrosion in sewers (2015-2018) ARC Linkage Projects View project Biodegradation of atenolol by an enriched nitrifying sludge: Products and pathways. Elsevier. https://doi.org/10.1016/j.cej.2016.11.153

Zonja, B., Delgado, A., Pérez, S., Barceló, D., 2015. LC-HRMS suspect screening for detection-based prioritization of iodinated contrast media photodegradates in surface waters. Environ. Sci. Technol. 49, 3464–3472. https://doi.org/10.1021/es505250q

Universitat de Girona